CO_2 Conversion into Formic Acid under Hydrothermal Conditions Using Biomass and Metals

University of Sheffield

Department of Chemical and Biological Engineering

Thesis submitted for the degree of Doctor of Philosophy

By: Ibrahim Alfayez

Supervisor:

Dr. James McGregor

January 2026

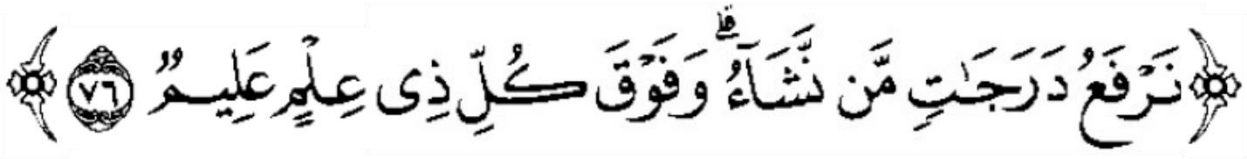

سورة يوسف

Which translates to:

“We raise to degrees whom We will, but over all those endowed with knowledge is the All-Knower (Allah)”

The noble Qur’an, Chapter13: Yusuf (Joseph)-Verse 76

(Translation of the meanings of THE NOBLE QUR’AN in the English language, Dr. Al-Hilali and Dr. Khan, 2013)

Abstract

Utilization of CO_2 provides a readily and inexpensive available source of carbon for different processes. Several studies have shown various products obtained from the utilization of CO_2 including formic acid which is an important chemical with various applications such as silage, pharmaceutical, and as an energy source. Formic acid can be produced from hydrothermal reduction of CO_2 with employment of proper reducing agent. Reductants, used in the hydrothermal hydrogenation of CO_2 into formic acid, can be divided into metals and organic-based. Metal reductants outperform non-metal reductants for the production of formic acid from CO_2 reduction under hydrothermal conditions. The formation of byproducts when non-metal reductants used could be the reason for their reported performance. Introducing metal reductants to non-metal reductants is believed to enhance the yield of formic acid as metals oxidation in-situ provides hydrogen for the reduction and shift the selectivity toward formic acid and act as a catalyst. Therefore, this work investigates the synergistic impact of combining metals and biomass as reductants on the production of formic acid under hydrothermal conditions. The results showed that combining Zn with glucose boosts the yield of formic acid threefold, 38 mM vs. 13 mM at 250 ºC, 2 h, and 50% filling volume. In addition, Zn enhances the selectivity toward more formic acid and less byproducts. Nevertheless, hydrogen gas was also a byproduct from this combination of reductants. Furthermore, the purity of the produced hydrogen gas was better than other hydrogen production such as aqueous phase reforming, APR, and metal to hydrogen processes. Moreover, the zinc oxide formed from this process can be used as a catalyst to produce propanoic acid from the same process. Therefore, this work presents an alternative way to enhance the performance of glucose as a sustainable reductant for the reduction of CO_2 into formic acid.

Acknowledgment

First and foremost, I extend my deepest gratitude and praise to Allah, the Almighty, for granting me the strength, wisdom, and perseverance to complete this research. I am sincerely thankful to the Government of the Kingdom of Saudi Arabia for generously supporting my academic journey through the Ministry of Education and the University of Hail. I am especially grateful to Dr. James McGregor for his invaluable guidance and dedicated supervision throughout the course of this work. I would also like to express my heartfelt appreciation to my family, friends, colleagues, laboratory technicians, and all those who have supported me, directly or indirectly, during this important phase of my academic and personal development.

Dedication

To my parents, 2025 was a tough year. May Allah have his mercy on you and reward you Jannah, paradise, in the company of those on whom Allah has bestowed his grace, the prophets, the people of truth, the martyrs, and the righteous - Amen.

Contents

List of figures

List of tables

Chapter 1: Introduction

There is a cost to everything, and the cost of industrial advancement is reflected on the whole globe. Heavy exploitation of natural resources, which has been the main source of energy, results in harmful impacts on our planet. The temperature of earth has risen since 1850, and subsequently the years from 2014 through 2023 were reported "the warmest".[1] Among multiple factors participating in global warming, carbon dioxide, CO_2, level in the atmosphere has been noticeably increased by 33 % in the period of 1959-2023.[2]–[4] The imbalance in the CO_2 level extends its harmful effects to impact other aspects on the planet, resulting, for instance, in changes in the ocean acidity that impact marine life.[4] The Intergovernmental Panel on Climate Change, IPCC, Climate Futures investigated different scenarios of CO_2 emission on five trends of CO_2: very high, high, halved, low, and very low from 2022 to 2100 and they concluded that stabilization of the temperature of the globe requires net zero CO_2 emission.[5] In fact, IPCC showed that more CO_2 needs to be captured from the atmosphere to satisfy low and very low CO_2 emission scenarios.[5]

Carbon dioxide, CO_2, can be used as a source of carbon for different chemical processes. CO_2 is a stable compound with a strong C=O bond making its usage challenging. CO_2 needs to be activated prior use, and its activation requires intensive energy input and/or introduction of catalysts or reducing agents. These challenges often limit the conventional CO_2 utilization processes as they trigger efficiency and scalability concerns.

Various solutions have been proposed to tackle CO_2 emissions and mitigate its effects on the environment. The solutions include but are not limited to controlling the existing processes to reduce CO_2 emissions or capturing and storing CO_2 to utilize it later. Utilizing the captured CO_2 not only participates in the reduction of the CO_2 amount emitted to the atmosphere but also presents a readily available source of carbon for different processes. In fact, finding another source of carbon will eliminate or at least reduce the dependency on natural resources if carbon is needed. The utilization of CO_2 in chemical processes presents a way to produce useful chemicals other than capturing and storing suggestions of CO_2. Formic acid is an important C_1 chemical with a variety of applications such as in silage, food preservative, and as a liquid organic hydrogen carrier, LOHC. Unlike methanol and hydrocarbons, formic acid needs fewer electron proton transfer steps for production which makes it easier to produce.

CO_2 gas is chemically captured by using an appropriate solvent. The type of solvents used for the purpose of CO_2 capturing varies based on their physical properties, chemical activities, and cost. Generally, CO_2 capturing solvents can be categorized based on their type. Borhani and Wang classified the type of solvents based on "family" as amine, ammonia, and salt solutions. [6] Each of amine, ammonia, and salt solutions has various models. For instance, monoethanolamine, MEA, is an example of amine-based CO_2 capturing solvent. Additionally, ammonia, NH_3, is also another type of CO_2 capturing solvent. Sodium hydroxide, NaOH, is an example of salt solution for capturing CO_2 gas. [6]

There are different views on the criteria on selecting CO_2 capturing solvent as different types have advantages and disadvantages.[6] NaOH is one of the suggested solvents which is a cost-effective choice, available, safe, and stable.[6] When CO_2 is captured in NaOH solution, the final product, or the final form in which CO_2 will be at is as sodium bicarbonate, $NaHCO_3$.

The conventional methods to produce formic acid from CO_2 conversion are electrochemical reduction and thermocatalytic hydrogenation. Electrochemical CO_2 reduction to formic acid requires high overpotential and faces challenges with stability and scale-up. On the other hand, thermocatalytic CO_2 hydrogenation to formic acid needs supported metal catalysts as well as a source of hydrogen which is typically produced from non-renewable sources.

Hydrogenation reactions, as the name suggests, require hydrogen. Hydrogen gas can be produced from both renewable and non-renewable sources. The available processes for hydrogen gas production are thermochemical processes, electrolytic means, and biological based processes. For example, aqueous phase reforming, APR, is an example of thermochemical processes whereas water splitting by solar energy is an example of electrolytic processes and microbial biomass conversion is an example of the biological ways to produce hydrogen gas.[7] Unfortunately, most of the produced hydrogen today comes from non-renewable sources. For instance, 95% of hydrogen gas produced in the United States from natural gas reforming process[8] which releases 8 kg of CO_2 per 1 kg of hydrogen produced.[9] Another way to produce hydrogen gas is liquid organic hydrogen carrier, LOHC. In LOHC, a chemical rich in hydrogen like methanol or formic acid, is produced and then transported and dehydrogenated as needed.[10] Note that the chemical in LOHC can be a side product from another process. Hydrogen can alternatively be produced in-

situ without the need of an external source of hydrogen by utilizing water at high temperature, HTW.[11] The only requirement for producing hydrogen from water at elevated temperatures is employing a reductant.

HTW refers to water at elevated temperatures and pressures where the properties of water change compared to normal conditions. At high temperatures and pressures, the properties of water such as density, dielectric constant, and viscosity change. For example, at 25 ºC and 1 bar, the density, dielectric constant, and diffusion coefficient are 998 $kg.cm^{-1}$, 78, and 7.74×10^{-8} $m^2.s^{-1}$ respectively.[12] However, at supercritical conditions, 450 ºC and 270 bar, water density, dielectric constant, and diffusion coefficient are 128 $kg.cm^{-1}$, 1.8, and 7.67×10^{-6} $m^2.s^{-1}$ respectively.[12] Thus, water properties at high operating conditions resemble the properties of conventional solvents. Thus, water properties at high operating conditions promotes reactions as the medium becomes active.

CO_2 can be used as a carbon source in different processes. The hydrogenation process of CO_2 into different useful products is an example. CO_2 hydrogenation reactions can produce various products such as CO, CH_4, hydrocarbons, methanol, formic acid and other chemicals.[13]

Formic acid production from CO_2 reduction under hydrothermal conditions has been reported using metal and nonmetal reductants with high selectivity toward formic acid at temperatures ranging from 200-300 ºC. Metal reductants such as Fe, Zn, and Al reported to produce formic acid when used to reduce CO_2 under hydrothermal conditions. For instance, formic acid yield of 78% was achieved using Zn metal only without any catalyst at 300 ºC from CO_2 reduction under hydrothermal conditions. [14]–[16]

Alternatively, biomass-based reductants have been employed for the reduction of CO_2 into formic acid under hydrothermal conditions. For example, Fernandez et al. examined an array of organic compounds as a reductant for the production of formic acid from the reduction of CO_2 under hydrothermal conditions and found that glucose yielded 65% of formic acid at 300 ºC when used to reduce bicarbonate. [17] Taking advantage of biomass reductant for processes like CO_2 reduction paves the way toward more options of biomass valorization for CO_2 utilization purposes and thus tackling the CO_2 increased emission.

From the presented information, two facts can be concluded i) the opportunity that captured CO_2 presents as a readily available source of carbon, and ii) the need to find an environmentally friendly source of hydrogen gas. Therefore, finding a way to present a solution to both issues is of great importance. Despite the advances presented in the CO_2 reduction into formic acid under hydrothermal conditions, optimization of biomass-based reductants, improving the yield as well as the selectivity of formic acid, and clearer understanding of the mechanistic pathways need vigorous investigation.

1.1. Objectives

This work aims to investigate the CO_2 reduction into formic acid reaction under hydrothermal conditions using glucose alone and in the presence of metals. The main role of glucose here is as a reducing agent to help convert CO_2 into formic acid. Additionally, the metals tested in this work are iron, Fe, zinc, Zn, and aluminum, Al in their zero-valence state. The metal addition is hypothesized to enhance yield and selectivity of formic acid under hydrothermal conditions. A similar role to glucose is expected from the addition of metals. Here are the objectives of this work:

- To identify the formed products at the given reaction conditions.
- To optimize the tested conditions for the best concentration of formic acid by varying the reaction times including the heating periods (1, 2, and 3 h), reaction temperatures (200, 250, and 300 ºC), and filling volumes (30, 50, and 70%).
- To trace and confirm the source of formic acid as there are two sources of carbon bicarbonate and glucose.
- To investigate the impact of adding metals, Fe, Zn, and Al, on the production of formic acid and other formed products.
- To check the reusability of the produced metal oxide for the production of formic acid.

Chapter 2: Literature Review

2.1. CO_2 mitigation options

One of the strategies to tackle the increased emission of CO_2 is via carbon capture, storage, and utilization of CO_2, aka CCUS. In this step, the CO_2 is first captured from industrial processes or directly from the air. The captured CO_2 can then be stored permanently, stored for utilization, or utilized directly CO_2 utilization aims to take advantage of the captured CO_2 by making use of it in another application as a raw material or converting it into a useful product. By doing so, the CO_2 can be captured and reused multiple times without being emitted to the environment.[18] The utilization of CO_2 can be split into two main routes, a) physical or direct use or non-conversion route, and b) chemical conversion.[19], [20]

The direct use of CO_2 means the use of CO_2 as is without any further treatment. Various applications are available for the CO_2 direct use including enhance oil and gas recovery, EOR and EGR, in fire extinguishers, as a refrigerant, and many others.[21], [22] On the chemical conversion of CO_2, the captured CO_2 is used as a feedstock to produce valuable products via chemical reactions. CO_2 can be used as a carbon source to produce products such as methanol, CO, dimethyl ether (DME), and many others.[19], [20]

The non-conversion route for CO_2 utilization is less popular and its overall impact on the CO_2 mitigation is limited.[23] On the other hand, the conversion route for CO_2 attained more attention as it seen as the solution to reach zero-emission goal.[18], [19], [22]Therefore, CO_2 hydrogenation is preferred over the other options given that the used hydrogen is obtained from a green and renewable source.

2.2. CO_2 Hydrogenation Processes

2.2.1. CO_2 Hydrogenation to Carbon Monoxide, CO

CO can be produced from the hydrogenation of CO_2 via a process called reverse water-gas shift reaction, RWGS, in the presence of catalysts. [24]

$$CO_2 + H_2 \leftrightarrow CO + H_2O;\ \Delta H_{298\,K} = 41.2\ kJ\ mol^{-1} \qquad \text{R.1}$$

Popular catalysts employed in these processes are metal-based catalysts such as copper-based[25]–[27], cerium-based[28]–[30], and supported noble metal catalysts.[13], [31] Cu-Ni/γ- Al_2O_3, Cu/Zn, Cu-Zn/γ- Al_2O_3, Cu/SiO_2 with and without potassium, K, promoter are example of the used metal catalysts. [25], [26]

Thermal stability of the catalyst is an important aspect to consider when endothermic processes are involved. Although copper-based catalysts exhibit weak thermal stability in the endothermic reaction of RWGS, solutions such as strengthening by adding a thermal stabilizer, e.g. Fe added to Cu/SiO_2, or applying epitaxial film to Cu/SiO_2 have been proposed.[32]

Despite their strong performance, cerium-based catalysts like Pt/CeO_2 deactivate when exposed to carbon, even in small quantities. [30] CO can be produced from CO_2 hydrogenation catalyzed by rhodium ion-exchanged zeolites promoted by lithium, Li/RhY, by increasing the ratio of Li/Rh above 10, where methane, CH_4, is preferably produced under this ratio.[13], [31] Additionally, the choice of metal precursor when preparing a noble metal catalyst plays a role in determining the selectivity toward possible products. For instance, a choice of acetate as a precursor makes CO as the main product as Arakawa et al. have shown.[33]

2.2.2. CO_2 Hydrogenation to Methane, CH_4

The Sabatier reaction is the reaction to produce methane from CO_2 hydrogenation. One of its plausible applications is to provide astronauts with water and fuel by converting CO_2, which exists in the atmosphere of Mars. [34]–[36]

$$CO_2 + 4H_2 \rightarrow CH_4 + 2H_2O;\ \Delta H_{298\,K} = -252.9\ kJ\ mol^{-1} \quad \text{R.2}$$

Catalysts, mainly metal-based over various supports, have been investigated. Nickel supported on oxide is one of the widely discussed catalysts. It is important to note that the type of support could improve the performance of the catalyst. For example, Cheng et al. showed that rice husk ash (RHA), as a support of nickel catalyst, is outperforming silica gel in the CO_2 methanation reaction due to the high surface area and dispersion of the nickel catalyst.[37]–[39] Additionally, due to its stability both thermally and structurally, RANEY nickel catalyst is well known for hydrogenation processes including methanation.[40]

Another way to produce methane from the hydrogenation of CO_2 is by directly conversion of post-combustion captured CO_2. Kothandaraman et al. proposed an entire process of converting post-combustion captured CO_2 into methane claiming thermal efficient and cost-effective approach.[41] The authors proposed a capture and conversion system of liquid phase CO_2 captured into methane using Ru catalyst and 2-EEMPA as a capture agent, which exhibits a conversion of hydrocarbons of more than 90% of captured CO_2. In that study, 2-EEMPA capturing solvent was tested at 170, 145, and 120 ℃ to probe the CO_2 conversion and the selectivity of CH_4, C_2H_6, and C_3-C_4, over 5 wt% Ru/Al_2O_3 catalyst, from which 170 ℃ was the highest for CO_2 conversion of 75.8% and selectivity of CH_4, C_2H_6, and C_3-C_4 87.4, 4.6, and 8% respectively. On the other hand, using only CO_2 gas in the same conditions exhibited higher CO_2 conversion, 82.6%, but less C_2H_6 and higher C_3-C_4. Other catalysts such as $Pd/ZnO/Al_2O_3$, Pd/ZnO, $Cu/ZnO/Al_2O_3$, Ni/Al_2O_3, and Ru/C were also tested. Nevertheless, Ru/C showed CO_2 conversion of 12.3%, which was less than that obtained over Ru/Al_2O_3.

2.2.3. CO_2 Hydrogenation to Hydrocarbons

CO_2 hydrogenation into hydrocarbons is through a modified Fischer-Tropsch synthesis, FT, where CO is replaced by CO_2. Hydrocarbons can be produced directly from CO_2 hydrogenation via two routes, a) methanol synthesis followed by conversion of methanol to hydrocarbons, and b) reaction of CO_2 hydrogenation follows two steps I) RWGS reaction then II) FT synthesis. [42], [43]

I. $CO_2 + H_2 \leftrightarrow CO + H_2O;\ \Delta H_{573\,K} = 38\ kJ\ mol^{-1}$ R.3

II. $CO + H_2 \rightarrow -CH_2- + H_2O;\ \Delta H_{573\,K} = -166\ kJ\ mol^{-1}$ R.4

The catalysts used for FT synthesis are either cobalt, which exhibits high performance to cost ratio and acts as a methanation catalyst when gas mixture fed is CO_2 and H_2, or iron oxides.[43]–[45] Iron oxides, however, perform well for both FT and RWGS and are preferred when hydrocarbons yield is wanted due to its olefinic nature. [43]–[45] It is also worth mentioning that a drawback of iron-based catalysts in CO_2 hydrogenation process is their deactivation due to the carbon deposited layer which poisoning it.[46] Promotors such as potassium are usually added to increase the production of hydrocarbons. Interestingly, potassium increases CO_2 conversion and can reverse H_2 storage at high temperature when in alanate phase, KA_1H_4.[47] Other promoters are manganese, which increases olefins/paraffin ratio and suppresses methane formation in both FT and CO_2

hydrogenation,[47], [48] copper,[49] ceria,[50] and Zr and Zn.[45] Moreover, the catalyst support plays an important role in keeping the catalyst stable during the reaction, alumina is the best then silica then titania. Nevertheless, the water produced in the reactions deactivates the catalysts and decreases the CO_2 hydrogenation reaction rate, therefore, in situ water removal is suggested.[51]

2.2.4. CO_2 hydrogenation to CH_3OH

Methanol can be synthesized by hydrogenation of CO_2 as in the following reaction[52], [53]:

$$CO_2 + 3H_2 \rightarrow CH_3OH + H_2O;\ \Delta H_{298\,K} = -49.5\ kJ\ mol^{-1} \qquad \text{R.5}$$

RWGS reaction is a side reaction that takes place when producing methanol by CO_2 hydrogenation. Since methanol production via CO_2 hydrogenation is an exothermic reaction, and to be thermodynamically favorable, manipulating reaction parameters by decreasing temperature and increasing pressure is required. However, due to the relative thermodynamic stability of CO_2, temperatures in excess of 513 K are required for methanol in CO_2 hydrogenation.[54] Two issues arise from the methanol production reactions from CO_2 hydrogenation a) both reactions produce water which can be a problematic as it deactivates the catalysts, b) RWGS reaction and the main reaction both use H_2, and thus, the production of methanol can be limited.[55], [56] Moreover, by-products such as hydrocarbons and higher alcohols are anticipated and thus, designing a methanol selective catalyst is essential.[54]

Copper and zinc, Cu and Zn, with variety of modifiers like Zr and Al are well known for this purpose. Doping Cr, Ze, and Th can improve copper thermal stability for methanol synthesis as Liaw and Chan presented. [57] Also, the addition of ZnO to Cu/ZrO_2 increases its activity whereas doping CuZnO by ZrO_2 increases both activity and selectivity. Noble metal catalysts have been investigated for the same purpose too where Pd is the most common applied. The support chosen for metal catalysts plays an important role in the catalyst performance, an example of this a study of comparing selectivity of different supports with La_2O_3 shown to have the best selectivity, 89% at 623 K.[54] Carbon nanotubes have been investigated and a study show turnover frequency, TOF, $1.5x10^{-2}s^{-1}$ at 523 K and 3 MPa over 16% $Pd_{0.1}Zn1$/CNTs(h-type).[58] Metal carbide such as MO_2C and Fe_3C could replace noble metals for methanol synthesis as they were shown to have comparable, to noble metals, methanol selectivity.[59]

Although methanol produced from gas phase CO_2 by hydrogenation is popular due to its rapid reaction rate, this reaction requires high temperature of 200-250 ℃ where the rate determining step for this conversion is the activation of CO_2.[60] An alternative way is to indirectly convert the post captured CO_2, which has been already activated, into methanol via intermediates such as formate. Since one of the main methods used to mitigate CO_2 emission is by post-combustion capture, captured CO_2 can be transformed directly with no need of separation from the capturing medium.

Addition of alcohol is shown to be beneficial for methanol synthesis by CO_2 hydrogenation. Nieminen et al. investigated the effect of the addition of alcohol in CO_2 hydrogenation to methanol over Cu/ZnO and copper chromite. Alcohol, specifically, 1- and 2-butanol solvents, play a catalytic role where they reduce the reaction temperature when compared to the production of methanol in the gas phase reaction.[61] Additionally, the addition of ethanol as a solvent showed its role as a catalyst toward converting CO_2 into methanol.[62]

The water formed from the conversion of CO_2 into methanol by hydrogenation shown to be a problem in the view of limiting the methanol yield. However, one proposed solution to this issue is in-situ continuous water removal. Nieminen et al. showed that effect when 3 Å, molecular 10 sieve was used, in 2-butanol solvent, for water removal continuously in which the methanol yield improved, noting that the higher ratio of the molecular sieve wight to the weight of catalyst, the better methanol yield, 55% methanol productivity, in g/kg/h, for 10:40 (g Cu/ZnO: g molecular sieve) versus 10% for 20:20 (g Cu/ZnO: g molecular sieve).[61]

Other heterogenous catalysts beyond Cu-based materials have also been investigated for the production of methanol from hydrogenating captured CO_2. Pd-based catalyst, specifically Pd/MgO have been shown to be effective for methanol production via ethyl carbonate as an intermediate. [62]

2.2.5. CO_2 Hydrogenation to Dimethyl Ether, DME

Dimethyl ether, DME, is a candidate to replace diesel due to its advantages including low emission of undesired gases, and high cetane number.[63] DME can be produced from CO_2 hydrogenation through either two steps or a single process. Two steps process is where the methanol is

synthesized first and then it undergoes a dehydration process to finally get DME whereas a single process is the one in which a bifunctional catalyst is used for both steps simultaneously where thermodynamic limitation of producing methanol is lower.[64]–[68]

Many types of catalysts for producing DME have been reported. Because the production process involves methanol, Cu-based catalysts are also employed here. Additionally, in the dehydration step, acidic catalysts such as zeolites and γ-Al_2O_3 are suggested. Although water produced from hydrogenation of CO_2 decreases γ-Al_2O_3 activity, it has no effect on HZSM-5.[69]–[74] Adding promoters such as Pd to copper based catalysts increase the selectivity of DME by 28%. [13], [75], [76]

2.2.6. CO_2 Hydrogenation to Formic Acid

Formic acid, the simplest form of carboxylic acids, is an important chemical for different applications and it can be produced from the hydrogenation of CO_2. Formic acid is a chemical used in applications including the leather and rubber industries, silage and food, anti-freezing agent, as well as an energy source.[9], [16], [77], [78] To give context on the market of formic acid, potassium formate, $KHCO_2$, is a formic acid salt used in multiple applications such as fertilizing, deicing agent, as well as a heat transfer fluid; its market is expected to grow by 40% to reach a total market value of $840 million in 2027.[79] Additionally, formic acid has been shown as a candidate to be a liquid organic hydrogen carrier. Hydrogen can be stored in formic acid by 4.3 wt.% of formic acid, in its pure form, and all of H_2 content can be retrieved. In addition, there is greater convenience in handling formic acid compared to H_2. [78], [80]

$$CO_2 + H_2 \rightarrow HCOOH;\ \Delta H_{298\,K} = -31.2\ kJ\ mol^{-1} \qquad \text{R.6}$$

Inorganic base addition shifts the equilibrium toward formate which could be then converted to formic acid using strong acid. [81] Homogenous ruthenium, Ru, based catalysts are widely applied in this process and many studies compare their performance. [82]

Furthermore, heterogenous catalysts used in CO_2 hydrogenation to formic acid are either a) bulk/nano-metal catalysts, which can be subdivided into supported catalysts, e.g. Au/TiO_2 and unsupported catalysts, e.g. Pd nanoparticle, and b) heterogenized molecular catalysts, either on solids such as SiO_2 based or on porous polymers such as metal organic frameworks, MOFs. [80]

Direct hydrogenation of CO_2 into formic acid using Pd/C and ionic liquid, IL, 1-butyl-3-methylimidazolium acetate, [Bmim][OAc], as a solvent, in the absence of base, had been investigated in liquid phase reaction. [83] ILs are organic ionic compounds, and they can be tailored by selection of ions to serve specific functions based on the desired applications. [83] Wu et al. investigated the conversion of CO_2 into formic acid using Pd/C and IL by first testing different IL solvents to probe the yield of formic acid. [Bmim][OAc] solvent exhibited the highest yield of formic acid, 1.42 mmol compared to other solvents such as [DBUH][OAc] where the formic acid yield was reported to be 0.99 mmol, in the presence of Pd/C catalyst at 40 ºC which seems promising for industrial application. [83]

Filonenko et al. tested the effect of supported and unsupported gold catalysts using different solvents and bases on the conversion of CO_2 into formats in liquid phase reaction and concluded that Au/Al_2O_3 is more active than Au/TiO_2, 215 versus 111 TON.[84] Additionally, the authors proposed that CO_2 hydrogenation to formate takes place between the gold and the support since each has a unique role in that process.[84] Their proposed mechanism was as the following: i) dissociation of H_2 occurs between the metal and its support from which hydroxyl and metal hydride produced, then ii) bicarbonate is formed at the support when CO_2 is adsorbed which interacts with the formed hydride to finally produce formate, which is proposed to be the rate determining step. [84]

Industrially, the production of formic acid is achieved via two steps:

Step 1: $CH_3OH + CO \rightarrow CH_3COOH$; $\Delta H_{298\,K} = -38.1\ kJ\ mol^{-1}$ R.7

Step 2: $CH_3COOH + H_2O \leftrightarrow HCOOH + CH_3OH$; $\Delta H_{298\,K} = 16.3\ kJ\ mol^{-1}$ R.8

The first step is the formation of methyl formate via methanol carbonylation, step 1, followed by hydrolysis of the formed ester, step 2, and then rectification of the products to yield formic acid. [78] The pressure of CO required in this process is as high as 85.5 MPa to obtain 50 wt.% formic acid at 100 ºC. [78]

2.3. Challenges for the existing CO_2 hydrogenation process

There are some challenges in the CO_2 hydrogenation processes such as thermodynamic and kinetic barriers, low conversion of CO_2, catalyst stability, product selectivity, and hydrogen source.

CO_2 is a stable compound, and this is one of the challenges when it comes to using it in a process, the strong C=O bond requires a huge energy input to activate it and make it ready to react with hydrogen in hydrogenation processes. Furthermore, when a catalyst is used for the CO_2 hydrogenation processes, the same issue arises which is the strong bonding of CO_2 on the surface of a catalyst which requires overcoming high energy barriers.[85], [86]

Low conversion of CO_2 is another challenge of CO_2 hydrogenation processes. For example, the conversion of CO_2 in CO_2 hydrogenation to methanol is about 21% at 220 ºC and in the presence of $Cu/Zn/ZrO_2$ catalyst.[87] Additionally, the CO_2 conversion in CO_2 hydrogenation to dimethyl ether, DME, is about 31% at 250 ºC and in the presence of Cu/Zn/Al/Zr+HZSM5.[71]

Product selectivity is another challenge in CO_2 hydrogenation processes. For example, in methanol synthesis from CO_2 hydrogenation, the selectivity toward methanol was reported to be about 68% when using Cu/Zn/ZrO2 catalyst at 220 ºC.[87] It is important to mention that although some catalyst show far higher methanol selectivity such as 99.5% when using $Cu/Zn/Ga/SiO_2$ catalyst in CO_2 hydrogenation to methanol, the CO_2 conversion is only 5.6%.[88]

Catalyst stability is another challenge in CO_2 hydrogenation processes. For instance, sintering is one of the main challenges for copper catalyst when it used in reverse water gas shift reaction, RWGS, to produce CO from the hydrogenation of CO_2 .[13] In addition, Ni-based catalysts were shown to deactivate as they interact with CO which is a product of CO_2 hydrogenation into methane at low temperature.[89]

One of challenges facing CO_2 hydrogenation processes is the source of hydrogen. Unfortunately, most of the produced hydrogen today comes from non-renewable sources. For instance, 95% of hydrogen gas produced in the United States from natural gas reforming process[8] which releases 8 kg of CO_2 per 1 kg of hydrogen produced.[9] The source of hydrogen is another aspect in which the challenges of CO_2 hydrogenation processes can be addressed. The hydrogen supply would be ideally obtained from a renewable source such as from a renewable electrolysis. However, more challenges arise when it comes to producing hydrogen from a renewable electrolysis process regarding the cost and the difficulty of the storage. The cost of producing hydrogen from a renewable source is high. For instance, the cost of producing hydrogen from a green renewable source using electrolysis is about \$2.2-7.3 per Kg of H_2 compared to \$0.6-1.3 per Kg of H_2 from

steam methane reforming, SMR. [90]–[92] Furthermore, the difficulty of storing the produce green hydrogen is another challenge for the hydrogen production from green sources such as electrolysis from a renewable source.[93]

2.4. Hydrothermal processes

An alternative way to produce formic acid is via utilization of CO_2 under hydrothermal conditions. In hydrothermal processes, the only requirement for hydrogen gas to be in-situ produced is employing a suitable reductant. Hydrogen can be produced in-situ without the need of an external source of hydrogen by utilizing water at high temperature, HTW.[11] At high temperatures and pressures, the properties of water such as density, dielectric constant, and viscosity change. For example, at 25 ºC and 1 bar, the density, dielectric constant, and diffusion coefficient are 998 $kg.cm^{-1}$, 78, and 774×10^{-8} $m^2.s^{-1}$ respectively. [12] However, at supercritical conditions, 450 ºC and 270 bar, water density, dielectric constant, and diffusion coefficient are 128 $kg.cm^{-1}$, 1.8, and 7.67×10^{-6} $m^2.s^{-1}$ respectively.[12]

The reductants used in hydrothermal processes can be metals or non-metals both cases have different ways to reduce the CO_2. In metal reductants the metal used undergoes oxidation and thus producing hydrogen gas and metal oxide as in the following equation

$$M(s) + H_2O\ (l) \rightarrow MO\ (s) + H_2(g) \qquad \text{R.10}$$

As seen in the reaction equation R.10, the production of H_2 will be one of the benefits of using metals here which will have effects on i) the total pressure of the process; ii) providing more in-situ hydrogen when compared to the no metals addition case. Since hydrogenation of CO_2 is one of the reactions happening in this kind of process, which is an exothermic reaction, and thus higher pressure is preferred in order to shift the reaction equilibrium toward the products side, i.e. to the side with lower number of moles of gas phase product according to Le Chatelier's principle. Furthermore, this is a hydrogenation process, and more hydrogen is needed for it to improve more.

On the other hand, in non-metal reductants, organic compounds, such as glucose, decompose into smaller compounds, and the formed compounds from the decomposition of glucose oxidized into other compounds, aldehydes to carboxylic acids an example of this, and thus during this

complicated process, hydrogen or equivalent reductants are produced which can then reduce the CO_2 into formic acid.

The hydrothermal process of converting CO_2 into formic acid has been reported by many researchers. Based on the literature, the types of work reported can be classified based on the used reductants into metals and non-metals reductants. Thus, sections 2.4.1 and 2.4.2 discuss further details about the reported studies.

2.4.1. Metal reductants

Metals have been used in the hydrothermal conversion of CO_2 into formic acid. Iron, Fe, [9], [94]–[99] zinc, Zn, [14]–[16], [98], [100], [101] aluminum, Al,[98], [102], [103] and manganese, Mn[98], [104] are examples of the used metals in such processes. It is also worth noting that in some cases, metal catalysts are used in conjunction with metal reductants.

I) Iron, Fe

Iron, Fe, has been studied in the literature for the conversion of CO_2 into formic acid under hydrothermal conditions. , [9], [94]–[99] Fe alone or in the presence of metal catalysts has been investigated at different conditions to study the formic acid production. First, the studies in which Fe powder as a reductant without any addition of metal catalysts are to be presented. The idea of metals addition generally is that the metal will oxidized throughout the reaction and thus H_2 gas will be produced which will eventually improve the production of formic acid. The variance in the reported yield data shows the importance of the reaction parameters such as reaction temperature, reaction time, filling volume, as well as the ratio of the starting materials. For instance, 35 % formic acid yield was reported when Fe as a metal reductant was used.[97] Additionally, 60%[96], 85%[9], and 90%[9] formic acid yields were also reported when Fe was used as a reducing agent.

For example, when the reaction temperature was reduced from 350 ºC [97] to 300 ºC [96], the reaction time extended to 120 minutes instead of 10 minutes, and the filling volume increased from 35 to 60 %, the yield of formic acid was shown to jump from 35 to 60 %. [96], [97] Increasing the reaction time improves the Fe oxidation and thus more H_2 gas is produced. Additionally, higher filling volume means higher pressure inside the system and thus favorable CO_2 hydrogenation into formic acid as the product side does not have gas phase compounds. [96] Moreover, increasing the

ratio of the starting materials was shown to impact the yield of formic acid where 6:16 to 2:24 variation in the $NaHCO_3$: Fe was shown to improve the yield of formic acid from 85 to 90 %. [9]

Nickel, Ni[9], [94], and copper, Cu [99][9] were the metal catalysts used in the literature along with Fe reductant for the production of formic acid under hydrothermal conversion of CO_2. The addition of Ni was shown to have no improvement on the production of formic acid as it was reported that the yield of formic acid when Ni was used with Fe to be 16 % only.[9], [94] The addition of Ni decreases the yield of formic acid as the yield was reported to be 60 % when no Ni was used.[96] Nevertheless, Ni could improve the yield of formic acid to 41 % if the proportions of the initial materials increased to 20:20:120 (mmol) of $NaHCO_3$:Fe:Ni.[105] The addition of Cu to Fe results in 60 % yield of formic acid at 300 ºC, 120 minutes, 55 % filling volume and 1:6:6 ratio of $NaHCO_3$:Fe:Cu.[9], [99]

II) Zinc, Zn

Zinc, Zn, is another metal that has been used in the literature for the production of formic acid from the conversion of CO_2 under hydrothermal conditions. [14]–[16], [98], [100], [101] Zn shows better performance when compared to Fe in terms of formic acid yield. For instance, the yield of formic acid was reported to be 78 % when only Zn was used at 300 ºC, 120 minutes, and 35 % filling volume.[14], [15] The better performance of Zn when compared to Fe, at the same conditions, can be attributed to the rapid oxidation of Zn into ZnO which took place in short reaction time of reaction time as short as 5 minutes.[15] Zn outperform Fe in oxidation due to reactivity of the metal as well as the standard reduction protentional. [106]

Additionally, the ratio of the CO_2 source to metal reductant is different in the Zn studies where it was reported to be 1:10 (mmol) $NaHCO_3$:Zn.[14], [15] Furthermore, the formation of Zn-H intermediate, confirmed by FT-IR, is believed to support and enhance the production of formic acid by providing hydrogen.[15] Similar to the Fe case, Zn was also tested in presence of metal catalysts to investigate the yield of formic acid. Ni catalyst has been reported in the literature with Zn metal as a reductant. At a lower temperature of 225 ºC and 2 h reaction time, the addition of Ni catalyst was shown to outperform the case in which no Ni was added by increasing formic acid yield to about 75% compared to 40%.[101] It also worth noting that the ratio of $NaHCO_3$:Zn in Ni addition studies was 1:6 (mmol).[101] Therefore, addition of Ni catalyst is beneficial as the

production of formic acid made possible at lower reaction temperature of 225 ºC.[101] The water filling volume was shown to influence the production of formic acid, more filling volume leads to higher autogenerated pressure, as suggested by many studies[9], [96], [99], however, when Zn alone and Zn and Ni as a catalyst were investigated, the water filling was not investigated and rather it was fixed at 35% and 60% respectively.[14], [15], [101] Additionally, 80% formate yield at an initial Zn of 8 mmol:1 mmol $NaHCO_3$ was achieved, however, the effect of altering the Ni amount while keeping the optimal values of $NaHCO_3$ at 1 mmol and Zn at 8 mmol has not investigated.[101]

III) Aluminum, Al

Aluminium, Al, is another metal reductant reported for the hydrothermal hydrogenation of CO_2 into formic acid. [98], [102], [103] Al was studied in the presence and in the absence of catalysts. First, Al performance as a reductant without any addition of catalyst stands somewhere between Fe and Zn. For example, 64% of formic acid yield was reported without any addition of catalyst at 300 ℃, 2 h, 35% water filling volume, and 1:6 $NaHCO_3$:Al.[102] Different metal catalysts have been investigated for the formic acid production in the presence of Al. Pd/C is one of the tested catalyst when employed at the same conditions, as that in the absence of a catalyst, vide supra, it was shown that the yield of formic acid improves to 72%.[77] When compare both cases of Pd/C addition and only Al metal at 300 ºC and 2 h, formic acid was shown to yield by 60% in the absence of Pd/C, however, introducing Pd/C resulted in the formation of acetic acid, CH_3COOH, as a byproduct while only slightly affecting the yield of formic acid, 70% formic acid yield for 0.5 g of Pd/C versus 60% formic acid yield without Pd/C.[77] Another study reported that using copper, Cu, as a catalyst gives a formate yield of 70% at 350 ℃, 2 h, 50% filling water, and 40:40:50 mmol initial reactants ratio.[107]

IV) Manganese, Mn

Manganese, Mn, as an alternative reducing agent was investigated. [98], [104] A yield of 76% was at 325 ℃, 1 h, 55% filling volume of water, 1:8 $NaHCO_3$:Mn.[104] However, the effect of introducing a catalyst to the process in the presence of Mn as a reducing agent has not been reported yet, and this could be a venue to explore whether or not the formic acid yield can be improved.

Table 1 shows a comparison of different reductant metals used for the formic acid production under hydrothermal conditions form the conversion of CO_2. The results collected in the table were picked based on conditions similarity as possible. Note that in Zn cases, there is no studied in which water filling volume was probed at the same other reaction conditions in the presence of catalysts. Observing the results listed in table .1, formic acid is best produced using Zn metal alone without any addition of metal catalysts.

Table 1: Summary of metal reductants and catalysts used for formic acid production

Reductant	**Catalyst**	**FA yield (%)**	**Reaction T (°C)**	**Reaction t (min)**	**Water filling (%)**	**$NaHCO_3$:reductant: catalyst (mmol)**	**Reference**
Fe	N/A	10.5	300	120	35	1:6:0	[99]
Fe	Ni	16	300	120	35	1:6:6	[94]
Fe	Cu	37	300	120	35	1:6:6	[9]
Zn	N/A	78	300	120	35	1:6:0	[101]
Zn	Ni	58	300	120	60	1:6:4	[101]
Al	N/A	64	300	120	35	1:6:0	[102]
Al	Pd/C	72	300	120	35	1:6:0.051	[77]
Mn	N/A	36	300	120	35	1:6:0	[104]

1 catalyst weight is 0.05 g

2.4.2. Non-metals reductants

Organic compounds can also act as reductants. There is a variety of organic compounds options such as glycerin[108], isopropanol[109], glucose[17][110][111], and others[112]. Being inexpensive, available, and green choice, biomass, along with CO_2, is another reductant option to produce formic acid under hydrothermal conditions.[17] In the process of formic acid production hydrothermally, both CO_2 and biomass react to produce formic acid.

Glycerin, which is produced from the transesterification of animal fats or vegetable was used as a reductant for the hydrothermal conversion of CO_2 into formic acid.[108] 90% formate yield was achieved using glycerin as a reductant and $NaHCO_3$ as a the CO_2 source at 300 ℃ and 90 minutes and water filling of 70%.[113] Additionally, methanol was studied as a reductant of $NaHCO_3$ into formate and it was shown to have insignificant production in the absence of catalyst, however, 68% formate yield was shown in the presence of Pd-Cu/C catalyst at 180 ℃ 16 h and 50% water filling.[114] Isopropanol, on the other hand, has been probed as a reductant and it was shown to have about 55% formate yield at 300 ℃ and 120 minutes and 70% water filling.[109] Furthermore, 2-pyrrolidone was probed as a reductant of $NaHCO_3$ into formate and it was shown to have the highest yield of formate at 350 ℃, 150 minutes, and 50% water filling.[112]

Glucose is another non-metal organic options which has been studied as a reducing agent in the hydrothermal process of CO_2 conversion into formic acid. Esposito and Antonietti reported the yields of lactic acid, 25%, formic acid, 5%, and acetic acid, 3% from glucose under hydrothermal using different bases at 220 ℃ for 120 s reaction time.[110] Among other biomasses, Fernández et al. 2018 investigated the reduction of CO_2 using $NaHCO_3$ as a CO_2 source and glucose into formic acid, at 300 ℃ and 180 minutes, and formic acid yield was 65%.[17]

Glucose was also probed in the presence of metal catalysts for formic acid production. Chinchilla et al. 2022 studied the impact of using different catalysts on the yield of formic acid from the hydrothermal hydrogenation of CO_2 with glucose at different reaction times and temperatures.[111] It was found that activated carbon as a catalyst showed the highest yield of 53% formic acid at 200 ℃ and 30 minutes whereas at higher temperature, 250 ℃, iron oxide, Fe_3O_4, was shown to have the best formic acid yield of 52%.[111] Konstantinova also investigated glucose as a biomass model for the process of hydrothermal CO_2 reduction with and without metal

catalysts.[115] Konstantinova concluded that using Ni as a metal bulk catalyst improved the concentration of formic acid by 150 % compared to the uncatalyzed case.[115]

It is important to stress that there is a significant difference between Fernández et al. 2018, Chinchilla et al. 2022, and Konstantinova 2022 studies in terms of formic acid origin. The difference is on the method used to trace the source of formic acid, and thus yield calculations. In other words, there are two sources of carbon in starting materials, CO_2 and glucose. For instance, Fernández et al. 2018 traced the source of the formed formic acid by altering the pH of the starting medium using base like NaOH to mimic the initial case where $NaHCO_3$ was used. Thus, the effect of alkaline medium on the reaction of $NaHCO_3$ and glucose into formic acid was probed, and it was concluded that formation of formic acid actually originated from the reduction of $NaHCO_3$.[17] On the other hand, Chinchilla et al. 2022 used another approach of tracing the source of formic acid by employing labelled agents. Furthermore, the source of formic acid when glucose was used as a reducing agent was 35% from reduction of $NaHCO_3$.[111] Konstantinova 2022 determined that the majority of the formed formic acid, 95%, comes from glucose decomposition rather than $NaHCO_3$ reduction based on the results from labelling studies. [115]

Glucose is non-toxic, and it can be obtained from sustainable sources. One downside of using glucose, however, is the formation of additional compounds beside the target one, formic acid. In fact, under hydrothermal conditions, and as the reaction temperature increases, the glucose decomposes based on the nature of the medium. Therefore, there will be two main possible reactions in the process of CO_2 conversion into formic acid under hydrothermal process using glucose as a reductant. The two main possible reactions in such a process are i) the hydrogenation or the conversion of CO_2 into formic acid, and ii) the degradation of glucose. The former process is straightforward; however, the latter is rather complex. The glucose could either be oxidized or the formed products form the glucose degradation oxidized into new products. After observing studies where glucose was used as a reductant for the CO_2 conversion into formic acid under hydrothermal conditions, besides formic, acetic, and lactic acids and a few others such as aldehydes, e.g. glyceraldehyde and pyruvaldehyde, and acids, e.g. propanoic acid, no more products were reported or investigated. Additionally, since the decomposition of glucose is expected to introduce more compounds, the new formed compounds could be even more valuable

than the target compound itself, therefore, it is of great interest to know the formed products, beside formic acid.

I) Glucose decomposition

Glucose decomposition has been investigated in literature at different conditions. A glucose molecule has 6 carbon atoms, the route to which glucose decomposes is affected by various variables, one of the main variables is the medium pH. [116]–[118] Kabyemela et al. 1999 presented glucose decomposition pathway where glucose can be isomerized into fructose which can yield products like acids or 5-HMF.[117] It can also decompose into one C_4 and one C_2 molecules, erythrose and glycolaldehyde which could further decompose or react to produce liquid products. Furthermore, glucose could produce acids via 1,6-anhydroglucose which are formed from glucose dehydration. Additionally, glucose can also decompose into two C_3 molecules, dihydroxyacetone and glyceraldehyde, both further produce liquid products via pyruvaldehyde as an intermediate. [117] Illustration of glucose decomposition is shown in scheme 1.

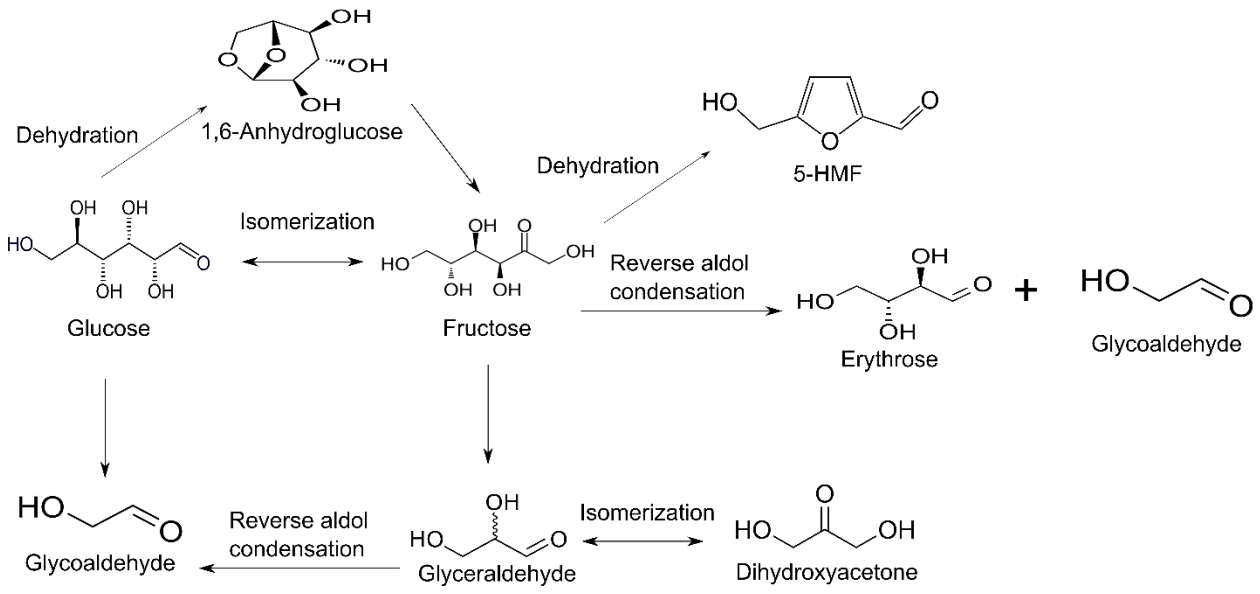

Scheme 1: Glucose decomposition pathway

Holgate 1993 studied both oxidation and hydrolysis of glucose at 500 ºC and 6 s reaction time aiming to identify the formed products from each process using HPLC.[119] Holgate 1993

reported various compounds formed from each process including carboxylic acids such as formic, acetic, and propanoic acids as well as ketones and aldehydes.[119] In addition, Esposito and Antonietti reported the formation carboxylic acids such as lactic, formic acetic acids from glucose under hydrothermal conditions.[110] Moreover, in addition to formic acid, acetic acid, lactic acid, glycoaldehyde, ethanol were also reported as byproducts form the hydrothermal conversion of CO_2 .[17] Formic, lactic, and acetic acids were also reported as products form the hydrothermal reduction of CO_2 using glucose as a reducing agent.[111] Konstantinova reported the formation of different carboxylic acids from the glucose and $NaHCO_3$ reduction under hydrothermal conditions. [115]

It is important to distinguish between metal reductants and catalysts. The main difference between metal reductants and catalysts is that metal reductants undergo oxidation and thus their final state is not the same as their initial state as metal oxide is the final product which is exactly the opposite of catalysts. The catalysts on the other hand participate in the reaction, however, they do not consume or converted in other products. Nevertheless, when metal reductants are used in hydrothermal processes, they produce metal oxide which is a catalyst giving the usage of metal reductants an advantage by playing two roles of reductants and catalysts.

Fernandez et al. reported that glucose outperforms other tested organic reductants as it reported to have a formic acid yield of 65%.[17] However, the byproducts compounds form glucose might be the reason why organic reductants are not as effective as the metal reductants. Therefore, finding a way to increase the selectivity toward formic acid while decreasing the formation of other compounds has not been reported in the literature yet. Although some of the formed compounds formed from the CO_2 conversion to formic acid under hydrothermal conditions using glucose as a reductant were reported, a complete carbon balance, identification, and quantification of all of the formed products in the liquid phase have not been reported. Therefore, it is of significant importance that the entered amount of carbon as well as the outlet or produced compounds are known in order to better understand the reaction and thus build a kinetic model in the future. Thus, part of this work herein will be endeavors to identify the formed products at different conditions and quantify them as well. Furthermore, metals reductants were shown to greatly produce formic acid under hydrothermal conditions.[9], [94]–[99], [14]–[16], [98], [100], [101], [98], [102], [103] Glucose and metal catalysts were also reported to improve the production of formic

acid.[111] Nevertheless, the best tested reductant metals in the literature for formic acid production form the conversion of CO_2 under hydrothermal conditions, Fe, Z, and Al, have not been investigated with glucose. The addition of metal reductants to glucose for the CO_2 reduction under hydrothermal conditions should increase the selectivity toward formic acid as both reductants can reduce CO_2 into formic acid which in turn should reduce the production of the byproduct form glucose decomposition. Therefore, this study includes the impact of metals addition, namely Fe, Zn, and Al, on the production of formic acid along with glucose as a biomass reductant.

Chapter 3: Methodology

3.1. Method

All of the reactions in this work were carried out in a 100-ml EZE-Seal reactor (Parker Autoclave Engineers, USA). There are three tubes connected to the reactor, two for the gas inlet and outlet as well as a liquid sampling line. The vessel of the reactor is also connected to an agitator which its chamber cooled by circulating water. The system is also equipped with a pressure gauge to monitor the pressure of the process throughout the reaction. A ceramic heating band is used to heat up the reactor. Both agitation speed and process temperature are controlled by a universal reactor controller, URC. More detailed information of the setup is presented in figure 1.

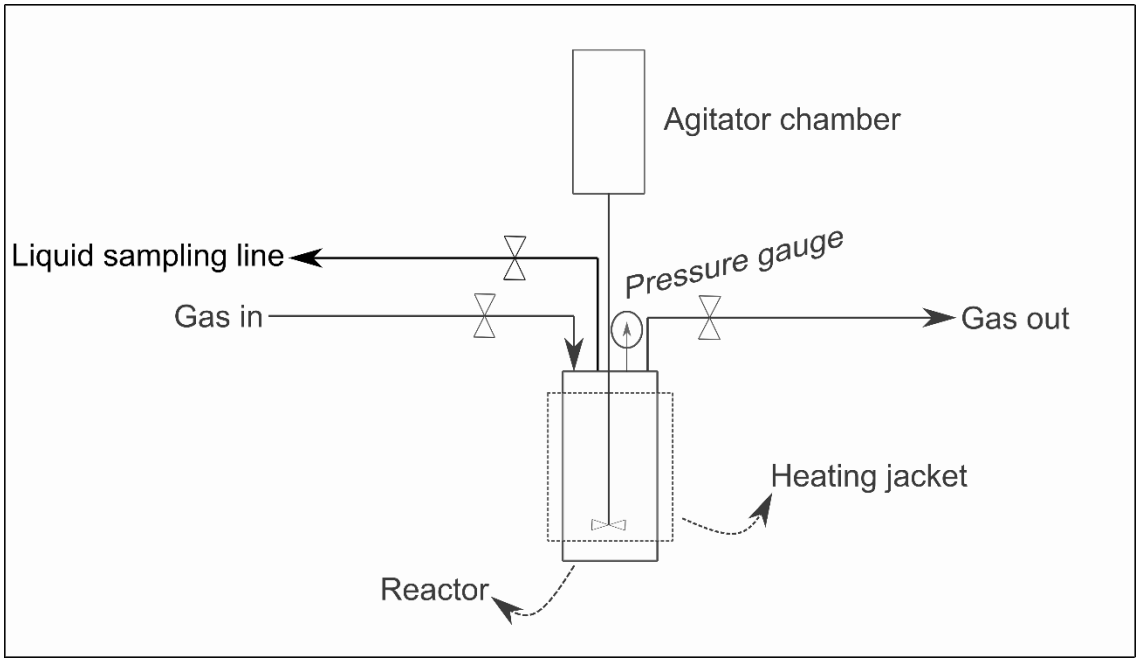

Figure 1: Reactor setup

3.2.1. Materials

Selecting the right form of CO_2 matters for the production of formic acid. In aqueous medium, CO_2 can exist in different forms based on the pH of the medium as illustrated in figure 2.

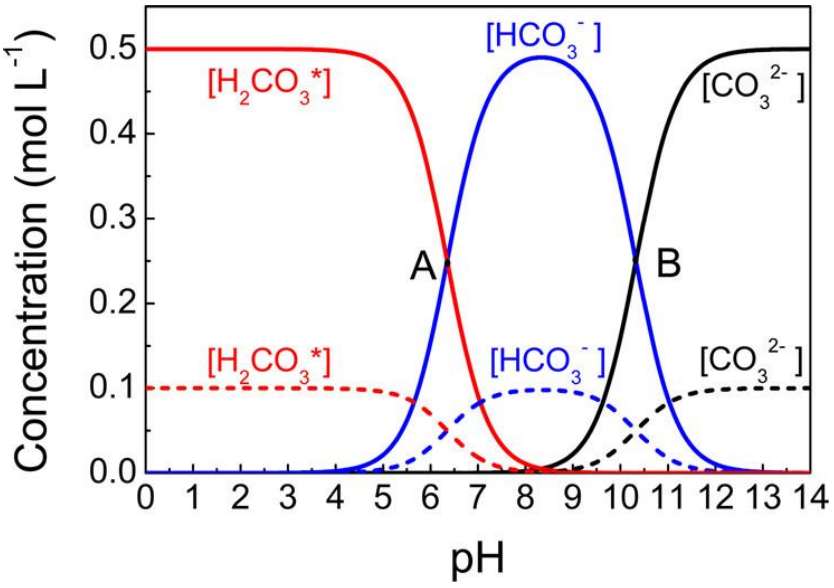

Figure 2: Form of CO_2 at different pH, reprinted with permission from (J. Phys. Chem. C 2015, 119, 1, 55-61)[1] Copyright (2024) American Chemical Society

As in figure 2, depending on the concentration, CO_2 can be in different forms at different pH values. For example, in acidic conditions, pH<5, CO_2 exists in the form of carbonic acid, H_2CO_3. Moreover, in a mild alkaline environment, pH between 8-10, CO_2 exists in the form of bicarbonate ions, HCO^-_3. Furthermore, at strong alkalinity conditions, pH>10, CO_2 exists in the form of carbonate ions, CO^-_3. Therefore, it is critical to know which form of CO_2 is best for formic acid production and thus maintain the relevant pH of the medium accordingly.

Since a mild basic medium, around pH of 8 [120], [121], was shown to be the best for formic acid production, and as the output of CO_2 capturing process of using NaOH is $NaHCO_3$, bicarbonate, HCO^-_3, provides the requirements as shown figure 2. [122][120], [121] In fact, in addition to being convenient when preparing the starting materials, using $NaHCO_3$ serves both purposes of i) providing CO_2 as well as ii) creating alkaline environment for better production of formic acid. Therefore, $NaHCO_3$ was the source of CO_2 in this work.

Table 2 lists the used materials in this work for reactions

Table 2: List of used materials for reactions

No.	**Name**	**Provider**	**Notes**
1	Ar gas	BOC	99.998% purity rating
2	Aluminum	Thermo Scientific Chemicals	-325 mesh (~ 44 μm), 99.5% (metals basis)
3	Deionized water	Purite	18.2MΩ.cm (Type-I)
4	D-(+)-Glucose	Sigma-Aldrich	≥99.5% (GC)
5	Iron	Sigma-Aldrich	≥99%, reduced, powder (~ 45 μm)
6	Sodium bicarbonate	Thermo Scientific Chemicals	99+%, Extra Pure
7	Sodium bicarbonate (^{13}C)	Sigma-Aldrich	98 atom % ^{13}C, 99% (CP)
8	Sodium Hydroxide	Thermo Scientific Chemicals	98%, extra pure, pellets
9	Zinc	Sigma-Aldrich	dust, <10 μm, ≥98%

The materials used for mobile phase of the HPLC, and for the preparation of standards are shown in table 3.

Table 3: List of used materials for analysis

No.	Name	Provider	Notes
1	Acetic acid	Fisher Scientific Chemicals	≥99%
2	Formic acid	Sigma-Aldrich	98-100%
3	Lactic acid	Sigma-Aldrich	≥85%
4	Oxalic acid	Fisher Scientific Chemicals	98%
5	Propanoic acid	Sigma Aldrich	≥99%
6	Sulfuric acid	Sigma-Aldrich	95-98%

3.2.2. Preparation of reactions

In all of the conducted experiments except for kinetic studies and volume change impact studies, 50 ml solution of 0.5 M $NaHCO_3$ and 0.05 M $C_6H_{12}O_6$ was prepared, see table 4 for exact quantities, well mixed, and its pH measured using a calibrated pH meter, 8100 Plus pH meter by ETI, then charged to the reactor vessel.

Table 4: Quantities of the materials used in grams

Experiment	**$NaHCO_3$ (g)**	**$C_6H_{12}O_6$ (g)**	**Fe (g)**	**Zn (g)**	**Al (g)**
No metal used, all at 50% filling volume experiments	2.1	0.45	0	0	0
Metals addition experiments	2.1	0.45	8.4	9.8	4.05

The reason for choosing 0.5 M and 0.05 M for $NaHCO_3$ and $C_6H_{12}O_6$ was to align with previous studies where 1:10 ratio of $NaHCO_3$: $C_6H_{12}O_6$ was suggested.[17], [115] Moreover, Konstantinova tested different initial concentrations of $NaHCO_3$ and it was shown that increasing the initial concentration of $NaHCO_3$ from 0.5 to 2 M resulted in slight increase in formic acid production Additionally, increasing the initial concentration of glucose beyond 0.05 M was shown to be not beneficial for the production of formic acid in similar study.[123] Furthermore, Konstantinova reported that increasing the initial concentration of glucose to 0.1 M resulted in char formation which was not only unbeneficial but also added challenges to cleaning after the reaction.[115]

For kinetic studies, there are three sets of initial concentrations 50 ml solutions which were 0.8 and 0.05, 0.5 and 0.05, and 0.5 and 0.1 M of $NaHCO_3$ and $C_6H_{12}O_6$ respectively prepared, well mixed, and charged to the vessel.

For the filling volume varying studies, 30- and 70-ml solutions of 0.5 M $NaHCO_3$ and 0.05 M $C_6H_{12}O_6$ were prepared, well mixed, and charged to the vessel.

The vessel is then attached to the stand of the reactor and secured. The level of the system is then checked and fixed as needed. Next, the system is purged, to expel any air inside the vessel, and then pressurized with inert gas, Ar or He, for 10 min to make sure there is no leak by monitoring the pressure. The heater is then attached to the vessel and secured. The reaction parameters are then entered via PID controller before starting the process. In all of the experiments, the agitator

speed was set to 500 rpm to ensure similar conditions across the experiments including the metals addition although the impact of the agitation was reported to be insignificant, less than 2% increase in formic acid concentration with agitation versus no agitation case, on the 0.5 M and 0.05 M studies as reported by Konstantinova due to low concentration of glucose, 0.05 M in the starting materials. [115] The parameters of all of the studies experiments are presented in table 5.

Table 5: Control parameters of all of the experiments conducted in this work

Study	**T (ºC)**	**t (h)**	**Filling volumes (ml)**	**Speed of agitator (rpm)**
1	200	1, 2, and 3	50	500
2	250	1, 2, and 3	50	500
3	300	1, 2, and 3	50	500
4	250	2	30	500
5	250	2	70	500

3.2.3. After the reaction

Once the reaction is over, the heating and agitation are stopped, and an ice-water container is used to immerse the vessel and thus quench the reaction. Once the process temperature reaches a temperature of 25 ºC. The gas phase products are released into a sampling bag or directed to analysis. The vessel is then detached and the liquid and solid, if any, are collected.

The pH of the liquid solution was measured using a calibrated pH meter, 8100 Plus pH meter by ETI. The liquid phase products were filtered through 0.2 µm syringe filter and then kept at 5 ºC for analysis. The solid phase residuals, if any, are filtered from the liquid phase medium using a

vacuum filtration. The residues are then washed with deionized water and dried in an isothermal oven overnight at 80 ºC then stored in glass vials for analysis.

3.3. Analysis techniques

Samples collected from reactions in this work are best classified by their phases. Gas, liquid, and solid samples are collected and therefore each of them analyzed separately.

3.3.1. Gas phase samples

The constituent of the formed compounds in the gas-phased was investigated using mass spectrometer, MS. Hiden HPR-20 EGA gas analysis by Hiden analytical was used for the identification of the gas phase products. The gas-phase content in the reactor was released directly to the MS unit via a three-way valve connection between the reactor gas outlet line and the MS unit inlet line. The MS inlet line has a capillary column, Quartz Inert Capillary, QIC, with a heater to avoid condensation. The inlet of the MS unit temperature was set to about 80-90 ºC. The electron-energy was set to 70 V, and the emission was set to 200 µA.

3.3.2. Liquid phase samples

The liquid samples in this work were mainly analyzed by high performance liquid chromatography, HPLC, gas chromatography coupled with a mass spectrometer, GC-MS, and nuclear magnetic resonance, NMR, spectroscopy to identify the formed compounds and quantify the identified by HPLC with UV-Vis and RI detectors.

HPLC-UV-Vis was used for qualification and quantification for all of the carboxylic acids and ketones whereas HPLC-RID was used for qualification of alcohols and qualification and quantification of sugars and bicarbonate, see the appendix for calibration curves. For liquid phase samples analyzed by HPLC, 0.2 µm syringe filter was used and 20 µL volume of the filtrate of each sample was directly injected to HPLC. HPLC analysis was conducted by using ECO 2080 HPLC by ECOM (Czech Republic). The apparatus is equipped with ECP 2010 pump, ECDA2800 ultraviolet-visible, photo diode array, UV-Vis PDA detector and RI2000 Refractive Index Detector in a sequence. MetaCarb 87H column by Agilent Technologies, USA (300×7.8 mm) connected to a MetaCarb 87H (50×4.6 mm) guard column by the same manufacturer. The output data of the

system were monitored and analyzed by Clarity software DataApex, Czech Republic. The mobile phase used for this purpose was diluted sulfuric acid, H_2SO4, 0.005 M at a flow rate of 0.6 ml/min. The oven temperature was 60 ℃ and the temperature of the detector was set at 30 ℃. The wavelength of the UV detector was set at 210 nm whereas the PDA was set to cover the ultraviolet-visible region, UV-Vis, from 200-800 nm. The UV-Vis detector was mainly used for all of the formed products except alcohols, sugars, and bicarbonates where RID was used for analysis. The detection limit of UV-Vis and RID were reported to be 1 pg – 1 ng and 10 ng – 1 µg respectively. [124] For the used UV-Vis detector, the noise level at 254 nm is ± 0.5×10-6 Au whereas the used RID's noise level is ±3 nano refractive index unit, nRIU as per manufacturer manual.

For GC-MS, 0.4 ml of each liquid sample was dissolved in methanol and final volume of 2 ml solution vial is used for GC-MS analysis. Shimadzu 2010 GC coupled with a QP2010 SE mass spectrometer, and an autosampler, AOC 20i, by Shimadzu, Japan, was used in this work for liquid samples. The carrier gas used was H_2 generated by a hydrogen generator, of purity >99.9995% by Parker. The injection port temperature was set to 250 ºC and the ionization source temperature was set to 200 ºC. The interface temperature, between the GC and the MS, was maintained to be 5 ºC higher than the program final temperature to avoid condensation. The column was used for GC-MS was HP-INNOWax with stationary phase of polyethylene glycol, 30 m × 0.25 mm and 0.2 µm film thickness by Agilent technologies, USA. The temperature program used was 40 ºC for a minute, then 200 ºC at 15 ºC/min for 7 minutes, then to 250 ºC at 15 ºC/min.

For NMR, the samples were analyzed using standard ^{1}H NMR, ^{1}H NMR with solvent suppression, and two ^{13}C NMR methods: CPD (normal ^{13}C spectrum) and DEPTQ. The DEPTQ method distinguishes carbons by the number of attached hydrogens, where CH and CH_3 peaks are phased up, while CH_2 and quaternary carbons are phased down. Additionally, a 2D NMR analysis was performed on one sample. The solvent used for the sample was D_2O. The NMR analysis was carried out by Dr. Khalid Doudin from the Chemistry Department at the University of Sheffield. Nuclear magnetic resonance (NMR): ^{1}H NMR spectra were recorded on Bruker Avance AVIII 400 MHz NMR spectrometers equipped with a 5mm solution state BBO probe with Z-gradient, the temperature was regulated at 25 ˚C and no spinning was applied to the NMR tube. Standard ^{1}H experiments were measured at 400.13 MHz using a 30° pulse for excitation, 64 k acquisition points over a spectral width of 20 ppm with 64 transients and a relaxation delay of 2 s. Chemical

shifts are given in ppm with respect to tetramethylsilane using the NMR solvent used as internal standards. Solvent suppression ^{1}H experiments were measured at 400.13 MHz using noesygppr1d pulse program for excitation, 64 k acquisition points over a spectral width of 20 ppm with 64 transients and a relaxation delay of 2 s. Chemical shifts are given in ppm with respect to tetramethylsilane using the NMR solvent used as internal standards.

3.3.3. Solid phase samples

The collected solid samples were primarily scanned by X-ray diffractometer, XRD, and Fourier transform infrared, FT-IR, spectrometer.

The solid content of the products was filtered by vacuum, washed with deionized water and dried in an isothermal oven overnight at 80 ºC then stored in glass vials for analysis. The crystalline structure of the collected solid samples were analyzed by XRD to confirm the formation and the type of oxides on the metal surfaces. XRD analysis conducted using XRD PANalytical Aeris. The device was set at a voltage of 40 kV and a tube current of 15 mA. The samples were scanned at 2θ range from 10 ° to 100 ° using nickel-filtered Cu Kα radiation (Kα1 λ = 1.540598 Å, Kα2 λ = 1.544426 Å). Measurements were conducted at 10 minutes scan rotating with reduced fluorescence mode with a step size of 0.02 °.

FTIR was used in this work to scan the collected liquid samples for the sake of identifying the functional group of the unknown compounds present in the collected samples. Additionally, FTIR was used to compare the collected solid samples against their fresh state to investigate any difference by observing binding compounds if any. For the liquid samples, a drop of the required liquid sample was analyzed against pure water spectra as a reference to infer the presence of any functional group of the compounds however, due to low concentration of the samples content, utilizing FTIR was not helpful as it was not able to detect any compounds in the liquid samples. Similarly, the spectra of the fresh solid samples versus the spent ones were about the same suggesting the need to seek other analysis techniques rather than FTIR. The used FT-IR spectrometer was Shimadzu IRAffinity-1S Fourier Transform Infrared Spectrometer, Shimadzu, Japan.

3.3.4. Calculation method

For both reactants, $NaHCO_3$ and $C_6H_{12}O_6$ the conversion was calculated using the following equation

$$Conversion\ (\%) = \frac{C_{initial} - C_{final}}{C_{initial}} \times 100 \qquad \text{E2.1}$$

where $C_{initial}\ and\ C_{final}$ are the molar concentration of each reactant. Note that All of the optimization, pH control, and metals addition reactions were duplicated, and the average values, as in E2.2, as well as the standard deviation, as in E2.3, are depicted in the figures in this work.

The average values were calculated using the following equation

$$Average = \frac{C_1 + C_2}{2} \quad \text{E2.2}$$

where $C_1 and\ C_2$ are concentrations for sample 1 and 2 for each product. Whereas the standard deviation was calculated using the following equation

$$Standard\ deviation = \sqrt{\frac{\sum(C - \bar{C})^2}{n-1}} \quad \text{E2.3}$$

where $C\ and\ \bar{C}$ are concentration of any sample and the average concentration of two samples respectively.

3.3.5. Statistical analysis

All of the concentration results from duplicated experiments for the formed carboxylic acids in the liquid phase samples from all of the different reactions sets were statistically analyzed to check whether or not the change in concentration with each independent variable is significant. The independent variables tested in this work are reaction time, reaction temperature, reactor filling volume, and reductants metals addition. A single factor Analysis of Variance, ANOVA, was carried out using Microsoft Excel for each of the formed products, namely oxalic, lactic, formic, acetic, and propanoic acids. The comparison threshold was set to 5%. The results of the statistical analysis are reported in each relevant chapter throughout the thesis. Furthermore, the detailed results for each compound in each reaction set can be found in the appendix for reference.

Chapter 4: Kinetic Studies and Liquid Phase Products Identifications

4.1. Kinetic studies

Understanding the behavior of a certain reaction requires a knowledge of its kinetics. Therefore, an initial study has been conducted investigating the reaction kinetics for the case of sodium bicarbonate, $NaHCO_3$, and glucose, $C_6H_{12}O_6$. A series of studies were performed to first identify the order of the reaction in both reactants, sodium bicarbonate and glucose. In these sets of studies, the initial concentration of one reactant is kept constant while changing the other, then alternating back by changing the fixed one and keeping the other fixed. Table 6 shows the initial concentration of each set of reactions.

Table 6: Kinetic studies initial concentrations

Set number	**$[NaHCO_3]_o$ (M)**	**$[C_6H_{12}O_6]_o$ (M)**
1	0.8	0.05
2	0.5	0.05
3	0.5	0.1

In these reactions, the temperature was set to 200 ºC, and the reaction time was the heating up period for each set to reach the set point from its initial temperature. Generally, the initial temperature was about 22 or 23 ºC, and the heating rate was kept the same by manipulating the heater setting to set the over vessel heater temperature to 500 ºC. Therefore, the time required for the system to reach the set point of 200 ºC was monitored and recorded to be ~16 minutes. Once the system reached the set point, the heater was turned off and removed to quench the reaction by

immersing the reactor in an ice bath until the temperature of the system returned to 25 ºC. Once the system is cooled, liquid samples are filtered through a 0.2 um syringe filter and kept at 5 ºC for analysis.

The liquid samples were analyzed by HPLC coupled with UV-Vis and refractive index, RI, detectors. The goal here is to measure the concentration of the reactants post the reactions. Since both glucose and bicarbonate poorly absorb UV light, RI detector was used in this case to monitor the concentration of both glucose and bicarbonate.

First of all, calibration curves of both glucose and bicarbonate were obtained from HPLC-RID and are shown in the appendix, figures 45 and 46. The conversion of the reactants, bicarbonate and glucose, after the reaction is presented in figure 3. It is also important to mention that the conversion of glucose is close to 98%, however, the data can still be used to determine the reaction order as long as there is a change of concentration over time.

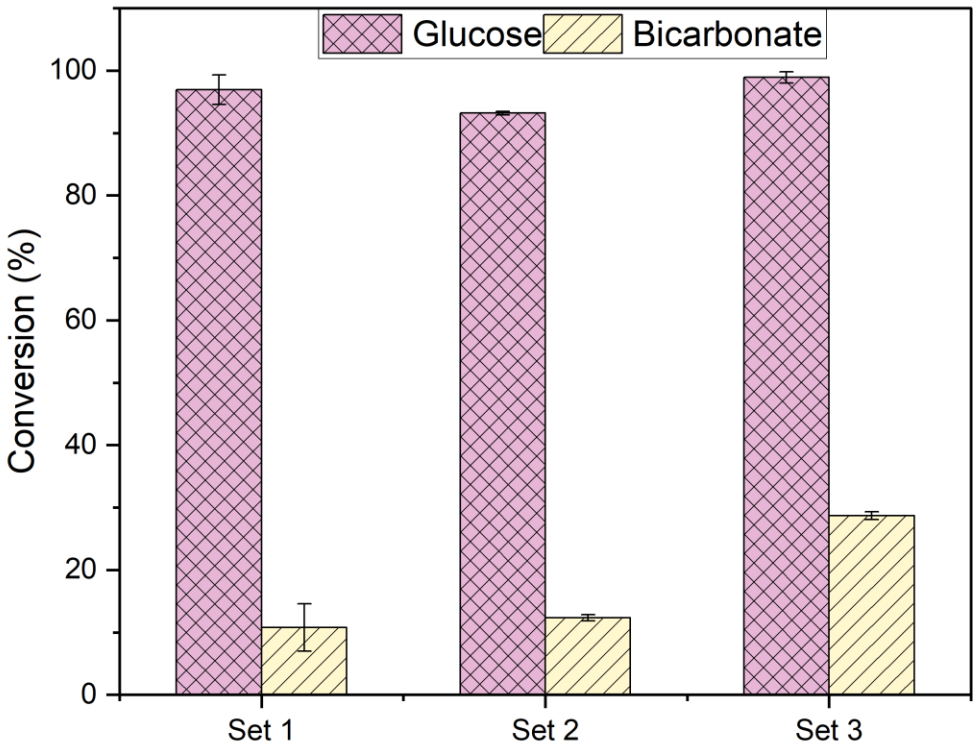

Figure 3: Reactants consumption, set 1: 0.8 & 0.05 M; set 2: 0.5 & 0.05 M; set 3: 0.5 & 0.1 M of sodium bicarbonates and glucose respectively, 200 ºC and 50% filling volume

It is worth considering how much of CO_2 would be in the gas phase during the reaction, to do so, the pressure of the process was monitored throughout the reaction and it was noted that the process pressure was the saturation pressure of water at 200 ºC at about 15.5 barg indicating low concentration of CO_2 was present in gas phase. Therefore, the solubility of CO_2 in the aqueous medium should be investigated at the given conditions. At 200 ºC, the solubility of CO_2 in water is about 0.105 mol/kg.MPa. [125]

In the case where 200 ºC studies were conducted, and knowing that 50 ml of water used in these experiments, and the pressure of the process is the saturation pressure of water at 200 ºC, i.e. 15.55 bar, the maximum solubility of CO_2 in water according to the figure above is 0.105 mol/kg.MPa × (1 kg/1000 g) × (1 MPa/10 bar) = 1.05×10^{-5} mol/g.bar. At the given conditions, (1.05×10^{-5} mol/g.bar * 50 g * 15.55 bar = 1.2×10^{-2} mol of CO_2 is soluble in water. Looking at the amount of CO_2 used up during the reaction at these conditions, 0.0634 M out of 0.5 M was used. In moles, that is 0.0634(mol/L) × 0.05(L) = 0.00317 mol or 3.2×10^{-3} mol. The amount of bicarbonate used at the given conditions is 72% less than the amount CO_2 can be soluble at 200 ºC.

Utilizing the calibration curve figures, the concentration of both reactants post reactions can be calculated, and then the rate can be calculated, at the tested temperature of 200 ºC, using E3.1.

$$Rate = \frac{\Delta C_i}{\Delta t} \quad \text{E3.1}$$

Where ΔC_i is the difference in concentration of a reactant between the initial and final states, and Δt is the period of time recorded from the initial to the final state. The rates of both reactants are presented in table 7.

Table 7: Kinetic studies data

Set number	**[$NaHCO_3$]o (M)**	**[$C_6H_{12}O_6$]o (M)**	**Rate (Ms^{-1}) wrt [HCO_3^-]**	**Rate (Ms^{-1}) wrt [$C_6H_{12}O_6$]**
1	0.8	0.05	8.97×10^{-5}	5.05×10^{-5}
2	0.5	0.05	6.61×10^{-5}	4.86×10^{-5}
3	0.5	0.1	1.49×10^{-4}	1.03×10^{-4}

The reaction order was calculated by utilizing the data from table 5 above and using the following relationships

$$Rate = k\,[HCO_3^-]^n[C_6H_{12}O_6]^m \qquad \text{E3.2}$$

The reaction orders in E3.2, n and m, can be determined by plugging data from table 7 and producing 3 equations as the following

$$5.05\times10^{-5} = k\,[0.8]^n[0.05]^m \qquad \text{E3.2.1}$$

$$4.86\times10^{-5} = k\,[0.5]^n[0.05]^m \qquad \text{E3.2.2}$$

$$1.03\times10^{-4} = k\,[0.5]^n[0.1]^m \qquad \text{E3.2.3}$$

Now, to determine n, divide E3.2.1 by E.3.2.2 to get the following

$$\frac{5.05\times10^{-5}}{4.86\times10^{-5}} = \frac{0.8^n}{0.5^n} \qquad \text{E3.2.4}$$

$$1.04 = (1.6)^n \qquad \text{E3.2.5}$$

Solve for n by taking the natural log,

$$n = \frac{\ln (1.04)}{\ln (1.6)} = 0.08 \qquad \text{E3.2.6}$$

From E3.2.6, n is approximated to be 0, similarly, m can be solved by dividing E3.2.2 by E3.2.3 and following the same procedure to end up with m = 1. In other words, the reaction is of zero order in $NaHCO_3$ and first order in $C_6H_{12}O_6$ which makes the overall reaction order first. Thus, E3.2 can be rewritten as

$$Rate = k\,[\mathrm{C_6H_{12}O_6}] \qquad \text{E3.3}$$

Now, the reaction rate constant, k, can be calculated using any of the data given in table 5 by plugging the relevant rate and glucose concentration. The average value of the reaction rate constant, k, from the available kinetic data is 1.22×10^{-4} s^{-1}.

To confirm the calculated orders of both of the reactants, making use of the collected data at 200 ºC for different reaction times 1, 2, and 3 h is carried out next. If the suggested first order of glucose is correct, then from following this relationship

$$\ln[GL] = \ln [GL]_o - kt \qquad \text{E3.4}$$

plotting the natural logarithm of glucose concentrations versus the relevant reaction time should result in a straight line which slope equals to k, the reaction rate constant. Thus, figure 4 presents a plot of the natural log of glucose concentrations versus the relevant reaction times.

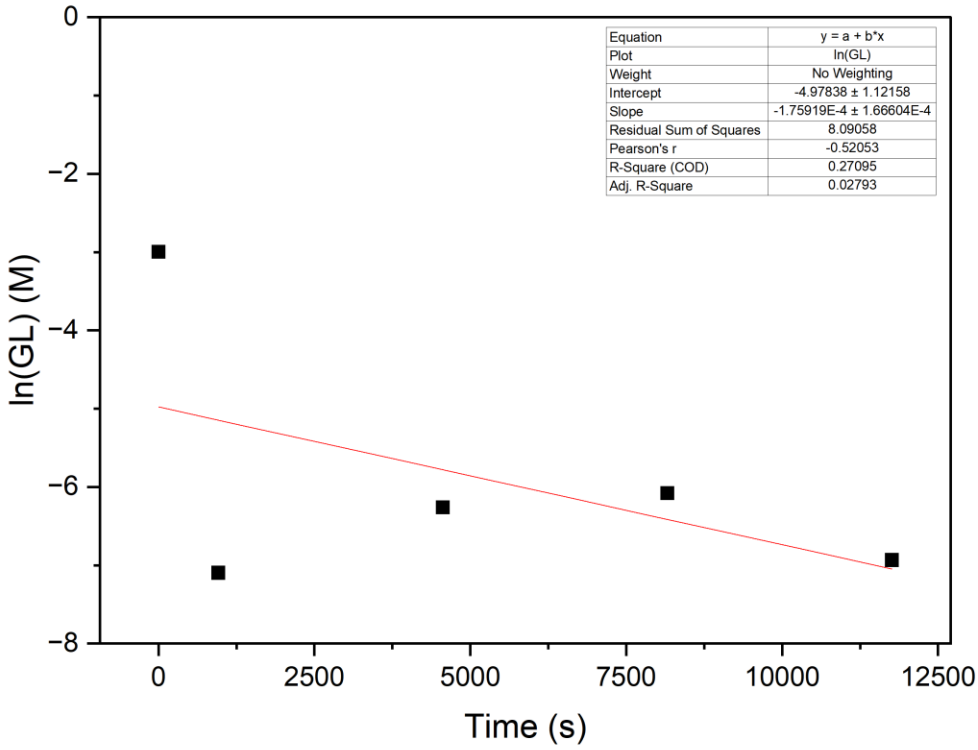

Figure 4: Natural log of glucose concentrations versus reaction times at 200 ºC, 0.5 M $NaHCO_3$ and 0.05 M $C_6H_{12}O_6$ at 50% filling volume

As figure 5 shows, plotting the natural log of glucose concentrations with their relevant reaction times resulted in a straight line with a slope of 1.8×10^{-4} s^{-1}.

4.1.1. Activation energy calculation

Now the order of the reaction is known, as well as the governing reaction rate equation, one can use data from different reaction temperatures to calculate the activation energy of the reaction, that is the energy needed for the reaction to start. To do so, utilizing E3.4 is the start

$$k = A\, e^{-\frac{E_a}{RT}} \quad \text{E3.4}$$

where k is the reaction rate constant, A is the frequency factor, Ea is the activation energy, R is the ideal gas constant, and T is the temperature in Kelvin.

Taking the natural logarithm for E3.4 yields

$$ln\,(k) = -\frac{E_a}{R} \times \frac{1}{T} + ln\,(A) \quad \text{E3.5}$$

From E3.5, one can use the data from different reactions at different temperatures to calculate the reaction rate constant, its natural logarithm, the inverse of the reaction temperature. From these data, plotting the values of the natural logarithm of the reaction rate constant versus the inverse of the temperature in Kelvin would result in a straight line with a slope of $-E_a/R$ as in the equation 3.5.

Table 8 shows the results of the calculated kinetics data at different reaction temperatures and reaction times. 4 reaction temperatures, namely 200, 225, 250, and 300 ºC, were probed at the filling volume of 50% to see the consumption of glucose. The last two columns to the right are the ones which can be plotted against each other in order to obtain the activation energy value.

Table 8: Kinetics data for different reactions wrt glucose, at 1 h reaction time

T (K)	**Rate (Ms^{-1})**	**K (s^{-1})**	**ln(k)**	**1/T**
473.15	1.34×10^{-5}	0.000267	-8.23	0.00211416
498.15	1.32×10^{-5}	0.000263	-8.24	0.00200803
523.15	1.35×10^{-5}	0.000269	-8.22	0.00191205
573.15	1.34×10^{-5}	0.000267	-8.23	0.00174520

From table 8, observing the calculated values for the ln(k) as a function of temperatures, one can see the inconsistent of the readings as the temperature elevated. In other words, ideally, the values of the ln(k) should decline as the temperature increases which is not the case here. It is expected as the temperature, as a single variable, cannot be isolated in this work as the pressure of the whole

system is a temperature-dependent. Furthermore, the reliance on high conversion data of glucose, over 95% conversion, is shown to introduce inaccuracy of the activation energy studies results. Therefore, the calculation of activation energy cannot be carried out in this work at this setup. Nevertheless, a limitation of this work is the inability to isolate reaction temperature as a single variable for kinetics studies and the reliance on high conversion data for glucose has led to obtaining inaccurate activation energy.

The overall reaction order was found to follow first order. The sodium bicarbonate concentration was found to have no impact on the rate equation in this study, i.e. zero order. A similar conclusion was made by Kabyemela et al. 1997 that glucose decomposition under hydrothermal conditions follows first order kinetic.[116] Therefore, this confirms what reported in the literature with the addition knowledge of the role of sodium bicarbonate in this work.

4.2. Identification of products: preliminary study at 250 ºC, 2 h, and 50 % filling volume results

In this work, there are two main reactions expected: i) glucose degradation, and ii) CO_2 hydrogenation. Two preliminary studies were conducted in order to collect liquid samples at the given conditions to probe the formed products. Therefore, the optimized conditions suggested by Konstantinova 2022[115] were considered for this regard. The method and details about the reactions set up as well as the analysis techniques can be found in the method section in chapter 2.

4.2.1. HPLC

The results from the liquid samples analysis using the HPLC can be shown in figure 5

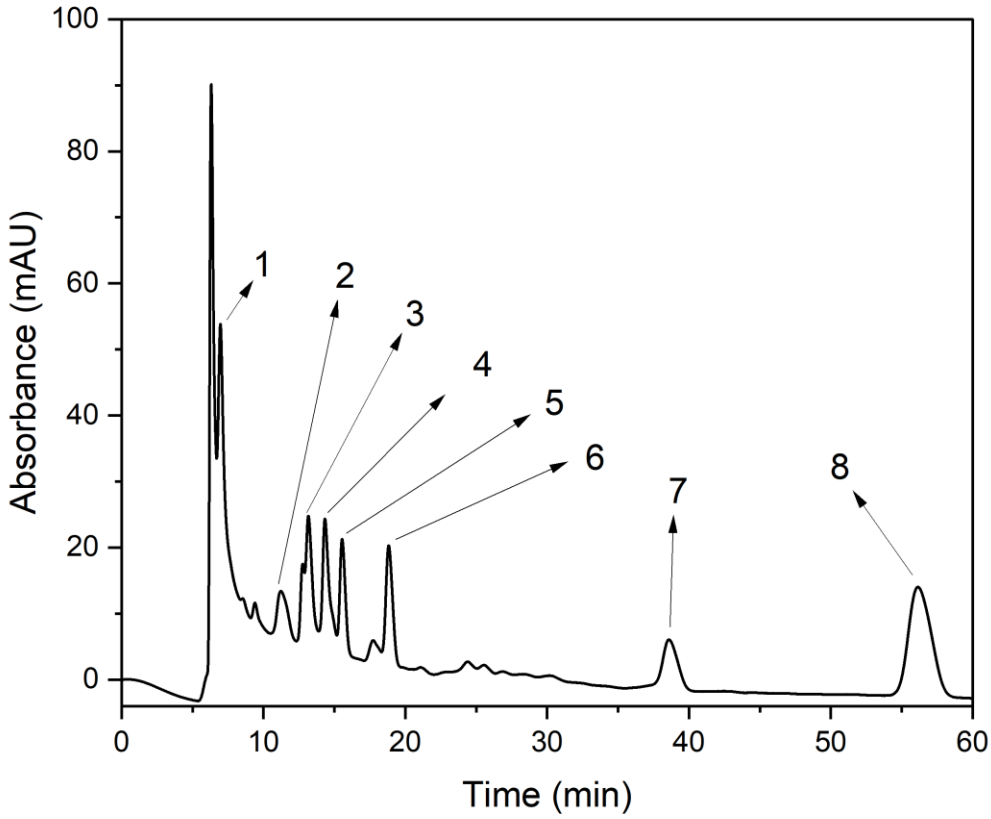

Figure 5: HPLC-UV-Vis chromatogram for 250 ºC - 2 h - 50%, 0.5 M $NaHCO_3$ and 0.05 M $C_6H_{12}O_6$

Figure 5 shows a chromatogram of 250 ºC, 2 h, 50% filling volume sample from HPLC coupled with UV-Vis detector. As shown in figure 5, there are multiple peaks suggesting multiple compounds formed from the reaction. Some of these peaks have already been identified by Konstantinova 2022,[115] however, two remain unidentified.

The aim here is to confirm the already identified products as well as try to find a way to identify the unknown compounds as they could be valuable, and to the best knowledge of the author, there is no similar study which looks at the identification of the formed compounds from the hydrothermal process of CO_2 hydrogenation using glucose as a reductant.

Table 9 shows the confirmed already identified products along with their retention times.

Table 9: Confirmed identified compounds in the liquid samples analyzed by HPLC-UV-Vis for the liquid samples obtained from 250 ºC - 2 h - 50% filling volume, 0.5 M $NaHCO_3$ and 0.05 M $C_6H_{12}O_6$

Peak No.	**Compound**	**Retention time (min)**
1	Oxalic acid	7
3	Lactic acid	13
4	Formic acid	14
5	Acetic acid	15
6	Propanoic acid *	18

The confirmation process of the identified products shown in table 7 was via two steps: the compound must a) match the retention time of an external standard, and b) match the maximum UV absorption, λ_{max}. The reason behind this is that there is a possibility of having different compounds elute at the same retention time and that can be tested by monitoring the λ_{max} as well. Compound number 5 in table 7 was labeled with an asterisk was reported by Konstantinova 2022[115] as acrylic acid which has the chemical formula of $C_3H_4O_2$, however, having an extra double bond should cause a red shift, absorption at a longer wavenumber, in the UV-Vis absorption spectrum to have λ_{max} of more than 205 nm which was not the case when looking at the UV-Vis spectrum of the compound elutes at 18 minutes. Therefore, propanoic acid standard which has an extra 2 hydrogen with the chemical formula of $C_3H_6O_2$ was injected as a standard and it was shown to satisfy the conditions of confirmation listed above.

To account for the formed compounds with appreciable amounts, 200 mAU.s peak area was set as a cutoff, meaning any compound with a peak area of 200 mAU.s and over will be considered for identification purposes. Thus, the peak areas of the compounds shown in the figure of the 250 ºC, 2 h, and 50% filling volume HPLC-UV-Vis chromatogram above with peak area of 200 mAU.s and above are presented in table 10.

Table 10: Formed compounds with their peak areas from HPLC-UV-Vis for the liquid samples obtained from 250 ºC - 2 h - 50% filling volume, 0.5 M $NaHCO_3$ and 0.05 M $C_6H_{12}O_6$

Peak No.	**Retention time (min)**	**Peak area (mAU.s)**	**Assignment**
1	7	541	Oxalic acid
2	11	418	--
3	13	283	Lactic acid
4	14	552	Formic acid
5	15	451	Acetic acid
6	18	627	Propanoic acid
7	38	210	--
8	56	1200	--

As shown in table 8 above, there are 8 major compounds formed from the hydrothermal process of CO_2 with glucose, 5 of them have been successfully confirmed.

Organic acids lactic, oxalic acids were also identified and present in all of the collected liquid samples. All of the aforementioned compounds except for propanoic acid have been reported

previously in similar work conducted by Konstantinova 2022. [115] However, acrylic acid was reported instead of propanoic acid, therefore injection of both compounds to HPLC carried out to ensure which is present in the collected samples of this work, and it was found that both UV-VIS spectrum and the retention time of propanoic acid to match what present in the liquid samples collected in this work. Therefore, propanoic acid is confirmed in the collected liquid samples. Additionally, propanoic acid and acrylic acid have been reported by Holgate 1993 when both oxidation and hydrolysis of glucose were studied at 500 ºC. [119]

Additionally, ketones, namely, acetone is present in some of the liquid samples. Acetone, in minor quantities, along with lactic, acetic, and formic acids, was also reported by Chinchilla et al. 2022 in similar work where glucose was used as s reducing agent for CO_2 reduction to formic acid. [111]

Alcohols, methanol, ethanol, and isopropanol were also detected in some of the liquid samples. Ethanol was mentioned in a study as a by-product from CO_2 reduction to formic acid using glucose.[17]

Revisiting the glucose decomposition scheme 1 in chapter 1, the suggested products to form from the glucose decomposition products are presented in scheme 2.

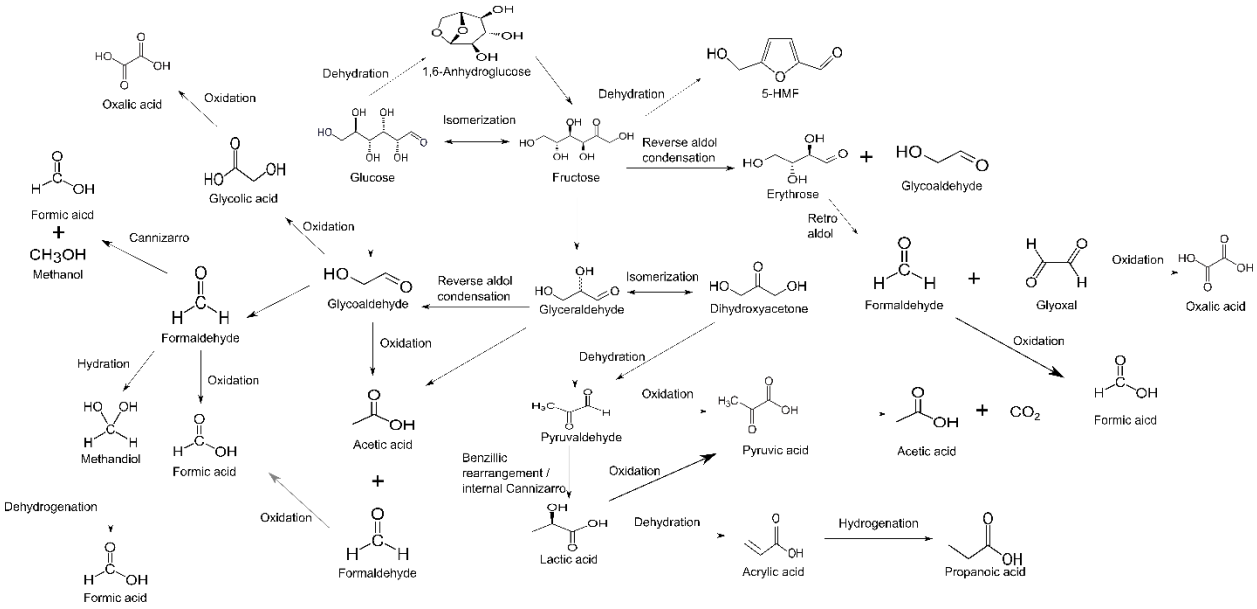

Scheme 2: Suggested pathways for different products from glucose decomposition via various reactions

As in the scheme 2, the formed fructose can either dehydrated into 5-HMF,[111], [117] undergo reverse aldol condensation to produce erythrose, C_4 compound, and glycolaldehyde, C_2 compound, [117], [126] or decompose into C_3 compounds, glyceraldehyde [117], [118], [126]–[128] which can then isomerized into dihydroxyacetone, DHA. [117], [126], [128], [129] The glycolaldehyde formed from the glucose decomposition can be oxidized to acetic acid or decompose into formaldehyde, an intermediate to finally form formic acid by either oxidation [130], hydration into methandiol then dehydrogenation into formic acid, or by internal Cannizzaro to formic acid and methanol.[131]

The products from the reverse aldol condensation of fructose, erythrose and glycolaldehyde, can produce variance of products from different processes such as formic acid via formaldehyde intermediate formed and oxalic acid via glyoxal intermediate both formed by erythrose retro-aldol reaction, or oxidation of glycolaldehyde to acetic acid. Alternatively, the C_3 compounds formed from the fructose decomposition, DHA and glyceraldehyde, can dehydrate to pyruvaldehyde which can then undergo a benzellic rearrangement to lactic acid. [128], [132], [133] Lactic acid can be a precursor to acrylic acid via dehydration.[130], [134] Nevertheless, propanoic acid is possible to form via hydrogenation of acrylic acid.

Balancing the total carbon entering and leaving the reactor is a powerful way to have an insight into the significance of identifying unknown compounds. For example, if the identified compounds contained most of the entered amount of carbon, then there will be no issue of ignoring the other formed compounds as this indicates an insignificant amount of carbon. Therefore, the total amount of carbon entered the system and obtained out of it is to be presented next.

The initial materials which are the source of carbon are $NaHCO_3$ and $C_6H_{12}O_6$. The amount of both reactants for the preliminary study as well as other studies later is 0.5 and 0.05 M of $NaHCO_3$ and $C_6H_{12}O_6$ respectively. Therefore, the total number of carbons at the beginning of the reaction was 25 $\times 10^{-3}$ and 15 $\times 10^{-3}$ moles of carbons from both $NaHCO_3$ and $C_6H_{12}O_6$ were calculated using E3.6 and shown in table 11.

$$Total\ amount\ of\ cabon\ in = 0.025\ mol\ NaHCO_3 \times \frac{1\ mol\ of\ carbon}{1\ mol\ of\ NaHCO_3} + 0.0025\ mol\ C_6H_{12}O_6 \times \frac{6\ mol\ of\ carbon}{1\ mol\ of\ C_6H_{12}O_6} \qquad \text{E.36}$$

Table 11: Moles balance of carbon for the liquid samples analyzed by HPLC and obtained from 250 ºC – 2 h - 50% filling volume, 0.5 M $NaHCO_3$ and 0.05 M $C_6H_{12}O_6$

Total moles of carbon in (mol)	39.88×10^{-3}
Total moles of carbon consumed (mol)	15.82×10^{-3}
Total moles of carbon formed* (mol)	4.96×10^{-3}
Difference (mol)	10.86×10^{-3}

*The moles of carbon formed are calculated from the identified compounds in the liquid phase only.

The total moles of carbon consumed was number of moles of the used glucose and bicarbonate post the reaction calculated by the difference of the initial and final amount of both reactants. Furthermore, the total moles of carbon formed was calculated from the concentration of formic, acetic, oxalic, lactic, and propanoic acids formed at the given conditions.

At the end of the reaction, the consumed carbon, calculated from the initial and final concentrations of both reactants, from both sources was 16 $\times 10^{-3}$ moles which represents about 40% of the entered number of moles of carbon. Furthermore, the total amount of carbon formed from the identified products was about 5 $\times 10^{-3}$ mol which represents only 31% the total consumed carbon. Therefore, identifying the unknown compounds is highly significant as about 70% loss of carbon was calculated. Note that the calculations were made for liquid phase products only.

From here, the journey of further identification search started. Compounds elute at 11, 38, and 56 minutes have bigger peak areas when compared to the identified ones, although peak areas alone are not sufficient evidence of their concentrations, knowing these compounds, they might be more valuable, in terms of cost or the ease of production, than other identified ones, is needed as it is needed for further studies on kinetics and reaction pathways. Note that only 38 and 56 are considered for identification as the peak at 11 has a lower than 200 nm UV absorption which

cannot be detected using the current device. Therefore, an educated systematic procedure is needed for identification if other analysis techniques fail.

Observing similar studies in literature, the formed compounds from glucose and sodium bicarbonates can be classified based on their functional groups for convenience. Carboxylic acids, aldehydes, ketones, and carbohydrates are anticipated to appear in the products. Therefore, it is essential to look for the anticipated compounds in the collected liquid samples first by injecting a standard of each to the HPLC. Furthermore, since glucose is a C_6 compound, the condition used for this step is not to exceed C_6 compound for each functional group as fragmentation to smaller compounds is believed to take place as shown in scheme 2.

First is to inject all the possible compounds based on the suggested reaction pathways from similar studies. Table 12 lists the possible compounds and their existence on the collected liquid phase samples.

Table 12: Possible compounds to form

C number	**Possible compounds**	**Detector**	**Seen in any liquid samples?**
C_1	Formic acid	UV-Vis and RID	Yes
	Formaldehyde	UV-Vis and RID	No
	Methanol	RID	Yes
C_2	Acetic acid	UV-Vis and RID	Yes
	Oxalic acid	UV-Vis and RID	Yes
	Glycolic acid	UV-Vis and RID	No
	Glycoaldehyde	UV-Vis and RID	Yes

	Acetaldehyde	UV-Vis and RID	No
	Ethanol	RID	Yes
C_3	Acetone	UV-Vis and RID	Yes
	Dihydroxyacetone	UV-Vis and RID	No
	Lactic acid	UV-Vis and RID	Yes
	Propanoic acid	UV-Vis and RID	Yes
	Acrylic acid	UV-Vis and RID	Yes
	Pyruvic acid	UV-Vis and RID	No
	Glyceraldehyde	UV-Vis and RID	No
	Pyruvaldehyde	UV-Vis and RID	Yes
	Isopropanol	RID	No
C_4	Butyric acid	UV-Vis and RID	No
C_5	Furfural	UV-Vis and RID	No
	Valeric acid	UV-Vis and RID	No
	Pentanone	UV-Vis and RID	No
	Levulinic aicd	UV-Vis and RID	No

C_6	5-HMF	UV-Vis and RID	No
	Glucose	RID	Yes
	Fructose	RID	No

4.2.2. GC-MS

GC-MS was utilized for the purpose of identifying the unknown compounds in the collected liquid samples from the hydrothermal conversion of CO_2 and glucose studies. Since most of the formed identified compounds are polar, polar columns can best fit the need in this analysis. Therefore, HP-Innowax column was first used to probe the separation of the formed compounds and compare them with the identified ones form the HPLC analysis. As both HPLC column and HP-Innowax have different principles of separating compounds, the solvents used in both techniques are not the same, the sample preparation methods, and the detection means make this identification task more challenging. Nevertheless, a similar study by Konstantinova [115] reported that employing GC-MS was not informative due to i) alkaline nature of the liquid sample, ii) low concentration of the products in the aqueous samples, and iii) poor sensitivity of the device toward formic acid.[115]Therefore, an initial test of different samples was conducted to confirm the claim that GC-MS is not suitable for the liquid samples from the hydrothermal conversion of CO_2 into formic acid using glucose as a reductant.

Solvent screening was carried out in order to determine which solvent is best for the liquid samples. Since the content of the collected liquid samples is polar, carboxylic acids mainly, finding a suitable polar solvent is vital to dissolve all of the liquid sample content. Therefore, solvents with different polarity were chosen, and acetone, hexane, and methanol were therefore probed, and it turned out that methanol dissolves the liquid samples better than the other tested solvents as acetone left some of the samples constituent undissolved whereas hexane created two-layers samples. Thus, methanol was used as a solvent for the collected liquid samples. In terms of the method used for the GC-MS, the following parameters in table 13 were used.

Table 13: GC-MS method for HP-Innowax column

Rate (ºC/min)	**Temperature (ºC)**	**Hold time (min)**
--	40	1
15	200	7
15	250	2

The results from running multiple samples were incomparable with the ones obtained from the HPLC. For example, no formic acid or lactic acid were detected using the GC-MS. Figure 6 shows a GC-MS chromatogram.

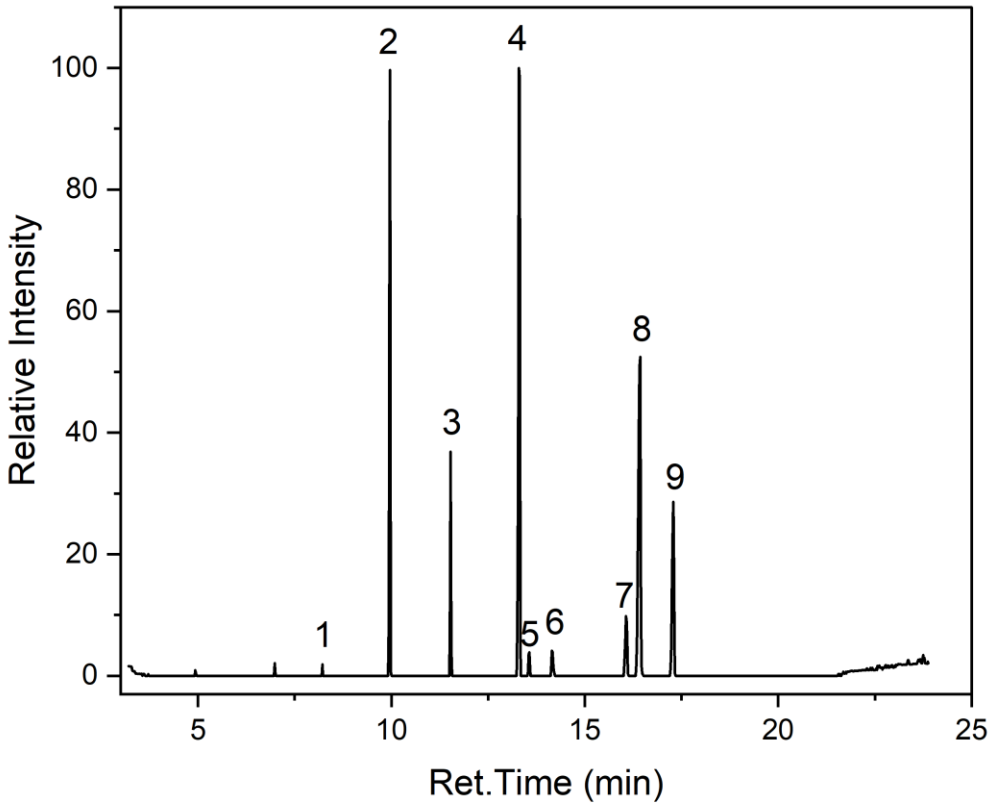

Figure 6: GC-MS chromatogram of a liquid sample collected at 250 ºC, 2 h, and 50% filling volume

The corresponding compound for each peak presented in figure 6 is listed along with their retention times in table 14.

Table 14: List of compounds name for each peak from GC-MS chromatogram of a liquid sample collected at 250 ºC, 2 h, and 50% filling volume

Peak number	**Retention time (min)**	**Compound name**	**Chemical formula**
1	8.217	2-Methyl Hexanoic acid	$C_7H_{14}O_2$
2	9.961	Dodecanoic acid, methyl ester	$C_{13}H_{26}O_2$
3	11.532	Hexadecanoic acid, 15-methyl-, methyl ester	$C_{18}H_{36}O_2$
4	13.308	Pentadecanoic acid, 14-methyl-, methyl ester	$C_{17}H_{34}O_2$
5	13.561	4-Hexen-2-one, 3-methyl-	$C_7H_{12}O$
6	14.156	n-Propyl acetate	$C_5H_{10}O_2$
7	16.07	Hexadecanoic acid, 15-methyl-, methyl ester	$C_{18}H_{36}O_2$
8	16.426	11-Octadecenoic acid, methyl ester	$C_{19}H_{36}O_2$
9	17.285	7-Tetradecyne	$C_{14}H_{26}$

Note that all of the detected compounds in the GC-MS look different when compared with the results from the HPLC. It is also important to understand why low carbon number carboxylic acids, such as formic, acetic and lactic for instance were not detected although they present in detectable

amounts as seen in HPLC-UV-Vis results. Therefore, it is worth testing the ability of the HP-INNOWax column as well as the MS detector in separating and detecting those compounds. Thus, injecting a sample from a prepared mixture of carboxylic acids, lactic; formic; acetic; and propanoic acid; using methanol as a solvent was tried next to see if there is a limitation of the system in detecting these compounds at the same parameters. Note that using methanol and carboxylic acids and heat might produce esters at high temperatures, and therefore, the scanning time was increased to cover as much of the sample constituents as possible. Table 15 lists the corresponding compounds for each peak form the obtained GCMS chromatogram.

Table 15: List of identified compounds name for each peak from GC-MS chromatogram of mixture of standards liquid sample

Peak number	**Retention time (min)**	**Compound name**	**Chemical formula**
1	3.3	Methyl formate	$C_2H_3O_2$
2	4.3	Methyl lactate	$C_4H_8O_3$
3	5.1	Acetic acid	$C_2H_4O_2$
4	5.7	Propanoic acid	$C_3H_6O_2$

Results from injecting a prepared mixture of standards, dissolved in methanol, to the GC-MS indicate that compounds of methyl lactate, methyl formate were detected as well as acetic acid and propanoic acid. In other words, this is evidence that there was esterification and thus corresponding to carboxylic acids alcohols were produced. Note that formic acid, which is the main product of interest here, was not detected. Therefore, the use of GC-MS for scanning the entire compounds in the collected samples without any treatment seemed not useful as results are incomparable to what obtained from HPLC. The same idea was reported by Konstantinova in which the GC-MS

was shown to be not effective technique to analyze samples obtained from the similar reactions.[115]

4.2.3. HPLC

HPLC seems to be the best available analysis technique for separating the sample constituent, gathering as many pieces of information as possible is needed as these could facilitate the identification process. The type of information that can be collected or inferred from the HPLC analysis are a) the column principle of separation, b) the maximum UV-Vis absorption, λ_{max}, c) the refractive index, RI, of the eluting compounds. The latter, however, seems ineffective because the last eluting compounds have either similar to the mobile phase refractive index or low sensitivity toward the RI detector. This information, a and b, can be then compiled and used for looking up compounds in UV spectra database.

First, understanding the separation principle helps in understanding the nature of the unknown compounds. The column used in this analysis was Agilent MetaCarb 87H for Organic Acids. This column is packed with a cation-exchange resin, H+ form. The main principle of separation is ion exclusion and other minor principles such as steric exclusion and partitioning.[135] Since the packing materials contains protons, H+, when a mixture of compounds is introduced to the column, weak organic acids in this study, the order of elution will be based on the pKa of the constituent compounds where low pKa compounds will elute first. The stronger the acid, the lower its pKa the earlier it elutes. To put this in test, three carboxylic acids contained in the liquid samples were identified, and thus their pKa can be compared with their retention time as table 16 presents.

Table 16: Carboxylic acids pKa

Compound	**Retention time (min)**	**pKa**[136]
Formic acid	14	3.74
Acetic acid	15	4.76

Propanoic acid	18	4.87

As shown in table 13, the values of the pKa and the retention time of different carboxylic acids can be correlated as lower pKa elutes first. Additionally, similar tables for comparing different standards injected to the HPLC and their relevant pKa values can be correlated to their retention time. From this, the last eluting unknown compounds should have high pKa values, i.e. less acidic, and this is one key piece of information.

The second piece of information that can be obtained from the HPLC is the maximum UV-Vis absorption, λ_{max}. While the UV-Vis detector was set at 210 nm, the Photo Diode Array Detector, PDAD, was set to scan over the range of both UV and Visible light spectrum, that is 200-800 nm. The λ_{max} values for the last eluting unknown compounds, elute at 38 and 56 minutes, are 223 and 232 nm respectively as depicted in the figures 8 and 9.

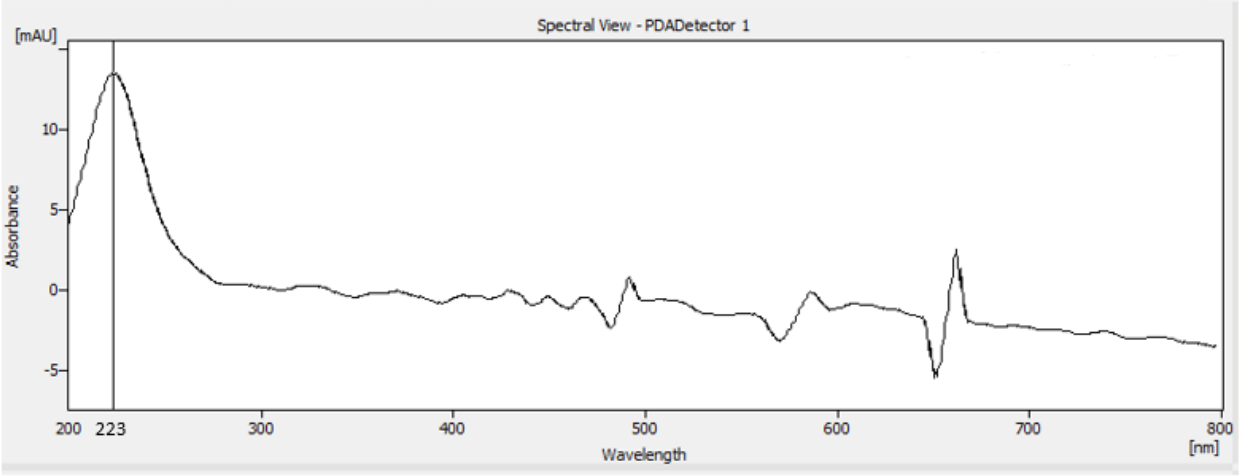

Figure 7: UV-Vis spectrum of unknown peak elutes at 38 min

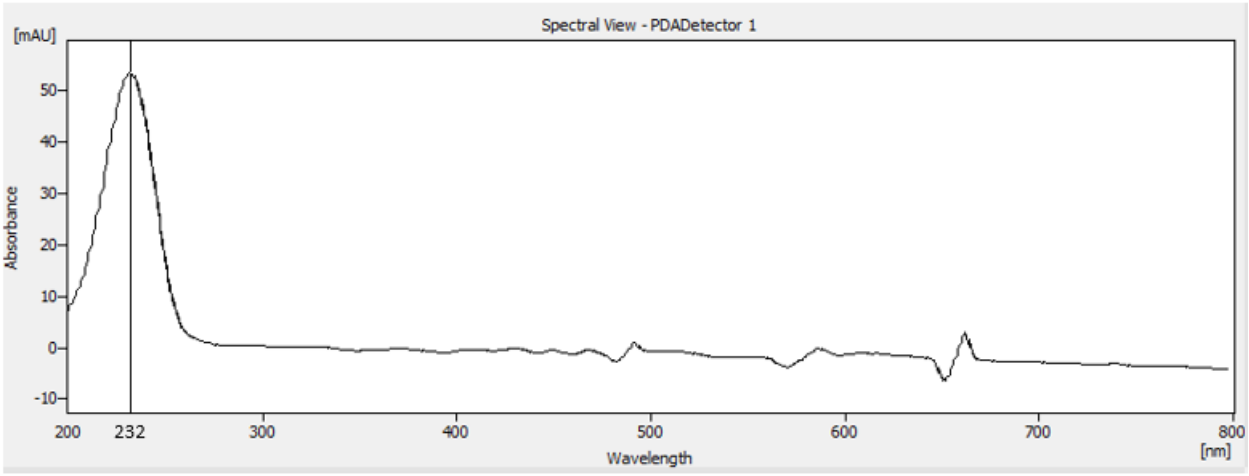

Figure 8: UV-Vis spectrum of unknown peak elutes at 56 min

Now, having both pieces of information, higher pKa values, as well as λ_{max}, UV spectra database can be used to look up compounds with similar λ_{max} and the candidates then can be filtered out based on their pKa.

UV spectra reference books used in this research,[137]–[142] and tables 17 and 18 shows the suggested candidates based on their λ_{max}values. Tables 17 and 18 present the candidates which have maximum UV absorption, λ_{max}, of 223 and 232 nm.

Table 17: Candidates with λmax of 223 nm[137]–[142]

Compound	**Chemical**	**Solvent**	**λmax (log (ε))**
Crotonaldehyde	C_4H_6O	EtOH	223 (4.18)
Crotonaldehyde, trans	C_4H_6O	H_2O; EtOH	223 (4.27); 220 (4.18)
Acetic anhydride, Acetoacetic acid,	$C_4H_6O_3$	Isooctane; pH 7.3;	224.5 (1.68); featureless 230-
Furan, 2,5-dihydro--2-methylene; 2-	C_5H_6O	MeOH; EtOH	239 (3.80); 223 (4.18); 232
2-Penten-4-yn-1-ol	C_5H_6O	n.s.g.(*)	223 (4.1)
2,4-Pentadien-1-ol, cis and trans	C_5H_8O	EtOH	223 (4.28)
2,4-Pentadien-1-ol; 3-Penten-2-one	C_5H_8O	EtOH, H_2O or EtOH	223 (4.4); 225 (4.05) or 224
Acrylic acid, beta dimethyl-	$C_5H_8O_2$	H_2O; H_2SO_3: 49.2	220.3 (4.08); 225.5 (4.06) and
Crotonic acid, x-methoxy	$C_5H_8O_3$	EtOH	223 (3.95), 234 (4.25), 221
2, 5-Furandicarboxyaldehyde	$C_6H_4O_3$	EtOH	223 (3.66)
2,4-hexadiyne-1-ol; 3,5-hexadiyne-2-ol;	C_6H_6O	EtOH	230.5 (2.60), 230 (2.45), 223
3-hexen-5-yn-2-ol	C_6H_8O	EtOH	223 (4.13)
2-Pentenoic acid, 3, 4-dihydroxy	$C_6H_8O_3$	EtOH	223 (4.13)
3,5-Hexadien-2-ol	$C_6H_{10}O$	EtOH	223 (2.4)

* n.s.g.: no solvent given

Table 18: Candidates with λmax of 232 nm[137]–[142]

Compound	**Chemical formula**	**Solvent**	**λmax (log (ε))**
Crotonic acid	$C_4H_6O_2$	82.2-100% H_2SO_4	232.3 (4.15)-235.5(4.21)
Isobutyric acid, lead salt	$C_4H_8O_2$	C_6H_{12}	232 (4.18)
3-Furoic acid	$C_5H_4O_3$	EtOH, H_2O	232 (3.36), 233 (3.40)
Furan,2,5-dihydro--2-	C_5H_6O	MeOH; EtOH	239 (3.80); 223 (4.18);
2(5H)-Furanone,3-hydroxy-	$C_5H_6O_3$	EtOH	232 (4.08)
Isovaleric acid; 2-Pentanoic	$C_5H_6O_3$	n.s.g., H_2O, n.s.g.	232.5 (4.1); 220 (4.26);
Methacrylic acid, methyl	$C_5H_8O_2$	n-C_6H_{14}	231s (2.0)
2, 4-Hexadiynoic acid;	$C_6H_4O_2$	EtOH,EtOH-0.2N	234 (3.26), 235 (3.32),
2,4-hexadiyne-1-ol; 3,5-	C_6H_6O	EtOH	230.5 (2.60), 230 (2.45),
trans-4-Hexen-2-ynoic acid	$C_6H_6O_2$	Et2O	232s(4.08)
2,4-Hexadiyne-1,6-diol	$C_6H_6O_2$	EtOH	220.5 (2.47), 232 (2.61)
Hex-5-en-3-ynoic acid	$C_6H_6O_2$	EtOH	232s(4.02)
Butadiene, 1-acetoxy-	$C_6H_8O_2$	heptane	232 (4.34)
2,4-	$C_6H_6O_4$	EtOH-NaOH	230 (4.10); 232 (3.99)
1, 3-Dioxane-4,6-dione, 2, 2-	$C_6H_8O_4$	MeOH	232 (4.04)
cis,cis-2,4-Hexadien-1-	$C_6H_{10}O$	EtOH; C_6H_{12}	231 (4.23); 231 (3.9),
3-Penten-2-one, 4-methyl-	$C_6H_{10}O$	C_6H_{12}; isooctane	232 (4.09)
Crotonic acid, 3-methoxy-,	$C_6H_{10}O_2$	MeOH	232 (4.13)
Crotonio acid	$C_6H_{10}O_4$	EtOH	232 (4.19)

The molar absorptivity, ε, is needed in order to confidently pick which of the suggested candidates is the one being looked for. The molar absorptivity, ε, can be calculated using Beer-Lambert law which relates the concentration to the absorbance as in equation 3.1.

$A = \varepsilon cl$ equation 3.1

Where A, ε, c, and l are absorbance, molar absorptivity, concentration, and length of optical path. For the unknown compounds, peaks at 38 and 56, one way to identify them is by using the spectra Databook. [137]–[142] To do so, both the UV maximum absorption, λ_{max}, as well as the molar absorptivity coefficient, ε, are needed for accurate prediction. The issue in the current case is that the concentration of each compound in different samples is unknown too. Nevertheless, one suggested way is to relate the results of the unknown peaks from different samples to each other by observing the peak areas. Then, take four or five results and order them in terms of the peak height at their maximum absorption, i.e. at 223 or 232 nm, what is the height of the peak at every sample…etc., then utilizing equation 3.1, plotting the absorbance versus the concentration yields a slope which should be equal to molar absorptivity times cuvette path length, ε and l. Note that the concentrations of these peaks at different samples are still unknown, however, assuming the highest response to be equal to 1, then estimate the rest with respect to 1 should roughly estimate the slope of the line.

First, this should be tested for known compounds in different samples and the results are to be checked with the reference book. Formic acid is an example here to see if this method gives a good prediction of molar absorptivity. Formic acid has been probed at different concentrations and its data are available for use, have a look at table 19.

Table 19: Formic acid concentration and UV response

Concentration (mM)	**Peak height (mAu)**
5	17.473
10	13.785
15	38.923

Assuming the highest response to have 1 mM and then calculate the rest accordingly, and the results should look like what is in table 20.

Table 20: Formic acid estimated concentration and UV response

Concentration (mM)	**Peak height (mAu)**
0.35	13.785
0.44	17.473
1	38.923

Plotting the data in the table above and obtain the slope of the straight line to calculate the molar absorptivity coefficient as in figure 10.

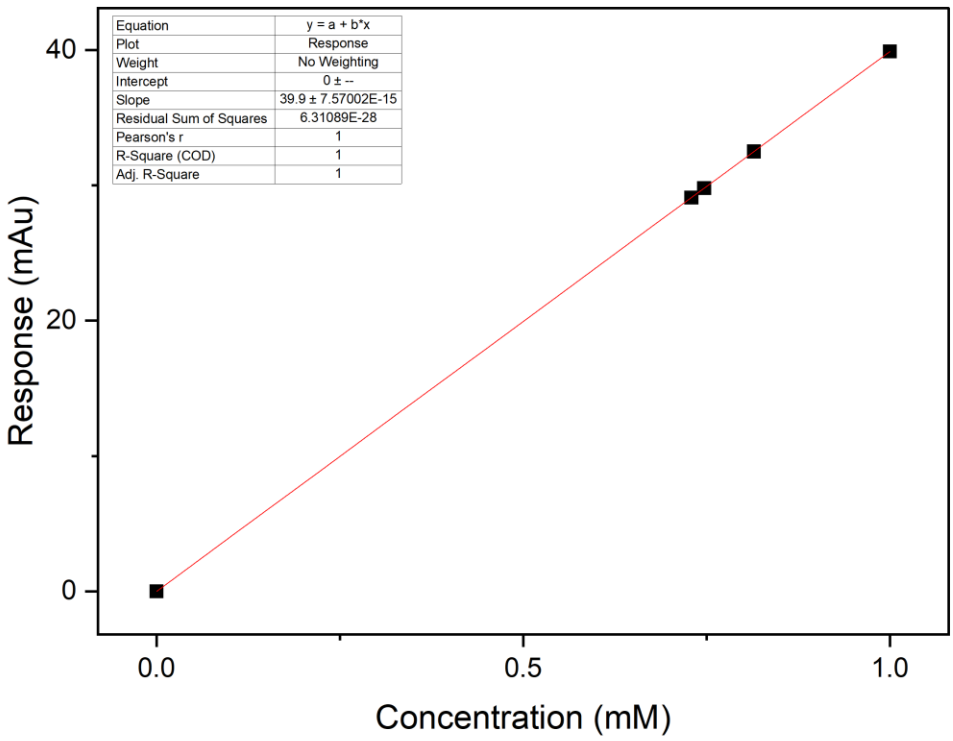

Figure 9: UV absorption of FA at different concentrations

Now, 38.923 is the molar absorptivity coefficient, and the path length is 1 cm, which is common in similar devices. Taking the logarithm of this value gives the log (ε) which can be used to look up data in spectra book reference. Therefore, the formic acid in this case can be said to have maximum absorbance of 208 nm and (1.6) is the log of its molar absorptivity. Comparing this to the spectra data book reference, Formic acid was reported to have max abs of 205 nm and (1.65). Therefore, this method gives a rough estimate, and it is good to start with.

Unknown compound eluted at 38 min

The same method will apply for the unknown peak at 38 min. Utilizing data for the peak at 38 from different analyzed samples and assigning each to a concentration relative to the highest concentration given in table 21.

Table 21: Compound eluted at 38 minutes concentration and UV response

Concentration (mM)	**Peak height (mAu)**
1	35.9
0.57	12.8
0.14	7.8
0.035	0.1
0	0

Plotting the data from the above table should yield a straight line with a slope equal to the molar absorptivity coefficient, ε, as in the previous test.

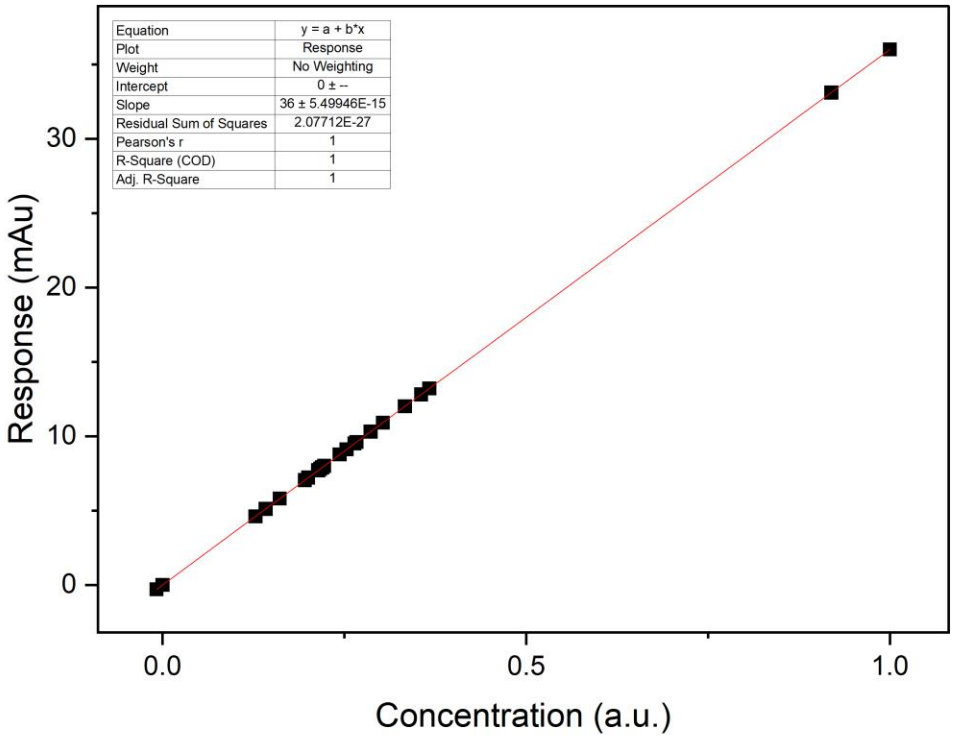

Figure 10: UV absorption of the unknown peak at 38 min at different concentrations

From the plot above in figure 11, the result will be 223 nm (1.5).

Unknown compound eluted at 56 min

The same procedure will be carried out for the compound eluted at 56 minutes and the relevant data are presented in table 22.

Table 22: Compound eluted at 56 minutes concentration and UV response

Concentration (mM)	**Peak height (mAu)**
1	349
0.57	200
0.14	48.5
0.035	12.4
0.025	8.9
0	0

Now, plotting data from the table above, table 19, gives a straight line as in figure 12.

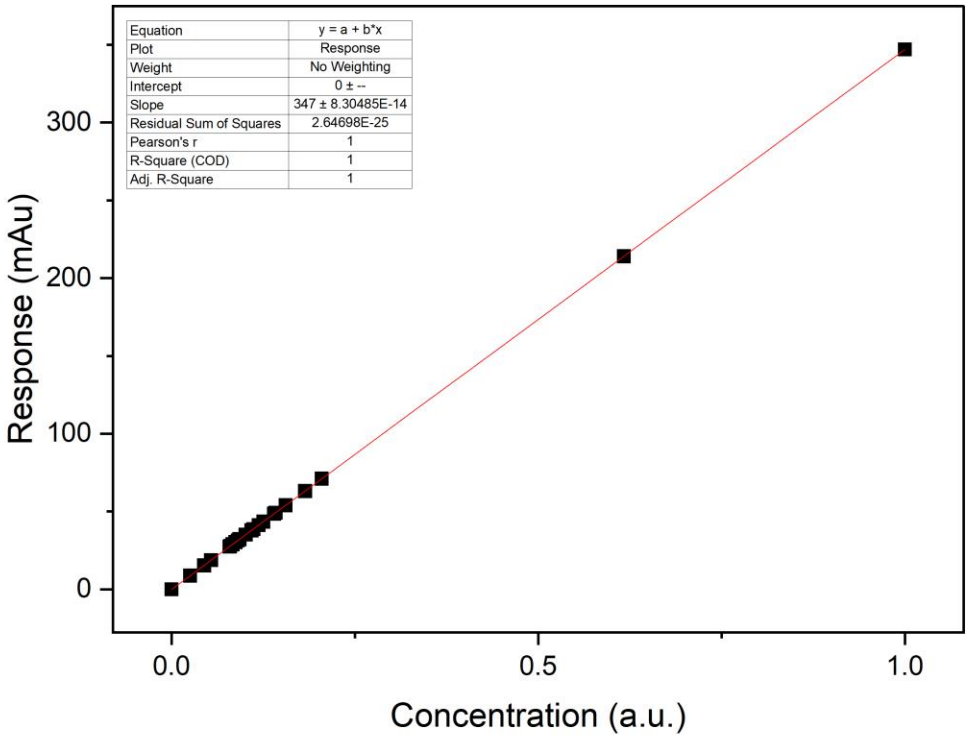

Figure 11: UV absorption of the unknown peak at 56 min at different concentrations

Slope from figure 12 can be used to calculate the molar absorptivity coefficient, which gives: 232 nm (2.5).

The obtained values for both compounds eluted at 38 and 56 can be used to filter out the candidates obtained from the spectra reference. By doing so, the 38 compound, which has λ_{max} and ε of 223 nm and 1.5 respectively, also can be written as 223 nm (1.5), is acetic anhydride or acetoacetic acid or acrylic acid alpha methoxy; all have similar chemical formula of $C_4H_6O_3$ and λ_{max} and ε of 224.5 nm (1.68). Now, the use of pKa becomes useful to filter out the suggested three compounds, and that by knowing that pKa of acetic anhydride is -7, strong acid, and thus it is impossible to elute later than weak acids and thus exclude it from the list. On the other hand, the pKa of acetoacetic acid is about 3.6 which suggests it eluting time to be before formic and acetic acid and thus to be excluded, leaving the last suggestion, acrylic acid alpha methoxy which has a pKa in the range of 4.5 to 5. Similarly, the compound eluted at 56 minutes has λ_{max} and ε of

232 nm (2.5) is either diacetylene glycol with a chemical formula of $C_6H_6O_2$ which has λ_{max} and ε of 232 nm (2.61) or methacrylic acid, methyl ester, with chemical formula of $C_5H_8O_2$ which has λ_{max} and ε of 231 nm (2.0) based on the collected data from the spectra database.

Since the peak at 56 minutes is higher in peak area, as well as UV absorption than the peak at 38 min, it is worth looking at it first. As shown in the above identification method, the peak at 56 min could be, according to the rough identification method, either diacetylene glycol or methacrylic acid, methyl ester. Since ester is more likely to form under the tested conditions, methacrylic acid, methyl ester standard was ordered to probe it using the HPLC as a starting point for verification.

Methacrylic acid, methyl ester was diluted in water and injected into HPLC to see if that is actually the unknown compound eluted at 56 minutes. Unfortunately, this compound eluted at 47 minutes, and it has a λ_{max} of 211 nm of unlike what it was reported in the spectra reference books. The type of solvent, n-hexane versus DI water, can change the UV absorption in both directions, blue and red shifts, however, by a few nanometers not by 19 nm.

Since this strategy was ineffective for identifying the unknown peaks detected by HPLC-UV-Vis at 56 minutes, it is pointless to proceed with the same strategy for identifying the other eluting peak at 38 minutes. Thus, finding another means for identifying or providing more information about the formed products is recommended.

4.2.4. Simple distillation method

Utilizing every single piece of information from the working principle of the HPLC column could help in identification. In the identification process, there was a stage in which the anticipated compounds were injected into the HPLC based on their availability. By doing so, further information can be obtained such as elution time behavior of different compounds from the same family based on the carbon number. For instance, ketones are expected to form from glucose degradation. Thus, acetone, dihydroxyacetone, DHA, and 2-pentanone were available in the lab and standard samples were prepared and injected into the HPLC.

2-pentanone elutes at the exact time of the second unknown compound, 56 minutes, however, the UV-Vis spectrum was not identical to the unknown compound and thus 2-pentanone is not present

in the liquid samples. However, along with acetone, the order of elution was as expected, i.e. acetone first 22 min at and 2-pentanone next at 56 min, as acetone is a C_3 and C_5 is the 2-pentanone, and the longer the carbon chain is, the longer it stays in the column. Although ketones injection was shown to be not helpful, they provide a very important piece of information. That is, the last eluting compounds could have lower boiling points as acetone with boiling point of 56 ºC elutes at 22 min and then 2-pentanone with boiling point of 101 ºC elutes at 56 min.

Separation of compounds in the sample based on their boiling points was then conducted aiming to separate the unknown compounds for further identifications. Therefore, both simple and fractional distillations at 98 ºC were chosen to see if there are any compounds in the sample with similar or lower boiling points. The reason for choosing 98 ºC was because water and formic acid were present in the sample and the purpose here is to isolate lower boiling points compounds for identification. The figures 13 and 14 show the distillation apparatus setup. Note the liquid sample used for the distillation was the collected from heating period to 200 ºC as they have the highest amount of unknown compounds.

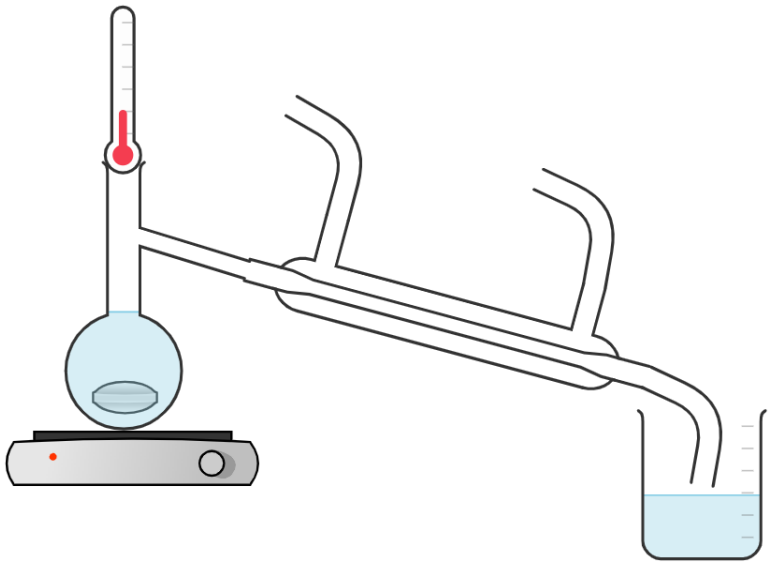

Figure 12: Simple distillation apparatus setup drawing

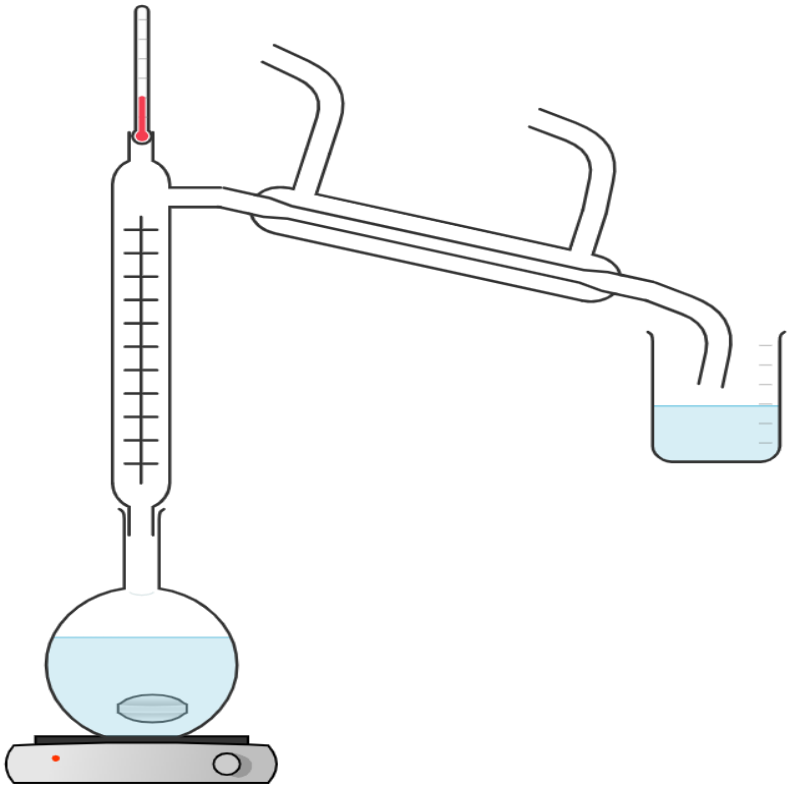

Figure 13: Fractional distillation apparatus setup drawing

The apparatus setup comprises of 1) heater with stirrer, 2) round-bottom flask, 3) fractional column for fraction distillation case, 4) condenser, and 5) collection container.

The procedure was straightforward, different components of distillation apparatus were attached, after charging 10 ml of the tested sample, as in the figures above, and then heating with stirring started up to the temperature set point, then the distillate capped in a glass vial and kept at 5 ºC for analysis. The aim here was to analyze the distillates from different samples using HPLC to see what constituents of the samples were separated in this method.

The separation method seemed useful as both unknown compounds eluted at 38 and 56 min were present in the distillate samples detected by HPLC-UV-Vis. The results from analyzing the distillates samples are presented in table 23.

Table 23: Distillates samples content detected by HPLC-UV-Vis

Sample / **Compound**	**Simple distillation**	**Fractional distillation**
Unknown at 38 min	4.5%	18.6%
Unknown at 56 min	89.2%	19.3%

As in table 20, simple distillation was shown to have better separation of the unknown peak eluted at 56 minutes. Therefore, further analysis of the collected distillate from the simple distillation using GC-MS was conducted. The same method and column were used for the GC-MS. The peaks from the GC-MS chromatogram for simple distillation sample are summarized in table 24.

Table 24: Assigned compounds from GC-MS analysis of distillate sample

Peak number	**Retention time (min)**	**Compound name**	**Chemical formula**
1	0.5	Isopropyl alcohol	C_3H_8O
2	0.6	Acetone	C_3H_6O
3	0.8	Acetoin	$C_4H_8O_2$
4	3.8	6-Methyl-1-heptanol	$C_8H_{18}O$

From the presented data, isopropanol is an alcohol, and alcohol does not strongly absorb UV light and thus it is excluded as a pure compound. On the other hand, acetone was also reported by Konstantinova [115] from GC-MS analysis, however, pure acetone eluted at different retention

time when injected to the HPLC and has a distinct UV-Vis spectrum. Therefore, it cannot be a pure acetone. The only possibility based on the given data is that the combination of alcohol and ketone resulted in the unknown compounds detected by HPLC and UV-Vis.

4.2.5. NMR

NMR analysis was carried out for both samples collected from normal reactions, i.e. 250 ºC 2 h and 50% filling volume, and the distillate samples collected post the distillation process. The NMR analysis was done for ^{13}C, and ^{1}H. For the liquid samples collected from 250 ºC, 2 h and 50% filling volume, the ^{13}C and ^{1}H results are depicted in figures 16 and 17.

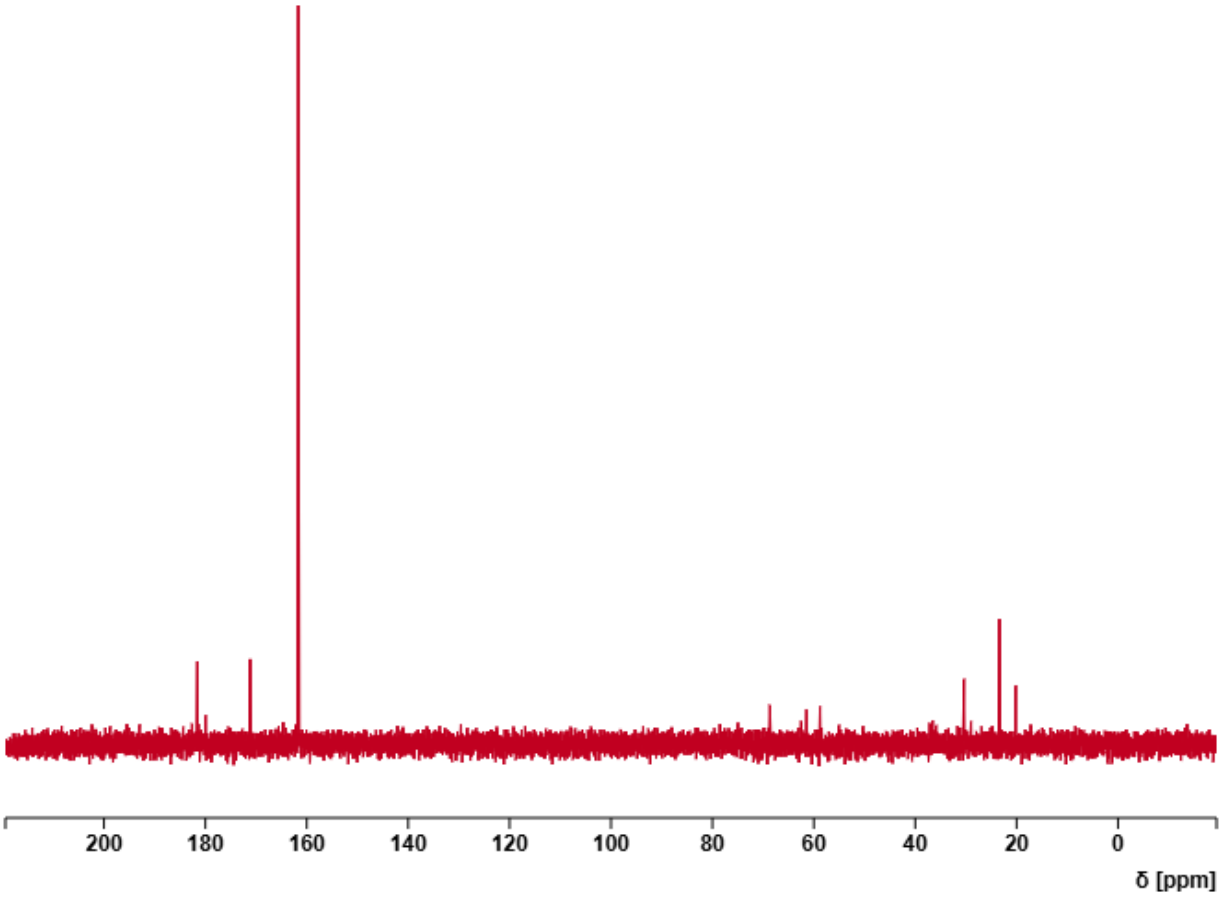

Figure 14: NMR spectrum for ^{13}C of sample from reaction 250 ºC, 2 h and 50% filling volume, 0.5 M $NaHCO_3$ and 0.05 M $C_6H_{12}O_6$

The peaks in figure 16 were assigned to compounds as the following: the peak at 160 ppm corresponds to carbonate, the peak at 171 ppm was attributed to formic acid, and peaks in the 180s ppm range are indicative of various carboxylic acids. Peaks from 68–76 ppm, suggesting CH groups bonded to oxygen (e.g., secondary alcohols or sugars), peaks from 58–63 ppm for CH_2 groups bonded to oxygen, and aliphatic CH_2 and CH_3 peaks below 40 ppm.

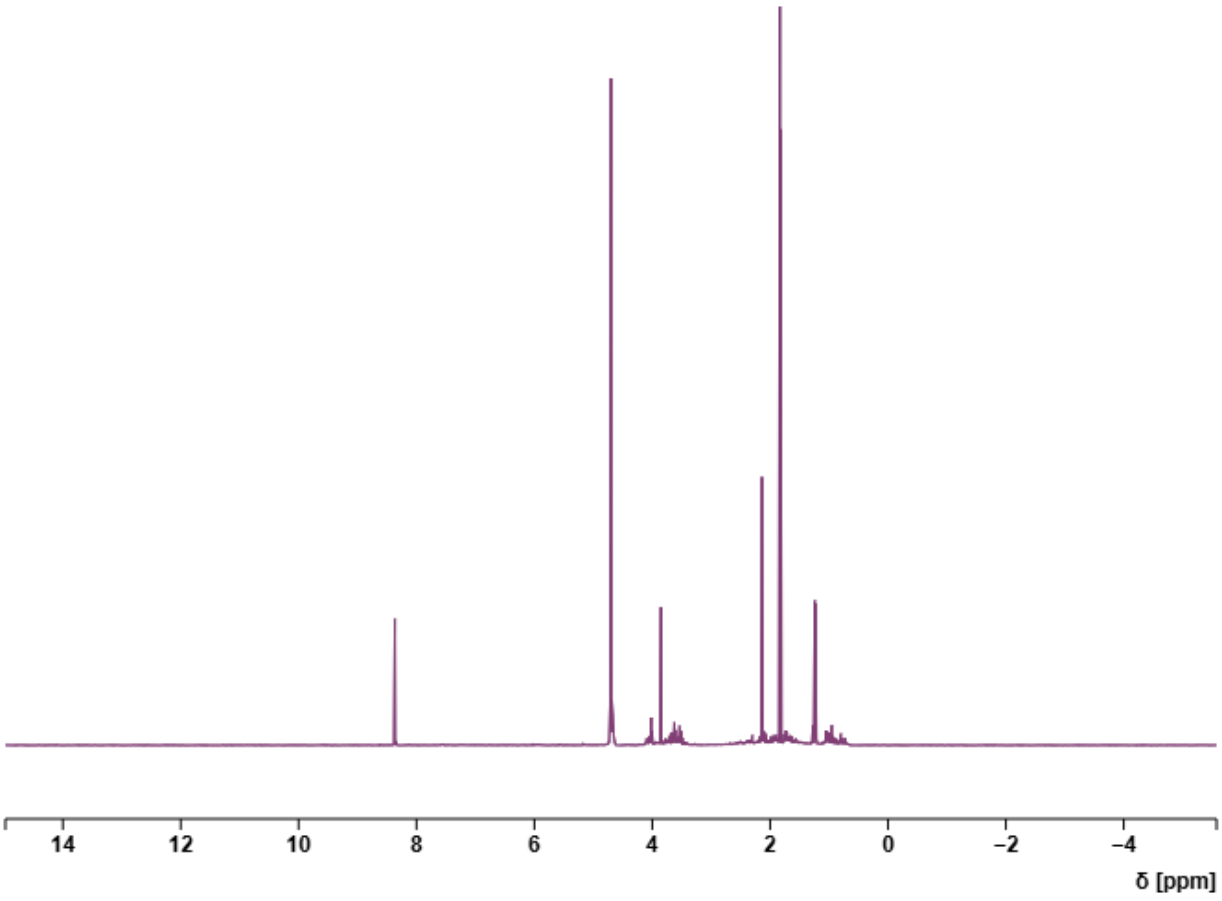

Figure 15: NMR spectrum for ^1H with solvent suppressed of sample from reaction 250 ºC, 2 h and 50% filling volume, 0.5 M $NaHCO_3$ and 0.05 M $C_6H_{12}O_6$

The ^1H NMR with solvent suppression showed a complex spectrum, with many peaks in the aliphatic region. A distinctive peak at 8.36 ppm was identified as formic acid as in figure 17.

For the distillate samples, the samples collected from the distillation process, the NMR spectra are presented in figure 18.

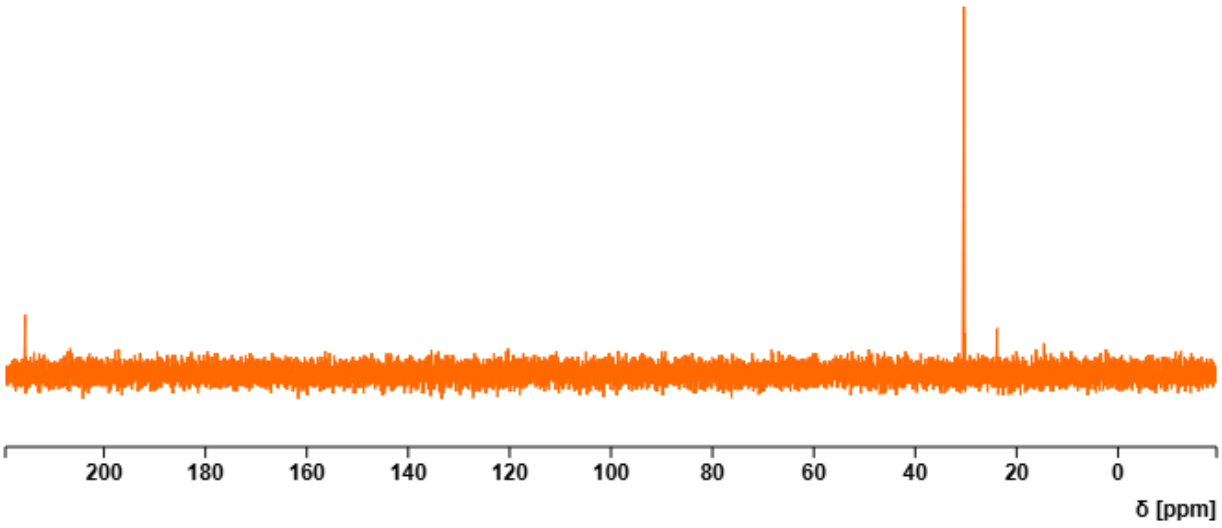

Figure 16: NMR spectrum for ^{13}C of distillate sample which collected from reaction heating period to 200 ºC, 16 min and 50% filling volume, 0.5 M $NaHCO_3$ and 0.05 M $C_6H_{12}O_6$

NMR analysis for the ^{13}C showed peaks at 215.4 ppm, 30.3 ppm, and 23.8 ppm as shown in figure 18.

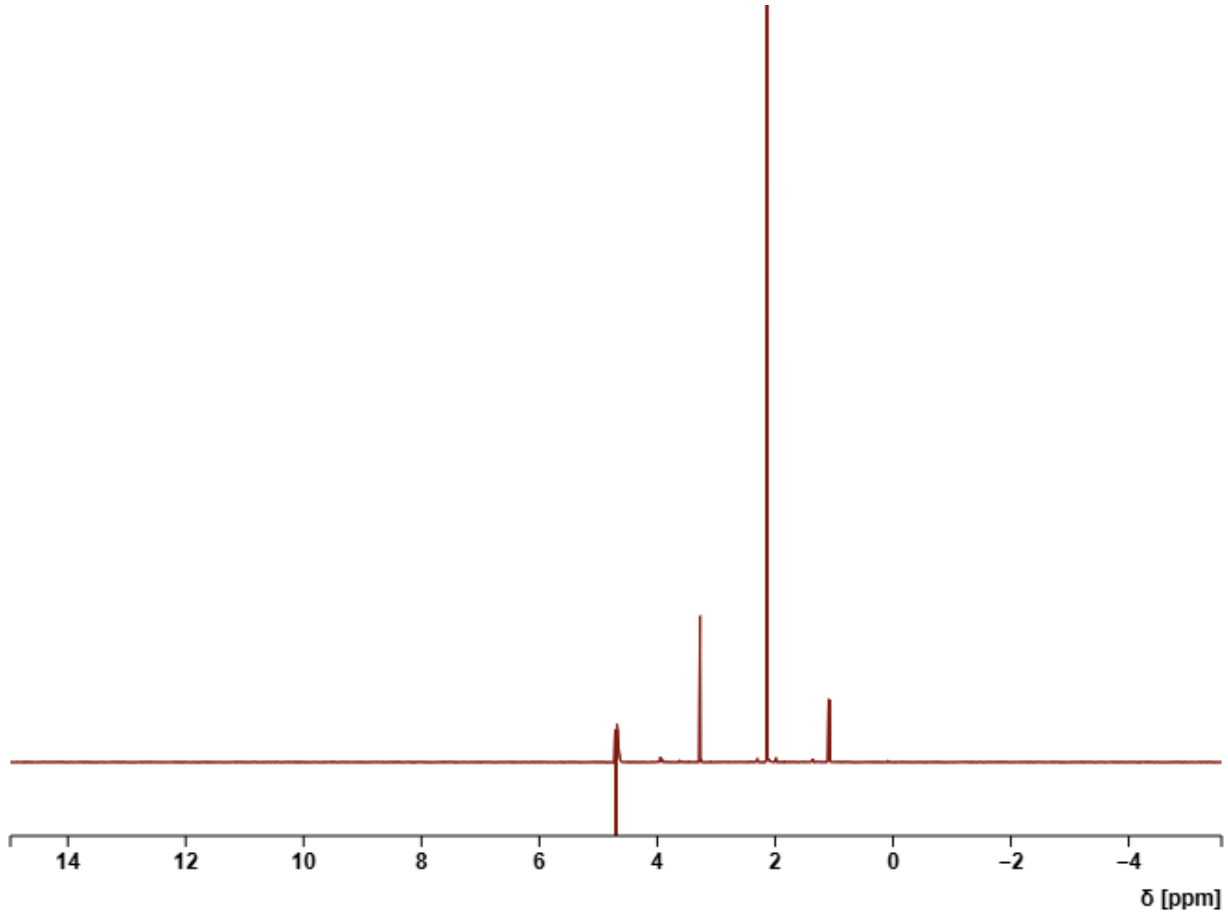

Figure 19: NMR spectrum for ^{1}H with solvent suppressed of sample from reaction distillate sample which collected from reaction heating period to 200 ºC, 16 min and 50% filling volume, 0.5 M $NaHCO_3$ and 0.05 M $C_6H_{12}O_6$

Peaks in figure 19 are at 1.08, 2.1, 3.2, and 3.9 ppm. To visualize and assign peaks better, 2D NMR analysis, i.e. plotting the spectra of ^{1}H against ^{13}C, was also carried out for the distillate samples and the 2D plot is shown in figure 20.

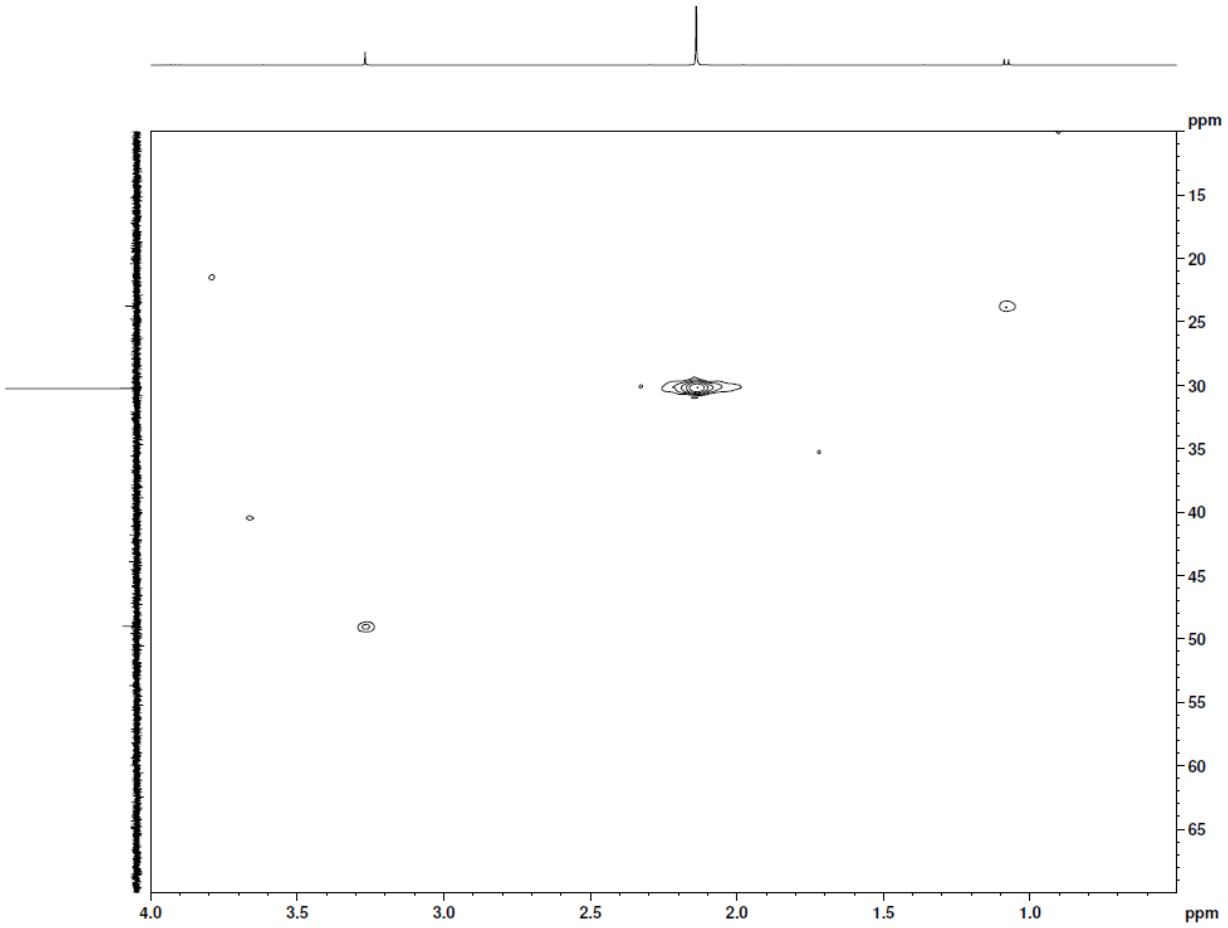

Figure 17: 2D NMR spectra for the distillate sample

In figure 20, ^{1}H at 1.08 ppm and ^{13}C at 23.8 ppm is isopropanol. ^{1}H at 2.1 ppm and ^{13}C at 30.3 ppm is acetone. ^{1}H at 3.2 ppm and ^{13}C at 49 ppm is methanol. The 215.4 ppm peak in figure 18 corresponds to the acetone carbonyl group. Since alcohols cannot be detected by UV-Vis, and acetone has a different retention time and UV maximum absorption, this suggestion was excluded.

4.3. Conclusion

Kinetic studies were conducted for the reaction of $NaHCO_3$ and $C_6H_{12}O_6$ at 200 ºC, 50% filling volume, and during the heating period to establish a reaction equation. Despite using high conversion data for glucose, the data showed, aligning with the literature for glucose, first-order kinetics for glucose, and zero-order kinetics for bicarbonate, and thus the reaction equation along with the reaction rate constant was reported in this work. By utilizing the available data from other

conducted reactions, the reported reaction rate constant was validated by plotting the natural log of glucose concentrations versus their relevant reaction times yielded a straight line with a slope of the reaction rate constant, comparable to the calculated value.

Further investigation on the activation energy for the given reaction was conducted next. It turned out that the utilization of the high conversion data for glucose, although beneficial for determining the reaction order and rate constant, led to inaccurate data for the reaction rate constant at higher reaction temperatures which is incorrect. Furthermore, the nature of the used setup could have played a role in not obtaining accurate data for the activation energy calculations as the system pressure increases with increasing the temperature. In other words, obtaining results at higher temperatures are necessary for activation energy calculations and thus, temperature should ideally be the only manipulated factor to impact the obtained results. Therefore, the activation energy calculations trials for this setup were shown to be unsuccessful.

Using glucose as a reductant introduces an array of products, and one aspect of this work was to shed a light on the qualifying the formed products first, then quantifying them to be able to accurately balance the moles of carbon in and out. Compared to similar studies, formic, acetic, lactic, and propanoic acid presence was confirmed in the collected liquid phase samples. However, three more compounds were detected using the UV-Vis coupled with the HPLC which needed identification. Mole balance calculations for the liquid phase known compounds and the consumed reactants revealed that only 31% of the consumed carbon was identified and thus further efforts needed to identify more of the detected compounds.

Two out of the three formed compounds were selected for further identification as the third was out of the detection range of UV-Vis. The possible compounds reported in the literature from similar studies were first injected and the results compared and none of them were among the unknown. GCMS was then used, and the results were incomparable to the obtained from HPLC which aligns with a previous study and thus GCMS was not suitable for this aim. NMR was employed next; however, the results were general and informative as the results suggested presence of carboxylic acids, sugars, and alcohols. Distillation, both simple and fractional, was carried out to separate the unknown from the liquid sample, and it was shown by HPLC analysis that simple distillation at 98 ºC was effective to separate one of the unknown successfully.

Therefore, analyzing the distillate was carried out next using GCMS and NMR and both suggested presence of methanol, acetone, and isopropanol. Since both alcohols cannot be detected by UV-Vis, and acetone has a different retention time and maximum UV absorption, this suggestion was excluded.

Using maximum UV absorption of the unknown compounds and estimating the molar absorptivity was done next as an initial step to look up possible compounds on spectra reference book. Two lists of possible candidates were compiled, then filtered using the estimated molar absorptivity. Since one of the unknowns was present in higher amount than the other, the suggested compound was obtained and then injected into the HPLC, however, the results were different than in the collected liquid phase samples. Therefore, the identification of the unknown compounds was stopped there as employing other analysis techniques such as HPLC-MS, which was unavailable at the time, is suggested for further investigation of the unknown compounds.

Chapter 5: Optimization Studies

5.1. Overview

The reaction variables such as reaction temperature, reaction time, and filling volume may influence the yield of the product. Here, the hydrothermal reaction of sodium bicarbonate, $NaHCO_3$, and glucose, $C_6H_{12}O_6$, is to be investigated by varying one reaction variable at a time. Setup, method, and analysis techniques can be found in detail in the method section in chapter 2.

200, 250, and 300 ºC have been tested in this work at different reaction times, 1; 2; and 3 hours, in order to see the impact they have on the yield of formic acid as well as the other formed products. However, observing the time it takes the system to heat up to the set point as the preliminary studies were conducted varied from similar studies in literature. For instance, the time it took the system used in this study to heat up from the initial state to 200 ºC was ~ 16 min. Additionally, when the reaction temperature set point is higher, then the system needs longer time to heat up to the set point. When the heat up time is compared with other hydrothermal studies in literature, there is a difference. For example, similar hydrothermal studies reported by Chinchilla et al. 2022 reported that 7 min was needed for the system to heat up from the initial state to the set point of 200 and 250 ºC.[111] Similarly, Fernandez et al. 2022 reported that it took their system 3 min to heat up to the set point of 300 ºC.[17] Therefore, and since the heating up time is quite long in this work compared to similar studies, 16 min versus 7 min to 200 ºC, it is necessary to examine if there is any conversion of the reactants or formation of the products during the heating period.

5.2. Results and discussion

5.2.1. Heating to 200, 250, and 300 ºC set points studies

Studies of the initial heating periods were carried out to see if there is any formation of products as well as to precisely report the reaction time by setting time zero as the time in which the system reached the temperature set point. Table 25 shows the time it took the system to reach the reaction temperature set point for all of the probed reaction temperatures.

Table 25: Time needed for the system to reach the temperature set point

Set T (˚C)	**Time to set point (min)**
200	16
250	28
300	42

As table 25 shows, the highest reaction temperature probed in this work, 300 ºC, the system needed about 42 min to get to the set point. To study the possibility of products formation during the heating period, several studies were conducted for all of the three reaction temperatures used in this work.

5.2.2. Reaction temperature of 200 ºC

The first tested set at the reaction of 200 ºC and 50% filling volume was the heating period. The formed products over the heating period, form room temperature to 200 ºC, are shown in figure 20.

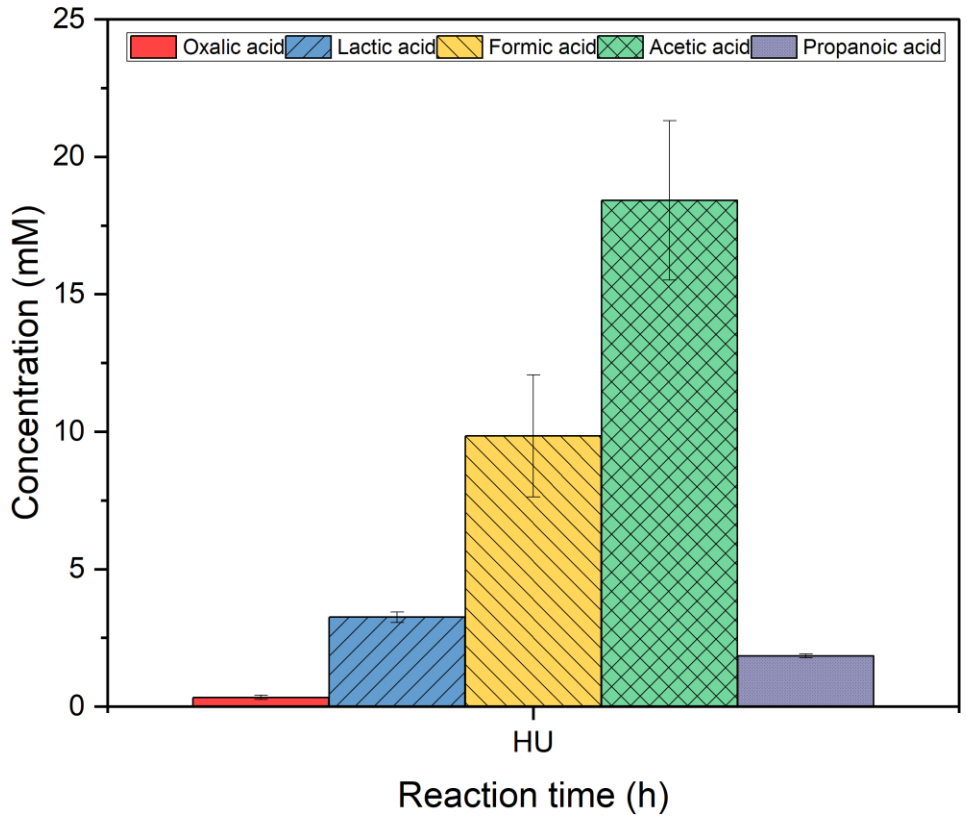

Figure 18: Formed products concentration during the heating period to 200 ºC; 0.5 M $NaHCO_3$ and 0.05 M $C_6H_{12}O_6$ at 50% filling volume

The formed carboxylic acids detected by HPLC-UV-Vis were oxalic, lactic, formic, acetic, and propanoic acids. The order of the produced compounds concentrations from the highest to the lowest were acetic, formic, lactic, propanoic and oxalic acids with the concentrations of 18.4, 9.8, 3.2, 0.3, and 1.8 mM respectively.

The concentrations of the formed compounds when the reaction time was 1 h at 200 ºC and 50% filling volume is depicted in figure 21.

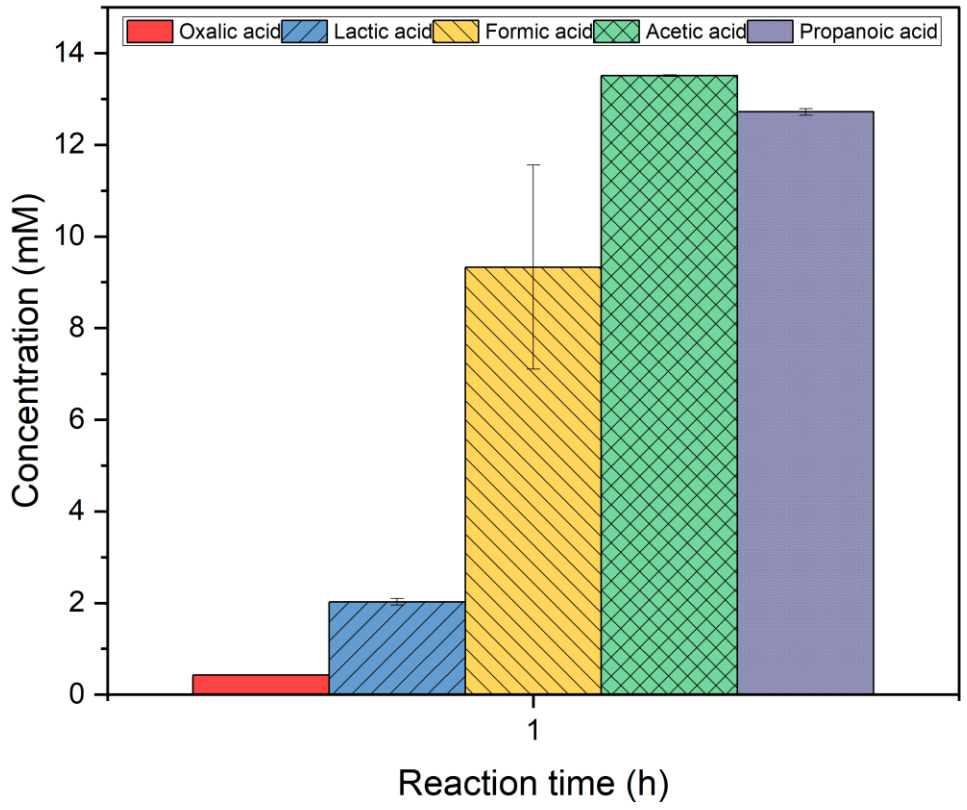

Figure 19: Formed products concentration up to 1 h at 200 ºC; 0.5 M $NaHCO_3$ and 0.05 M $C_6H_{12}O_6$ at 50% filling volume

The order of compounds based on the concentrations, high to low, when the reaction time was 1 h at 200 ºC and 50% filling volume were acetic, propanoic, formic, lactic, and oxalic acids with concentrations of 13.5, 12.7, 9.3, 2, and 0.4 mM respectively.

When the reaction time increased to 2 h, the concentrations of the formed compounds are shown in figure 22.

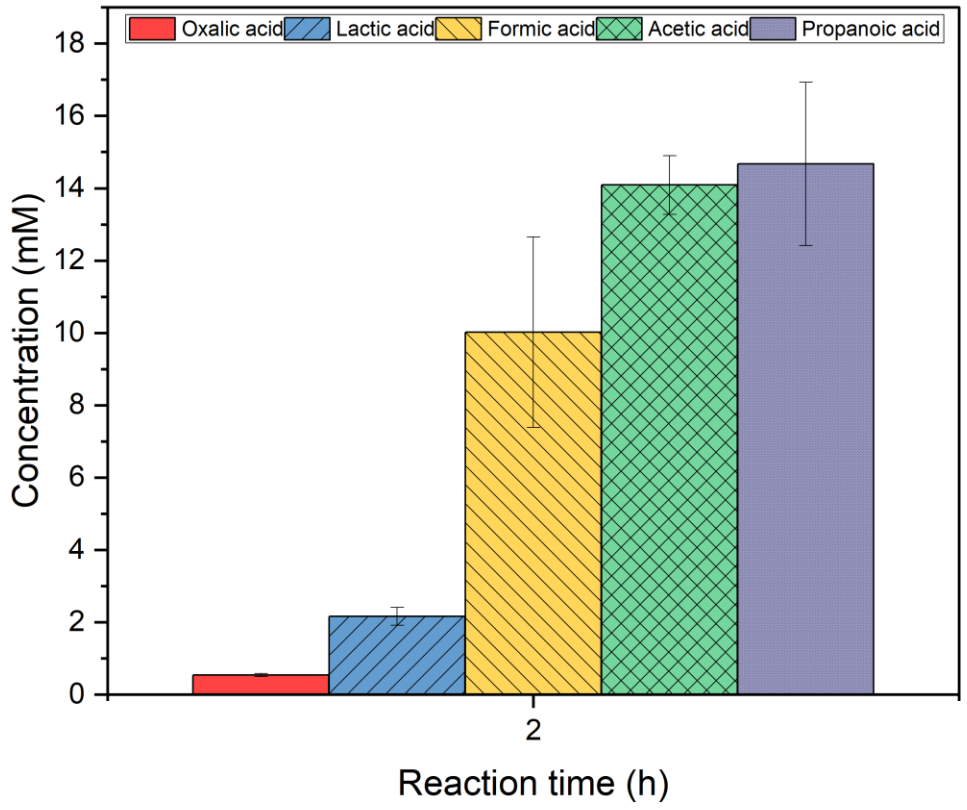

Figure 20: Formed products concentration up to 2 h at 200 ºC; 0.5 M $NaHCO_3$ and 0.05 M $C_6H_{12}O_6$ at 50% filling volume

The order of the formed compounds, by concentrations from the highest to the lowest, were propanoic, acetic, formic, lactic, and oxalic acids. The relevant concentrations of the compounds were 14.6, 14.1, 10, 2.2, and 0.5 for propanoic, acetic, formic, lactic, and oxalic acids respectively.

The formed compounds when the reaction time was increased to 3 h at 200 ºC and 50% filling volume are presented in figure 23.

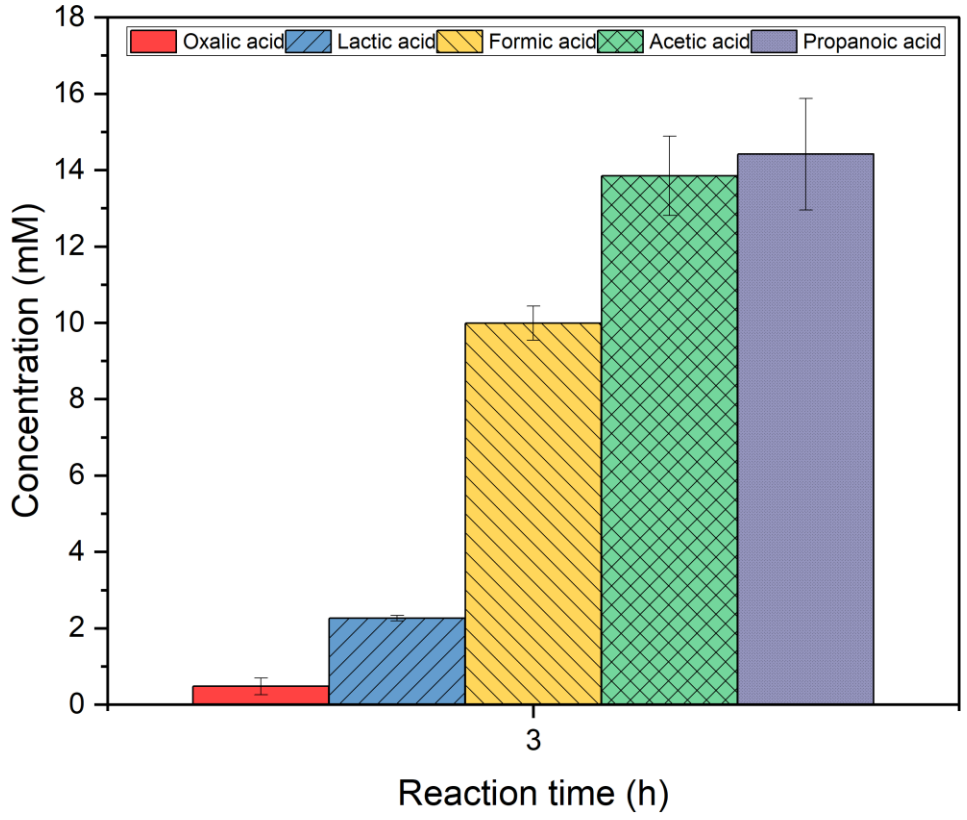

Figure 21: Formed products concentration up to 3 h at 200 ºC; 0.5 M $NaHCO_3$ and 0.05 M $C_6H_{12}O_6$ at 50% filling volume

The order of the formed compounds based on their concentrations form the highest concentration to the lowest concentration were propanoic, acetic, formic, lactic, and oxalic acids with concentrations of 14.4, 13.8, 10, 2.3, and 0.4 mM respectively.

For comparison, the formed products from all of the tested reaction times at 200 ºC and 50% filling volume are presented side to side in figure 24.

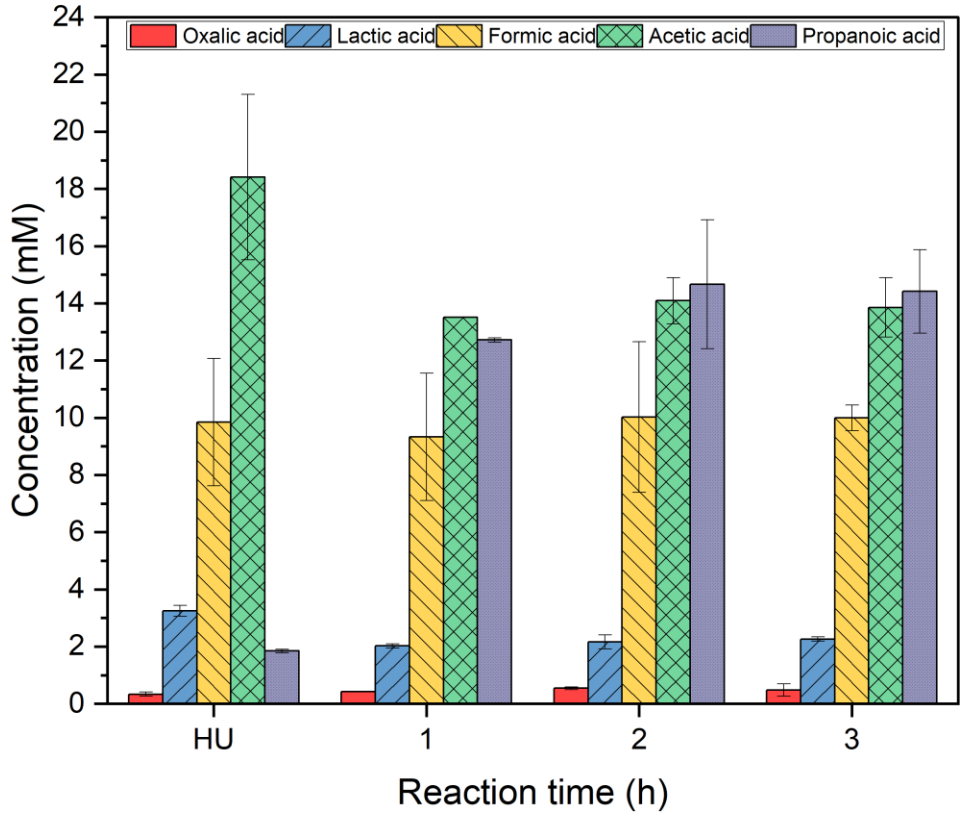

Figure 22: Formed products concentration at different reaction times at 200 ºC; HU: heating period, 0.5 M $NaHCO_3$ and 0.05 M $C_6H_{12}O_6$ at 50% filling volume

The confirmed products concentrations were traced in this work. Oxalic, lactic, formic, acetic, and propanoic acids concentrations were monitored by analyzing the collected liquid samples using HPLC-UV-Vis. It is worth noting that there are other products formation at some of the tested conditions such as ethanol, isopropanol, and acetone. As shown in figure 24, from left to right, there were compounds formation during the heating period to 200 ºC which took about 16 minutes. Moreover, the same formed compounds from the preliminary studies, at 250 ºC and 2 h, formed here as well. Different compounds exhibited different behaviors as the reaction time was varied. While some of the formed compounds were produced rapidly during the heating period, others were formed later on as the reaction time progressed. Additionally, some of the formed compounds stayed the same regardless of changing the reaction time. For instance, the concentrations of oxalic

and formic acids were the same in all of the tested reaction times, including the heating period to 200 ºC. On the other hand, some compounds formed in higher concentrations first, and then exhibited declining as the reaction time was increased. For example, acetic acid was produced by a concentration of 18.5 mM. At the end of the reaction period, its concentration declined as the reaction time was increased to longer reaction times. Notably, and at the same time, the concentration of propanoic acid was minimal during the heating period, less than 2 mM, before it increased as the reaction time progressed. Note that the formation of propanoic acid is related to the disappearance of acetic acid as the reaction time increases. Statistically, the change of all of the formed compounds' concentrations at 200 ºC when reaction time varied, heating, 1, 2, and 3 h, is significant. The calculated P-value for oxalic, lactic, formic, acetic, and propanoic acids are 0.027, 0.000216, 0.012, 8.3×10^{-5}, and 0.0012 respectively.

Tracking the conversion of both reactants, bicarbonates HCO_3^-, and glucose, $C_6H_{12}O_6$, would be helpful to see which needed longer time to convert. Figure 25 presents the concentration of both reactants as a function of reaction time including the heating period to 200 ºC.

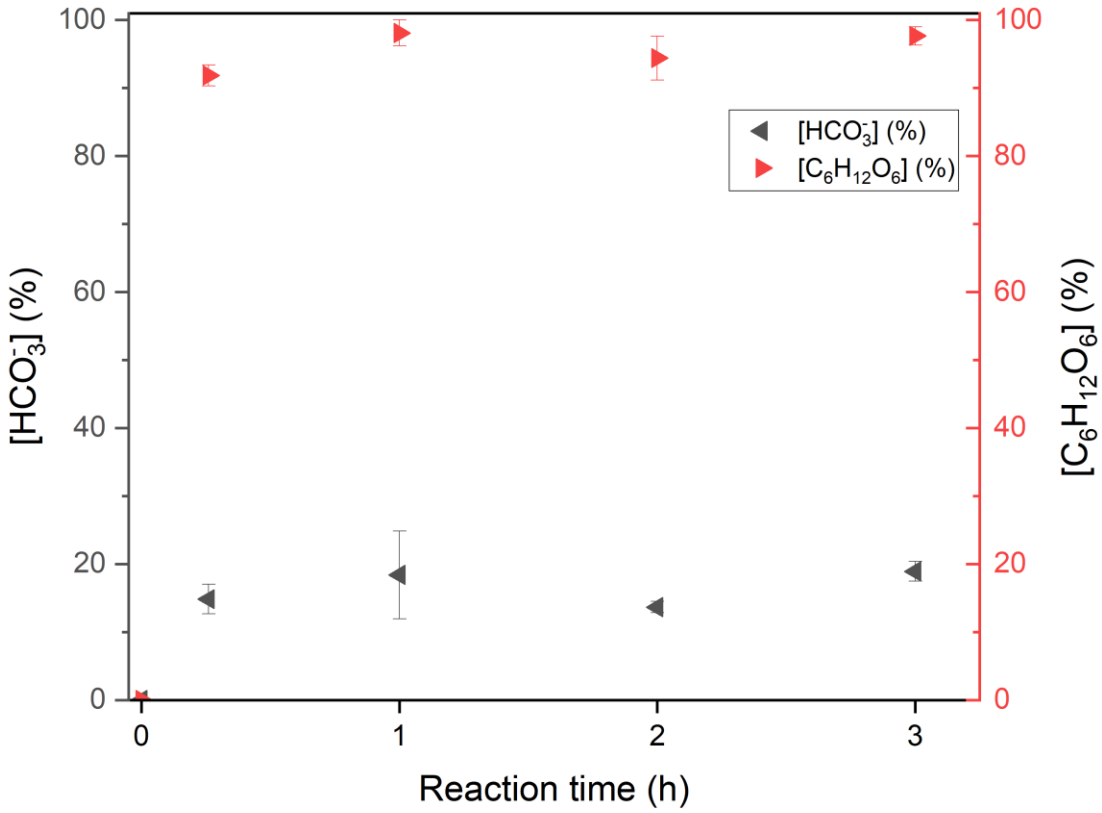

Figure 23: The conversion of the reactants at different reaction times at 200 ºC

During the heating period, the conversion of the reactants was 13 and 93% of bicarbonate and glucose respectively as shown in figure 25. When the reaction time was longer, that was the heating period and 1 h after that, the conversion of the reactants was 18 and 96% of bicarbonate and glucose respectively. Furthermore, when the reaction time was heating period and 2 h, the conversion was 13 and 94% of bicarbonate and glucose respectively. Finally, when the reaction time was the heating period and 3 h, the consumption of the reactants was 19 and 97% of bicarbonate and glucose respectively.

As mentioned earlier in the chapter, other products were formed in some of the tested cases. Here an observation was made for the formation of ethanol and acetone at 200 ºC. Table 26 presents the relevant peak areas for each compound.

Table 26: Average peak areas obtained from HPLC-RID for ethanol, in mV.min, and UV-VIS, in mAU.min, for acetone at 200 ºC

	Ethanol (±)	**Acetone (±)**
Heating period	0	593 (14)
1 h	969 (71)	848 (1.2)
2 h	906 (37)	772 (58)
3 h	0	617 (37)

As in table 26, ethanol was produced at 1 and 2 h reaction times, however, it was neither detected for the heating period samples nor at 3 h reaction time for the 200 ºC studies. The production of ethanol was the highest at 1 h reaction time before it was shown to decline at 2 h reaction time. On the other hand, acetone was detected for all of the tested reaction times at 200 ºC studies. The behavior of acetone can be said to reach its highest production at 1 h reaction time after which it was shown to decline at longer reaction time.

When the reaction time exceeded the heating period to 1 h, the concentration of lactic acid decreased by 38%, see figure 24. At the same time, the appearance of ethanol was observed when the reaction time exceeded the heating period to 1 and 2 h, see table 26. This suggests that the previously reported decomposition of lactic acid to ethanol under hydrothermal conditions by Shen et al. 2014[143] occurred here.

Similar to the other tested reaction times, products formed during the heating period. Formation of the products during the heating period has not been reported in the literature. The reason for that is because the volume of the reactor used in similar studies as well as the heating method used were different than what used in this study. For instance, the volume of the reactor in this work is 100 ml whereas the volume of the reactors used in Chinchilla et al. 2022 and Fernandez et al. 2022 were 10 and 15.6 ml respectively.[17], [111] Consequently, the period it took the reactor to reach

the set temperature was shorter than it did in this work. For example, similar hydrothermal studies reported by Chinchilla et al. 2022 reported that 7 minutes was needed for the system to heat up from the initial state to the set point of 200 and 250 ºC.[111] Similarly, Fernandez et al. 2022 reported that it took their system 3 minutes to heat up to the set point of 300 ºC.[17] Furthermore, the heater used in this work was a ceramic band heater that is installed on the top of the reactor vessel unlike preheated alumina bed used by Fernandez et al. 2022 or fluidized bed heater in Chinchilla et al. 2022. [17], [111]

The product distribution varies as the reaction time progressed from the heating period to 2 h. During the heating period, acetic acid was the highest formed product, 18.4 mM, whereas propanoic acid was the lowest formed product, 1.8 mM. As the reaction time progressed to 1 h, the opposite happened where the concentration of acetic acid decreased by 27% and the propanoic acid concentration increased from 1.8 to 12.7 mM. Although this reaction temperature, 200 ºC, was reported in Chinchilla et al. 2022 work, other formed compounds beside formic acid were not reported. [111] Chinchilla et al. 2022 reported a slight decline in the yield of acetic acid at 200 ºC from 40% to 37% as the reaction time proceeded from 1 to 2 and 3 h. It is worth noting that the formation of products during the heating period was not investigated in that study due to shorter time needed to reach the setpoint, 7 min. Additionally, propanoic acid was not reported by Chinchilla et al. 2022, only formic, acetic, and lactic acids were reported as the main products.

The simultaneous decreasing of acetic acid and increasing of propanoic acid suggests the pathway of propanoic acid production in this process. In other words, the production of propanoic acid is acetic acid dependent. As the reaction time exceeded the heating period, the concentration of acetic acid declined by 27%, see figure 24. At the same time, the concentration of propanoic acid inclined when the reaction time exceeded the heating period from 2 M to ~13 mM, see figure 24. One possibility is that the product from the decomposition of lactic acid, i.e. ethanol,[143] and the present acetic acid converted into ethyl acetate via esterification before the outcome of this reaction, ethyl acetate, reacted with carbon monoxide, via ethyl acetate carbonylation into propanoic acid,[144] to finally produce propanoic acid, see scheme 3.

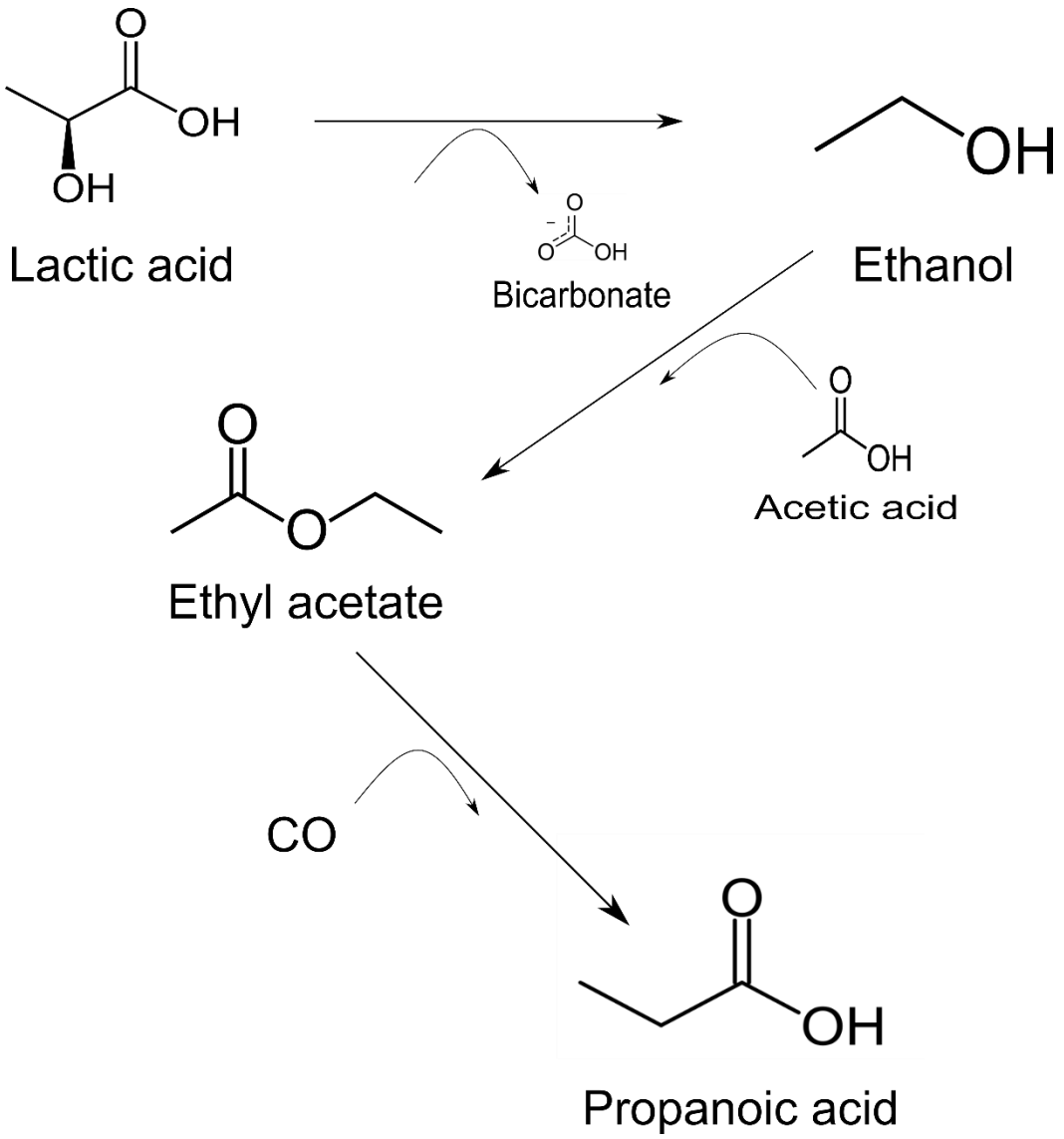

Scheme 3: Proposed mechanism for propanoic acid production

Another explanation is as the following, acetic acid can be produced from ethanol,[145]–[148] and thus, a reverse process from acetic acid to ethanol is possible. Propanoic acid can be produced via ethanol carbonylation as in R.9.[149]–[154]

$$C_2H_6O + CO \rightarrow C_3H_6O_2;\ \Delta H_{298\,K} = -143.2\ kJ\ mol^{-1} \qquad \text{R.9}$$

As ethanol was formed at 200 ºC at short reaction time and disappeared at longer time, the decrease in acetic acid concentration was accompanied by an increase in propanoic acid, this supports the formation of propanoic acid from the acetic acid via the formation of ethanol. Ethanol forms from acetic acid though reduction followed by the carbonylation of the formed ethanol to propanoic acid. Ethanol was reported as a by-product from CO_2 reduction study under subcritical conditions using glucose.[17] Though the formed ethanol was not quantified in this study, it paved the way for quantification investigation in the future studies to correlate the formation of both ethanol and propanoic acid. This presents an alternative way to produce either acetic, ethanol, or propanoic acid from this method by controlling the reaction time at 200 ºC.

5.3. Reaction temperature of 250 ºC

Similar to the first reaction temperature, 250 ºC was then tested at 3 different reaction times including the heating period. Figure 26 presents the concentrations of the formed products during the heating period. Note that the preliminary studies conducted and reported in chapter 3 were at the same reaction temperature, 250 ºC, however, they were limited to 2 h reaction time.

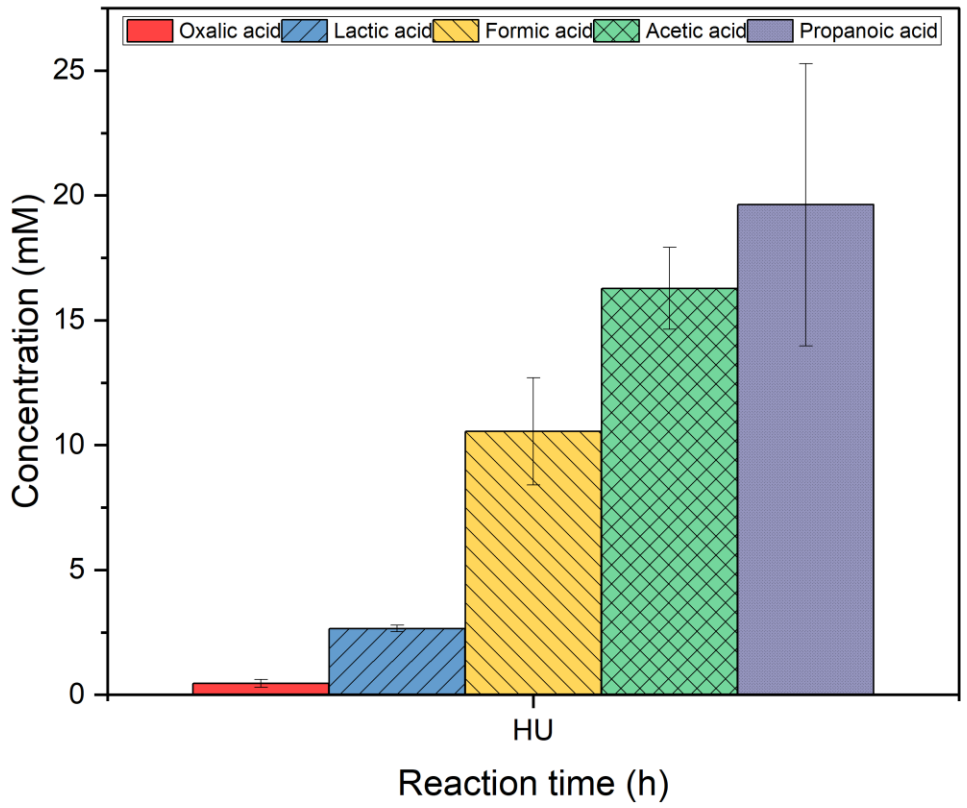

Figure 24: Formed products concentration during the heating to 250 ºC; 0.5 M $NaHCO_3$ and 0.05 M $C_6H_{12}O_6$ at 50% filling volume

The order of the formed compounds based on their concentrations from the highest to the lowest during the heating period to 250 ºC were propanoic, acetic, formic, lactic, and oxalic acids. The concentrations of the formed compounds were 19.6, 16.3, 10.5, 2.6, and 0.4 mM of propanoic, acetic, formic, lactic, and oxalic acids respectively.

The concentrations of the formed compounds when at 1 h reaction time at 250 ºC and 50% filling volume are shown in figure 27.

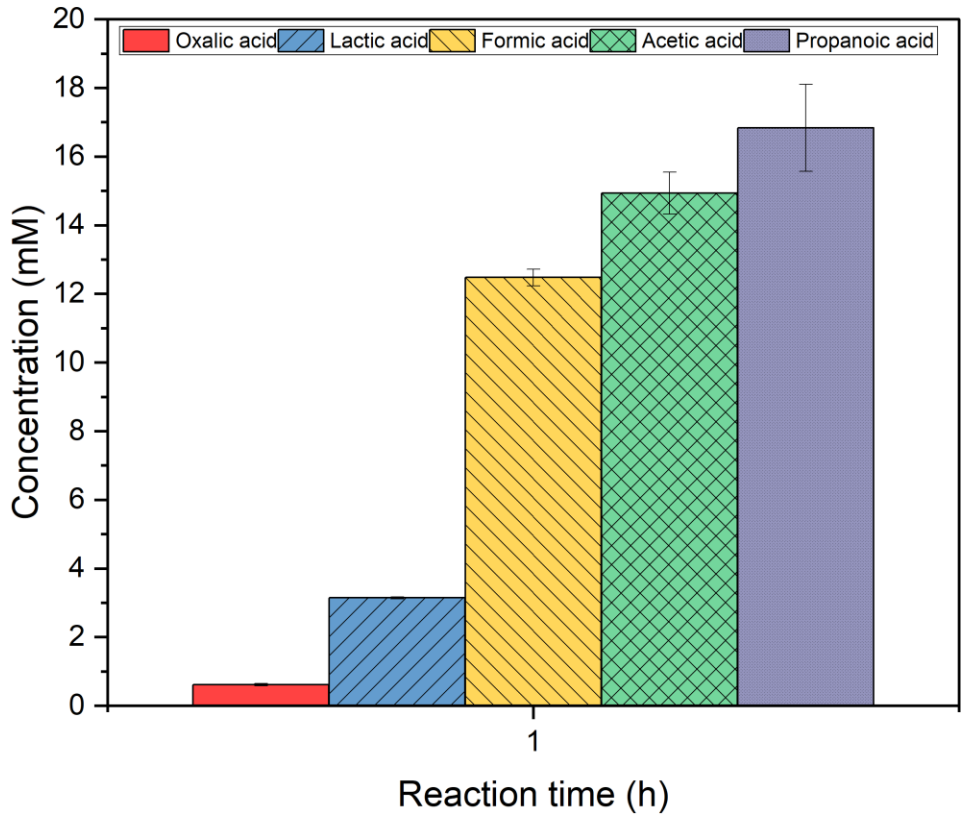

Figure 25: Formed products concentration up to 1 h at 250 ºC; 0.5 M $NaHCO_3$ and 0.05 M $C_6H_{12}O_6$ at 50% filling volume

The trend of the concentration of the formed compounds from the highest concentrations to the lowest at 1 h were propanoic, acetic, formic, lactic, and oxalic acids, and the concentrations were 16.8, 14.9, 12.4, 3.1, and 0.6 mM respectively.

When the reaction time increased to 2 h, the formed compounds and their relevant concentrations are illuminated in figure 28.

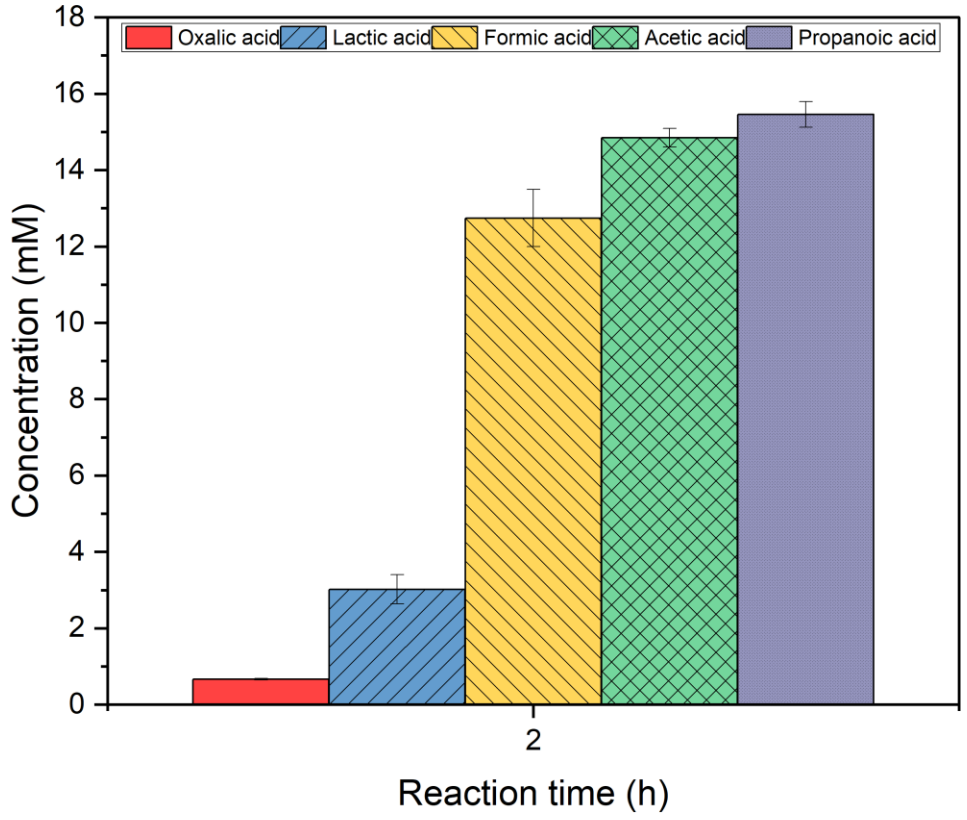

Figure 26: Formed products concentration up to 2 h at 250 ºC; 0.5 M $NaHCO_3$ and 0.05 M $C_6H_{12}O_6$ at 50% filling volume

The formed products ordered by their concentrations form the highest to the lowest were propanoic, acetic, formic, lactic, and oxalic acids. The concentrations of the formed compounds were 15.4, 14.8, 12.7, 3, and 0.6 mM of propanoic, acetic, formic, lactic, and oxalic acids respectively.

As the reaction time was increased to 3 h, the formed compounds are shown in figure 29.

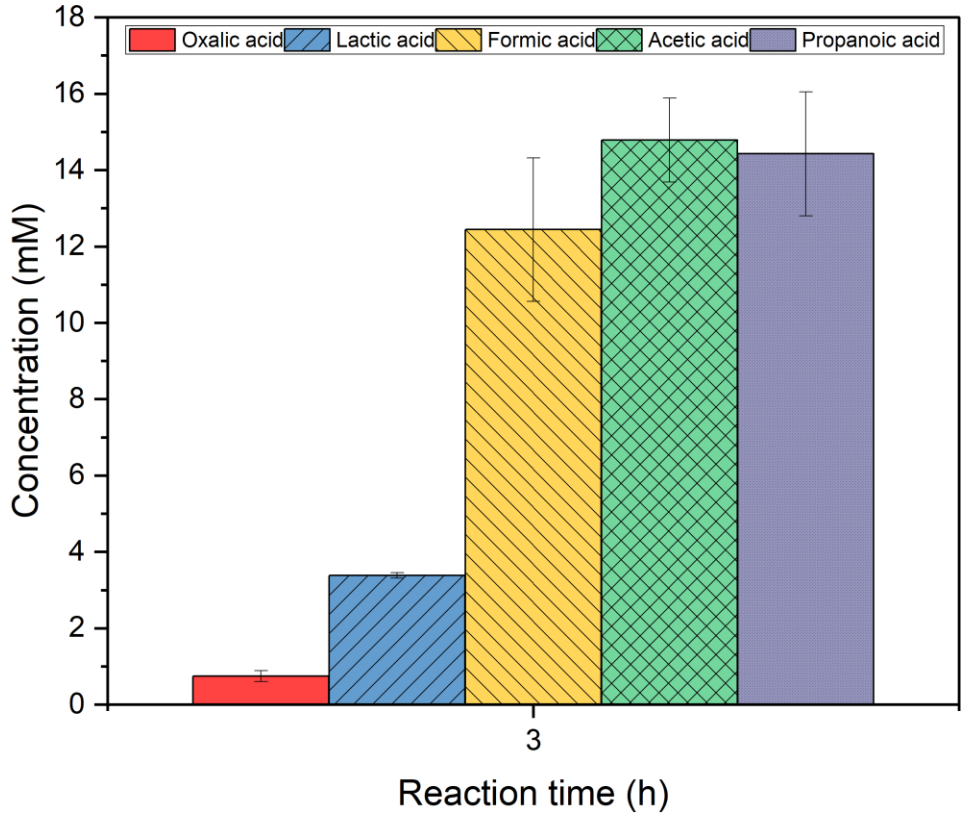

Figure 27: Formed products concentration up to 3 h at 250 ºC; 0.5 M $NaHCO_3$ and 0.05 M $C_6H_{12}O_6$ at 50% filling volume

At 3 h, acetic acid was the highest, then propanoic, formic, lactic, and oxalic acids. The concentrations of the formed compounds were 14.7, 14.4, 12.4, 3.4, and 0.7 mM of acetic, propanoic, formic, lactic, and oxalic acids respectively.

For better comparison, all of the formed compounds at 250 ºC at 50% and different reaction times are presented side-to-side in figure 30.

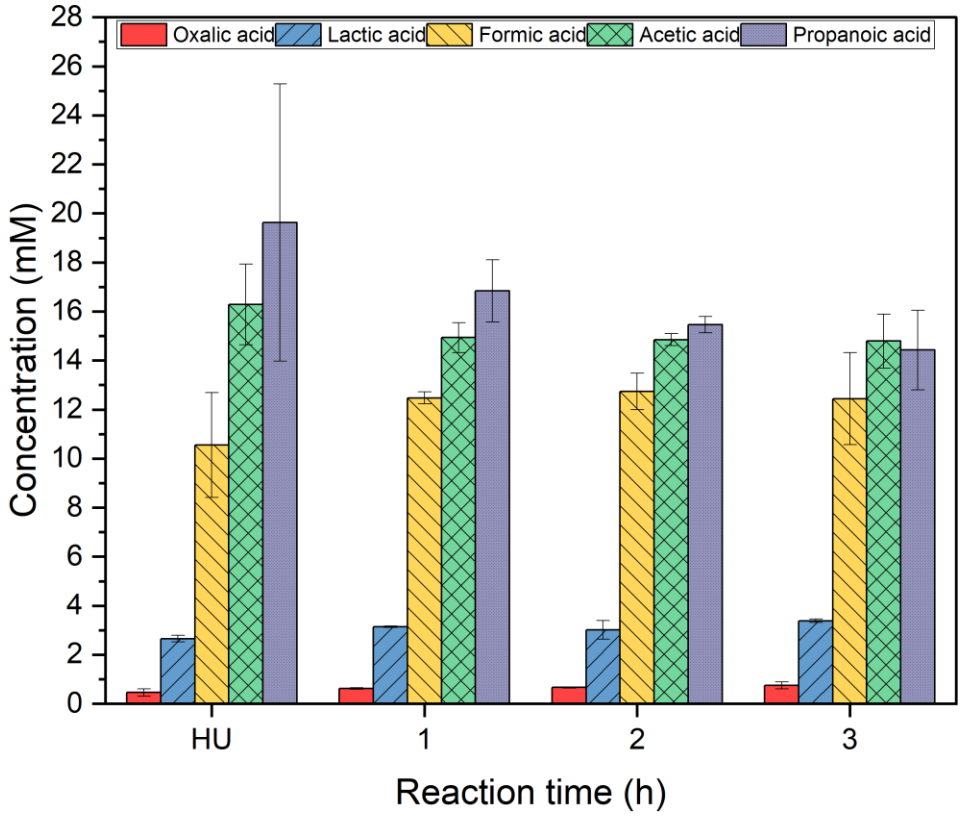

Figure 28: Formed products concentration at different reaction times at 250 ºC; HU: heating period, 0.5 M $NaHCO_3$ and 0.05 M $C_6H_{12}O_6$ at 50% filling volume

The heating period for the reactions conducted at 250 ºC was about 28 minutes for the system to reach the set point temperature. As figure 30 shows, and just like the case at 200 ºC, there were formations of different products during that period. All of the observed products obtained at 1, 2, and 3 h reaction times were observed after the heating period. Oxalic and lactic acids exhibit similar constant behavior as the reaction time was varied. However, formic acid concentrations improved as the reaction time was increased longer than the heating period and the highest concentration of formic acid was observed at 250 ºC, and 2 h reaction time at 50% filling volume. Nevertheless, while other products showed constant or increased behaviors as the reaction time was increased, acetic and propanoic acids exhibited the opposite. The concentrations of both acetic and propanoic acids were declining as the reaction time was increased to 1, 2, and 3 h. Statistically,

the change of all of the formed compounds' concentrations at 250 ºC when reaction time varied, heating, 1, 2, and 3 h, is insignificant. The calculated P-value for oxalic, lactic, formic, acetic, and propanoic acids are 0.2, 0.1, 0.5, 0.5, and 0.4 respectively.

To have a wider view of the behaviors of all of the participants, figure 31 depicts the reactants conversion at all of the tested reaction times.

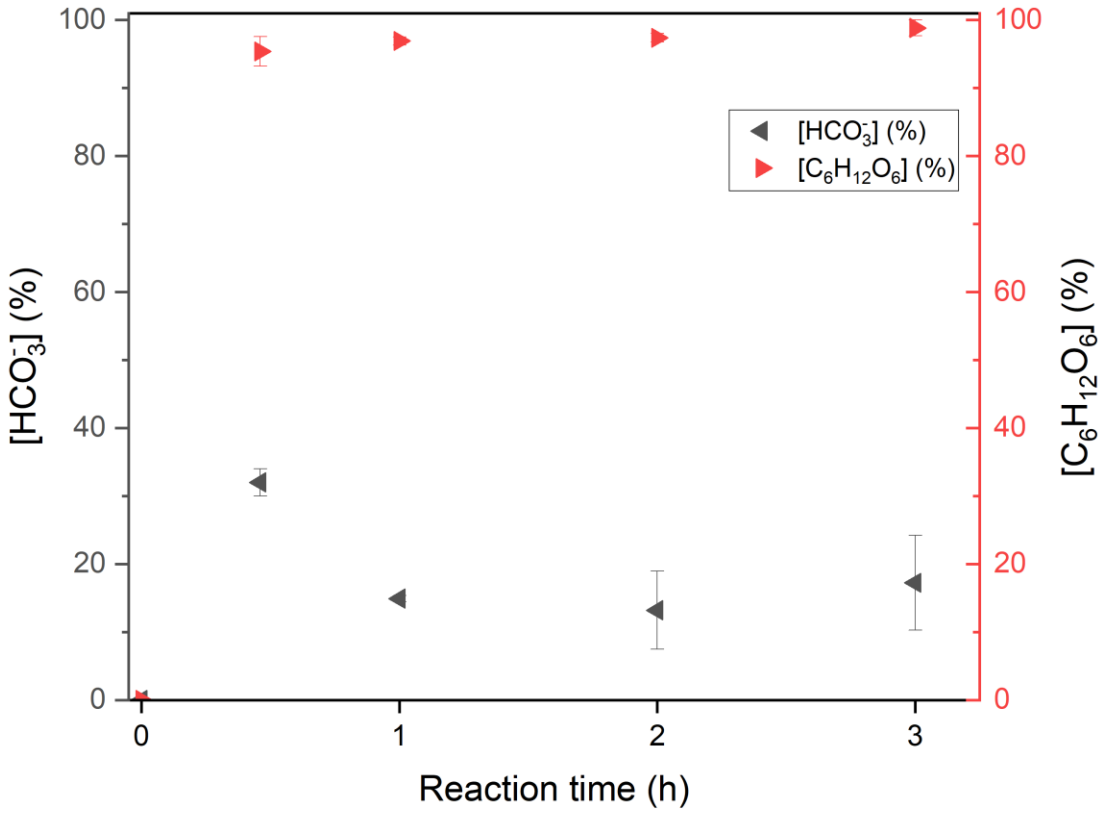

Figure 29: The conversion of the reactants at different reaction times at 250 ºC

The behaviors of both reactants, as in figure 23, exhibited a similar trend after the heating period. That is, no significant change was observed in the consumption of both reactants as the reaction time was increased 1-, 2-, and 3 h after the heating period. However, when comparing the results of heating up plus 1, 2, and 3 h with the heating up period only, improvement can be seen in the glucose consumption, longer reaction time meant better decomposition. Nevertheless,

bicarbonates were consumed better during the heating period when compared to the other tested reaction times.

Formic acid was found to have the highest concentration at 250 ºC, 2 h, and 50% filling volume with 12.7 mM. Similar observation was reported by Konstantinova 2022. [115] The autogenerated pressure from water is temperature dependent. Therefore, increasing the reaction temperature increases the pressure of the process. For instance, the pressure of saturation of water at 200 ºC is 15 bar and 40 at 250 ºC. The process of CO_2 hydrogenation into formic acid is an exothermic process,[155], [156] and thus the improvement of the formic acid production can be attributed to the increased pressure at 250 ºC according to Le Chatelier's principle.

5.4. Reaction temperature of 300 ºC

The highest reaction temperature in this work was 300 ºC, and the formation of different products was tracked from the liquid samples analysis at different reaction times. At 300 ºC, the reaction times probed were 1, 2, and 3 h including the heating up period. Figure 32 shows the results of the concentrations of the formed products at the heating period to 300 ºC.

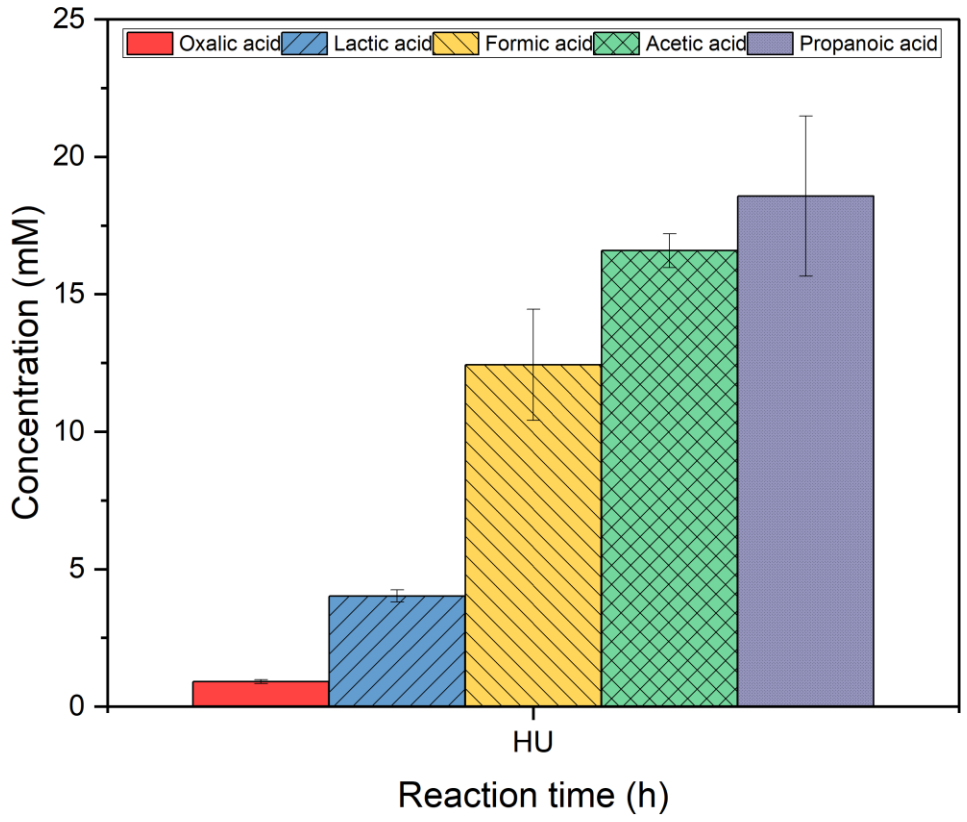

Figure 30: Formed products concentration during heating to 300 ºC; 0.5 M $NaHCO_3$ and 0.05 M $C_6H_{12}O_6$ at 50% filling volume

The formed compounds during the heating period at 300 ºC and 50% filling volume, ordered from the highest concentrations to the lowest, were propanoic, acetic, formic, lactic, and oxalic acids. The concentrations of the formed compounds were 18.5, 16.5, 12.4, 4, and 0.9 mM of propanoic, acetic, formic, lactic, and oxalic acids respectively.

The formed compounds at the reaction time of 1 h and 50% filling volume are illustrated in figure 33.

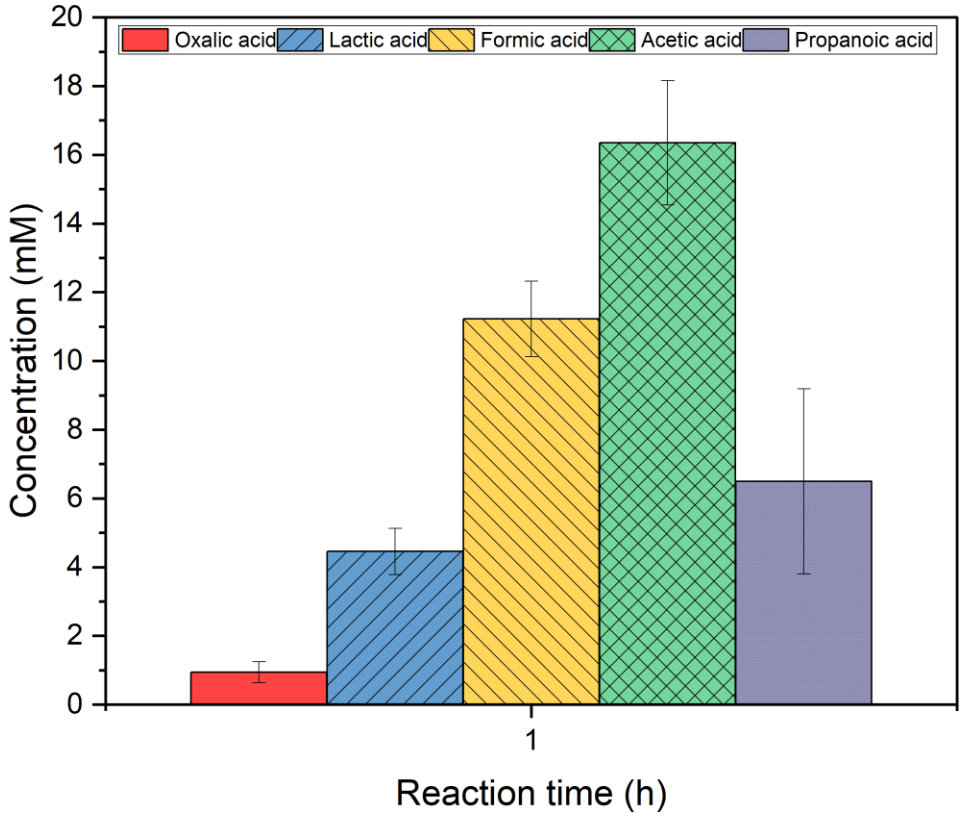

Figure 31: Formed products concentration up to 1 h at 300 ºC; 0.5 M $NaHCO_3$ and 0.05 M $C_6H_{12}O_6$ at 50% filling volume

The formed compounds at 1 h from the highest concentrations to the lowest were acetic, formic, propanoic, lactic, and oxalic acids. The concentrations of the formed compounds were 16.3, 11.2, 6.4, 4.4, and 0.9 mM of acetic, formic, propanoic, lactic, and oxalic acids respectively.

The formed compounds and their relevant concentrations as the reaction time was set to 2 h are presented in figure 34.

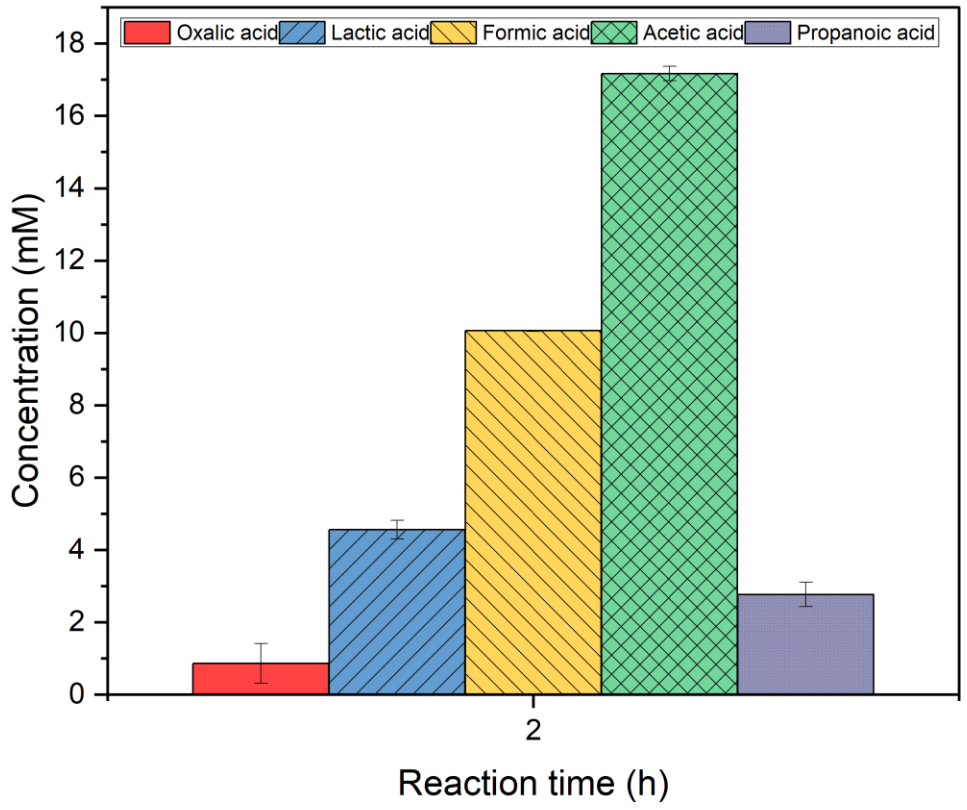

Figure 32: Formed products concentration up to 2 h at 300 ºC; 0.5 M $NaHCO_3$ and 0.05 M $C_6H_{12}O_6$ at 50% filling volume

The order of the formed concentrations at 2 h from the highest to the lowest concentrations were acetic acid with 17.1 mM, formic acid with 10 mM, lactic acid with 4.5 mM, propanoic acid with 2.7 mM and oxalic acid with 0.8 mM.

The formed compounds at the reaction time of 3 h are shown in figure 35.

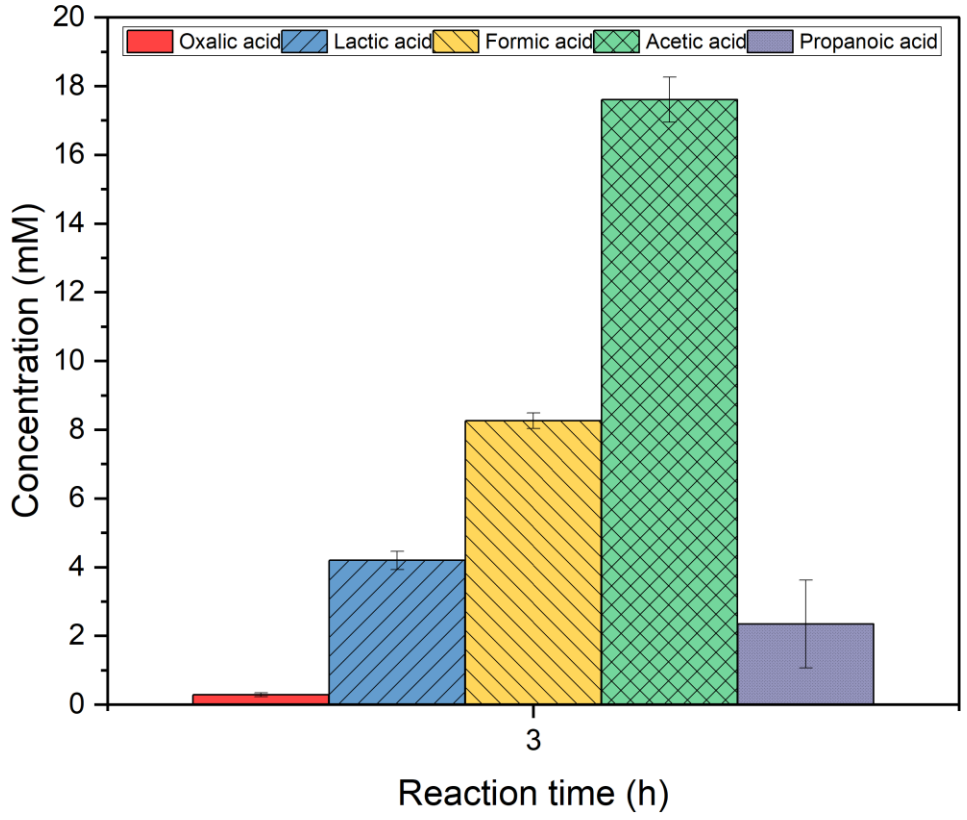

Figure 33: Formed products concentration up to 3 h at 300 ºC; 0.5 M $NaHCO_3$ and 0.05 M $C_6H_{12}O_6$ at 50% filling volume

At 3 h, acetic acid was the highest in concentration with 17.6 mM, formic acid with 8.2 mM, lactic acid with 4.2 mM, propanoic acid with 2.3 mM, and oxalic acid with 0.3 mM.

The formed compounds from all of the tested times at 300 ºC are shown in figure 36 for comparison.

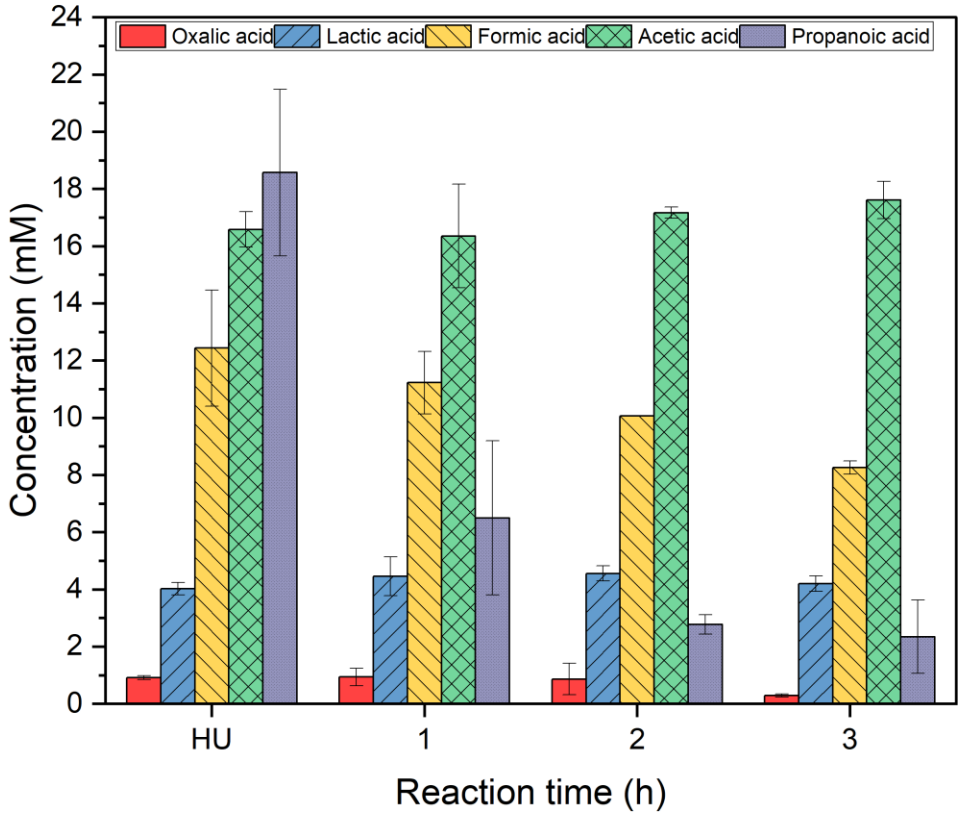

Figure 34: Formed products concentration at different reaction times at 300 ºC; HU: heating period, 0.5 M $NaHCO_3$ and 0.05 M $C_6H_{12}O_6$ at 50% filling volume

While the reaction time seems to have no impact on the concentrations of oxalic and lactic acids at 200 and 250 ºC, this trend changed at 300 ºC. Although oxalic acid concentration remained the same at different reaction times, the lactic acid concentrations improved as the reaction time proceeded past the heating period. Nevertheless, the concentration of formic declined by 10% as the reaction time was increased over the heating period to 1 h. Similarly, the concentration of propanoic acid exhibited decline to reach its lowest point at 3 h. Acetic acid concentration, on the other hand, was slightly increasing as the reaction time progressed to 3 h at 300 ºC. Statistically, the change of all of the formed compounds' concentrations at 300 ºC when reaction time varied, heating, 1, 2, and 3 h, is insignificant. The calculated P-value for oxalic, lactic, formic, and acetic acids are 0.3, 0.6, 0.08, and 0.6 respectively. However, this is not the case for propanoic acid which

concentration changes with respect to the reaction times, heating, 1, 2, and 3 h, is statistically significant with P-value of 0.0043.

In terms of the reactants, figure 37 presents their conversion at the tested reaction times.

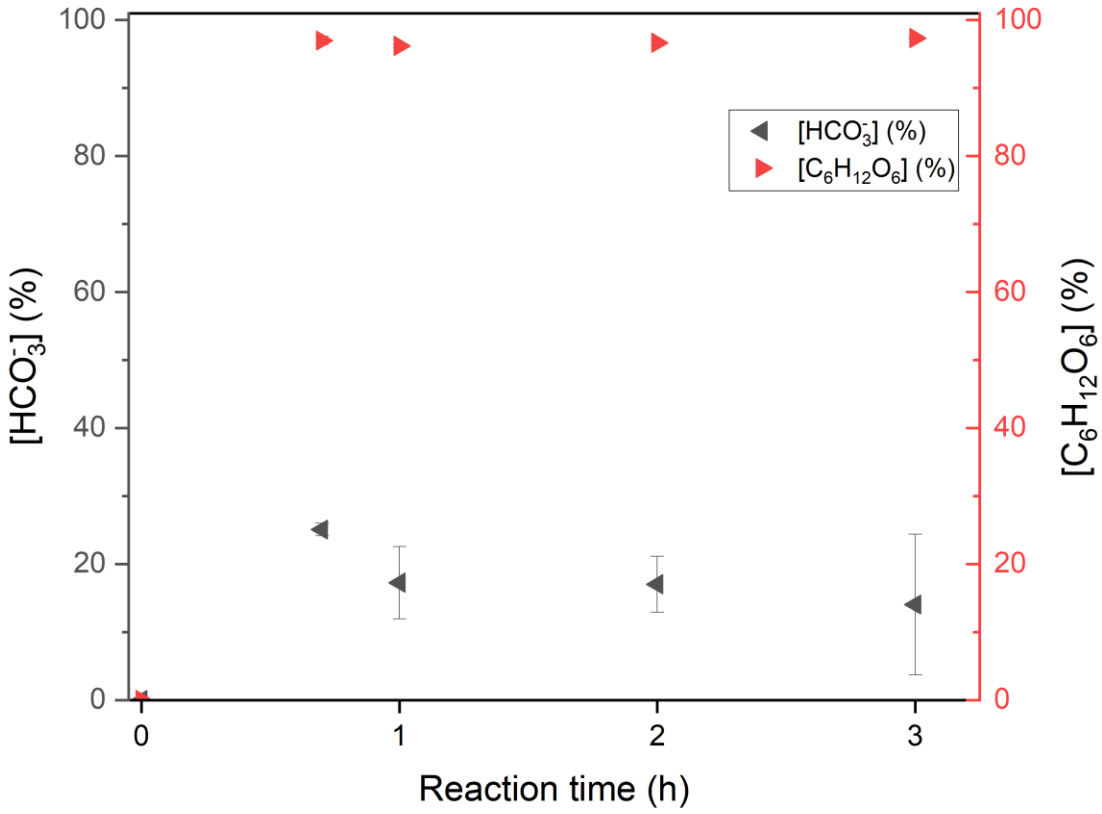

Figure 35: The conversion of the reactants at different reaction times at 300 ºC

As in the previous case at 250 ºC, the conversion of glucose at 300 ºC was similar as in figure 37 above. However, the consumption of bicarbonates exhibited declining behaviors as the reaction time was increased over the heating up period to 1-, 2-, and 3 h.

Unlike the case at 200 ºC where acetone and ethanol were detected, ethanol was the only additional detected in the liquid samples collected from the 300 ºC studies. The average of the detected ethanol in term of peak areas from the RID coupled with HPLC, in mV.min, is illustrated in table 27.

Table 27: Average peak areas obtained from HPLC-RID for ethanol in mV.min

	Ethanol (±)
Heating period	183 (106)
1 h	264 (45)
2 h	288 (38)
3 h	316 (64)

Formic acid concentration declined at 300 ºC as the reaction time increased. This is in agreement with what was reported by multiple studies where formic acid reported to decomposes at higher temperatures.[94], [115], [157] Observing the trend of bicarbonates conversion from figure 37 and relate it to the concentration of formic acid from the figure 36, formic acid concentration was declining as the reaction time increases and that what happens to the consumption of bicarbonates suggesting that formic acid is actually produced from the conversion of bicarbonates instead of glucose. It could also be that the formic acid decomposes into CO_2 and H_2, and as the reaction medium is alkaline, the CO_2 will be in the form of bicarbonates as shown in figure 1 in chapter 1. Unfortunately, a limitation of this study is not testing the gas phase products for the optimization

studies due to low pressure of the process after cooling, it is worth considering a method to investigate the formed products in the gas phase in the future studies.

Propanoic acid concentration declined as the reaction time progressed from the heating period to 3 h. At the same time, there was a slight increase in concentration of the formed acetic acid, especially at 2 and 3 h reaction times. The formation of propanoic acid was explained in the 200 ºC section 4.3 to originate from acetic acid via ethanol, see 200 ºC in chapter 5, The reverse process is shown here, where the decline in the propanoic acid was accompanied by an increase in the concentration of acetic acid as well as the appearance of ethanol as the reaction time progressed from heating period to 3 h at 300 ºC. Since the concentration of both lactic and acetic acid remain unchanged at the tested reaction times, and the fact that propanoic acid concentration declined was accompanied by ethanol inclined, this suggests that the reverse reaction, equation 4.1, took place at 300 ºC. Oxalic, lactic, formic, acetic, and propanoic acids were detected in the collected liquid samples. As the decomposition scheme shows, and based on the obtained products, there are different pathways through which each of the aforementioned compounds can form. The alkali presence in the reaction medium facilitates the isomerization of glucose into fructose while preventing the dehydration of glucose into 1,6-anhydroglucose. [158], [159]

Revisiting scheme 2 under the identification section in chapter 3, oxalic acid can be produced via two routes, via fructose, erythrose, and glyoxal intermediates, or via glycolaldehyde and glycolic acid intermediates. Lactic acid on the other hand can only be obtained via fructose, glyceraldehyde and/or DHA, and pyruvaldehdye. Formic acid, beside the reduction of bicarbonate, can be obtained from different routes such as fructose, erythrose, and formaldehyde intermediates; or glycolaldehyde and formaldehyde intermediates from glucose decomposition. Acetic acid can be produced from glucose decomposition via glycolaldehyde intermediate, or via lactic acid and pyruvic acid intermediates. Propanoic acid can be obtained from the hydrogenation of acrylic acid which is produced via lactic acid dehydration.

Comparing the amount of formic acid produced from the $NaHCO_3$ and glucose with the case in which NaOH and glucose was used, 93% of formic acid was obtained from the CO_2 reduction. The remaining 7% is a comparable amount of oxalic acid to formic acid, ~ 0.7 mM : 0.8 mM, and therefore, the formation of oxalic and formic acid is suggested via fructose and erythrose

intermediates. In other words, formic acid is suggested to be produced via formaldehyde intermediate which agrees with what suggested by Chinchilla et al. [111] Similarly, acetic and propanoic acid has a comparable concentration with approximately 1:1 ratio, both at 15 mM, suggesting their formation via the lactic acid intermediate, via oxidation and dehydration respectively.

5.5. Reaction temperature impact on the products distribution

I. Heating periods

The formed products during the heating period have been shown previously, however, the goal of this is to present the same data in terms of temperature. The resulting products from the heating periods are shown in figure 38.

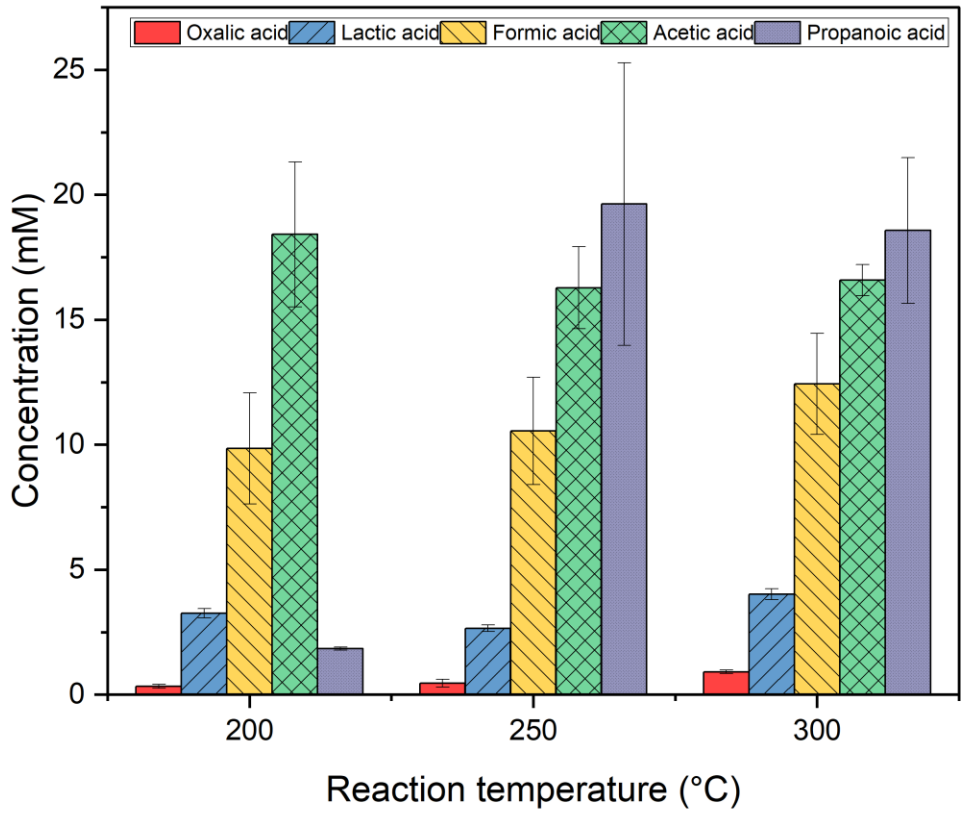

Figure 36: Products formed during the heating periods, 0.5 M $NaHCO_3$ and 0.05 M $C_6H_{12}O_6$ at 50% filling volumes

All of the formed products except for acetic acid have shown an increase in their concentration as the heating period progresses from 200 to 300 ºC. The significant change in concentration among the formed products is for the propanoic acid as the system heated from 200 to 250 ºC. Moreover, at the same time, acetic acid concentration declined slightly as the system heated from 200 to 250 ºC. The decline in acetic acid concentration and the incline in the propanoic acid concentration from 200 to 300 ºC could be related. As the system further heated to 300 ºC, oxalic, lactic, formic, and acetic acid concentrations slightly improved whereas propanoic acid slightly declined.

II. 1 h reaction time

Figure 39 presents the concentration of the formed products as the reaction temperature was 200, 250, and 300 ºC at 1 h.

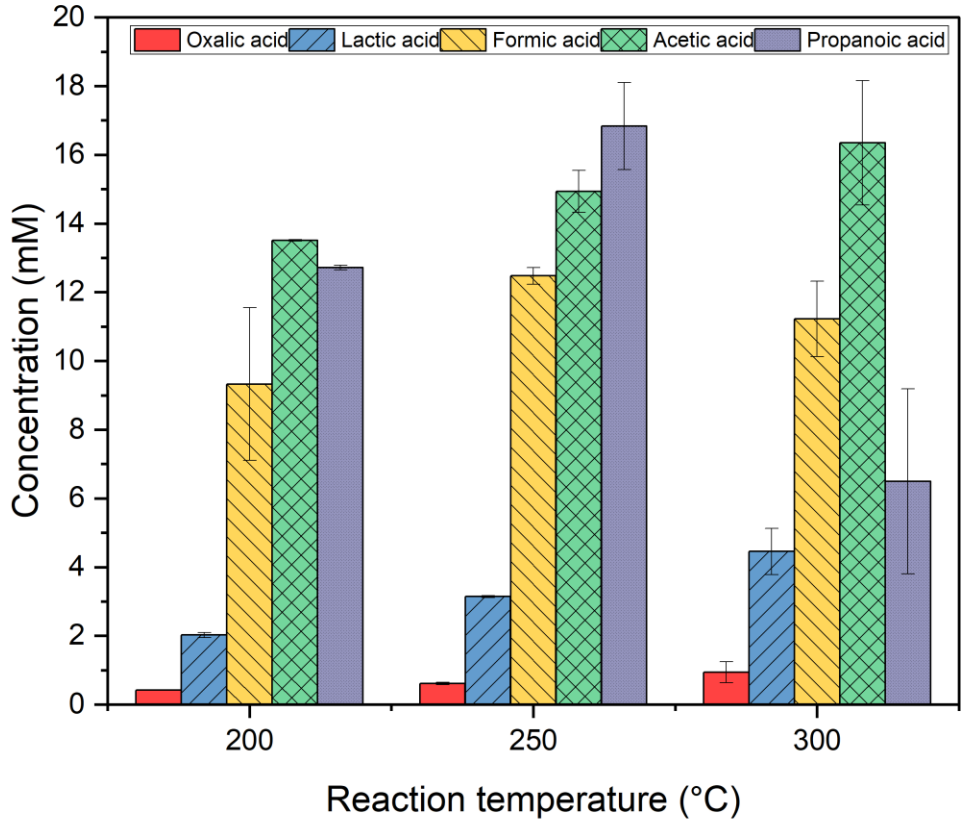

Figure 37: Products formed at 1 h and different temperatures, 0.5 M $NaHCO_3$ and 0.05 M $C_6H_{12}O_6$ at 50% filling volumes

At the reaction time of 1 h, oxalic, lactic, and acetic acids concentrations increase with the temperature suggesting higher temperature favoring for formation. On the other hand, formic and propanoic acids showed a different trend as the reaction temperature increased. Formic acid concentration was better when the reaction temperature increased to 250 ºC, however, further increasing to 300 ºC was not beneficial suggesting decomposition at higher temperature. Similarly, propanoic acid concentration declined as the reaction temperature progressed to 300 ºC. Statistically, the change of all of the formed compounds' concentrations at 1 h when reaction

temperatures varied, 200, 250, and 300 ºC, is significant for lactic and propanoic acids and insignificant for oxalic, formic, and acetic acids. The calculated P-value for oxalic, lactic, formic, acetic, and propanoic acids are 0.13, 0.02, 0.2, 0.2, and 0.02 respectively.

III. 2 h reaction time

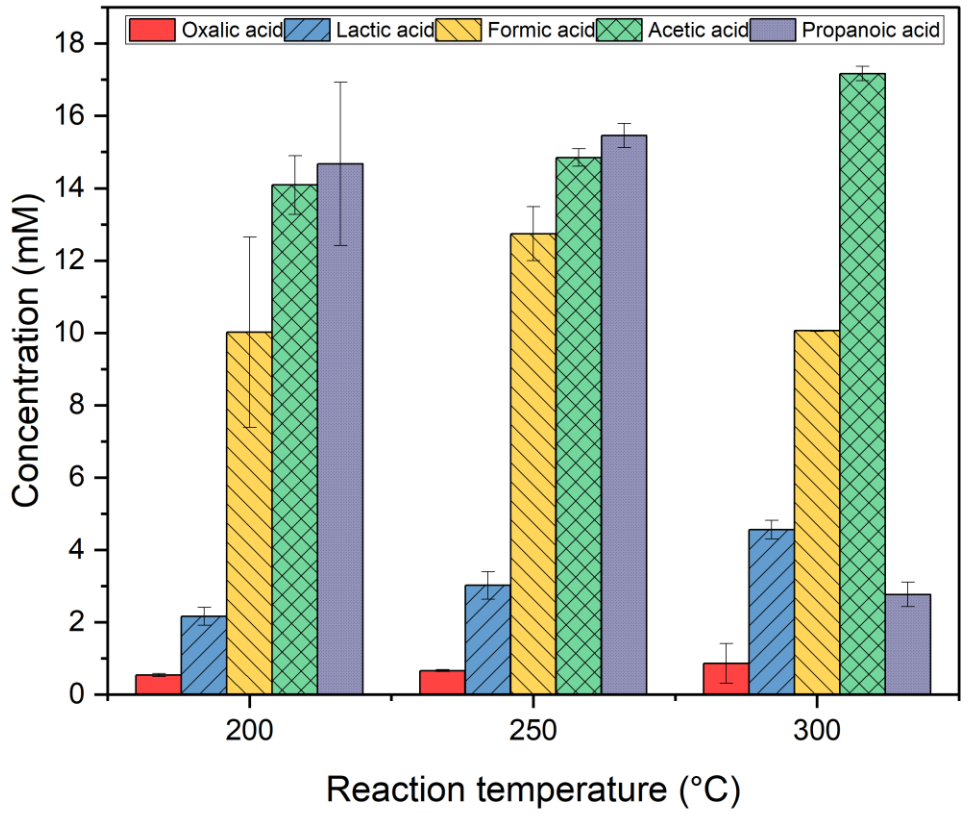

Figure 38: Products formed at 2 h and different reaction temperatures, 0.5 M $NaHCO_3$ and 0.05 M $C_6H_{12}O_6$ at 50% filling volumes

At the reaction time of 2 h, the concentrations of the formed products improved as the reaction temperatures increased from 200 to 250 ºC. However, when the reaction temperature further increased into 300 ºC, the oxalic, lactic, and acetic acid concentrations improved, nevertheless, formic and propanoic acid concentrations declined. Statistically, the change of all of the formed compounds' concentrations at 2 h when reaction temperatures varied, 200, 250, and 300 ºC, is

significant for lactic, acetic and propanoic acids and insignificant for oxalic and formic acids. The calculated P-value for oxalic, lactic, formic, acetic, and propanoic acids are 0.6, 0.009, 0.3, 0.2, and 0.004 respectively.

IV. 3 h reaction time

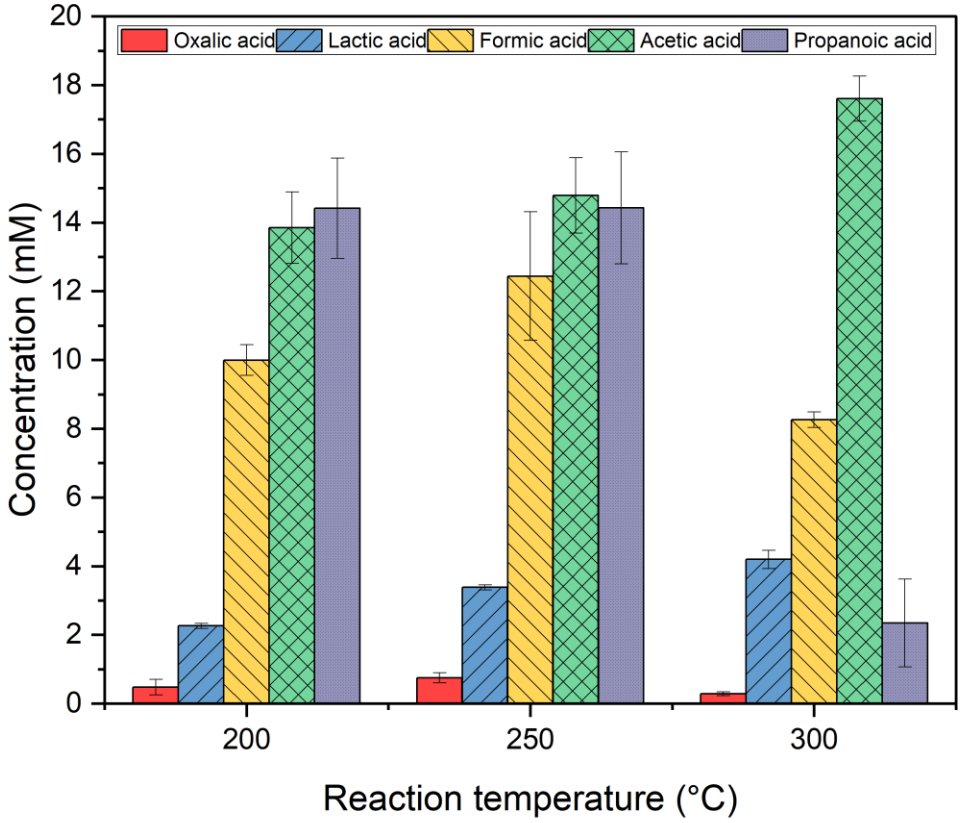

Figure 39: Products formed at 3 h and different reaction temperatures, 0.5 M $NaHCO_3$ and 0.05 M $C_6H_{12}O_6$ at 50% filling volumes

When the reaction time was set to 3 h, the concentrations of oxalic, lactic, formic, and acetic acids improved as the reaction temperature increased from 200 to 250 ºC. However, propanoic acid was specifically showed similar concentration as in 200 ºC. Furthermore, when the reaction temperature increased to 300 ºC, oxalic, formic, and propanoic acids declined in concentrations, whereas lactic and acetic acids improved. Statistically, the change of all of the formed compounds'

concentrations at 3 h when reaction temperatures varied, 200, 250, and 300 ºC, is significant for lactic and propanoic acids and insignificant for oxalic, formic, and acetic acids. The calculated P-value for oxalic, lactic, formic, acetic, and propanoic acids are 0.13, 0.003, 0.07, 0.06, and 0.006 respectively.

Overall, the products distribution of the tested reaction times and reaction temperatures showed different behaviors. All of the products improved as the reaction temperature increased from 200 to 250 ºC. However, increasing the reaction temperature further to 300 ºC presented various behaviors as some compounds further increase in concentrations while other sharply declined. Formic acid and propanoic acids disfavor higher reaction temperatures beyond 250 ºC. Glucose is decomposed into oxalic, lactic, formic, acetic, and propanoic acids. Oxalic, lactic, and acetic acids favor higher reaction temperatures except for oxalic acid at 3 h. In other words, lactic and acetic acids are stable final products whereas oxalic and propanoic acids degraded as the reaction temperature progressed. Formic acid concentration followed an increase to the maximum at 250 ºC and 2 h after which it declined. Therefore, the results obtained present with evidence the optimal conditions for each of the reported products.

5.6. Filling volume: 30, 50, and 70 ml

The filling volume is one of the variables that has been shown to impact the yield of formic acid in processes where metals reductants were used for the CO_2 reduction under hydrothermal conditions. [9], [96], [99] Therefore, the filling volume was varied in this study to see its impact on formic acid as well as the other formed products. 30, 50, and 70 %, or ml, were tested while keeping the concentration of the reactants fixed, the reaction time at 2 h, and the reaction temperature at 250 ºC. Figure 42 illustrates the behavior of the formed products as the filling volume varied.

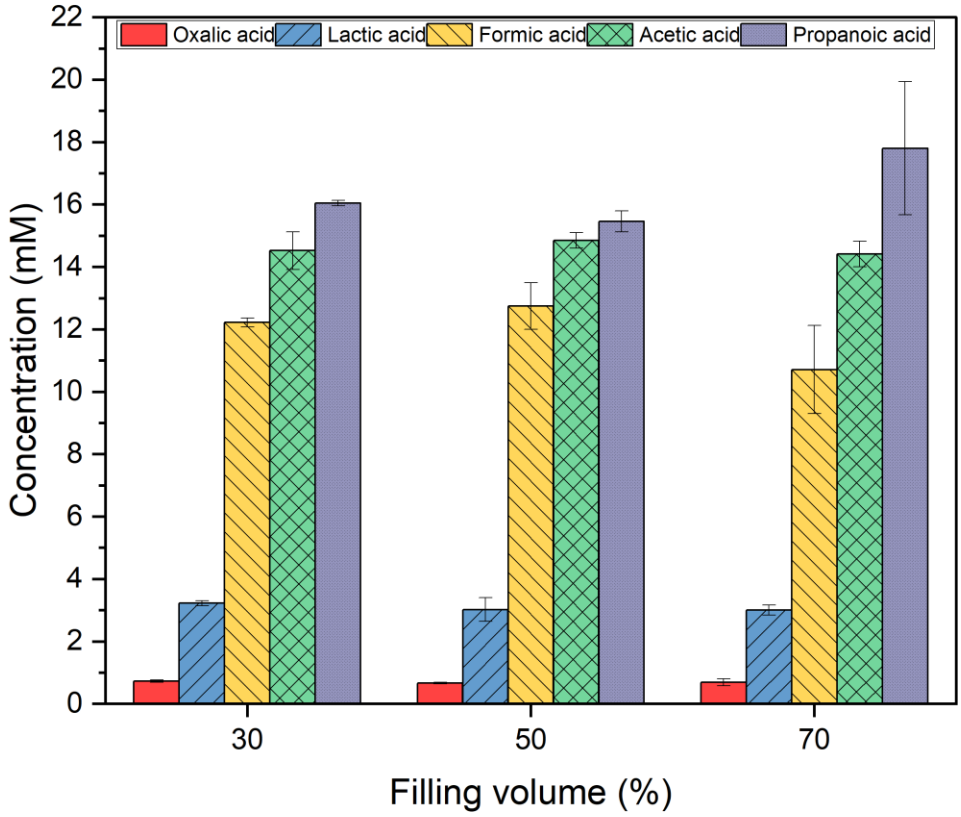

Figure 40: Formed products concentration at different filling volumes; initial concentrations 0.5 M $NaHCO_3$ and 0.05 M $C_6H_{12}O_6$; 2 h reaction time; at 250 ºC

Statistically, the change of all of the formed compounds' concentrations at 250 ºC and 2 h when reactor filling volume varied, 30, 50, and 70 %, is insignificant for oxalic, lactic, formic, acetic, and propanoic acids. The calculated P-value for oxalic, lactic, formic, acetic, and propanoic acids are 0.7, 0.6, 0.2, 0.6, and 0.3 respectively.

The conversion of the reactants at different filling volumes is presented in figure 43.

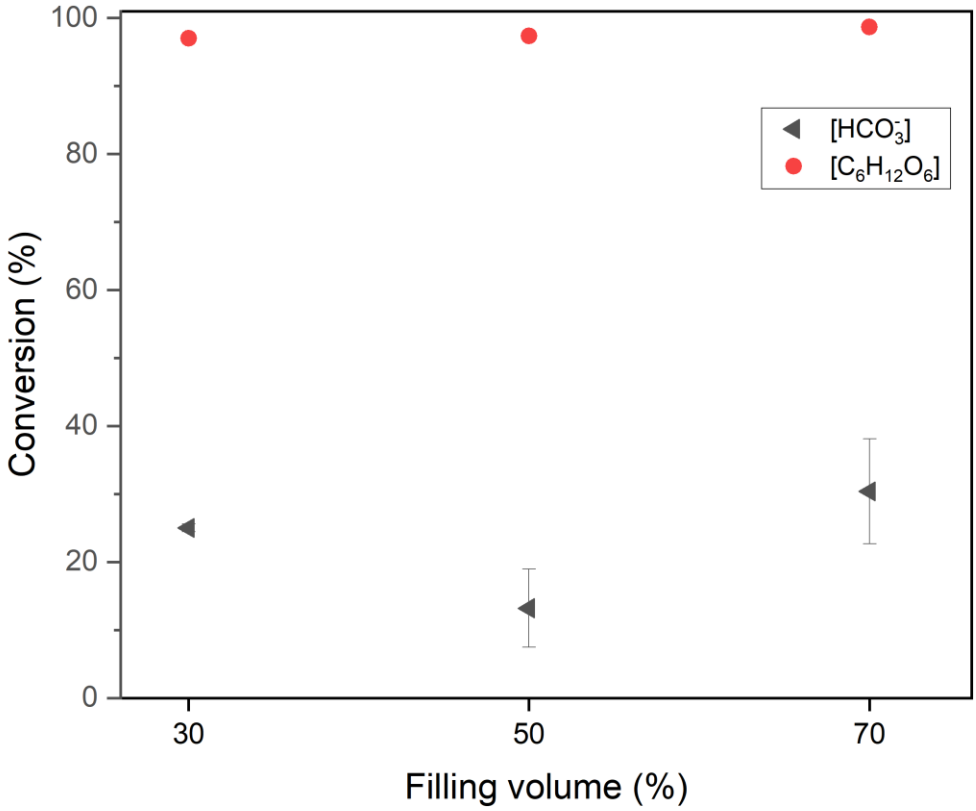

Figure 41: The conversion of the reactants at different filling volumes at 250 ºC and 2 h

The conversion of the reactants at different filling volumes, as shown in figure 43, was constant for glucose, however, for bicarbonates, the conversion declined when the filling volume was 50% compared to the other cases at 30 and 70%. As there was not a significant change in the concentrations of the formed products when the filling volume was varied, the discrepancy in the conversion of bicarbonates could be due to experimental error.

Generally speaking, the filling volume did not significantly impact the formed products. Although the filling volume did not significantly impact most of the products, lactic and propanoic acids were shown to have improved in their concentrations at higher filling volume of 70%. Additionally, formic acid concentration decreased as the filling volume increased to 70%.

Glucose is a biomass, and although filling volume was reported in the literature to impact the formic acid yield when $NaHCO_3$ and metal reductants were used, [9], [96], [99] this was not the case for biomass reductants. In fact, Yang et al. reported constant yield formic acid at different filling volumes when 2-pyrrolidone was used as a reductant.[160] In the studies where metal reductants were used, [9], [96], [99] the yield of formic acid was reported to increase as the filling volume was increased.

When metal reductants were employed as in the studies in literature, the metals undergo oxidation and thus resulting in a production of hydrogen gas, the hydrogen gas increases the pressure of the process and thus favoring the yield of formic acid by shifting the equilibrium toward formic acid in the CO_2 hydrogenation into formic acid reaction. Additionally, for the metal reductants studies, when the filling volume increases, less headspace, i.e. empty volume inside the vessel, is available for the produced hydrogen gas and thus higher pressure is achieved as pressure and volume inversely correlated, $P \propto \frac{1}{V}$.

This is not the case here as glucose is unlike metal reductants, it does not produce hydrogen and thus no increase in the pressure of the process was observed. The pressure in this study remains constant as the only variable that affects it is the temperature which is fixed in the filling volume studies. In fact, the mechanisms of reactions take place between metal reductant and biomass reductant are different. For example, in metal reductants cases, formic acid is produced by bicarbonate reduction via the electrons released upon metal oxidation. On the other hand, for glucose reductant case, the products of glucose decomposition are what undergo oxidation or other reactions and thus reducing bicarbonate into formic acid. Therefore, this presents one of the differences in controlling variables that affect the production of formic acid from the reduction of CO_2 under hydrothermal conditions when utilizing metals and non-metals reductants.

5.7. Source of formic acid

In all of the conducted reactions, there are two sources of carbon, sodium bicarbonate and glucose. The possible reactions to occur at the studies conditions which could produce formic acid are: i) reduction of CO_2 and ii) glucose decomposition. It is of great importance to trace the origin of formic acid in order to precisely obtain the yield, understanding the reaction mechanism, as well

as monitoring the source of formic acid along with formic acid concentrations in subsequent studies.

There are two ways to investigate the source of formic acid, by controlling the pH of the medium, or by using labelled reagents. In the typical reaction using $NaHCO_3$, the pH of the starting materials is about 8.3. Therefore, a way to test if formic acid originated by glucose, same reaction procedure should be followed, the only exception is replacing $NaHCO_3$ by NaOH aiming for a starting pH of 8.3. Furthermore, labelling materials with isotopes of carbon for instance could be utilized here and then analyzed by a special technique like nuclear magnetic resonance spectroscopy, NMR.

5.7.1. Starting material pH control studies

Maintaining the pH at 8.3 without using $NaHCO_3$ was conducted to test if formic acid can be produced. Sodium hydroxide, NaOH, was used to control the pH of the medium. First, a solution of 1 M NaOH was prepared, and then the required volume needed to adjust the pH to 8.3 was added to the mixture and charged into the reactor.

The same procedure as in the typical reactions was followed, and the collected liquid samples were analyzed using HPLC. The results from these studies are to be compared with the original reactions, $NaHCO_3$ and glucose, to see how much formic acid is formed in the pH control studies. Figure 44 illustrates the formed formic acid from the pH control studies as well as the original reactions, at 250 ºC, 2 h, and 50% filling volume.

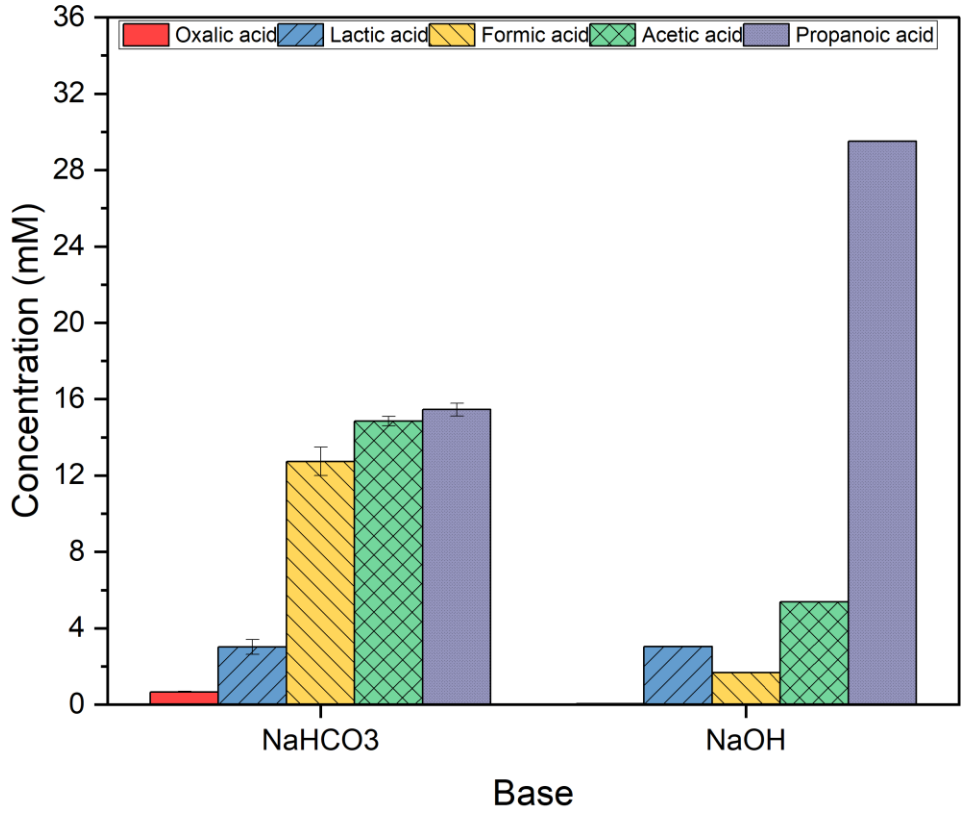

Figure 42: Formed products from different bases $NaHCO_3$ and NaOH at 250 ºC, 2 h, and 50% filling volume. (0.5 M $NaHCO_3$, and 0.05 M $C_6H_{12}O_6$)

As shown in figure 44, the same identified compounds also formed when NaOH was used except for oxalic acid. It is also worth noticing that the consumption of glucose in both studies, with NaOH and with $NaHCO_3$, were about the same, averaging 0.0485 M of glucose consumed. Since formic acid was the compound of interest, 6% of formic acid was produced when NaOH was used to adjust the pH of the medium in the presence of glucose.

Comparing the concentrations of the formed compounds while varying the base type, propanoic acid was the highest in concentration, 9.4 mM, followed by acetic, 2.7 mM, lactic, 1.5 mM, and formic, 0.8 mM, acids when NaOH was used to maintain the pH of the starting medium at 8.3. On the other hand, the order of the produced compounds when sodium bicarbonate was used were

propanoic, acetic, formic, lactic, and oxalic acids. It is also worth noting that pH was measured pre and post the reaction, and there was a decline from 8.3 to about 3 after the reaction.

Formic acid was produced in low concentration when the NaOH was used instead of $NaHCO_3$, 1.6 mM versus 12.7 mM for NaOH versus $NaHCO_3$ respectively. Similar observation was reported by Fernandez et al. 2018, where NaOH effect was investigated, and thus formic acid was found to be produced from $NaHCO_3$ reduction rather than glucose decomposition. [17] Note that there is a difference in the reaction temperature between this work and Fernandez et al. 2018, 250 ºC vs. 300 ºC. One observation to be mentioned here is the pH of the solution post the reaction. In the literature, there is no report on the pH of the solution after the reaction, thus, measuring the pH of the products medium for both NaOH controlled as well as $NaHCO_3$ studies was carried out. It turns out that pH of the NaOH controlled study was acidic, pH less than 3, whereas the other case, $NaHCO_3$, was basic, pH over 8. Therefore, confirming the source of formic acid using pH control method is incomparable with the case where $NaHCO_3$ was used despite the initial pH values being the same. In other words, when using $NaHCO_3$, the pH stays in alkaline region throughout the reaction. Therefore, similar future studies are encouraged to employ a buffer agent to maintain the pH throughout the reaction in order to mimic the original case in which $NaHCO_3$ was used.

5.7.2. Labelling studies

An alternative way of using labelled reagent was also carried out to trace the origin of formic acid. Labelled sodium bicarbonate, $NaH^{13}CO_3$, was used instead of normal $NaHCO_3$ and the liquid samples were probed by NMR to trace the source of carbon in formic acid.

The collected liquid samples from the labelled studies were analyzed by HPLC-UV-VIS to compare them with the unlabeled samples before analyzing them using NMR, 30° pulse sequence. The results of the formed products from both labelled and unlabeled samples, duplicated, are presented in terms of average peak areas in table 28.

Table 28: Average peak area for selected products, 250 ºC, 2 h, 50% for labelled and unlabeled studies, (OA: oxalic acid, LA: lactic acid, FA: formic acid, AA: acetic acid, PA: propanoic acid)

	Peak area (mAU.min)	
	Labelled	**Unlabeled**
OA	332.22	540.86
LA	233.09	282.26
FA	251.87	552.16
AA	317.99	451.50
PA	463.16	627.02

Results from the labelled and unlabeled studies from the HPLC-UV-VIS are in disagreement although the same procedure for both studies were identical as shown in table 28. Formic acid is the target compound for tracing here and has different peak areas when the samples from labelled and unlabeled studies were compared. In fact, formic acid concentration in the labelled studies is about half the concentration of formic acid in unlabeled studies. The same case is observed for oxalic acid with about 38% difference. Nevertheless, lactic acid has comparable results from labelled and unlabeled studies, less than 18% difference, and acetic and propanoic acids have difference within 30% for both cases.

It is worth testing the behavior of the starting materials using HPLC in order to compare the cases of labelled and unlabeled studies to ensure they are comparable. Table 29 presents the average values of the obtained peak areas for bicarbonate, HCO_3^-, and glucose, GL.

Table 29: Starting materials peak area (in mV.min), 0.5 and 0.05 M SB and GL from HPLC-RID

	Starting material		
	Labelled	**Unlabelled**	**Diff (%)**
HCO_3^-	8910.4	8978.6	0.8
GL	2956.5	2851.6	3.7

As table 29 shows, the respond of the detector for reactants in both labelled and unlabeled studies was comparable. Less than 1% change between the labelled and unlabeled samples for bicarbonate, HCO_3^-, and less than 4% change between the labelled and unlabeled samples for glucose, GL.

Since there was a difference in the concentration of formic acid between labelled and unlabeled samples detected by HPLC, it might be worthless to proceed with NMR as the samples were incomparable. However, the same conclusion was obtained from the NMR analysis in which the labelled samples had lower formic acid concentration than the unlabeled samples as shown in figure 45.

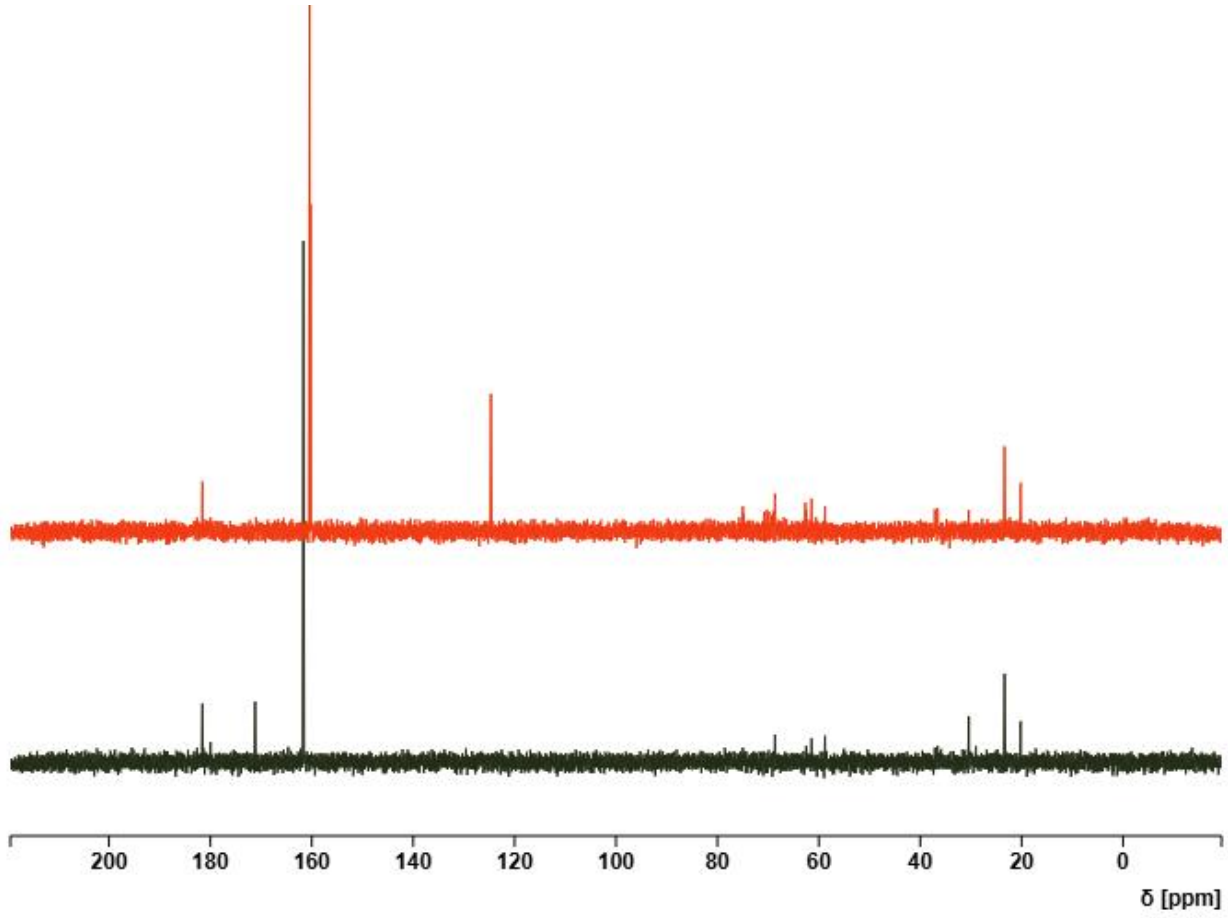

Figure 43: NMR ^{13}C results for labelled (red/top spectrum) and unlabeled (black/bottom spectrum) samples

The peak at about 171 ppm is assigned to formic acid, and as in figure 45, the concentration of formic acid in the sample from the labelled studies, spectra in red, is lower than the concentration of formic acid obtained from the unlabeled studies, spectra in black. This confirms the same conclusion obtained from the HPLC analysis that the concentration of formic acid in the labelled samples is lower than the unlabeled samples.

There was variation in the concentration of formic acid between the labeled ^{13}C samples and the unlabeled ones. NMR analysis was used in various studies to trace formic acid by employing labelled CO_2. In fact, there are disagreements in the previous studies on the origin of formic acid at hydrothermal reduction of CO_2 using glucose. Fernandez et al. 2018 showed that $NaHCO_3$ is the source from which formic acid was reduced.[17] On the other hand, Konstantinova, 2022 and suggested that more than 95% of the formed formic acid was from the degradation of glucose.[115]

Nevertheless, Chinchilla et al. 2022 report was between the aforementioned extremes by suggesting that about 35% of the formed formic acid originated from the reduction of formic acid.[111] All of the aforementioned studies did not report analyzing liquid samples collected from labelled and unlabeled studies using HPLC. Kinetic isotope effect, KIE, could be the reason for the variation in formic acid concentration when the labeled ^{13}C agent was used in this study. In KIE, the difference in mass changes the outcome of the reaction which makes it a useful tool used in kinetic studies to determine reaction pathways. Nevertheless, deuterium, D_2, is usually used in kinetic studies as it has 2 protons compared to ^{1}H which results in noticeable effect.[161] In fact, labelled carbon, ^{13}C, has been reported to have insignificant impact as the KIE was reported in different studies to not exceed 1.1.[161]–[163] Therefore, other than KIE may be the reason of the decline in the concentration of formic acid when labelled ^{13}C was used and that question to be answered in similar future work.

5.8. Conclusion

Optimization studies were conducted at three reaction temperatures, 200, 250, and 300 ºC at three different reaction times, 1, 2, and 3 h including the heating periods. As the volume of the vessel in this work is bigger than what was used in similar studies in literature, longer heating periods were expected for each set of reactions to reach the set point. Since longer time was needed to heat up the system, there was a possibility of glucose decomposition during the heating period, therefore, studies of the products formation from heating periods were conducted. Carboxylic acids, namely oxalic, lactic, formic, acetic, and propanoic acids were detected in the liquid samples from heating studies. This presents a way to produce comparable concentrations of any of the aforementioned compounds during the heating periods without the need for longer reaction time.

Formic acid is the main target compound in this study, thus, the optimal conditions among the tested temperatures and reaction times were 250 ºC, 2 h, and 50% filling volume where formic acid concentration reached about 13 mM. Filling volume was tested as it was reported to impact the yield of formic acid when metal reductants were used. Therefore, additional set of studies were conducted in which the filling volume of 30 and 70% were probed to investigate the effect on the yield of formic acid. It turned out that filling volume had insignificant impact on the yield of formic acid as its concentration was slightly affected.

In this study, there were two sources of carbon from which formic acid can be produced, bicarbonate and glucose. Therefore, it is essential to trace the origin of formic acid to better understand the reaction mechanism and thus clearly suggest the reaction pathway. Thus, two sets of studies were carried out to trace the source of formic acid, first, by maintaining the initial pH of the reactant at 8.3 while using NaOH in replace of $NaHCO_3$, second, by employing a labelled $NaH^{13}CO_3$. The results of pH control studies showed that about 93% of the formed formic acid originate from the reduction of bicarbonate. Unfortunately, the labelled studies carried out in this were misinformative as the concentration of formic acid is incomparable between the labelled and unlabeled samples as shown by both HPLC and NMR.

Chapter 6: Role of Metal Reductants on Formic Acid Production

6.1. Influence of the metals on the reaction

The addition of zero-valent metals to the hydrothermal conversion of CO_2 into formic acid is hypothesized to have two main effects. First, the formation of H_2 gas from reducing H_2O as well as reducing the reactant, $NaHCO_3$, into formate salt, $HCOO^-$ which can be further hydrogenated into the desired final product, formic acid, HCOOH. Second, the formed metal oxide would act as a catalyst for the production of formic acid as it was shown by Chinchilla et al. 2022 where formic acid yield was 49% and 45% for Fe_3O_4 and Fe_2O_3 respectively compared to 44% with no catalyst. [111] The standard reduction potential, E^o, of the Fe, Zn, and Al are -0.04, -0.763, and -1.67 V respectively. [106] The more negative the E^o the greatest the ability to donate electrons.

6.2. Results and discussion

6.2.0.1. The conversion of sodium bicarbonate

The conversion of the starting materials exhibited variation for different metals used. Table 30 shows the conversion of bicarbonate, and glucose for no metal, N/A, Fe, Zn, and Al studies.

Table 30: Reactants conversion in % of no metal, N/A, Fe, Zn, and Al studies; 0.5 M $NaHCO_3$ and 0.05 M $C_6H_{12}O_6$ at 50% filling volume with 1:6 mmol ratio of $NaHCO_3$:metal

	N/A	**Fe**	**Zn**	**Al**
Glucose	97.4	99.0	99.2	97.8
HCO_3^-	13.2	32.3	14.9	50.9

The conversion of sodium bicarbonate can be monitored by observing the concentration of it post the reaction and compare it with its initial one. As table 30 shows, different behaviors were observed on different metals. For the Fe, Zn, and Al cases, the conversion of bicarbonate was approximately 0.16, 0.0744, and 0.2547 M respectively indicating that the highest quantity of bicarbonate was consumed in the presence of Al.

For the case in which only bicarbonate and Zn were tested, the same amount of bicarbonate was consumed, with the average of 0.0748 M. It is worth noting that formic acid was the only liquid formed in the liquid phase sample analyzed for the case in which only bicarbonate and Zn were tested.

6.2.0.2. The conversion of glucose

Similarly, the conversion of glucose for different metals can be monitored by observing the final concentration of glucose and comparing it to its initial state. Unlike sodium bicarbonate, glucose exhibited the same conversion behavior regardless of the metal used. The average conversion of glucose in all of the tested metals was about 0.0493 M.

6.2.1. Fe

Iron powder was used as a reducing agent in this work to see its impact on the formation of the formed products, especially formic acid. Figure 46 illustrates the concentration of different formed products when no metals were added.

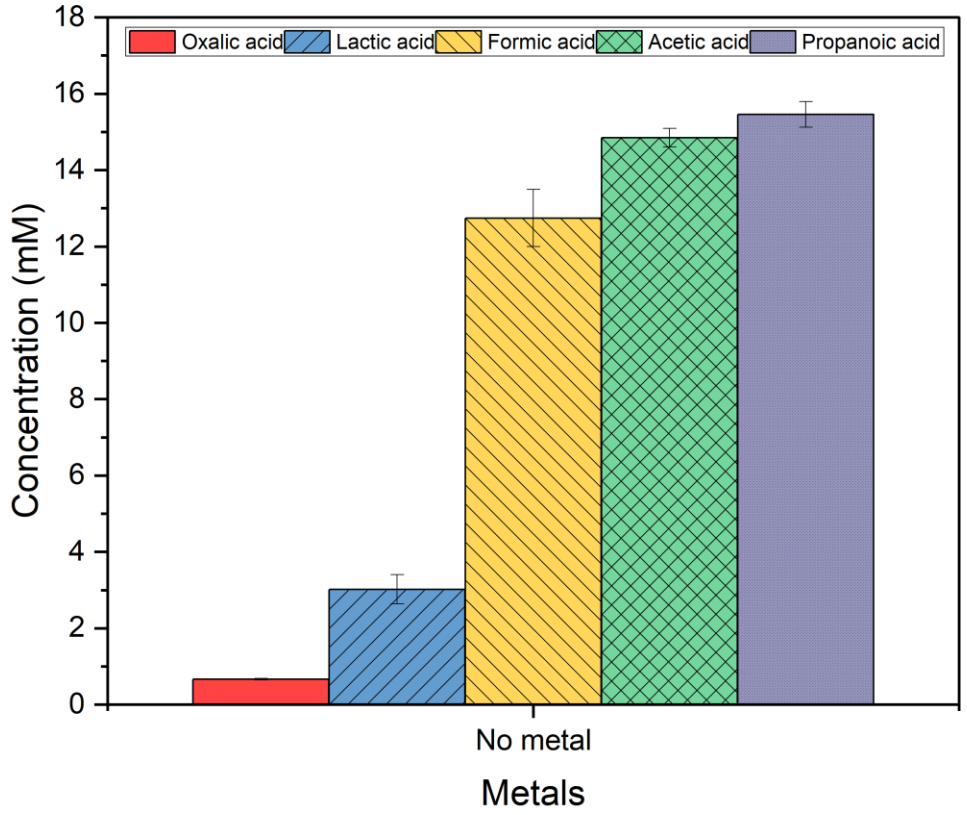

Figure 44: The formed products with no metal; 250 ºC, 2 h, 0.5 M $NaHCO_3$ and 0.05 M $C_6H_{12}O_6$ at 50% filling volume

The formed compounds ordered by their concentrations from the highest to the lowest were propanoic, acetic, formic, lactic and oxalic acids with concentrations of 15.4, 14.8, 12.7, 3, and 0.6 mM respectively.

Figure 47 illustrates the concentrations of the formed compounds when Fe reductant was added.

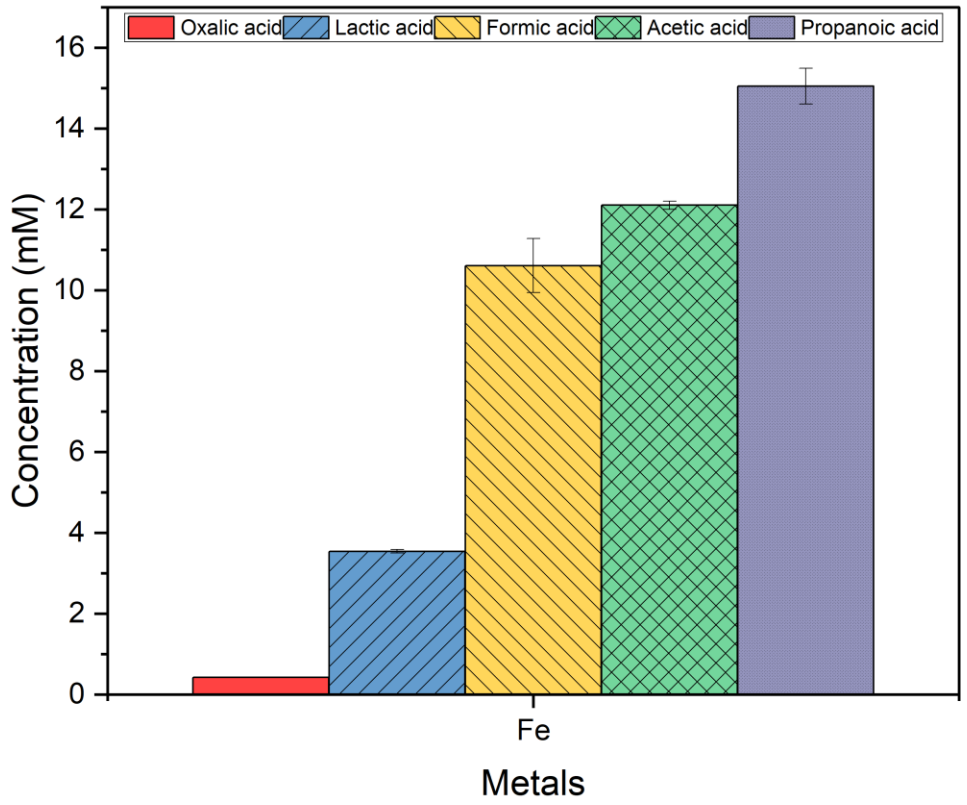

Figure 45: Fe addition effect on the formed products concentrations; 250 ºC, 2 h 0.5 M $NaHCO_3$ and 0.05 M $C_6H_{12}O_6$ at 50% filling volume with 1:6 mmol ratio of $NaHCO_3$:Fe

The order of the compounds based on their concentrations when Fe was added were propanoic, acetic, formic, lactic, and oxalic acids. The concentrations of the formed compounds were 15, 12.1, 10.6, 3.5, and 0.4 mM of propanoic, acetic, formic, lactic, and oxalic acids respectively.

Figure 48 presents the formed compounds from both cases, with and without Fe metal, for comparison.

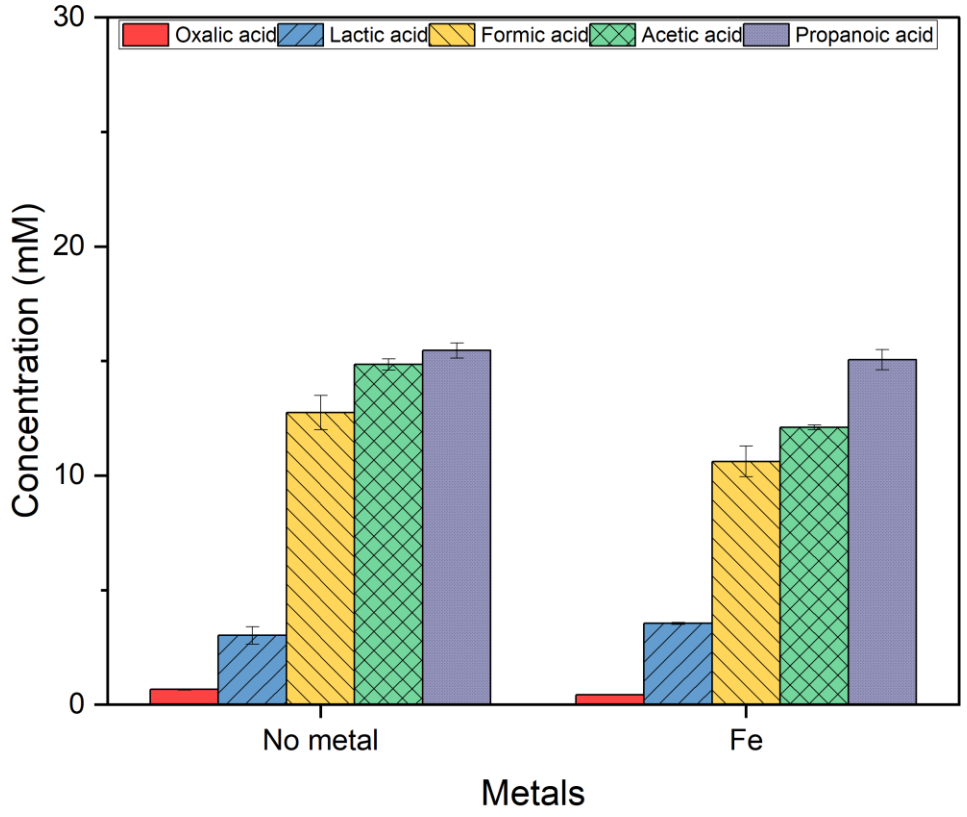

Figure 46: Fe addition effect on the formed products concentrations versus no metal; 250 ºC, 2 h 0.5 M $NaHCO_3$ and 0.05 M $C_6H_{12}O_6$ at 50% filling volume with 1:6 mmol ratio of $NaHCO_3$:Fe

As in figure 48, the same formed products from the case in which no metal was added formed when Fe powder was used as a reductant. Some compounds exhibited differences in the concentration at the compared two cases whereas others remain unchanged. Specifically, oxalic, lactic, and propanoic acids remained unchanged in both cases suggesting that Fe addition has no impact on the production of these compounds. On the other hand, formic and acetic acids concentrations declined when Fe metal was added suggesting influence of Fe on the production of formic and acetic acids. Statistically, the change of all of the formed compounds' concentrations at 250 ºC and 2 h at 50% filling volume when Fe reductant was added, is significant for oxalic and acetic acids and insignificant for lactic, formic, and propanoic acids. The calculated P-value for oxalic, lactic, formic, acetic, and propanoic acids are 0.006, 0.2, 0.09, 0.005, and 0.4 respectively.

To have a clear picture of what happened in both cases, with and without metal Fe addition, products in the gas phase should be monitored too. Thus, table 31 shows the pressure of the process in both cases at time zero, the beginning of the reaction at the desired reaction temperature, which is the same throughout the reaction, and at the end when the reactor cooled down to room temperature.

Table 30: Process pressure at different studied cases, Fe vs. no metal addition

Case	**Pressure at t=0 (barg)**	**Pressure post reaction after cooling (barg)**
No metal	40	<=10
Fe powder	40	<=10

Data from table 31 can be used as a first indication of the compounds formed in the gas phase. For the case in which metal Fe was added, the process pressure exhibited the same behavior as the case in which no metal was added.

The gas-phase products after the reactions were scanned by drawing a gas sample of the process post the reaction and after cooling the system to room temperature and running it through a mass spectrometer, MS, to see what compounds have formed in the gas phase for both Fe and without metal cases. Analysis of the gas phase sample using the MS can be shown in figure 49.

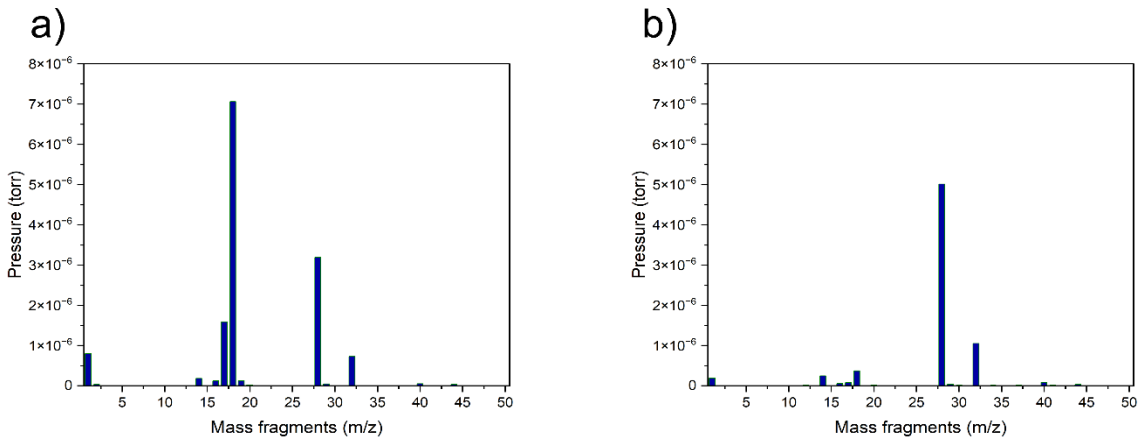

Figure 47: Gas phase products for the case where Fe was used (a) and with no Fe (b), collected from 250 ºC, 2 h, and 50% filling volume once cooled to room temperature ($NaHCO_3$: Fe is 1:6 mmol)

The constituents of the gas phase sample for the case where Fe was added in mass/charge, m/z, are: 1, 2, 14, 16, 17, 18, 19, 20, 28, 29, 32, 40, and 44 which represent H_2, water vapor, CO and O_2, as the proportion of O_2 to N_2 in this case does not represent air, Ar, and small amount of CO_2 . On the other hand, for the case in which no Fe was used, the m/z are: 1, 14, 16, 17, 18, 28, 29, 32, and 40 which represent H_2, water vapor, air, and small amount of Ar gas. The gas-phase products for the no metal case, figure b in figure 49, represent a typical thermal degradation which fits perfectly for glucose decomposition. However, when Fe was added, more fragments are present in the gas-phase suggesting catalytic behavior. The dominant fragments ion in each case is CO for the no metal case, and water vapor for the Fe addition case. Comparing the Fe addition case with no metal case, there was an increase in hydrogen and a decline in the CO observed in the no metal case.

The collected solid sample, Fe metal, was filtered, washed and dried before XRD analysis. The XRD analysis was conducted to investigate the oxidation occurring to the metal Fe from the hydrothermal reaction. Figure 50 presents the XRD result for the collected Fe sample.

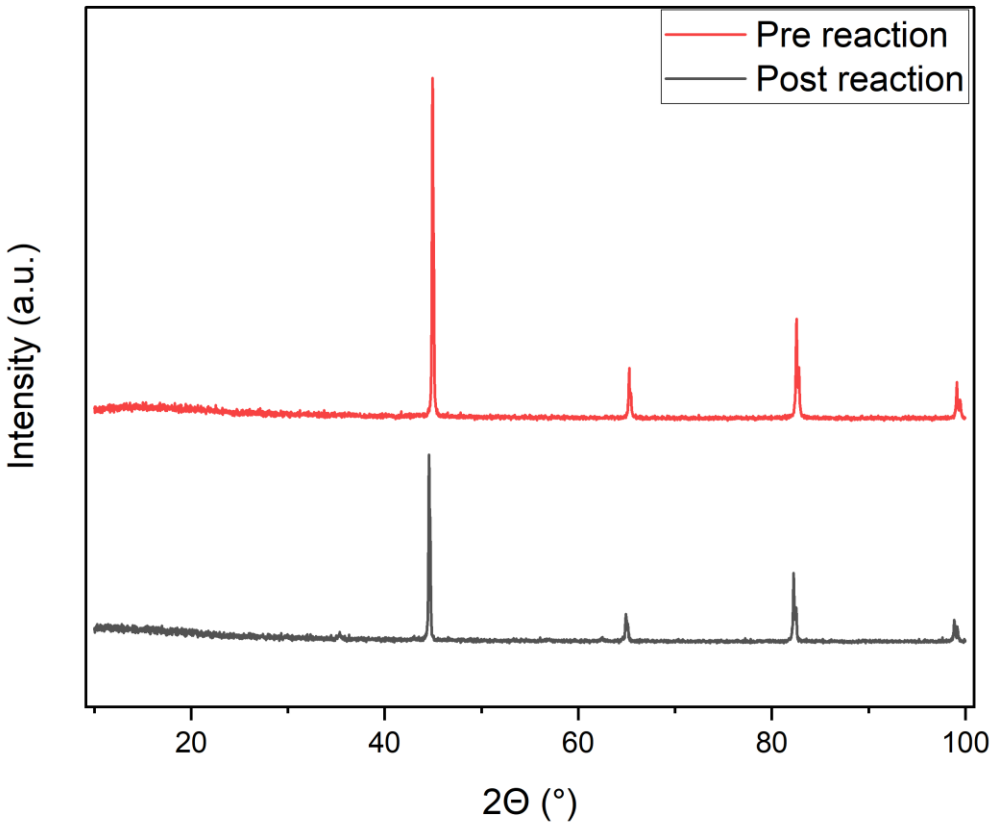

Figure 48: Fe metal solid sample pre reaction (top) and post reaction (bottom) at 250 ºC, 2 h, and 50% filling volume

XRD analysis for the collected solid sample from the Fe addition reactions have peaks at 35, 44, 62, 65, 82, and 99º as shown in figure 50.

The addition of Fe metal to the reaction of $NaHCO_3$ and glucose at 250 ºC, 2 h, and 50% filling volume was not beneficial as the concentration of all of the formed products declined except for the lactic acid which slightly improved to 3.5 mM from 3 mM where no Fe was used. Fe addition was shown to improve the yield of formic acid in different studies. For instance, Duo et al. 2016 showed that Fe addition was beneficial for the formic acid production under hydrothermal conditions as the yield was reported to reach 90%.[96] Additionally, another study reported formic acid yield of 40% when Fe was used as a reductant to the hydrothermal reduction of CO_2 into formic acid. [97] Nevertheless, the main difference between the aforementioned studies and this

work is the glucose as an additional reductant. An explanation could be that two reductants, Fe and glucose, compete against each other leading to retardation of the products would normally form when one of them is used alone as in scheme 4.

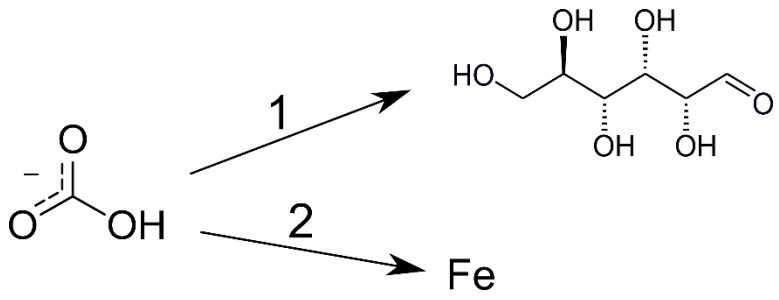

Scheme 4: Competition between two reductants to react with bicarbonate

As in scheme 4, a bicarbonate molecule would react with either glucose or glucose-decomposed products in the case in which no Fe is added. However, when Fe is added, this present another reactant for bicarbonate molecule and thus, the normally produced products from the no Fe addition case would naturally vary when Fe is added and this explains the variation in the concentration of the formed products between the two cases as shown in figure 48. Additionally, the reason for formic acid production improvement when Fe was used in literature was attributed to the formation of hydrogen gas as an indicator of the metal being oxidized. This was not the case here as the pressure was monitored throughout the reaction and there was no change in the pressure when compared to the case in which no Fe was used as illustrated in table 30. This suggests that the formation of hydrogen gas during the process may not occur as suggested by pressure readings. Moreover, a further indication of low oxidation of Fe is the amount of hydrogen present in the collected gas-phase samples as in figure 49. Furthermore, XRD of the collected Fe post the reaction confirms this where the intensity of the oxidation of Fe is low, small peak at 34-35º which represents Fe oxide in figure 50, compared to the reported similar studies with Fe only.[9] In XRD, small peak area indicates lower concentrations of the target compound in the scanned sample. Although Jiang et al. 2017 reported Fe_3O_4 peaks at around 30, 35, 57, and 63º 2θ, and here only the one at about 35º 2θ is present, that is because the tested temperature and initial ratio of water:Fe in Jiang et al. 2017 work were 300 ºC for 2 h reaction time and 2 ml:6 mmol, 250 ºC and 50 ml: 8 mmol in this work. [9] It is also worth mentioning that Fe oxidation favors high temperatures T ≥

275 ºC. [96] which explains the case in this work as the reaction temperature tested for Fe addition is 250 ºC.

6.2.2. Zn

Zinc, Zn, was another metal used in this work to see its impact on the formed products. As was the case when Fe was used, the type products formed from the Zn addition are similar to the other cases with Fe and with no metals added. Figure 51 presents the concentration of various products at no metals case.

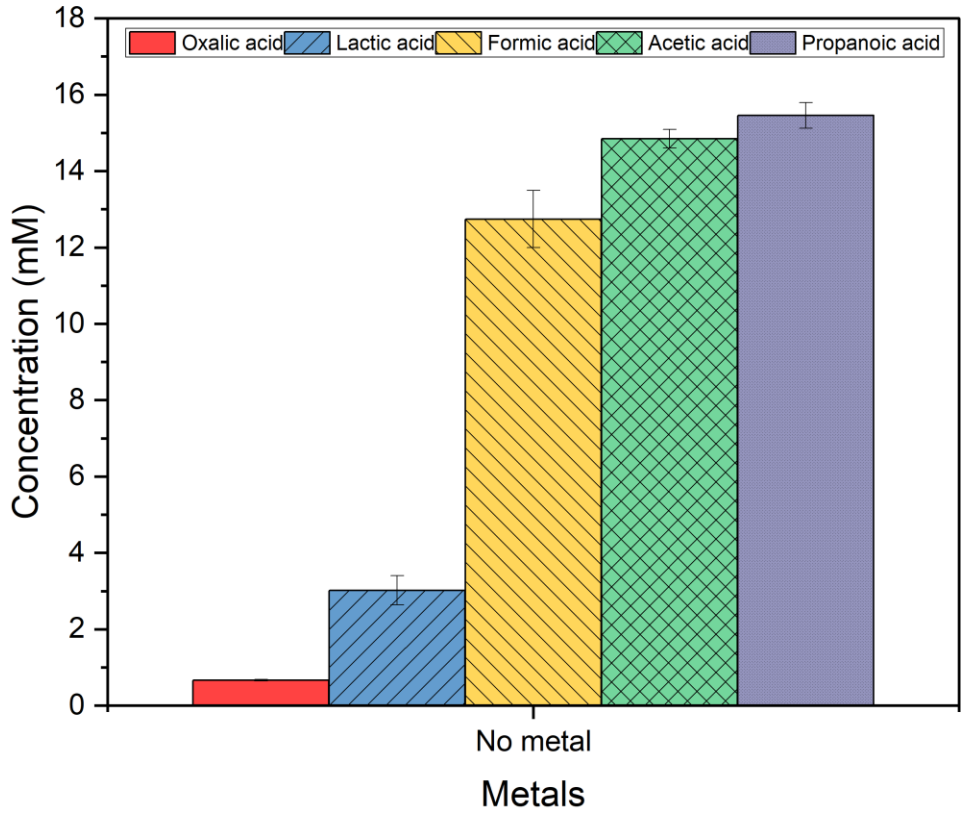

Figure 49: The formed products with no metal; 250 ºC, 2 h, 0.5 M $NaHCO_3$ and 0.05 M $C_6H_{12}O_6$ at 50% filling volume

The formed compounds ordered by their concentrations from the highest to the lowest were propanoic, acetic, formic, lactic and oxalic acids with concentrations of 15.4, 14.8, 12.7, 3, and 0.6 mM respectively.

Figure 52 illustrates the concentrations of the formed compounds when Zn reductant was added.

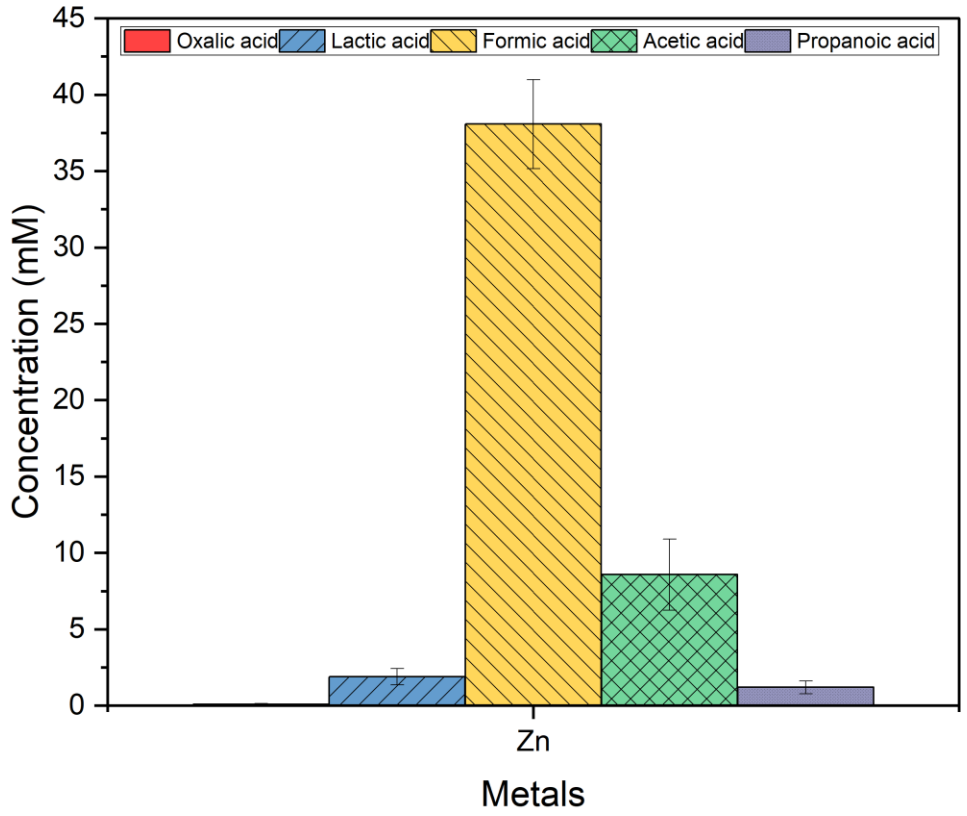

Figure 50: Zn addition effect on the formed products concentrations; 250 ºC, 2 h, 0.5 M $NaHCO_3$ and 0.05 M $C_6H_{12}O_6$ at 50% filling volume with 1:6 mmol ratio of $NaHCO_3$:Zn

In the case where Zn was added, the concentrations of each of the formed compounds were 38 mM of formic acid, 8.5 mM of acetic acid, 1.2 mM of propanoic acid, 1.8 mM of lactic acid and 0.08 mM of oxalic acid.

For the sake of comparison, the concentrations of the formed products from both cases, with and without Zn metal, are shown in figure 53.

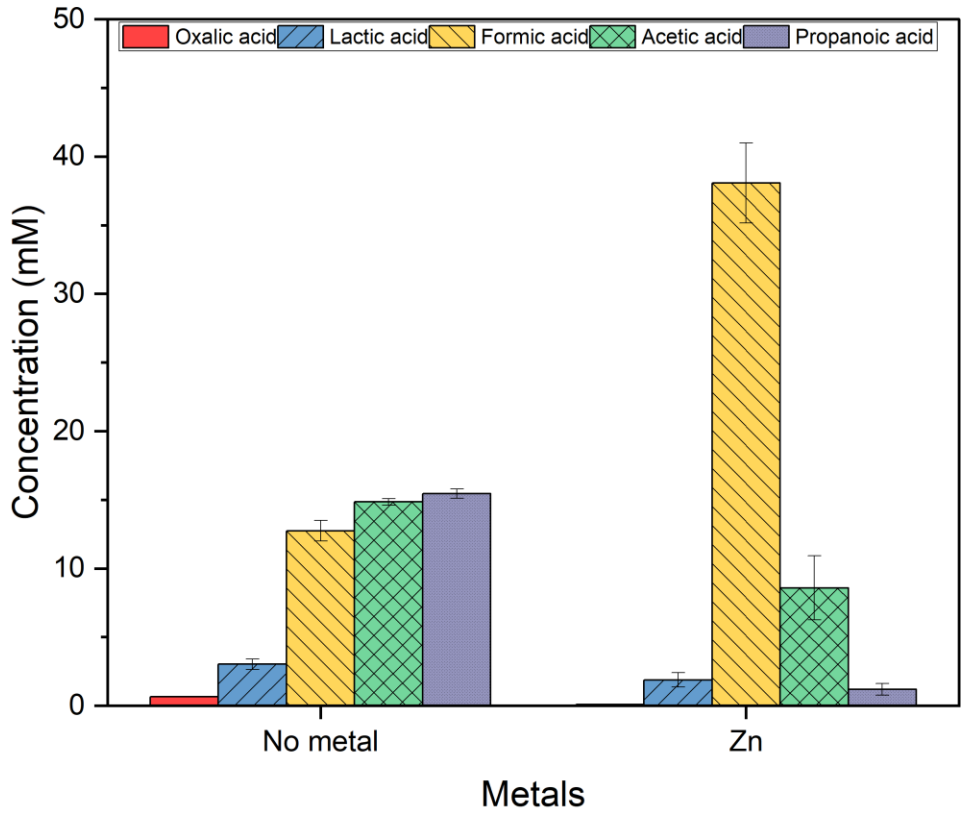

Figure 51: Zn addition effect on the formed products concentrations versus no metal; 250 ºC, 2 h, 0.5 M $NaHCO_3$ and 0.05 M $C_6H_{12}O_6$ at 50% filling volume with 1:6 mmol ratio of $NaHCO_3$:Zn

As in figure 53, the concentrations of all of the formed products exhibited different behavior with Zn addition. Oxalic acid, for instance, was produced in a trace amount when compared to the other cases. Additionally, lactic, acetic, propanoic acids exhibited declining in the formation compared to the other cases. Nevertheless, formic acid on the other hand was shown to have the height amount of production when Zn was added. The selectivity toward formic acid formation significantly increased when Zn was used as a reductant. In fact, formic acid increased by about three folds, 38 vs. 10 mM and 38 vs. 13 mM, when Zn was used compared to both cases where Fe was added as well as when no metal was added respectively. Statistically, the change of all of the

formed compounds' concentrations at 250 ºC and 2 h at 50% filling volume when Zn reductant was added, is significant for oxalic, formic, and propanoic acids and insignificant for lactic, and acetic acids. The calculated P-value for oxalic, lactic, formic, acetic, and propanoic acids are 0.004, 0.1, 0.007, 0.06, and 0.0007 respectively.

It is also important to monitor the process pressure in order to see the impact on the formation of the gas phase products. One variable that can be easily monitored is the process pressure. The following table, 32, presents the values of the process pressure for both no metal and Zn addition cases.

Table 31: Process pressure at different studied cases, Zn vs. no metal addition

Case	**Pressure at t=0 (barg)**	**Pressure post reaction after cooling (barg)**
No metal	40	<=10
Zn powder	62	30

As in table 31, the process pressure was higher when the system reached the temperature set point, at time zero, when compared to the no metal addition case by about 22 barg. Note that the pressure from t=0 to the end of the reaction remained the same for both with and without metal studies. Furthermore, when the system cooled down to room temperature, the system pressure was also higher when compared to the case in which no metal was added by 20 barg.

The gas-phase products were also analyzed for the case in which Zn was used as a metal reductant using mass spectrometer, MS. The gas-phase sample was released to the MS to investigate the formed products in the gas phase, and the figure 54 presents the constituents of the gas phase.

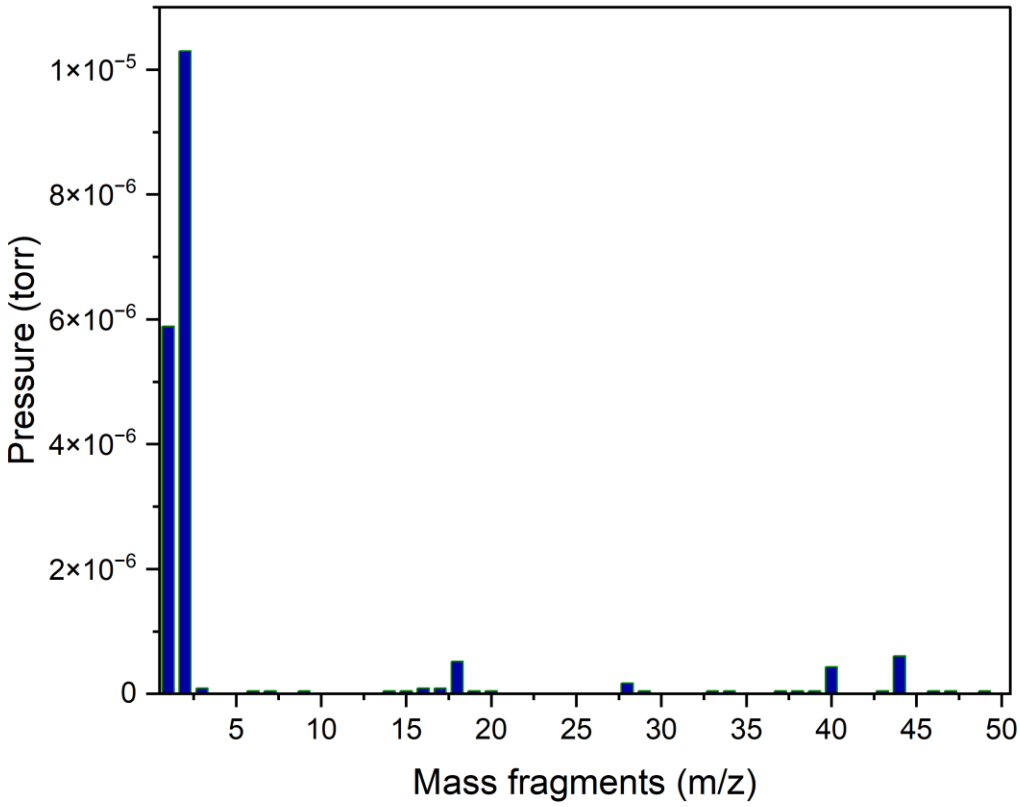

Figure 52: Gas phase products for the case where Zn was used

As shown in figure 54, the gas phase has a significant amount of H_2 gas as expected, and the constituents of the gas phase in high amounts are: H_2, 1, and 2 m/z, water vapor, 18 m/z, CO, 28 m/z, Ar, 40 m/z and CO_2 , 44 m/z.

The collected solid sample by XRD was analyzed to confirm the oxidation of the metal. Figure 55 illustrates the XRD result for the collected Zn metal after the reaction. The metal was filtered, washed and then dried before scanning it using XRD.

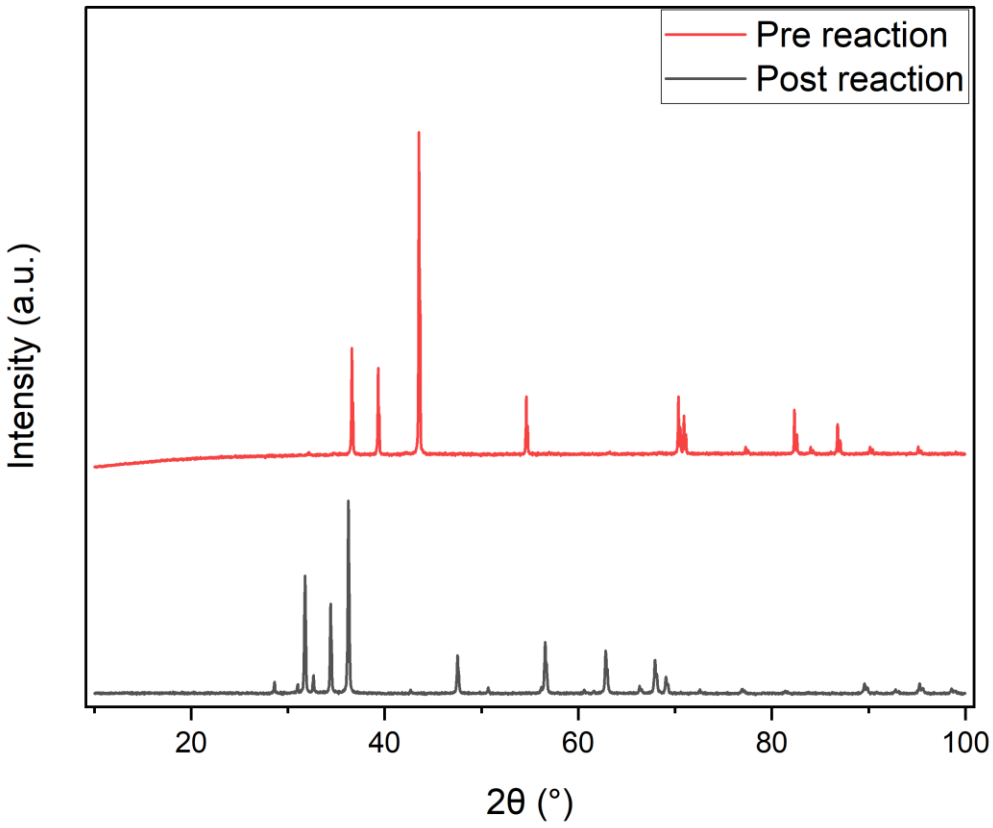

Figure 53: Zn metal solid sample pre reaction (top) and post reaction (bottom) at 250 ºC, 2 h, and 50% filling volume

The results from the XRD analysis for the collected Zn metal post the reaction showed oxidation in the metal. As in figure 55, multiple peaks were observed. For instance, at 32, 34, 36, 48, 56, 63, and 68º.

The addition of Zn metal as a reductant along with glucose improved both the concentration and the selectivity of formic acid. Zn was shown in the literature to outperform the other tested metal reductants in terms of formic acid production form the hydrothermal reduction of CO_2 . As in table 1 in chapter 1, the yield of formic acid was reported to be 78% when metal Zn was used as a reductant.[101] On the other hand, Fe at the same conditions, the yield of formic acid was only 10.5%. [99] The excellent performance of Zn as a metal reductant was attributed to the formation of Zn-H intermediate which is believed to be a crucial intermediate for the reduction of CO_2 into

formic acid as it provides hydrogen. [14], [15] Nevertheless, Zn addition requires a high reaction temperature of 300 ºC or more if no catalyst is used.

The oxidation of Zn is a rapid process. Jin er al. 2014 reported the fast oxidation of Zn to ZnO at half a minute and further oxidation follows up to 10 minutes at 300 ºC. [15] This could explain the better performance of Zn when compared to Fe at hydrothermal processes. Furthermore, the oxidation of Zn into ZnO can be monitored via a) the pressure of the process at the beginning of the reaction, b) the constituent of the collected gas-phase samples, and c) the pattern of XRD for the collected solid samples. For the process pressure, there was a jump in the pressure when Zn metal was used to reach as high as 62 barg at the beginning of the reaction and about 30 barg when the system was cooled to the room temperature as shown in table 31. Moreover, hydrogen gas was the highest in the product distribution probed by the MS as shown in figure 54. Lastly, the pattern of XRD for the collected solid samples from the Zn addition studies as in figure 55, show multiple oxidation peaks were observed. The structure of Zn metal is Wutzite, hexagonal, structure, and the oxidation peaks can be seen in different positions in the provided graph. For instance, at 31.8º (100), 34.4 º (002), 36.2 º (101), 47.5 º (110), 56.5 º (103), 62.9 º (112), 67.9 º (201). [101] Therefore, the results obtained from the analysis of XRD are in agreement with the gas phase results, and it shows better oxidation for the metal when compared to the case in which Fe was used.

When Zn was used, 3-fold increase in the formic acid production was seen as in figure 53. Looking at the conversion of both reactants in both cases with and without Zn, one can clearly see the similarity in conversion between both cases as in table 30 in section 6.2.01 and 6.2.0.2. Therefore, Zn addition can be said to shift the selectivity toward more formic acid rather than other formed products form glucose decomposition. Revisiting the reaction scheme 2 in chapter 3 and looking at the formed products in the case where Zn was used, no oxalic acid was detected, low quantities of propanoic and lactic acids formed, and acetic acid about fourth the quantity of formic acid, one can suggest the shift in pathway. The glucose decomposition into glycolaldehyde, via glucose or fructose, is suggested as the main glucose decomposition pathway when Zn metal was used. The formed acetic acid is suggested to originate from the oxidation of glycolaldehyde whereas formic acid is suggested to be produced via formaldehyde intermediate. In addition, since no methanol was detected in the liquid samples from the Zn addition studies, the internal Cannizzaro of

formaldehyde into formic acid is unlikely to occur. As minor amounts of lactic and propanoic acids were detected, a minor isomerization of glucose into fructose is suggested. Therefore, the suggested main pathway when Zn was added is shown in scheme 5.

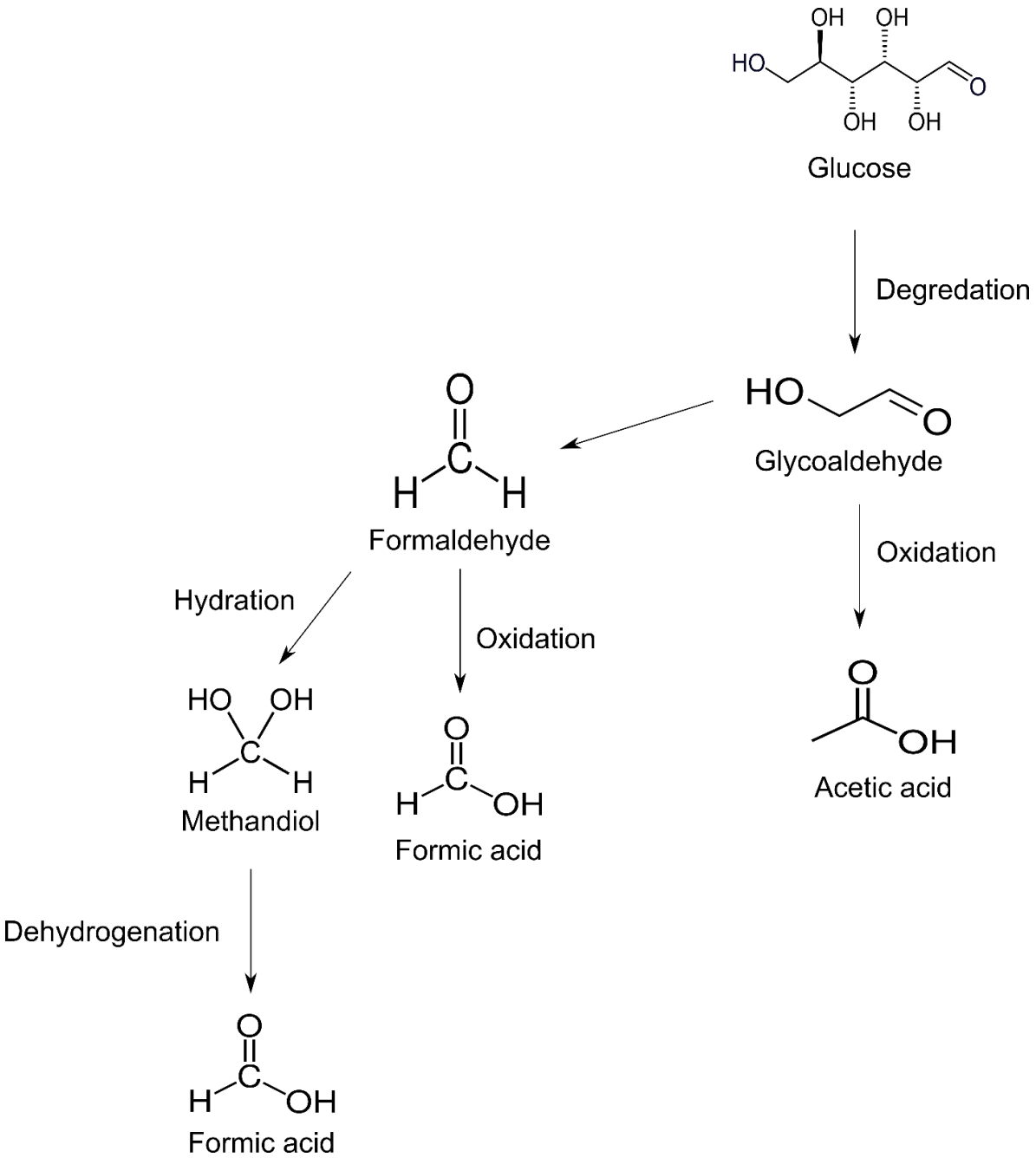

Scheme 5: The proposed pathway for formic acid and acetic acid production when Zn was used as a reductant

The number of moles of the hydrogen gas produced from the Zn addition can be calculated using the ideal gas law, knowing that the final pressure of the vessel once it was cooled to room temperature was 30 barg, as in table 31, the volume of the vessel being the unfilled remaining volume, i.e. 50 ml as the vessel volume is 100 ml and filling was 50%. This gives 0.063 mol of gas is in the vessel at the given conditions. Assuming all of this gas is hydrogen, as it has the highest share of gas-phase product shown in figure 54, the volume of hydrogen gas produced can be calculated using gas volume at STP occupies 22.5 L/mol, which gives about 1.4 L of hydrogen. Jin et al. 2024 reported 74 ml of hydrogen produced at 300 ºC and 2 h using Zn and $NaHCO_3$ [15], however, the volume of the reactor as well as the ratio of filling were 5.7 ml and 35% respectively. In other words, the expected volume of hydrogen can be calculated to be about 1.3 L if a larger reactor of 100 ml was used at 35% filling volume and similar reaction temperature of 300 ºC. Nonetheless, this work with a lower temperature of 250 ºC but higher filling volumes produces higher volume of hydrogen which could be due to either glucose presence or more water available.

The hydrogen produced in this work can be compared to the hydrogen production process in aqueous phase reforming, APR, in which oxygenated chemicals used to produce hydrogen gas. [164]–[166]Various organic compounds reported in the literature as a feedstock for APR. An example is glucose. Since glucose was also used here, it is worth comparing the yield of H_2 at similar or near conditions.

Wen et al. 2008 study used catalyst, Ni/ Al_2O_3 to produce H_2 from glucose in aqueous phase reforming process.[164] In their study, 1 g catalyst, Ni/ Al_2O_3, 90 g H_2O, 2.4 wt.% glucose at 533 K for 4 h. Different loading catalysts were used for the APR process, and the highest composition of H_2 in mol% was 48.5% with CO_2 presence in the gas phase with 45.2%, CO with 0.3%, CH_4 with 5.4%, and C_2-C_6 hydrocarbons of 0.5%. with 48 wt.% Ni/ Al_2O_3 with 15.1% H_2 yield. Therefore, the produced H_2 needs to be further purified from other unwanted gases.

There is another study for H_2 production using alkali enhanced hydrothermal reforming of biomass derives compounds to produce H_2 free of CO_2. [167] In that study, 6 g glucose was one of the compounds they tested for H_2 production. The reactor was 400 ml, 5 wt.% Pt/AC catalyst, and the amount of catalyst was 1.2 g, $Ca(OH)_2$ 15 g, 90 g H_2O. The conditions were 533 K, 4 h and pressure

was autogenous pressure. From this, 82% H_2 was produced along with CH_4 at 16% and C_3H_8 at 1.4 and trace of CO and CO_2. The STP volume of H_2 was calculated for other compounds but not for glucose, however, based on the reported molar concentration of H_2, glucose sits between glycerol and mannitol, and their STP volume for H_2 from the reactions were 0.7 and 0.6 L/g, meaning H_2 from glucose has an STP H_2 volume of ~ 0.65 L/g of glucose. [167] Compared to this study, and amount of glucose used was about 0.45 g and the STP volume of the produced H_2 was calculated to be about 1.4 L.

Another study investigated the production of H_2 gas from zero-valent iron powder.[168] In that study, H_2 production was shown to be about 15 bar from a reaction of 40 mmol, 5 μm Fe powder, and 40 ml of 1 M KOH, pH of 14, in a 100 ml autoclave at 160 ºC and 25 bar using 6 bar CO_2 gas initially. The product from this process is > 80 wt.% Fe_3O_4 solid. The reaction time was 16 h. Although higher temperature was used in this work, 250 ºC, but the produced H_2 is more in less time and there is no need for any pressure for the process. Therefore, the usage of Zn in this work presents a way to produce H_2 which paves the way for future studies to optimize the suggested process for better performance.

6.2.3. Al

Aluminum, Al, was another metal used in this work to study its addition impact on the formation of formic acid and other products. The formed products when Al was added are similar to the other tested cases, i.e. other metals and no additional metals. The concentrations of the formed compounds in the case where no metal was added are shown in figure 56.

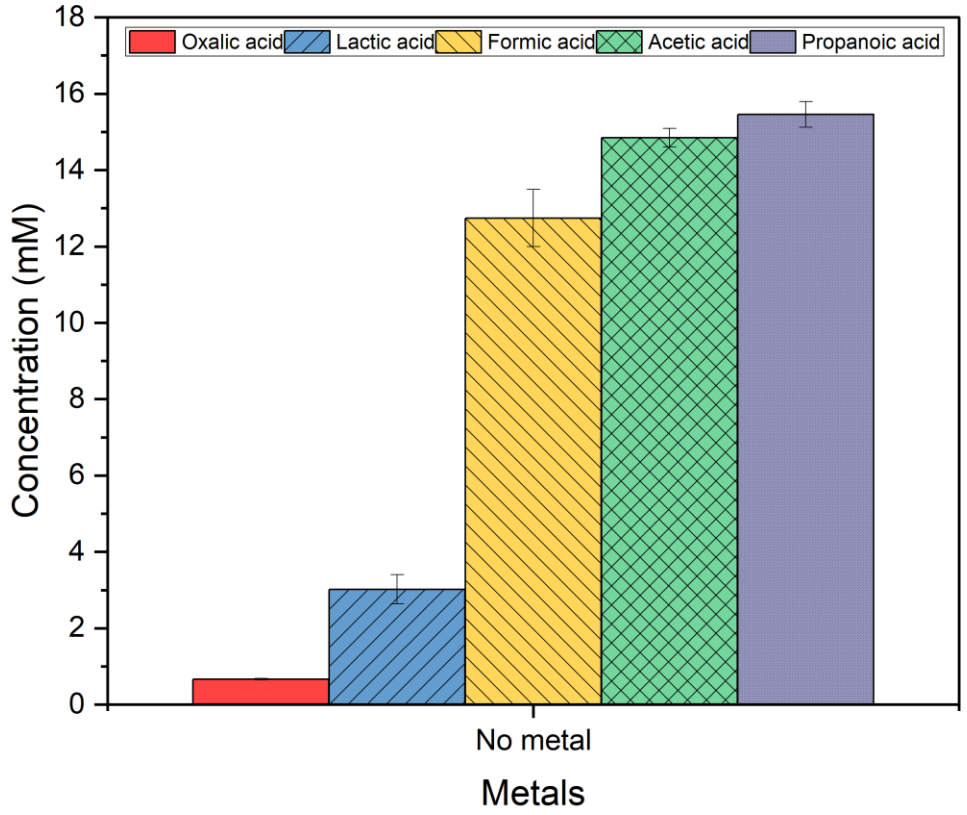

Figure 54: The formed products no metal; 250 ºC, 2 h, 0.5 M $NaHCO_3$ and 0.05 M $C_6H_{12}O_6$ at 50% filling volume

The formed compounds ordered by their concentrations from the highest to the lowest were propanoic, acetic, formic, lactic and oxalic acids with concentrations of 15.4, 14.8, 12.7, 3, and 0.6 mM respectively.

Figure 57 illustrates the concentrations of the formed compounds when Al reductant was added.

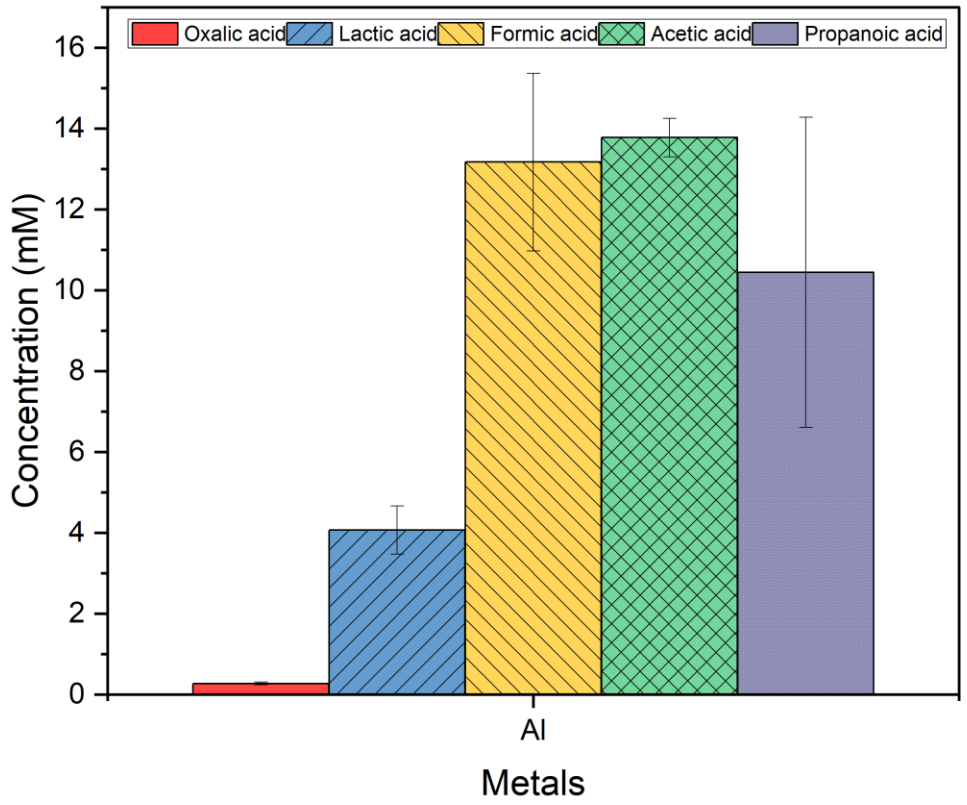

Figure 55: Al addition effect on the formed products concentrations; 250 ºC, 2 h, 0.5 M $NaHCO_3$ and 0.05 M $C_6H_{12}O_6$ at 50% filling volume with 1:6 mmol ratio of $NaHCO_3$:Al

The concentrations of the formed compounds when Al metal was added, ordered from the highest to the lowest, were acetic, formic, propanoic, lactic and oxalic acids and their concentrations were 13.7, 13.2, 10.4, 4.1, and 0.3 mM respectively.

The concentrations of the formed compounds from both cases, with and without Al are illustrated in figure 58.

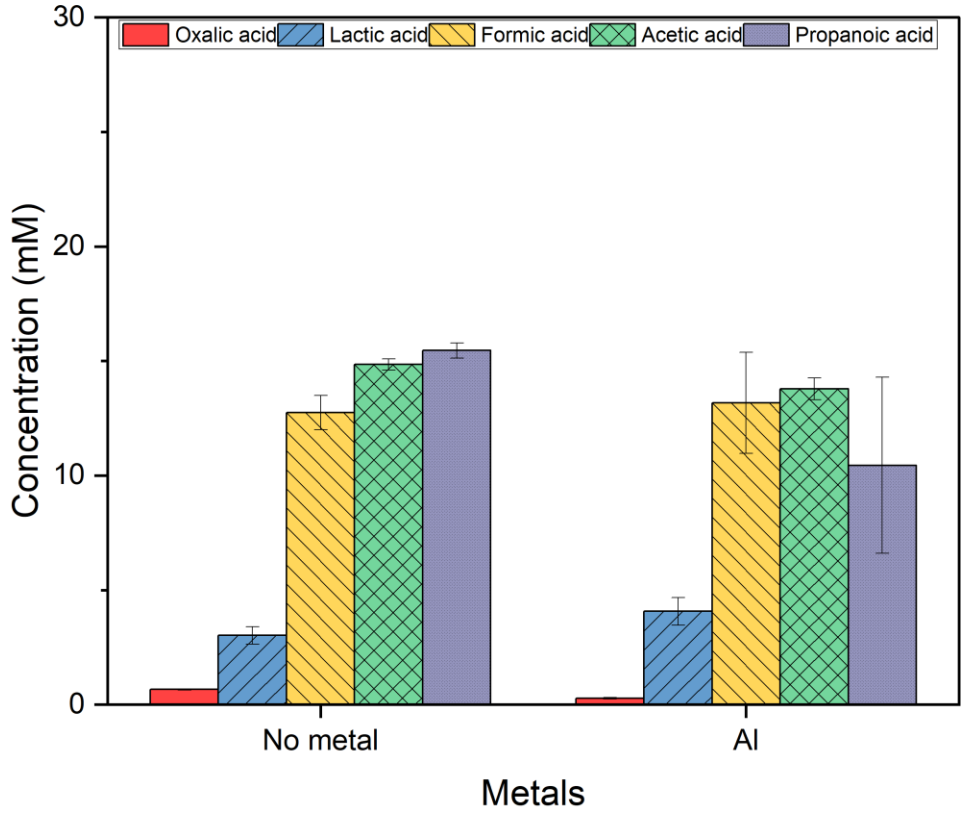

Figure 56: Al addition effect on the formed products concentrations versus no metal; 250 ºC, 2 h, 0.5 M $NaHCO_3$ and 0.05 M $C_6H_{12}O_6$ at 50% filling volume with 1:6 mmol ratio of $NaHCO_3$:Al

Figure 58 presents the formed products when Al metal was used and compared it with the case in which no metal was used. Lactic and formic acids concentration exhibited a slight increase when Al metal was used. However, all other formed products exhibited decline in their concentrations when the case of Al addition compared to the no metal addition results. Statistically, the change of all of the formed compounds' concentrations at 250 ºC and 2 h at 50% filling volume when Al reductant was added, is insignificant for all of the formed carboxylic acids except for oxalic acid. The calculated P-value for oxalic, lactic, formic, acetic, and propanoic acids are 0.006, 0.2, 0.8, 0.1, and 0.2 respectively.

It is also beneficial to observe the pressure of the process at the start of the reaction as well as when the system is cooled to see if there is any formation of gases. Table 33 presents the pressure readings for the system at Al and no metal addition cases.

Table 33: Process pressure at different studied cases, Al vs. no metal addition

Case	**Pressure at t=0 (barg)**	**Pressure post reaction after cooling (barg)**
No metal	40	<=10
Al powder	60	~12

The process pressure was higher when the metal Al was used compared to the case in which no metal was used. At time zero, 60 barg was recorded for the process pressure, higher than the no metal addition case by about 20 barg. Furthermore, when the system was cooled to room temperature, the pressure of the system was recorded at 12 barg, slightly higher than no metal addition case.

The system was coupled to the MS to detect what gases were present at the end of the reaction where the system was cooled to room temperature. Figure 59 presents the constituent of the collected gas sample after cooling the reactor.

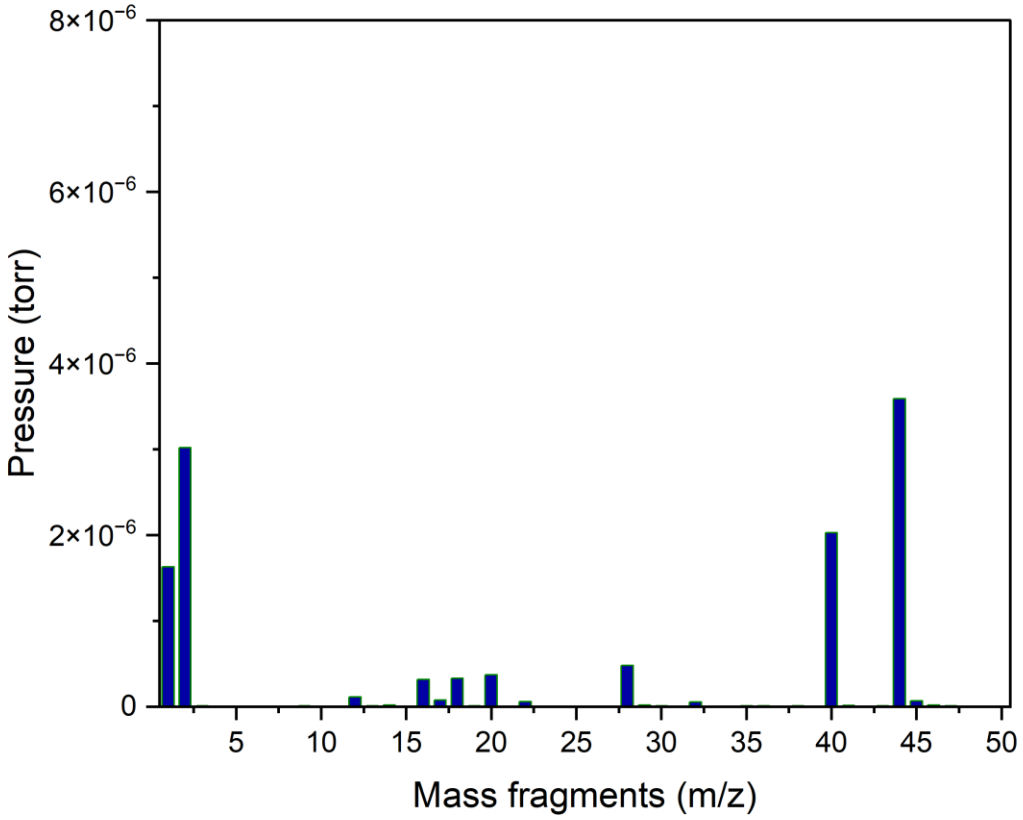

Figure 57: Gas phase products for the case where Al was used

The increase in the process pressure should be related to the formation of gases. As in figure 59, there formation of both H_2, m/z=1 and 2, gas and CO_2 , m/z=44. Other detected gases were water vapor, m/z=18, CO, m/z=28, Ar, m/z=40.

Observing the formation of H_2 gas, it is expected that the Al metal was oxidized better than Fe and therefore H_2 was produced. Comparing the Al addition to no metal case, the dominant products in the gas phase sample for the Al were CO_2 and H_2. On the other hand, there was a sharp decline in CO compared to no metal case. The produced hydrogen is anticipated as Al underwent oxidation and thus produces hydrogen gas and aluminum oxide. Furthermore, the presence of CO_2 and H_2 along with the decline in the CO suggests that water gas shift reaction occurred in the case of Al as shown in R.12.

$H_2 + CO_2 \leftrightarrow CO + H_2O;\ \Delta H_{298} = 41.2\ kJ\ mol^{-1}$ R.12

The collected Al solid sample was scanned by XRD to see if oxidation occurred. The solid sample was filtered post the reaction, washed, and then dried before XRD analysis. Figure 60 illustrates the pattern of the surface of Al post the reaction.

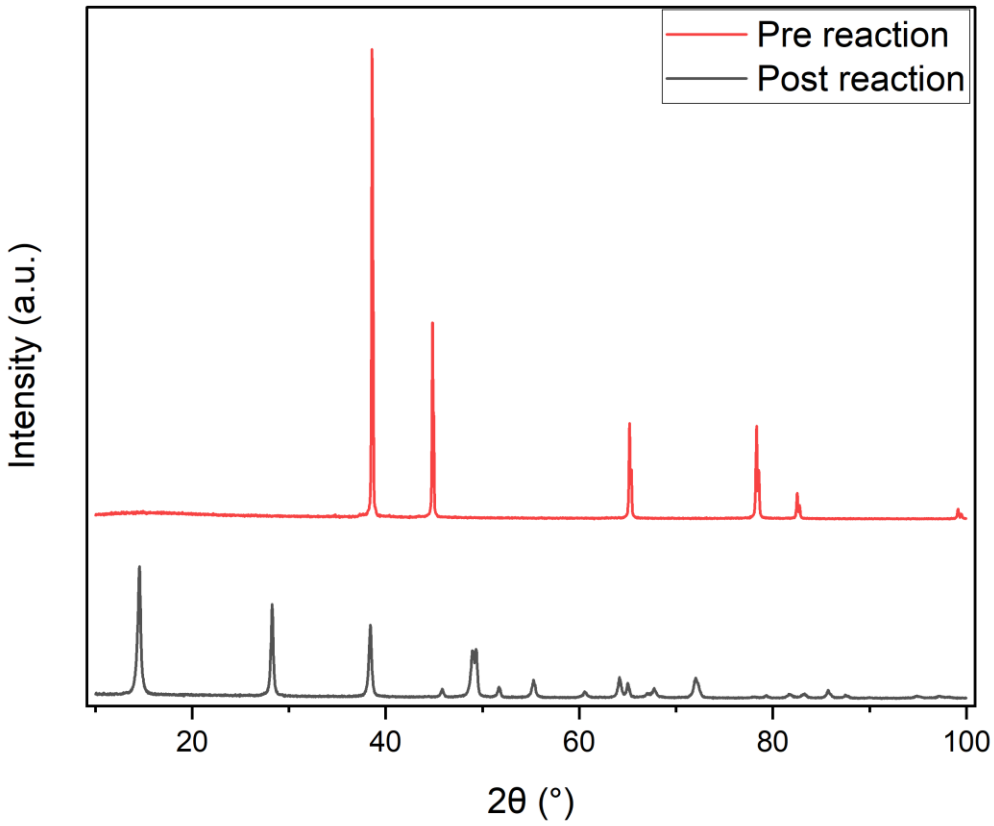

Figure 58: Al metal solid sample pre reaction (top) and post reaction (bottom) at 250 ºC, 2 h, and 50% filling volume

As in figure 60, the detected peaks from the XRD studies were 14.5, 28, 38, 44, 49, 55, 65, and 72 º.

Formic acid was slightly increased in concentration when Al was used. When compared to Fe and Zn, Al should sit in the middle if metals were ordered based on the formic acid yield. 64% of formic acid yield was reported when Al was used as a metal reductant at 300 ºC and 1:6

$NaHCO_3$:Al ratio. [102] For comparison reference, Fe[99] and Zn[101] were reported to have 10.5 and 78% yield of formic acid at 300 ºC and 1:6 $NaHCO_3$:metal ratio. However, in this work, as both glucose and temperature are the difference, the concentration of formic acid from the metal addition studies were 10.6, 38.1, and 13.2 mM for Fe, Zn, and Al respectively. Therefore, the same order holds in this study as the reported ones.

Although there is evidence of Al oxidation, there are still peaks related to Al suggesting that not Al was not fully oxidized. For instance, peaks at 38, 44, 65 º are for Al. Yet, other peaks at 14.5, 28, 49, 55, and 72º are evidence for Al oxidation as they are related to Boehmite, AlO(OH) as observed by Rio et al. 2021. [103] Additionally, Zhong et al. 2016 reported the same effect on the metal aluminum being oxidized into AlO(OH) in the presence of Pd/C catalyst at 300 ºC, 35% filling volume and 2 h reaction time. [77] Nevertheless, Al tends to naturally form a protective oxide layer, [169]–[171] this could be a reason for the ineffectiveness of using Al in this work.

The process pressure declined to 12 barg after cooling down to the room temperature. This is unlike the case of Zn where the difference in the pressure at the beginning of the reaction and the beginning of the reaction where no metal was used remained after cooling down to the room temperature. When compared to the other cases, Fe; Zn; and no metal, the proportion of CO_2 gas in the case where Al was used is higher. Then, H_2 gas is next in the highest proportion. Followed by others like CO and water vapor. It is also worth noting that Ar was used for purging pressure testing prior to the reaction, and the result in this figure is probably due to Ar remining in the outlet gas lines.

One explanation could be the formation of other gases than hydrogen gas which could have dissolved in the aqueous medium from the gas phase as the system cooled down in the case where Al was used. CO_2 for example have more solubility in water at room temperature when compared to H_2.[172] This explanation can be supported by the results of the gas-phase products of Al studies from figure 59 where CO_2 was detected along with H_2.

Analyzing the conversion of the reactants can suggest the production of CO_2 gas as more bicarbonates were consumed for the Al studies as in table 30 in section 6.2.01. Lyu et al. 2015 reported the presence of CO_2 gas in the collected gas samples from the hydrothermal CO_2 reduction into methanol using Al over Cu catalyst. [107] Moreover, CO_2 and H_2 were also reported to be

produced when Al and $NaHCO_3$ were used to produce formic acid, however, the produced CO_2 increased as CO_2 source, $NaHCO_3$, increased. [102]

More importantly, the decline in the pressure of the system when it was cooled down could be due to the solubility of CO_2 back in the aqueous medium. If this is true, then the concentration of the reactant, bicarbonate, should be higher at the end of the reaction, i.e. less consumption, unlike what is reported in table 30. However, CO_2 can reduce the pH of the medium, and thus, the form in which CO_2 can exist is not as bicarbonate but carbonic acid, see figure 1 in chapter 1, which cannot be detected using RID used in conjunction with HPLC in this work for monitoring the reactants.

In summary, high yield of formic acid when Zn was used can be related to the production of hydrogen gas which is believed to positively impact the process by supporting hydrogenation process in the hydrogenation of CO_2 into formic acid under hydrothermal conditions in the presence of glucose. Additionally, when comparing the cases in which Fe and Al were used, although Al case produced hydrogen gas, yet the formation of the important intermediate of Zn-H in Zn case may be the reason of the better yield and selectivity of formic acid.

6.3. Reusing ZnO

After testing Fe, Zn, and Al, Zn was shown to have the best yield of formic acid which is the target product here. These results, although glucose is present in this case, agree with what has been reported in the literature for the hydrothermal conversion of CO_2 into formic acid, see table 1 in chapter 1. The additional note to be mentioned here is that the formed products form the reactions where no metals were used were also affected by the additional Zn and the selectivity was switched toward more formic acid formation as in figure 61.

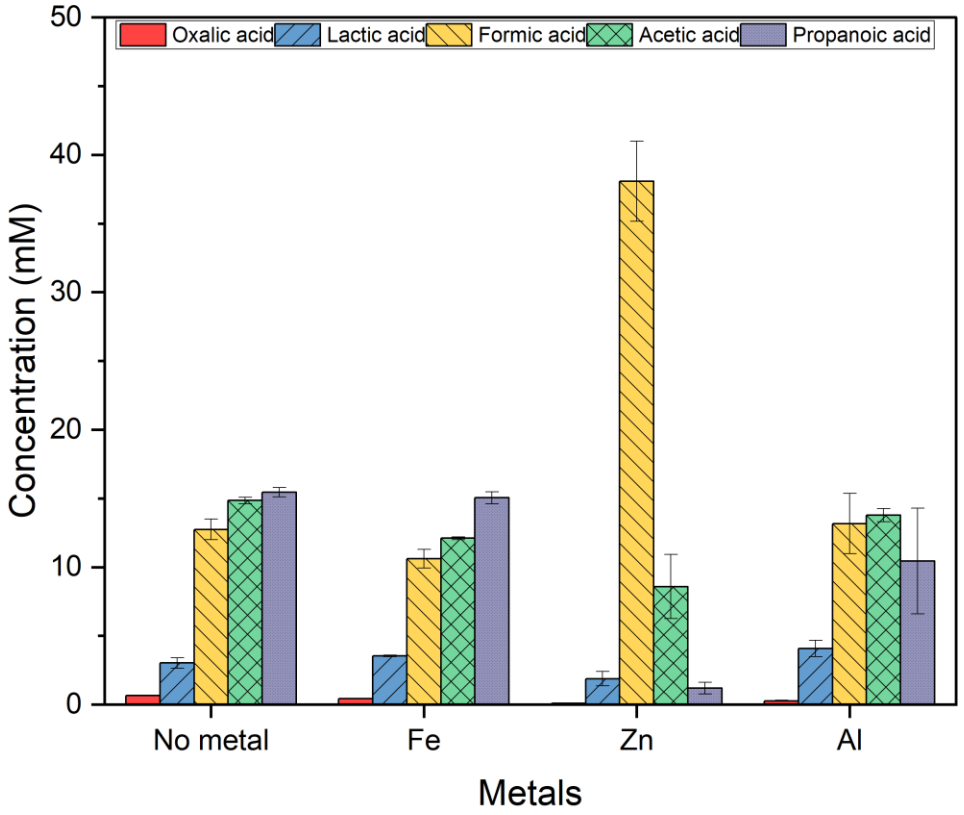

Figure 59: Metals addition effect on the formed products concentrations and no metal, 250 ºC, 2 h, 0.5 M $NaHCO_3$ and 0.05 M $C_6H_{12}O_6$ at 50% filling volume with 1:6 mmol ratio of $NaHCO_3$:metals

Although the solid sample of the Zn collected post the reaction was oxidized as shown in figure 55, it is worth looking at reusing the dried zinc oxide and examining the efficacy of the recycled materials. To test this, the collected solid sample, which was filtered post the reaction, washed, and dried is to be used again with the same proportion of the reactants, that is 0.5 and 0.05 M of $NaHCO_3$ and $C_6H_{12}O_6$ mixed and filled up to 50% filling volume of the reactor. The solid Zn was placed in the vessel along with the other reactant, and the same procedure was repeated but with the collected zinc oxide to investigate the activity of Zn oxide in this process.

The exact same procedure of heating rate, reaction time, cooling method, as well as solid sample treatment was adopted for the sake of comparison. The collected liquid samples were similarly

analyzed by HPLC to see the effect of this metal oxide, Zn oxide, on the formed products, and figure 62 shows the results compared to the cases where no metals were added.

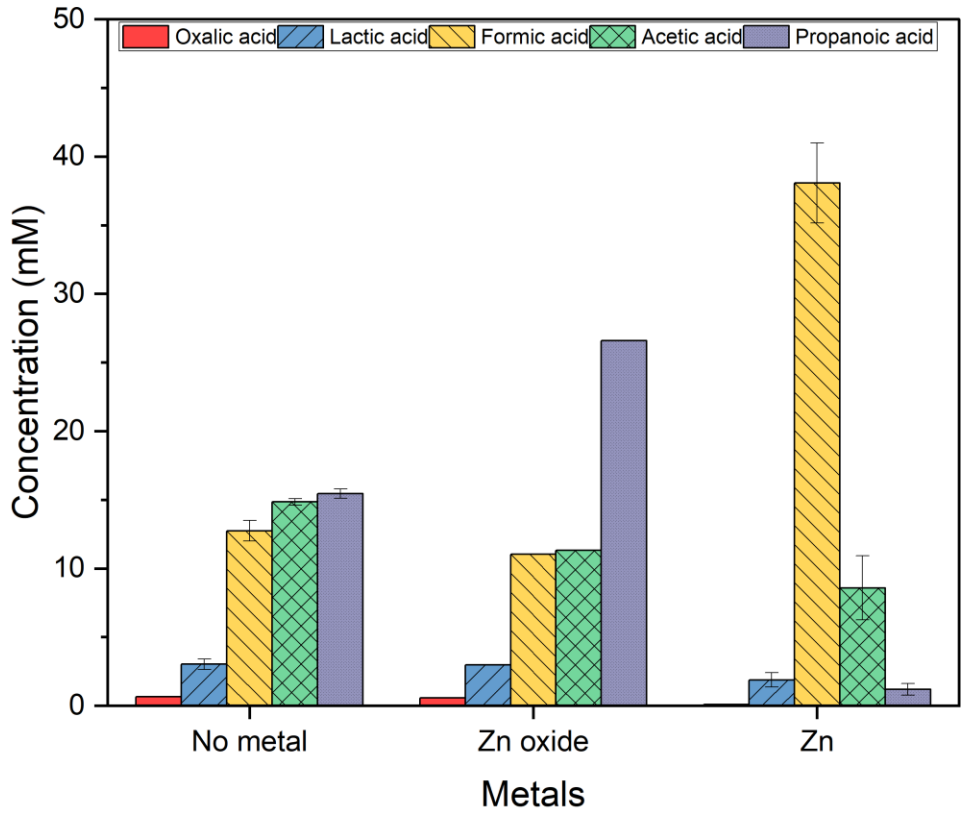

Figure 60: Zn oxide reuse versus no metals and Zn addition case, 250 ºC, 2 h, 0.5 M $NaHCO_3$ and 0.05 M $C_6H_{12}O_6$ at 50% filling volume

As shown in figure 62, the same products formed as in the case where no metal was used when the Zn oxide was used. Oxalic and lactic acids exhibited the same concentration as in the case where no metal was used. However, Formic and acetic acids were not the case, they exhibited declining in their concentrations compared to the no metal addition case. Nevertheless, propanoic acid concentration was about 73% more in the case in which Zn oxide was used.

The used zinc oxide in this study was collected after the reaction, filtered, washed, and dried for XRD analysis. Figure 63 presents the XRD results for the collected zinc oxide.

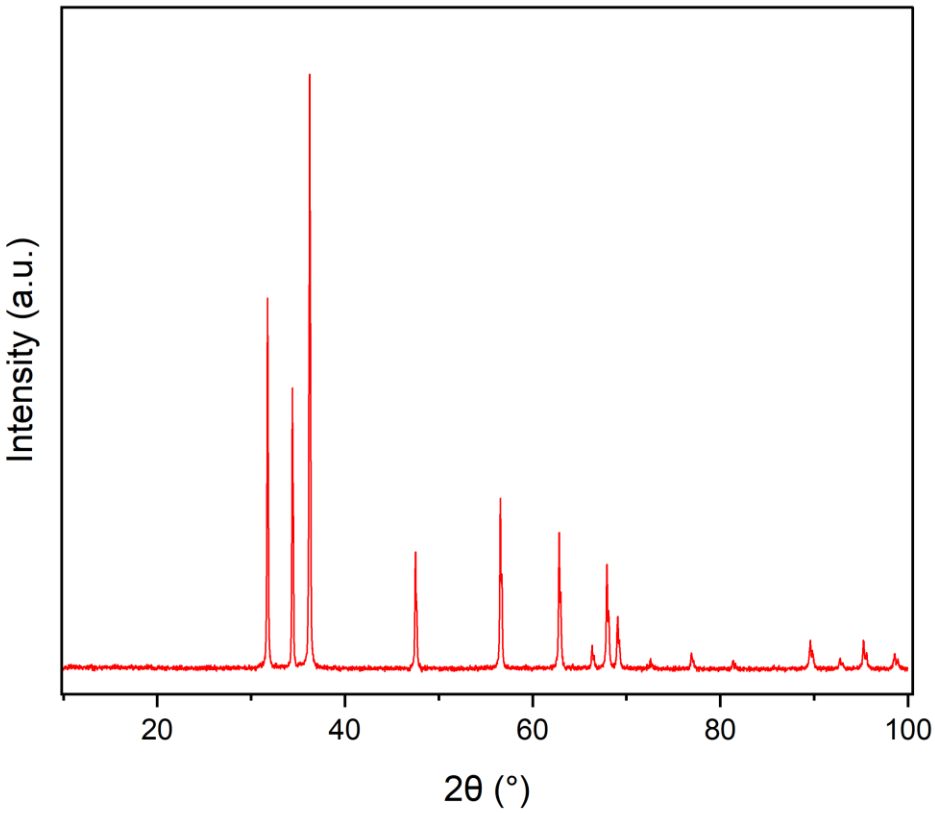

Figure 61: XRD pattern for the reused zinc oxide, 250 ºC, 2 h, 0.5 M $NaHCO_3$ and 0.05 M $C_6H_{12}O_6$ at 50% filling volume

The XRD analysis for the reused zinc oxide remained the same after the reaction as shown in figure 63 when compared to the collected after Zn metal studies, see figure 55.

Reusing Zn oxide is proved to be not beneficial for production of formic acid. Zn oxide is not a well-known catalyst for CO_2 hydrogenation to formic acid. Zeng et al. 2014 tested ZnO for the CO_2 hydrogenation into formic acid, and there was only 13% yield compared to 78% when only metal Zn was used. [14] Therefore, the role of using Zn oxide for the formic acid production via CO_2 hydrogenation is expected to be ineffective. Nonetheless, the high concentration of propanoic acid when the zinc oxide was used is noticeable as shown in figure 62. Therefore, searching for newly formed products in the collected liquid sample using HPLC is essential.

Comparing the retention times for all of the detected compounds using HPLC-UV-VIS and RID results in two unique compounds detected by RID at 22.5 min and 24.4 min and another one detected by UV-VIS at 34.5 min. The compounds at 22.5 min 24.4 min were already identified, thanks to the intensive identification endeavors carried out in this work, see chapter 3 for more information. The compounds are ethanol, and 2-propanol, aka isopropanol. However, the other one eluted at 34.5 minutes is unknown.

The collected information can be restated as the following, the usage of zinc oxide produces propanoic acid greatly compared to the no catalyst and Zn cases, at the same time, two different compounds were detected using HPLC, one of them is identified, that is isopropanol, which could form from the oxidation of acetone, while the other is unknown. From the information given, and since the unknown compound at 34.5 minutes detected by the UV-VIS but not by RID, and the maximum UV absorption, λ_{max}, is about 200 nm it is high likely an aldehyde. Furthermore, since both propanoic acid and isopropanol are C_3 compounds, there is a possibility of them being produced via Cannizzaro reaction where 2 aldehydes at basic medium converted into carboxylic acid and alcohol. Moreover, the medium is alkaline, which favors Cannizzaro reaction, as well as the catalyst used here, zinc oxide, is a basic catalyst. However, if the formed compound is propionaldehyde, then it does not undergo Cannizzaro reaction as it has hydrogen atom in the alpha position. Instead, the same proposed pathway for propanoic acid via ethanol carbonylation in chapter 4 is still applied here. In fact, the oxidation of Zn into ZnO produces hydrogen gas, and along with the CO_2 present in the media, a reverse water gas shift reaction may occur, and thus CO could be produced. Indeed, CO is one of the gas-phase products when Zn was used as shown in figure 54. Nevertheless, ethanol and CO are what needed for the ethanol carbonylation into propanoic acid.

6.4. Zn metal as a reductant for CO_2 hydrogenation into formic acid

Zn metal was used as a reducing agent for the production of formic acid under hydrothermal conditions. A study on using Zn with CO_2 , in the form of $NaHCO_3$, under hydrothermal conditions was carried out and the results of the collected liquid sample are presented here. Figure 64 compares the cases in which only $NaHCO_3$, Zn, and DI water were used (labelled Zn w/o GL) with the other tested cases where no metal was used and Zn when Zn was used.

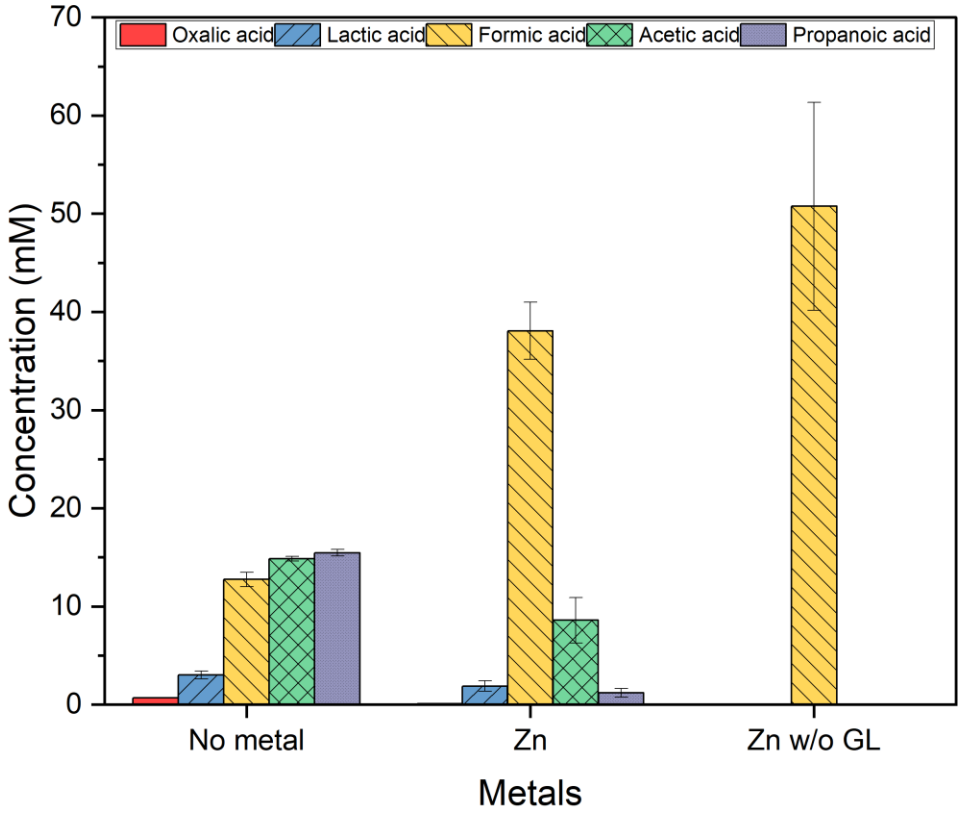

Figure 62: No metal; with Zn; and Zn without glucose, Zn w/o GL, results, reactions carried out at 250 ºC, 2 h, and 50% filling volume, 0.5 M $NaHCO_3$, 0.05 $C_6H_{12}O_6$, and 1:6 ratio of $NaHCO_3$:Zn

Figure 64 shows that formic acid was the only formed product when only Zn was used as a reductant unlike the other cases, where Zn and glucose, and glucose only were used. Since there was no glucose in the CO_2 hydrogenation with Zn case, no more compounds were expected as only reduction of bicarbonates into formic acid took place. The formic acid produced in the case where only Zn was used as a reductant was about 51 mM compared to the case in which a combination of Zn and glucose were used as reductants, 38.1 mM. Although Zn alone produces higher amounts of formic acid compared to Zn and glucose together, the use of both reductants at the same time presents several advantages. First, using Zn with glucose increases the selectivity toward formic acid thus, less byproducts formation could be attained. In fact, Zn addition to

glucose presents a way to make the process more feasible and cost-effective as further separation and treatments of the products steps could be eliminated. Second, using glucose along with Zn presents a sustainable option for reductants as less amount of Zn is required for formic acid production. Moreover, when comparing the ratio of Zn: $NaHCO_3$ in this wok with what reported in the literature, less of Zn was used in this work, 1:6 vs. 1:8 in the literature [14]–[16], [173], and therefore, less reliance on metals which require extraction and more exploitation of metals including extraction and refining processes. Third, this work presents the potential for both types of reductants, which can be considered a benchmark for future optimization work which could present another sustainable option for reductants besides metals by reducing the amount of metals needed for similar formic acid production. Lastly, at the tested temperature in this work, 250 ºC, more formic acid yield was obtained compared to metals alone where higher reaction temperature of 300 ºC was needed. Overall, this work presents the production of formic acid in higher yield than what reported in the literature at lower ratio of metal Zn, lower reaction temperature, and lower filling volume.

XRD analysis was done for the case in which only Zn was used as a reductant. The results from the XRD showed the same oxidation pattern as the case in which glucose was used, see figure 54. Meaning the oxidation across all of the Zn addition studies was the same in terms of oxidation peaks positions and intensity.

Formic acid was the only product from the CO_2 reduction into formic acid using Zn as a reductant. The same was presented in the literature, where Zn was reported to outperform other reducing agents such as Fe and Al. In the literature, formic acid was shown to be produced from the hydrothermal reduction of CO_2 using metals including Zn. [14]–[16], [173] However, the reported studies were conducted at elevated reaction time of 300 ºC and lower filling volumes of 35%. [14]–[16], [173] In this work, 250 ºC; 2 h and 50% filling volume were used and therefore, variation is expected. Zhong et al. 2019 reported ~55% yield of formic acid when Zn was used as a reductant at 250 ºC and 60% filling volume, where yield was calculated as carbon in fromate to the carbon of initial $NaHCO_3$. [101] In this work, the yield of formic acid from the case in which only Zn was used as a reductant is 67.5%. Better yield was achieved in this work due to smaller reductant size of 10 µm whereas Zhong et al. used 74 µm or 200 mesh zinc. [101]

6.5. Conclusion

The addition of metal reductants to the glucose to study the impact on formic acid and other formed products was the main objective of this chapter. First, Fe was tested as a metal reductant at 250 ºC, 2 h, and 50% filling volume and the liquid, gas, and solid samples were analyzed, and pressure of the process was monitored throughout the reaction. The addition of Fe with glucose did not improve the yield of formic acid. However, other formed products were shown to improve such as lactic and propanoic acid. Therefore, Fe addition enhances glucose decomposition via fructose decomposition to glyceraldehyde which is the precursor of pyruvaldehyde from which lactic and propanoic acid were suggested to originate.

Zn addition was shown to improve the yield of formic acid by three folds. At the same time, other formed products were suppressed which increased the selectivity toward formic acid. The pressure of the process was 55% higher when Zn metal was used as a reductant in conjunction with glucose. Analysis of the gas-phase products confirmed the dominance of hydrogen gas which is anticipated as Zn underwent oxidation and thus hydrogen gas is released which is the responsible for increasing the process pressure. Observing that other formed products' yields declined when Zn was added, and given the fact that in both cases, where Zn was added and when without it, the same conversion of the reactants achieved, the formic acid pathway from the glucose decomposition when Zn added was suggested. In this case, glycolaldehyde which can be obtained from either glucose or fructose decomposition was believed to be the intermediate from which formic acid was produced via oxidation of formaldehyde.

Al was the third metal reductants tested in this work along with glucose. Al was not beneficial for enhancing formic acid yield in this work as it was only 3% increased when Al was added. On the other hand, lactic acid yield was shown to increase when Al was used. This suggests that Al addition favors the decomposition of glucose to lactic acid. The process pressure was observed to increase once reached the temperature set point of 250 ºC. The analysis of the gas sample confirmed the dominance of both hydrogen gas and CO_2. The conversion of the glucose in the case in which Al was used was the same as all of the cases, however, the conversion of bicarbonate was higher which explains the higher presence of CO_2 in the gas phase samples. In addition, the presence of CO_2 in the gas phase sample when Al was used suggested that the equilibrium of

carbonate, bicarbonate and CO_2 was affected, and thus, instead of ending up with bicarbonate in the solution post the reaction, the consumed CO_2 stayed in the gas phase.

Overall, the ordered in which metal affects the yield of formic acid still holds as reported in literature as Zn>Al>Fe even with the presence of glucose. Nevertheless, the formed ZnO from the case in which Zn was added was then studied to see if it can still be reused for formic acid production. It was shown that reusing ZnO was not beneficial for the production of formic acid as it less produced, however, it showed great enhancement of the yield of propanoic acid. Nevertheless, since formic acid and acetic acids originate mainly from glycolaldehyde, using ZnO favors the decomposition of glucose via fructose then pyruvaldehyde which is the way from which propanoic acid is produced.

Chapter 7: Conclusion and Recommendations

7.1. Conclusion

In this work, the process of producing formic acid from the conversion of CO_2 in the presence of glucose alone, and in the presence of zero-valent metals, specifically, Fe, Zn, and Al were studied. Preliminary kinetics studies were conducted at heating to 200 ºC at different concentrations of the starting material and the kinetics studies showed that the reaction of $NaHCO_3$ and $C_6H_{12}O_6$ is a first order in $C_6H_{12}O_6$ and zero order in $NaHCO_3$ making the overall reaction follows first order kinetic. It is worth noting that the methodology used in this work could not report the activation energy as the reaction temperature, as a variable, cannot be isolated without variation in the process pressure. In addition, the reliance on high conversion glucose data, although worked for determining the reaction order, failed to establish activation energy calculation.

Probing the formation of different products at the 250 ºC, 2 h, and 50% filling volume was conducted. The purpose of doing that was to investigate if more products form from this process as $C_6H_{12}O_6$ is expected to introduce more products beside the most popular reported simple carboxylic acids, formic, acetic, and lactic acids. New products were detected in this work. Acetone, ethanol and isopropanol were identified, however, there are more products that need identification as the employed analysis techniques used in this work were unsuccessful. The approach followed for identifying the unknown compounds in this study although informative was unable to identify the unknown compounds formed from the process.

The optimal temperature and reaction time at which formic acid is highly produced were chosen based on literature as well as optimization studies in which three different reaction temperatures, 200; 250; and 300 ºC; and three different reaction times, 1; 2; and 3 hours; at a filing volume of 50% were investigated. Then the optimal case, among the tested cases, in which the concentration of the formic acid was the highest, was then used to check if the filling volume has any impact on the formic acid. Therefore, two additional filling volumes, besides 50%, 30 and 70%, were investigated to study the impact of filling volume on the formed products. From the optimization studies the optimal conditions among the tested conditions, for the production of formic acid was found to be 250 ºC, 2 h, and 50% filling volume, which agrees with previous studies.

The observation of appearing and disappearing of ethanol at 200 and 300 ºC, the decline of acetic acid production with incline of propanoic acid at 200 ºC, and the decline of propanoic acid production with incline of acetic acid at 300 ºC, suggested the pathway for the propanoic acid production via ethanol carbonylation.

The difference between the volume of the vessel used in this work and the heating method and the reported studies presented a variation in the heating time needed for the system to reach the set point. Although looks a drawback of this work, it actually suggested a new venue in which the formation of products could be produced during the heating process. Therefore, a unique aspect of this study is probing the formation of different products as the system heating period from room temperature to the set point. As the setup of this work is quite different than what was reported in the literature, the heating period was longer and thus formation of products during this period was anticipated. The results from heating period reactions showed that all of the formed products under the tested conditions were similarly produced during the heating period, however, at different concentrations. In other words, CO_2 reduction into formic acid using glucose under hydrothermal conditions could produce the same product at shorter reaction time if the heating rate is controlled.

As there were two sources of carbon in the initial reaction medium, bicarbonate and glucose, it is of great importance to trace the origin from which formic acid was obtained. Therefore, pH control studies using NaOH were conducted. The outcome of these studies showed that only 16% of the formic acid comes from glucose. An additional point was made in this study concerning pH after the reaction. In pH controlling studies, the pH pre and post the reaction was measured, and as the reaction progressed there was a decline in the pH of the medium ending up with acidic medium compared to the case in which $NaHCO_3$ was used where pH was basic for both pre- and post reaction. This suggests that tracing the origin of formic acid in this process by controlling the pH required employing a buffer solution in which pH stays the same throughout the reaction so the results can be then compared. Furthermore, NMR analysis was conducted for this work using labelled carbon sodium bicarbonate, $NaH^{13}CO_3$, however, the concentration of formic acid from the labelled studies was lower than the concentration of formic acid form unlabeled studies which made the usage of NMR for the tracing purposes in this work unsuccessful.

Metals reductants in their zero-valent state, Fe; Zn; and Al, have been shown to have a great impact on the formation of formic acid in CO_2 hydrogenation under hydrothermal conditions with Zn to have the highest yield of formic acid. Combining two reductants from different sources, metals and biomass, has not been reported at all. Therefore, introducing same reported metals to bicarbonates and glucose was then probed, which is another unique aspect of this work. The aim here was to increase the yield and selectivity toward formic acid. Among the tested metal reductants, the addition of Zn reductant along with glucose increased both the selectivity and the yield of formic acid. Formic acid concentration reached 38 mM with Zn addition compared to 13 mM without Zn. The other formed products were declined when Zn was used which was attributed to favoring the CO_2 reduction to formic acid over formation of other produced from glucose degradation. Therefore, formic acid pathway was suggested via glycolaldehyde which is believed to be a precursor of formic and acetic acid from glucose degradation. Additionally, H_2 gas was produced from this process as a by-product with better purity and without catalysts compared to H_2 production methods like APR, and metals to hydrogen processes.

The addition of Fe and Al as reductants along with glucose for the CO_2 hydrogenation into formic acid under hydrothermal conditions was shown to be ineffective. Fe was partially oxidized and thus not much hydrogen was produced which reflected on similar to no metals addition case production. On the other hand, Al, although a strong reductant, was shown to be ineffective to be added with glucose for formic acid production. The formation of CO_2 gas was suggested to be over the formation of H_2 gas, which was observed by the change in process pressure and analysis of the gas-phase samples, and therefore, slight improvement of formic acid was observed compared to no metal case.

Although the reuse of the oxidized Zn at the same conditions was shown to have adverse effects on the production of formic acid as it was shown to be produced in lower concentration, it can still be used in similar process as a catalyst to produce propanoic acid. The outcome of the ZnO reusage studies showed the improvement in the production of propanoic acid by about 73%.

Overall, this work provides insight into future kinetic studies as more compounds formation was detected, identified, and reported. Moreover, this work also provided information about the required conditions, i.e. reaction temperature and time, to produce a specific compound in higher

concentration. Furthermore, this work presents an alternative way to produce hydrogen from a batch process employing Zn and glucose reductants with no need for catalyst or external pressure. Lastly, the formed ZnO is not wasted as this work showed that using ZnO as a catalyst improved propanoic acid production which suggests an alternative way to produce propanoic acid from glucose and ZnO under hydrothermal conditions.

7.2. Recommendations for future work

1. Identification of Compounds Formed from CO_2 Hydrogenation into Formic Acid Using Glucose Under Hydrothermal Conditions

The hydrothermal conversion of CO_2 into formic acid using glucose as a reductant is a complex chemical process, particularly within the temperature range of 200–300 ºC, with reaction durations from 1 to 3 hours and a 50% reactor filling volume. From such a process, a variety of products are formed. Identifying these compounds is critical to understanding the underlying mechanisms and optimizing the reaction pathways. As the employed analysis techniques were not informative of the other formed compounds, other analysis techniques are therefore suggested for similar future work. Since HPLC-UV-Vis and HPLC-RID were the main analysis techniques used for analyzing the liquid phase samples, it is recommended to keep using the same separation method but with another detector. For instance, High-Performance Liquid Chromatography-Mass Spectrometry, HPLC-MS, is especially suited for this analysis due to its dual capabilities the separation efficiency of HPLC and the sensitivity and specificity of MS. This method is particularly advantageous when dealing with complex mixtures where unknown compounds become hard to identify.

2. Quantification of Acetone, Ethanol, Isopropanol, and Newly Identified Compounds

Quantitative analysis of reaction products, including acetone, ethanol, and isopropanol, is crucial for evaluating the efficiency and selectivity of the CO_2 hydrogenation process. These compounds are common reduction products in hydrothermal systems involving biomass-derived compounds like glucose, and their formation pathways can provide essential information about reaction stoichiometry and kinetics.

By determining the concentrations of these compounds at different time points and under varying conditions, one can develop a stoichiometric map of the reaction. This map is instrumental in identifying limiting reagents, estimating conversion efficiency, and proposing balanced chemical equations that reflect real-world yields. Furthermore, tracking the appearance and evolution of newly identified compounds over time provides kinetic insights that help differentiate between primary and secondary reaction pathways. This data not only serves mechanistic studies but also informs the design of separation and purification processes downstream, ensuring economic feasibility and environmental compliance in scaled-up systems.

3. Optimization Studies for the Zn and Glucose System

Zinc, Zn, plays a dual role in the hydrothermal reduction of CO_2 it acts as a reductant and potentially as a catalyst. When paired with glucose, Zn can significantly influence the yield and selectivity of formic acid. Optimization of this binary system requires a comprehensive investigation of several parameters, including the Zn-to-glucose ratio, particle size of Zn, reaction time, temperature, and pH.

Smaller Zn particles have a higher surface area-to-volume ratio, potentially increasing reaction rates due to greater reactive surface exposure. Conversely, larger particles might offer slower, more controlled release of electrons or maintain structural integrity over longer durations. Reaction temperature and time influence not just kinetics but also product distribution, with higher temperatures potentially favoring gas-phase products or leading to glucose degradation.

Ultimately, optimizing the Zn–glucose system aims to minimize resource use while maximizing yield, particularly for formic acid, which is a high-value product and a potential hydrogen carrier. The results will contribute to designing a scalable, sustainable process with lower environmental and economic costs.

4. Quantification of Gas-Phase Products

While the primary focus is often on liquid-phase products like formic acid, it is equally important to monitor and quantify gas-phase products in hydrothermal CO_2 reduction. Common gases

formed in such systems include CO_2, CO, CH_4, H_2, and possibly others. These gases are key indicators of side reactions, thermal degradation, or alternative reduction pathways.

Gas chromatography, especially GC-TCD, Thermal Conductivity Detector, or GC-MS, is the preferred technique for analyzing gas compositions. Gas samples are typically collected using inline analysis or gas-tight syringes or gas sampling bags immediately after the reactor cools to ambient temperature. Calibration with certified gas standards allows accurate quantification.

Understanding the gas-phase profile is essential for a complete carbon balance and to estimate the extent of CO_2 conversion. It also provides insight into reaction selectivity—whether carbon ends up as formic acid, alcohols, or methane—and reveals whether competing reactions (e.g., methanation) are significant. Additionally, the amount of H_2 produced or consumed can offer clues about reaction mechanisms and help determine the theoretical efficiency of the system as a hydrogen storage or production method.

5. Investigating the Source of Formic Acid Using pH-Controlled Buffer Systems

Determining the true origin of formic acid in the reaction mixture is vital for mechanistic studies. Glucose and CO_2 can both contribute to formic acid formation, but their relative contributions remain ambiguous under uncontrolled pH conditions. By introducing buffer systems to maintain a stable pH, especially mimicking conditions where $NaHCO_3$ is present, one can better isolate the roles of each reactant.

Buffers like phosphate or carbonate systems can maintain the reaction medium at specific pH levels during the hydrothermal process. When compared with non-buffered or variably buffered reactions, the presence and yield of formic acid under fixed pH conditions help determine whether CO_2 reduction or glucose degradation predominates in its formation.

Using isotopically labeled compounds, e.g., ^{13}C-labeled CO_2, in combination with mass spectrometry further enables direct tracking of carbon atoms. If formic acid contains ^{13}C, it clearly originates from CO_2, whereas unlabeled formic acid suggests derivation from glucose. This isotopic approach, combined with controlled pH environments, offers a robust framework for pinpointing formic acid's source.

Such studies are crucial not just academically, but also for industrial application, where the precise control of input materials and reaction conditions can make the difference between a viable or unviable process.

6. Economic Analysis of the Optimized Hydrogen Production Process

Once the process has been chemically optimized, an economic evaluation becomes imperative. This analysis determines whether the hydrothermal conversion of CO_2 into formic acid, using Zn and glucose, is financially viable for industrial or decentralized applications, such as hydrogen carriers or carbon-neutral fuels.

Key economic factors include the cost of raw materials, e.g., Zn, glucose, water, energy requirements for heating system, reactor material costs, and operational labor. The recyclability of Zn, as ZnO or other forms, and the potential reuse of unconverted glucose significantly affect overall cost. Additionally, the yield and purity of formic acid, as well as the value of co-products, such as ethanol and H_2, contribute to profitability.

Eventually, this analysis will help determine whether the proposed route offers a competitive advantage over existing hydrogen production or CO_2 utilization technologies, paving the way for further development or commercialization.

Appendix

1. Calibration curves

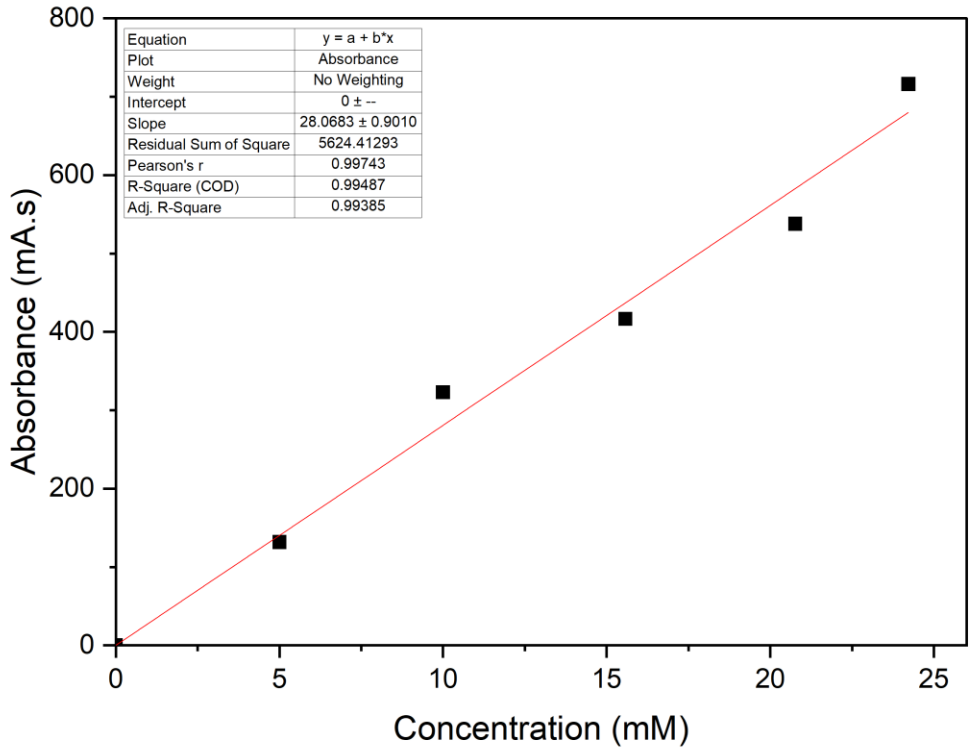

Figure 63: Calibration curve of acetic acid by HPLC-UV-Vis

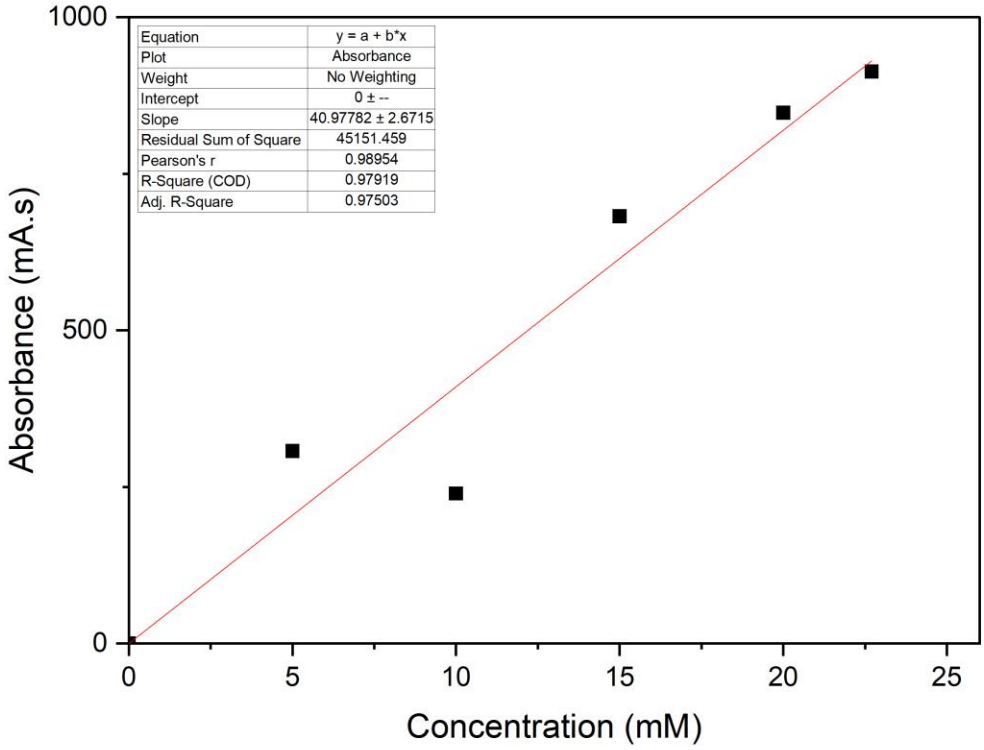

Figure 64: Calibration curve of formic acid by HPLC-UV-Vis

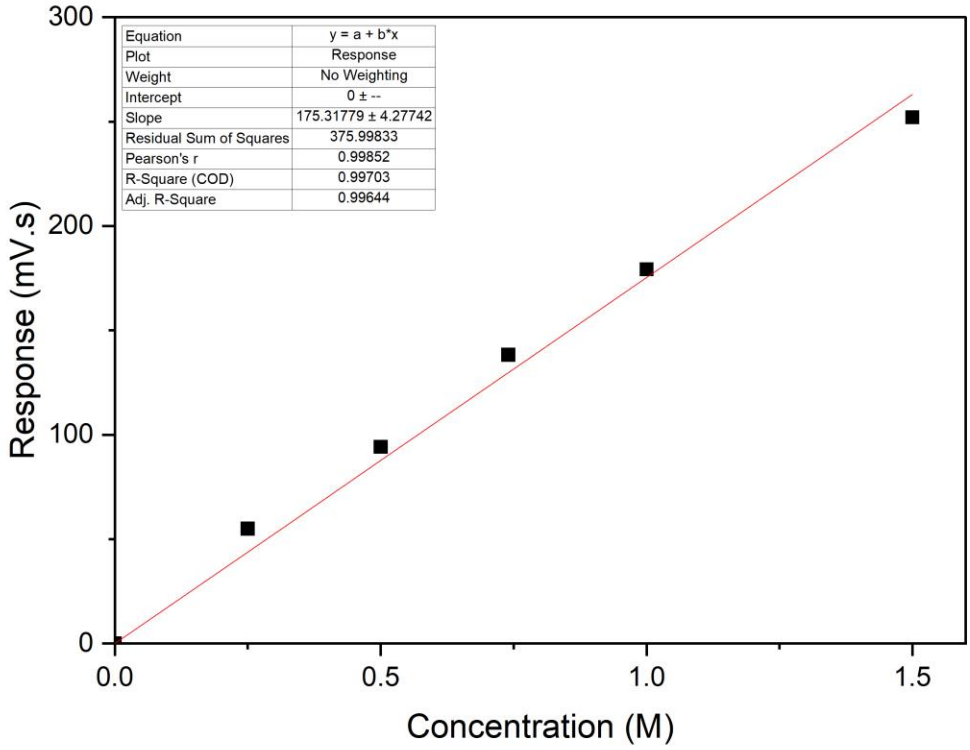

Figure 65: Calibration curve of glucose by HPLC-RID

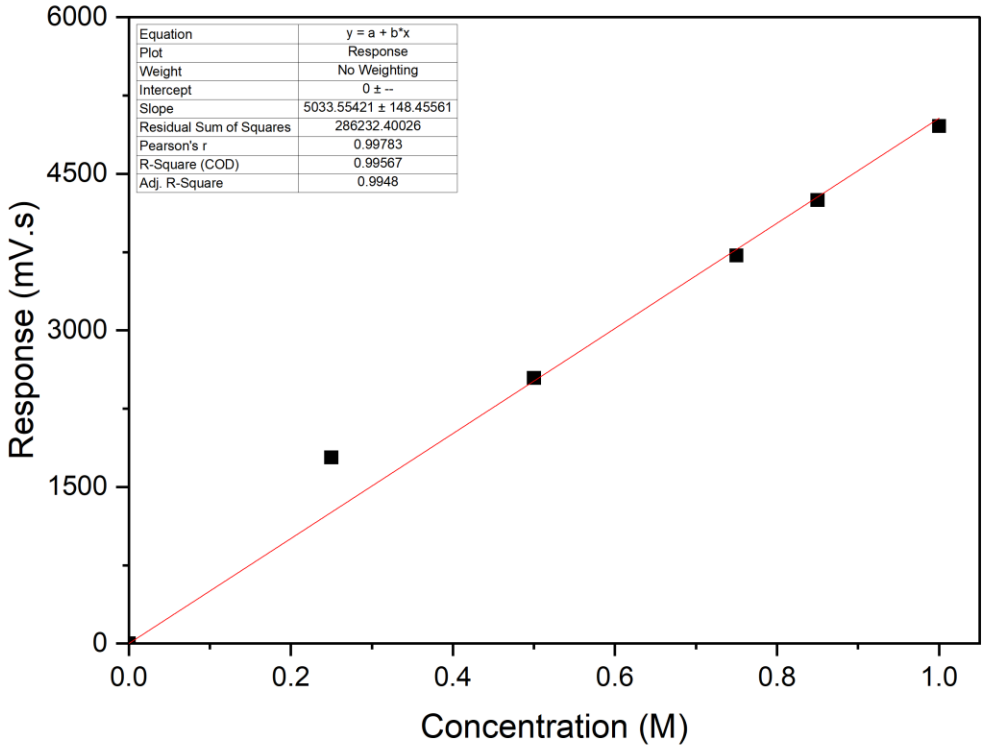

Figure 66: Calibration curve of bicarbonate by HPLC-RID

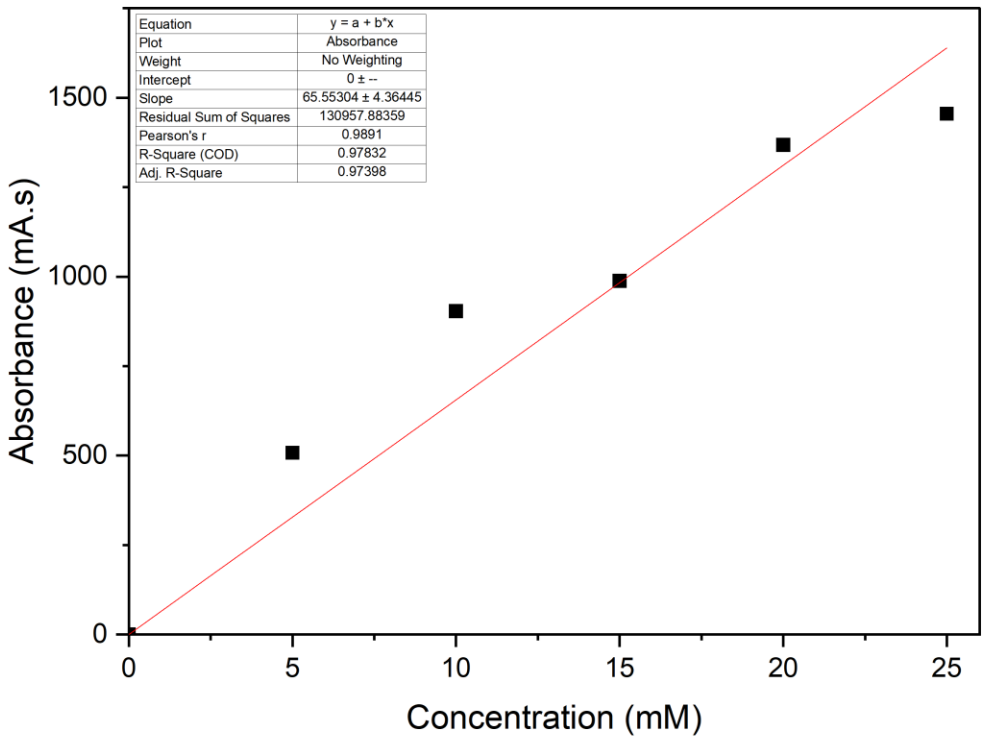

Figure 67: Calibration curve of lactic acid by HPLC-UV-Vis

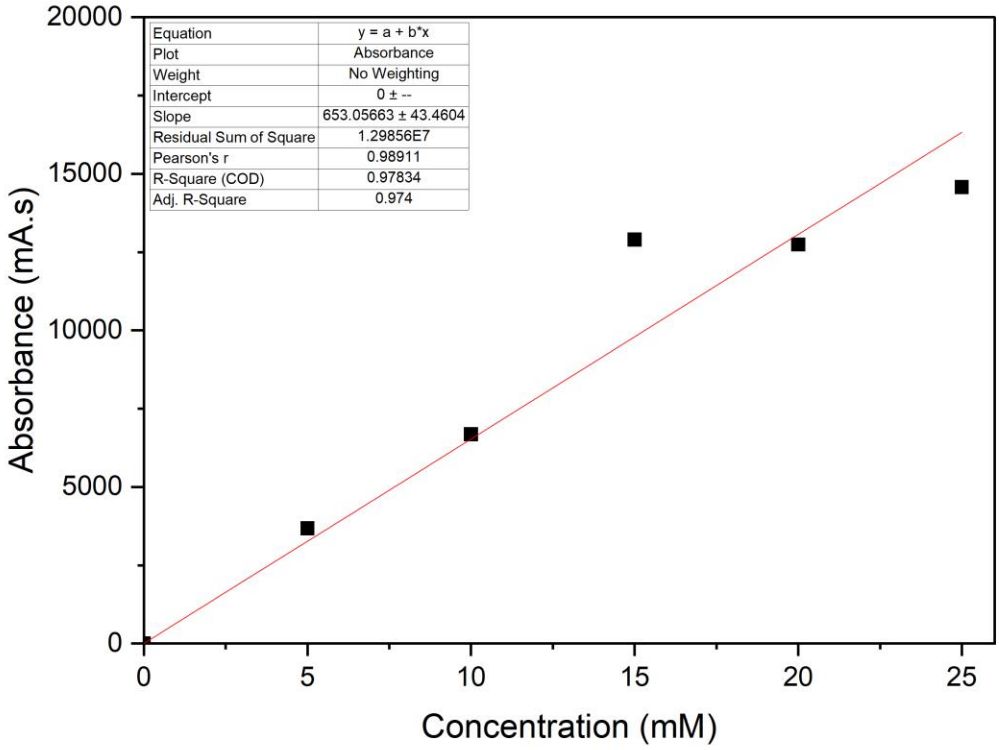

Figure 68: Calibration curve of oxalic acid by HPLC-UV-Vis

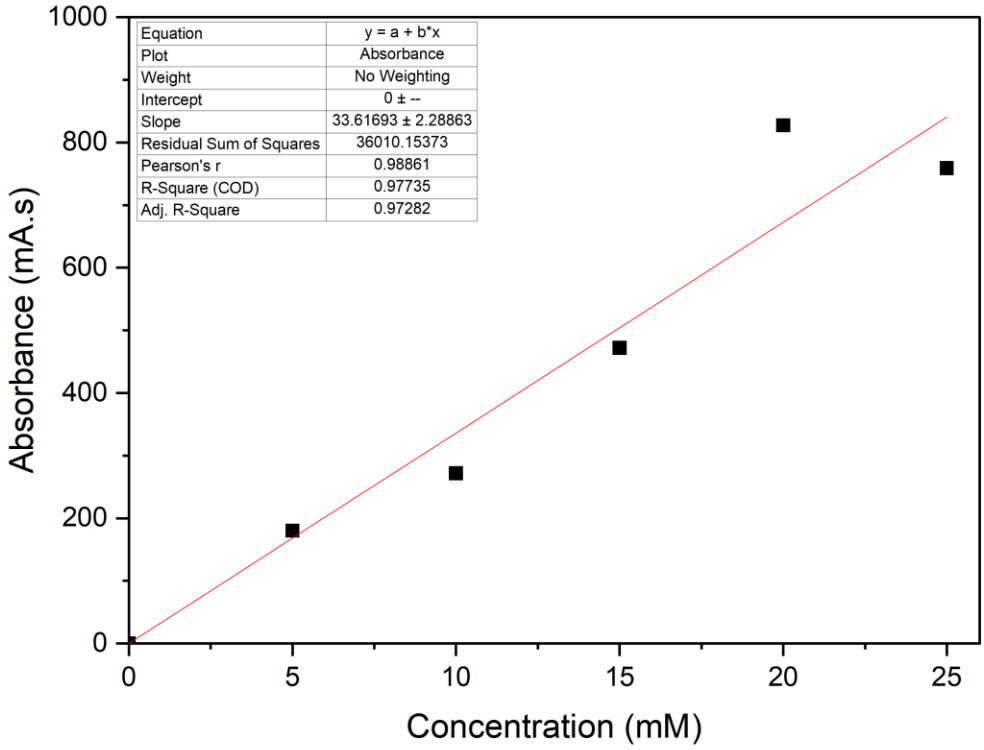

Figure 69: Calibration curve of propanoic acid by HPLC-UV-Vis

2. Statistical analysis results

OA: oxalic acid, LA: lactic acid, FA: formic acid, AA: acetic acid, and PA: propanoic acid.

1. Reaction times: heating, 1, 2, and 3 h for each compound at 200 ºC

   Anova: Single Factor

OA SUMMARY

Groups	Count	Sum	Average	Variance
Heating	2	0.001049	0.000525	1.72E-08
1	2	0.846675	0.423338	6.55E-05
2	2	1.085999	0.543	0.001981
3	2	0.955798	0.477899	0.04923

ANOVA

Source of Variation	SS	df	MS	F	P-value	F crit
Between Groups	0.361235	3	0.120412	9.393065	0.027742	6.591382
Within Groups	0.051277	4	0.012819			
Total	0.412512	7				

Anova: Single Factor

LA

SUMMARY

Groups	Count	Sum	Average	Variance
Heating	2	0.078067	0.039033	2.11E-05
1	2	4.047663	2.023831	0.005338
2	2	4.324364	2.162182	0.062389
3	2	4.525024	2.262512	0.005515

ANOVA

Source of Variation	SS	df	MS	F	P-value	F crit
Between Groups	6.738608	3	2.246203	122.6366	0.000216	6.591382
Within Groups	0.073264	4	0.018316			
Total	6.811871	7				

Anova: Single Factor

FA

SUMMARY

Groups	Count	Sum	Average	Variance
Heating	2	0.478008	0.239004	0.002763
1	2	18.6586	9.329301	4.949176
2	2	20.04528	10.02264	6.929051
3	2	19.98549	9.992745	0.198849

ANOVA

Source of Variation	SS	df	MS	F	P-value	F crit
Between Groups	137.2051	3	45.73504	15.14425	0.011941	6.591382
Within Groups	12.07984	4	3.01996			
Total	149.285	7				

Anova: Single Factor

AA

SUMMARY

Groups	Count	Sum	Average	Variance
Heating	2	1.364805	0.682403	0.004395
1	2	27.02103	13.51051	0.000357
2	2	28.17532	14.08766	0.653011
3	2	27.69988	13.84994	1.078301

ANOVA

Source of Variation	SS	df	MS	F	P-value	F crit
Between Groups	259.0751	3	86.35836	198.975	8.29E-05	6.591382
Within Groups	1.736064	4	0.434016			
Total	260.8112	7				

Anova: Single Factor

PA

SUMMARY

Groups	Count	Sum	Average	Variance
Heating	2	0.643313	0.321657	0.140918
1	2	25.43355	12.71678	0.005248
2	2	29.33751	14.66875	5.08397
3	2	28.82806	14.41403	2.140723

ANOVA

Source of Variation	SS	df	MS	F	P-value	F crit

Between Groups	282.4145	3	94.13817	51.08668	0.001203	6.591382
Within Groups	7.370859	4	1.842715			
Total	289.7854	7				

2. Reaction times: heating, 1, 2, and 3 h for each compound at 250 ºC

Anova: Single Factor

OA SUMMARY

Groups	Count	Sum	Average	Variance
Heating	2	0.919237	0.459619	0.023628
1	2	1.234813	0.617407	0.001175
2	2	1.326671	0.663335	0.000594
3	2	1.495022	0.747511	0.02106

ANOVA

Source of Variation	SS	df	MS	F	P-value	F crit
Between Groups	0.087701	3	0.029234	2.517088	0.19691	6.591382
Within Groups	0.046456	4	0.011614			
Total	0.134157	7				

Anova: Single Factor

LA SUMMARY

Groups	Count	Sum	Average	Variance
Heating	2	5.311378	2.655689	0.017423
1	2	6.286796	3.143398	0.000922
2	2	6.037992	3.018996	0.145084

3	2	6.76256	3.38128	0.005342

ANOVA

Source of Variation	SS	df	MS	F	P-value	F crit
Between Groups	0.549824	3	0.183275	4.343741	0.094934	6.591382
Within Groups	0.168771	4	0.042193			
Total	0.718595	7				

Anova: Single Factor

FA SUMMARY

Groups	Count	Sum	Average	Variance
Heating	2	21.10536	10.55268	4.59246
1	2	24.94937	12.47468	0.060898
2	2	25.48295	12.74148	0.5591
3	2	24.87796	12.43898	3.517186

ANOVA

Source of Variation	SS	df	MS	F	P-value	F crit
Between Groups	6.103497	3	2.034499	0.932225	0.503043	6.591382
Within Groups	8.729644	4	2.182411			
Total	14.83314	7				

Anova: Single Factor

AA SUMMARY

Groups	Count	Sum	Average	Variance
Heating	2	32.56029	16.28014	2.708318
1	2	29.87138	14.93569	0.369989
2	2	29.69565	14.84782	0.060354
3	2	29.57998	14.78999	1.2082

ANOVA

Source of Variation	SS	df	MS	F	P-value	F crit
Between Groups	3.055984	3	1.018661	0.937376	0.501153	6.591382
Within Groups	4.346862	4	1.086715			
Total	7.402845	7				

Anova: Single Factor

PA SUMMARY

Groups	Count	Sum	Average	Variance
Heating	2	39.26349	19.63175	31.9811
1	2	33.67175	16.83588	1.617245
2	2	30.91175	15.45587	0.111263
3	2	28.84856	14.42428	2.650823

ANOVA

Source of Variation	SS	df	MS	F	P-value	F crit
Between Groups	30.57844	3	10.19281	1.121308	0.439688	6.591382
Within Groups	36.36043	4	9.090107			
Total	66.93887	7				

3. Reaction times: heating, 1, 2, and 3 h for each compound at 300 ºC

Anova: Single Factor

OA

SUMMARY

Groups	Count	Sum	Average	Variance
Heating	2	1.82126	0.91063	0.005006
1	2	1.877673	0.938837	0.093996
2	2	1.725394	0.862697	0.300995
3	2	0.573993	0.286997	0.002739

ANOVA

Source of Variation	SS	df	MS	F	P-value	F crit
Between Groups	0.577068	3	0.192356	1.910487	0.269329	6.591382
Within Groups	0.402737	4	0.100684			
Total	0.979805	7				

Anova: Single Factor

LA

SUMMARY

Groups	Count	Sum	Average	Variance
Heating	2	8.044773	4.022387	0.046882
1	2	8.913496	4.456748	0.456845
2	2	9.113532	4.556766	0.067774
3	2	8.39744	4.19872	0.071039

ANOVA

Source of Variation	SS	df	MS	F	P-value	F crit

Between Groups	0.355052	3	0.118351	0.736767	0.582533	6.591382
Within Groups	0.64254	4	0.160635			
Total	0.997592	7				

Anova: Single Factor

FA

SUMMARY

Groups	Count	Sum	Average	Variance
Heating	2	24.86283	12.43142	4.101982
1	2	22.44997	11.22498	1.202891
2	2	20.11314	10.05657	0.0002
3	2	16.51622	8.258112	0.051623

ANOVA

Source of Variation	SS	df	MS	F	P-value	F crit
Between Groups	18.95691	3	6.318971	4.718559	0.084024	6.591382
Within Groups	5.356695	4	1.339174			
Total	24.31361	7				

Anova: Single Factor

AA

SUMMARY

Groups	Count	Sum	Average	Variance
Heating	2	33.16875	16.58437	0.379928
1	2	32.70775	16.35388	3.278133
2	2	34.33327	17.16663	0.038919
3	2	35.2163	17.60815	0.429781

ANOVA

Source of Variation	SS	df	MS	F	P-value	F crit
Between Groups	1.934498	3	0.644833	0.625025	0.635556	6.591382
Within Groups	4.126761	4	1.03169			
Total	6.061259	7				

Anova: Single Factor

PA SUMMARY

Groups	Count	Sum	Average	Variance
Heating	2	37.13855	18.56927	8.49434
1	2	12.99622	6.49811	7.232515
2	2	5.539679	2.769839	0.113449
3	2	4.686151	2.343075	1.63597

ANOVA

Source of Variation	SS	df	MS	F	P-value	F crit
Between Groups	344.9856	3	114.9952	26.3203	0.004288	6.591382
Within Groups	17.47627	4	4.369068			
Total	362.4618	7				

4. Reaction temperature: 200, 250, and 300 ºC for each compound at 1 h

Anova: Single Factor

OA SUMMARY

Groups	Count	Sum	Average	Variance
200	2	0.846675	0.423338	6.55E-05
250	2	1.234813	0.617407	0.001175
300	2	1.877673	0.938837	0.093996

ANOVA

Source of Variation	SS	df	MS	F	P-value	F crit
Between Groups	0.271146	2	0.135573	4.270627	0.132526	9.552094
Within Groups	0.095236	3	0.031745			
Total	0.366383	5				

Anova: Single Factor

LA

SUMMARY

Groups	Count	Sum	Average	Variance
200	2	4.047663	2.023831	0.005338
250	2	6.286796	3.143398	0.000922
300	2	8.913496	4.456748	0.456845

ANOVA

Source of Variation	SS	df	MS	F	P-value	F crit
Between Groups	5.9316	2	2.9658	19.21246	0.019489	9.552094
Within Groups	0.463106	3	0.154369			
Total	6.394705	5				

Anova: Single Factor

FA

SUMMARY

Groups	Count	Sum	Average	Variance
200	2	18.6586	9.329301	4.949176
250	2	24.94937	12.47468	0.060898
300	2	22.44997	11.22498	1.202891

ANOVA

Source of Variation	SS	df	MS	F	P-value	F crit
Between Groups	10.03254	2	5.016269	2.422162	0.23651	9.552094
Within Groups	6.212965	3	2.070988			
Total	16.2455	5				

Anova: Single Factor

AA

SUMMARY

Groups	Count	Sum	Average	Variance
200	2	27.02103	13.51051	0.000357
250	2	29.87138	14.93569	0.369989
300	2	32.70775	16.35388	3.278133

ANOVA

Source of Variation	SS	df	MS	F	P-value	F crit
Between Groups	8.084732	2	4.042366	3.323877	0.173397	9.552094
Within Groups	3.64848	3	1.21616			
Total	11.73321	5				

Anova: Single Factor

PA

SUMMARY

Groups	Count	Sum	Average	Variance
200	2	25.43355	12.71678	0.005248
250	2	33.67175	16.83588	1.617245
300	2	12.99622	6.49811	7.232515

ANOVA

Source of Variation	SS	df	MS	F	P-value	F crit
Between Groups	108.3388	2	54.16941	18.35213	0.02077	9.552094
Within Groups	8.855008	3	2.951669			
Total	117.1938	5				

5. Reaction temperature: 200, 250, and 300 ºC for each compound at 2 h

Anova: Single Factor

OA

SUMMARY

Groups	Count	Sum	Average	Variance
200	2	1.085999	0.543	0.001981
250	2	1.326671	0.663335	0.000594
300	2	1.725394	0.862697	0.300995

ANOVA

Source of Variation	SS	df	MS	F	P-value	F crit
Between Groups	0.104288	2	0.052144	0.515308	0.642133	9.552094
Within Groups	0.303571	3	0.10119			

Total	0.407859	5

Anova: Single Factor

LA

SUMMARY

Groups	Count	Sum	Average	Variance
200	2	4.324364	2.162182	0.062389
250	2	6.037992	3.018996	0.145084
300	2	9.113532	4.556766	0.067774

ANOVA

Source of Variation	SS	df	MS	F	P-value	F crit
Between Groups	5.8886	2	2.9443	32.09069	0.009436	9.552094
Within Groups	0.275248	3	0.091749			
Total	6.163848	5				

Anova: Single Factor

FA

SUMMARY

Groups	Count	Sum	Average	Variance
200	2	20.04528	10.02264	6.929051
250	2	25.48295	12.74148	0.5591
300	2	20.11314	10.05657	0.0002

ANOVA

Source of Variation	SS	df	MS	F	P-value	F crit

Between Groups	9.734617	2	4.867308	1.949952	0.286693	9.552094
Within Groups	7.488351	3	2.496117			
Total	17.22297	5				

Anova: Single Factor

AA

SUMMARY

Groups	Count	Sum	Average	Variance
200	2	28.17532	14.08766	0.653011
250	2	29.69565	14.84782	0.060354
300	2	34.33327	17.16663	0.038919

ANOVA

Source of Variation	SS	df	MS	F	P-value	F crit
Between Groups	10.28989	2	5.144946	20.5173	0.017782	9.552094
Within Groups	0.752284	3	0.250761			
Total	11.04218	5				

Anova: Single Factor

PA

SUMMARY

Groups	Count	Sum	Average	Variance
200	2	29.33751	14.66875	5.08397
250	2	30.91175	15.45587	0.111263
300	2	5.539679	2.769839	0.113449

ANOVA

Source of Variation	SS	df	MS	F	P-value	F crit
Between Groups	202.0928	2	101.0464	57.10254	0.004095	9.552094
Within Groups	5.308681	3	1.76956			
Total	207.4015	5				

6. Reaction temperature: 200, 250, and 300 ºC for each compound at 3 h

Anova: Single Factor

OA SUMMARY

Groups	Count	Sum	Average	Variance
200	2	0.955798	0.477899	0.04923
250	2	1.495022	0.747511	0.02106
300	2	0.573993	0.286997	0.002739

ANOVA

Source of Variation	SS	df	MS	F	P-value	F crit
Between Groups	0.214139	2	0.107069	4.39836	0.128245	9.552094
Within Groups	0.073029	3	0.024343			
Total	0.287168	5				

Anova: Single Factor

LA SUMMARY

Groups	Count	Sum	Average	Variance
200	2	4.525024	2.262512	0.005515
250	2	6.76256	3.38128	0.005342
300	2	8.39744	4.19872	0.071039

ANOVA

Source of Variation	SS	df	MS	F	P-value	F crit
Between Groups	3.779167	2	1.889583	69.21921	0.003089	9.552094
Within Groups	0.081896	3	0.027299			
Total	3.861062	5				

Anova: Single Factor

FA SUMMARY

Groups	Count	Sum	Average	Variance
200	2	19.98549	9.992745	0.198849
250	2	24.87796	12.43898	3.517186
300	2	16.51622	8.258112	0.051623

ANOVA

Source of Variation	SS	df	MS	F	P-value	F crit
Between Groups	17.64847	2	8.824236	7.026302	0.07379	9.552094
Within Groups	3.767659	3	1.255886			
Total	21.41613	5				

Anova: Single Factor

AA SUMMARY

Groups	Count	Sum	Average	Variance
200	2	27.69988	13.84994	1.078301

250	2	29.57998	14.78999	1.2082
300	2	35.2163	17.60815	0.429781

ANOVA

Source of Variation	SS	df	MS	F	P-value	F crit
Between Groups	15.29991	2	7.649956	8.449003	0.058542	9.552094
Within Groups	2.716281	3	0.905427			
Total	18.01619	5				

Anova: Single Factor

PA

SUMMARY

Groups	Count	Sum	Average	Variance
200	2	28.82806	14.41403	2.140723
250	2	28.84856	14.42428	2.650823
300	2	4.686151	2.343075	1.63597

ANOVA

Source of Variation	SS	df	MS	F	P-value	F crit
Between Groups	194.4424	2	97.2212	45.37734	0.005724	9.552094
Within Groups	6.427516	3	2.142505			
Total	200.8699	5				

7. Reactor filling volumes: 30, 50, and 70% for each compound at 2 h and 250 ºC

Anova: Single Factor

OA

SUMMARY

Groups	Count	Sum	Average	Variance
30	2	1.4425	0.72125	0.001337
50	2	1.326671	0.663335	0.000594
70	2	1.384837	0.692419	0.0123

ANOVA

Source of Variation	SS	df	MS	F	P-value	F crit
Between Groups	0.003354	2	0.001677	0.35353	0.72801	9.552094
Within Groups	0.014231	3	0.004744			
Total	0.017585	5				

Anova: Single Factor

LA

SUMMARY

Groups	Count	Sum	Average	Variance
30	2	6.442334	3.221167	0.006299
50	2	6.037992	3.018996	0.145084
70	2	6.004416	3.002208	0.027986

ANOVA

Source of Variation	SS	df	MS	F	P-value	F crit
Between Groups	0.059399	2	0.029699	0.496731	0.651115	9.552094
Within Groups	0.179369	3	0.05979			
Total	0.238768	5				

Anova: Single Factor

FA

SUMMARY

Groups	Count	Sum	Average	Variance
30	2	24.43382	12.21691	0.020945
50	2	25.48295	12.74148	0.5591
70	2	21.41282	10.70641	1.993823

ANOVA

Source of Variation	SS	df	MS	F	P-value	F crit
Between Groups	4.465508	2	2.232754	2.602411	0.221095	9.552094
Within Groups	2.573868	3	0.857956			
Total	7.039376	5				

Anova: Single Factor

AA SUMMARY

Groups	Count	Sum	Average	Variance
30	2	29.037	14.5185	0.363396
50	2	29.69565	14.84782	0.060354
70	2	28.82965	14.41483	0.165409

ANOVA

Source of Variation	SS	df	MS	F	P-value	F crit
Between Groups	0.204459	2	0.10223	0.520554	0.639633	9.552094
Within Groups	0.589159	3	0.196386			
Total	0.793618	5				

Anova: Single Factor

PA SUMMARY

Groups	Count	Sum	Average	Variance
30	2	32.08294	16.04147	0.006778
50	2	30.91175	15.45587	0.111263
70	2	35.60655	17.80328	4.558033

ANOVA

Source of Variation	SS	df	MS	F	P-value	F crit

Between Groups	5.971458	2	2.985729	1.915536	0.291037	9.552094
Within Groups	4.676074	3	1.558691			
Total	10.64753	5				

8. Fe reductant addition for each compound at 2 h and 250 ºC and 50% filling volume

Anova: Single Factor

OA

SUMMARY

Groups	Count	Sum	Average	Variance
No metal	2	1.326671	0.663335	0.000594
Fe	2	0.858573	0.429287	4.38E-05

ANOVA

Source of Variation	SS	df	MS	F	P-value	F crit
Between Groups	0.054779	1	0.054779	171.851	0.005769	18.51282

Within Groups	0.000638	2	0.000319
Total	0.055416	3	

Anova: Single Factor

LA

SUMMARY

Groups	Count	Sum	Average	Variance
No metal	2	6.037992	3.018996	0.145084
Fe	2	7.089164	3.544582	0.002176

ANOVA

Source of Variation	SS	df	MS	F	P-value	F crit
Between Groups	0.27624	1	0.27624	3.751731	0.192362	18.51282
Within Groups	0.14726	2	0.07363			
Total	0.423501	3				

Anova: Single Factor

FA

SUMMARY

Groups	Count	Sum	Average	Variance
No metal	2	25.48295	12.74148	0.5591
Fe	2	21.22489	10.61245	0.445682

ANOVA

Source of Variation	SS	df	MS	F	P-value	F crit
Between Groups	4.532766	1	4.532766	9.02239	0.095262	18.51282
Within Groups	1.004782	2	0.502391			

Total	5.537547	3				

Anova: Single Factor

AA

SUMMARY

Groups	Count	Sum	Average	Variance
No metal	2	29.69565	14.84782	0.060354
Fe	2	24.20782	12.10391	0.010904

ANOVA

Source of Variation	SS	df	MS	F	P-value	F crit
Between Groups	7.529064	1	7.529064	211.3167	0.004699	18.51282
Within Groups	0.071259	2	0.035629			
Total	7.600323	3				

Anova: Single Factor

PA

SUMMARY

Groups	Count	Sum	Average	Variance
No metal	2	30.91175	15.45587	0.111263
Fe	2	30.10159	15.05079	0.192062

ANOVA

Source of Variation	SS	df	MS	F	P-value	F crit
Between Groups	0.164089	1	0.164089	1.081934	0.407499	18.51282
Within Groups	0.303325	2	0.151662			

Total	0.467413	3

9. Zn reductant addition for each compound at 2 h and 250 ºC and 50% filling volume

Anova: Single Factor

OA SUMMARY

Groups	Count	Sum	Average	Variance
No metal	2	1.326671	0.663335	0.000594
Zn	2	0.169895	0.084947	0.002186

ANOVA

Source of Variation	SS	df	MS	F	P-value	F crit
Between Groups	0.334532	1	0.334532	240.7325	0.004128	18.51282
Within Groups	0.002779	2	0.00139			
Total	0.337312	3				

Anova: Single Factor

LA SUMMARY

Groups	Count	Sum	Average	Variance
No metal	2	6.037992	3.018996	0.145084
Zn	2	3.772959	1.886479	0.282069

ANOVA

Source of Variation	SS	df	MS	F	P-value	F crit
Between Groups	1.282594	1	1.282594	6.005303	0.133879	18.51282

Within Groups	0.427154	2	0.213577
Total	1.709748	3	

Anova: Single Factor

FA

SUMMARY

Groups	Count	Sum	Average	Variance
No metal	2	25.48295	12.74148	0.5591
Zn	2	76.14449	38.07225	8.529414

ANOVA

Source of Variation	SS	df	MS	F	P-value	F crit
Between Groups	641.6479	1	641.6479	141.1997	0.007008	18.51282
Within Groups	9.088514	2	4.544257			
Total	650.7364	3				

Anova: Single Factor

AA

SUMMARY

Groups	Count	Sum	Average	Variance
No metal	2	29.69565	14.84782	0.060354
Zn	2	17.16483	8.582417	5.429521

ANOVA

Source of Variation	SS	df	MS	F	P-value	F crit
Between Groups	39.2553	1	39.2553	14.30098	0.063353	18.51282

Within Groups	5.489875	2	2.744938
Total	44.74518	3	

Anova: Single Factor

PA SUMMARY

Groups	Count	Sum	Average	Variance
No metal	2	30.91175	15.45587	0.111263
Zn	2	2.385405	1.192703	0.18193

ANOVA

Source of Variation	SS	df	MS	F	P-value	F crit
Between Groups	203.438	1	203.438	1387.742	0.00072	18.51282
Within Groups	0.293193	2	0.146596			
Total	203.7312	3				

10. Al reductant addition for each compound at 2 h and 250 ºC and 50% filling volume

Anova: Single Factor

OA SUMMARY

Groups	Count	Sum	Average	Variance
No metal	2	1.326671	0.663335	0.000594
Al	2	0.551036	0.275518	0.001294

ANOVA

Source of Variation	SS	df	MS	F	P-value	F crit

Between Groups	0.150402	1	0.150402	159.3684	0.006216	18.51282
Within Groups	0.001887	2	0.000944			
Total	0.15229	3				

Anova: Single Factor

LA

SUMMARY

Groups	Count	Sum	Average	Variance
No metal	2	6.037992	3.018996	0.145084
Al	2	8.142458	4.071229	0.357989

ANOVA

Source of Variation	SS	df	MS	F	P-value	F crit
Between Groups	1.107193	1	1.107193	4.401718	0.170793	18.51282
Within Groups	0.503073	2	0.251537			
Total	1.610267	3				

Anova: Single Factor

FA

SUMMARY

Groups	Count	Sum	Average	Variance
No metal	2	25.48295	12.74148	0.5591
Al	2	26.34207	13.17104	4.845614

ANOVA

Source of Variation	SS	df	MS	F	P-value	F crit

Between Groups	0.184523	1	0.184523	0.068282	0.818302	18.51282
Within Groups	5.404714	2	2.702357			
Total	5.589237	3				

Anova: Single Factor

AA

SUMMARY

Groups	Count	Sum	Average	Variance
No metal	2	29.69565	14.84782	0.060354
Al	2	27.55481	13.7774	0.228927

ANOVA

Source of Variation	SS	df	MS	F	P-value	F crit
Between Groups	1.145796	1	1.145796	7.921682	0.106456	18.51282
Within Groups	0.289281	2	0.14464			
Total	1.435076	3				

Anova: Single Factor

PA

SUMMARY

Groups	Count	Sum	Average	Variance
No metal	2	30.91175	15.45587	0.111263
Al	2	20.89114	10.44557	14.72922

ANOVA

Appendix

Source of Variation	SS	df	MS	F	P-value	F crit
Between Groups	25.10313	1	25.10313	3.383062	0.207243	18.51282
Within Groups	14.84048	2	7.420241			
Total	39.94362	3				

Bibliography

[1] "Climate Change: Global Temperature | NOAA Climate.gov." https://www.climate.gov/news-features/understanding-climate/climate-change-global-temperature#:~:text=The%20roughly%202%2Ddegree%20Fahrenheit,significant%20increase%20in%20accumulated%20heat (accessed Nov. 25, 2024).

[2] "How do we know climate change is happening? | Grantham Institute – Climate Change and the Environment | Imperial College London." https://www.imperial.ac.uk/grantham/publications/climate-change-faqs/how-do-we-know-climate-change-is-happening/#:~:text=Models%20only%20show%20a%20temperature,of%20global%20warming%20since%201850 (accessed Nov. 25, 2024).

[3] "Atmospheric CO2 ppm by year 1959-2023 | Statista." https://www.statista.com/statistics/1091926/atmospheric-concentration-of-co2-historic/ (accessed Nov. 25, 2024).

[4] "Climate Change: Atmospheric Carbon Dioxide | NOAA Climate.gov." https://www.climate.gov/news-features/understanding-climate/climate-change-atmospheric-carbon-dioxide (accessed Nov. 25, 2024).

[5] IPCC, "Technical summary," in *Climate change 2022 – impacts, adaptation and vulnerability*, Cambridge University Press, 2023, pp. 37–118.

[6] T. N.Borhani and M. Wang, "Role of solvents in CO2 capture processes: The review of selection and design methods," *Renew. Sustain. Energy Rev*, vol. 114, p. 109299, Oct. 2019, doi: 10.1016/j.rser.2019.109299.

[7] " Office of ENERGY EFFICIENCY & RENEWABLE ENERGY," *Hydrogen Production Processes*. https://www.energy.gov/eere/fuelcells/hydrogen-production-processes (accessed Mar. 15, 2023).

[8] "Hydrogen Production Processes | Department of Energy." https://www.energy.gov/eere/fuelcells/hydrogen-production-processes (accessed Nov. 25, 2024).

[9] C. Jiang, H. Zhong, G. Yao, J. Duo, and F. Jin, "One-step water splitting and NaHCO 3 reduction into hydrogen storage material of formate with Fe as the reductant under hydrothermal conditions," *Int. J. Hydrogen Energy*, vol. 42, no. 27, pp. 17476–17487, Jul. 2017, doi: 10.1016/j.ijhydene.2017.03.022.

[10] T. He, Q. Pei, and P. Chen, "Liquid organic hydrogen carriers," *Journal of Energy Chemistry*, vol. 24, no. 5, pp. 587–594, Sep. 2015, doi: 10.1016/j.jechem.2015.08.007.

[11] H. Takahashi *et al.*, "CO2 reduction using hydrothermal method for the selective formation of organic compounds," *J. Mater. Sci.*, vol. 41, no. 5, pp. 1585–1589, Mar. 2006, doi: 10.1007/s10853-006-4649-5.

[12] A. A. Galkin and V. V. Lunin, "Subcritical and supercritical water: a universal medium for chemical reactions," *Russ. Chem. Rev.*, vol. 74, no. 1, pp. 21–35, Jan. 2005, doi: 10.1070/RC2005v074n01ABEH001167.

[13] W. Wang, S. Wang, X. Ma, and J. Gong, "Recent advances in catalytic hydrogenation of carbon dioxide.," *Chem. Soc. Rev.*, vol. 40, no. 7, pp. 3703–3727, Jul. 2011, doi: 10.1039/c1cs15008a.

[14] X. Zeng *et al.*, "New insights into highly efficient reduction of CO2 to formic acid by using zinc under mild hydrothermal conditions: a joint experimental and theoretical study.," *Phys. Chem. Chem. Phys.*, vol. 16, no. 37, pp. 19836–19840, Oct. 2014, doi: 10.1039/c4cp03388d.

[15] F. Jin *et al.*, "Highly efficient and autocatalytic $H2_2$ dissociation for CO_2 reduction into formic acid with zinc.," *Sci. Rep.*, vol. 4, p. 4503, Mar. 2014, doi: 10.1038/srep04503.

[16] D. Roman-Gonzalez *et al.*, "2Hydrothermal CO2 conversion using zinc as reductant: Batch reaction, modeling and parametric analysisof the process," *J. Supercrit. Fluids*, vol. 140, pp. 320–328, Oct. 2018, doi: 10.1016/j.supflu.2018.07.003.

[17] M. Andérez-Fernández, E. Pérez, A. Martín, and M. D. Bermejo, "Hydrothermal CO 2 reduction using biomass derivatives as reductants," *J. Supercrit. Fluids*, vol. 133, pp. 658–664, Mar. 2018, doi: 10.1016/j.supflu.2017.10.010.

[18] S. Valluri, V. Claremboux, and S. Kawatra, "Opportunities and challenges in CO2 utilization.," *J. Environ. Sci. (China)*, vol. 113, pp. 322–344, Mar. 2022, doi: 10.1016/j.jes.2021.05.043.

[19] International Energy Agency, *Putting CO2 to Use: Creating value from emissions*. OECD, 2019.

[20] E. Alper and O. Yuksel Orhan, "CO 2 utilization: Developments in conversion processes," *Petroleum*, vol. 3, no. 1, pp. 109–126, Mar. 2017, doi: 10.1016/j.petlm.2016.11.003.

[21] A. Rafiee, K. R. Khalilpour, and D. Milani, "CO2 conversion and utilization pathways," in *Polygeneration with Polystorage for Chemical and Energy Hubs*, Elsevier, 2019, pp. 213–245.

[22] "Carbon Utilization: A Vital and Effective Pathway for Decarbonization - Center for Climate and Energy SolutionsCenter for Climate and Energy Solutions." https://www.c2es.org/document/carbon-utilization-a-vital-and-effective-pathway-for-decarbonization/ (accessed Dec. 17, 2025).

[23] Z. Turakulov *et al.*, "Assessing various CO utilization technologies: a brief comparative review," *J. Chem. Technol. Biotechnol.*, vol. 99, no. 6, pp. 1291–1307, Jun. 2024, doi: 10.1002/jctb.7606.

[24] C. Song, "Co_2 conversion and utilization: an overview," in *Co_2 conversion and utilization*, vol. 809, C. Song, A. F. Gaffney, and K. Fujimoto, Eds. Washington, DC: American Chemical Society, 2002, pp. 2–30.

[25] Y. Liu and D. Liu, "Study of bimetallic Cu–Ni/γ-Al2O3 catalysts for carbon dioxide hydrogenation," *Int. J. Hydrogen Energy*, vol. 24, no. 4, pp. 351–354, Apr. 1999, doi: 10.1016/S0360-3199(98)00038-X.

[26] C.-S. Chen, W.-H. Cheng, and S.-S. Lin, "Study of reverse water gas shift reaction by TPD, TPR and CO2 hydrogenation over potassium-promoted Cu/SiO2 catalyst," *Applied Catalysis A: General*, vol. 238, no. 1, pp. 55–67, Jan. 2003, doi: 10.1016/S0926-860X(02)00221-1.

[27] F. S. Stone and D. Waller, "Cu-ZnO and Cu-ZnO/Al2O3 catalysts for the reverse water-gas shift reaction. The effect of the Cu/Zn ratio on precursor characteristics and on the activity of the derived catalysts," *Topics in Catalysis*, vol. 22, no. 3–4, pp. 305–318, 2003.

[28] L. Wang, S. Zhang, and Y. Liu, "Reverse water gas shift reaction over Co-precipitated Ni-CeO2 catalysts," *Journal of Rare Earths*, vol. 26, no. 1, pp. 66–70, Feb. 2008, doi: 10.1016/S1002-0721(08)60039-3.

[29] A. Trovarelli, "Catalytic Properties of Ceria and CeO_2 -Containing Materials," *Catalysis Reviews*, vol. 38, no. 4, pp. 439–520, Nov. 1996, doi: 10.1080/01614949608006464.

[30] A. Goguet, F. Meunier, J. Breen, R. Burch, M. Petch, and A. Faurghenciu, "Study of the origin of the deactivation of a Pt/CeO catalyst during reverse water gas shift (RWGS) reaction," *J. Catal.*, vol. 226, no. 2, pp. 382–392, Sep. 2004, doi: 10.1016/j.jcat.2004.06.011.

[31] K. Kitamura Bando, K. Soga, K. Kunimori, and H. Arakawa, "Effect of Li additive on CO2 hydrogenation reactivity of zeolite supported Rh catalysts," *Applied Catalysis A: General*, vol. 175, no. 1–2, pp. 67–81, Dec. 1998, doi: 10.1016/S0926-860X(98)00202-6.

[32] C. S. Chen, J. H. Lin, J. H. You, and C. R. Chen, "Properties of Cu(thd)2 as a precursor to prepare Cu/SiO2 catalyst using the atomic layer epitaxy technique.," *J. Am. Chem. Soc.*, vol. 128, no. 50, pp. 15950–15951, Dec. 2006, doi: 10.1021/ja063083d.

[33] H. Kusama, K. K. Bando, K. Okabe, and H. Arakawa, "CO2 hydrogenation reactivity and structure of Rh/SiO2 catalysts prepared from acetate, chloride and nitrate precursors," *Applied Catalysis A: General*, vol. 205, no. 1–2, pp. 285–294, Jan. 2001, doi: 10.1016/S0926-860X(00)00576-7.

[34] N. Perkas, G. Amirian, Z. Zhong, J. Teo, Y. Gofer, and A. Gedanken, "Methanation of Carbon Dioxide on Ni Catalysts on Mesoporous ZrO2 Doped with Rare Earth Oxides," *Catal. Lett*, vol. 130, no. 3–4, pp. 455–462, Jul. 2009, doi: 10.1007/s10562-009-9952-8.

[35] J. Sehested *et al.*, "Discovery of technical methanation catalysts based on computational screening," *Top. Catal.*, vol. 45, no. 1–4, pp. 9–13, Aug. 2007, doi: 10.1007/s11244-007-0232-9.

[36] P. J. Lunde and F. L. Kester, "Carbon dioxide methanation on a ruthenium catalyst," *Ind. Eng. Chem. Proc. Des. Dev.*, vol. 13, no. 1, pp. 27–33, Jan. 1974, doi: 10.1021/i260049a005.

[37] F.-W. Chang, T.-J. Hsiao, and J.-D. Shih, "Hydrogenation of CO_2 over a Rice Husk Ash Supported Nickel Catalyst Prepared by Deposition−Precipitation," *Ind. Eng. Chem. Res.*, vol. 37, no. 10, pp. 3838–3845, Oct. 1998, doi: 10.1021/ie980152r.

[38] F.-W. Chang, T.-J. Hsiao, S.-W. Chung, and J.-J. Lo, "Nickel supported on rice husk ash — activity and selectivity in CO2 methanation," *Applied Catalysis A: General*, vol. 164, no. 1–2, pp. 225–236, Dec. 1997, doi: 10.1016/S0926-860X(97)00173-7.

[39] F.-W. Chang, M.-T. Tsay, and S.-P. Liang, "Hydrogenation of CO2 over nickel catalysts supported on rice husk ash prepared by ion exchange," *Applied Catalysis A: General*, vol. 209, no. 1–2, pp. 217–227, Feb. 2001, doi: 10.1016/S0926-860X(00)00772-9.

[40] S. Sane, J. M. Bonnier, J. P. Damon, and J. Masson, "Raney metal catalysts: I. comparative properties of raney nickel proceeding from Ni-Ai intermetallic phases," *Appl. Catal.*, vol. 9, no. 1, pp. 69–83, Jan. 1984, doi: 10.1016/0166-9834(84)80039-1.

[41] J. Kothandaraman *et al.*, "Integrated Capture and Conversion of CO2 to Methane Using a Water-lean, Post-Combustion CO2 Capture Solvent.," *ChemSusChem*, vol. 14, no. 21, pp. 4812–4819, Nov. 2021, doi: 10.1002/cssc.202101590.

[42] L. Torrente-Murciano, R. S. L. Chapman, A. Narvaez-Dinamarca, D. Mattia, and M. D. Jones, "Effect of nanostructured ceria as support for the iron catalysed hydrogenation of CO2 into hydrocarbons.," *Phys. Chem. Chem. Phys.*, vol. 18, no. 23, pp. 15496–15500, Jun. 2016, doi: 10.1039/c5cp07788e.

[43] K. Fujimoto and T. Shikada, "Selective synthesis of C2-C5 hydrocarbons from carbon dioxide utilizing a hybrid catalyst composed of a methanol synthesis catalyst and zeolite," *Appl. Catal.*, vol. 31, no. 1, pp. 13–23, Jan. 1987, doi: 10.1016/S0166-9834(00)80663-6.

[44] J.-F. Lee, W.-S. Chern, M.-D. Lee, and T.-Y. Dong, "Hydrogenation of carbon dioxide on iron catalysts doubly promoted with manganese and potassium," *Can. J. Chem. Eng.*, vol. 70, no. 3, pp. 511–515, Mar. 2009, doi: 10.1002/cjce.5450700314.

[45] P. S. Sai Prasad, J. W. Bae, K.-W. Jun, and K.-W. Lee, "Fischer–Tropsch Synthesis by Carbon Dioxide Hydrogenation on Fe-Based Catalysts," *Catal. Surv. Asia*, vol. 12, no. 3, pp. 170–183, Sep. 2008, doi: 10.1007/s10563-008-9049-1.

[46] X. Guo, D. Mao, S. Wang, G. Wu, and G. Lu, "Combustion synthesis of CuO–ZnO–ZrO2 catalysts for the hydrogenation of carbon dioxide to methanol," *Catal. Commun.*, vol. 10, no. 13, pp. 1661–1664, Jul. 2009, doi: 10.1016/j.catcom.2009.05.004.

[47] R. W. Dorner, D. R. Hardy, F. W. Williams, and H. D. Willauer, "K and Mn doped iron-based CO2 hydrogenation catalysts: Detection of KAlH4 as part of the catalyst's active phase," *Applied Catalysis A: General*, vol. 373, no. 1–2, pp. 112–121, Jan. 2010, doi: 10.1016/j.apcata.2009.11.005.

[48] L. Xu *et al.*, "The promotions of MnO and K2O to Fe/silicalite-2 catalyst for the production of light alkenes from CO2 hydrogenation," *Applied Catalysis A: General*, vol. 173, no. 1, pp. 19–25, Oct. 1998, doi: 10.1016/S0926-860X(98)00141-0.

[49] T. Herranz, S. Rojas, F. J. Pérez-Alonso, M. Ojeda, P. Terreros, and J. L. G. Fierro, "Hydrogenation of carbon oxides over promoted Fe-Mn catalysts prepared by the microemulsion methodology," *Applied Catalysis A: General*, vol. 311, pp. 66–75, Sep. 2006, doi: 10.1016/j.apcata.2006.06.007.

[50] Q. Fu, H. Saltsburg, and M. Flytzani-Stephanopoulos, "Active nonmetallic Au and Pt species on ceria-based water-gas shift catalysts.," *Science*, vol. 301, no. 5635, pp. 935–938, Aug. 2003, doi: 10.1126/science.1085721.

[51] M. P. Rohde, D. Unruh, and G. Schaub, "Membrane application in fischer−tropsch synthesis to enhance co_2 hydrogenation," *Ind. Eng. Chem. Res.*, vol. 44, no. 25, pp. 9653–9658, Dec. 2005, doi: 10.1021/ie050289z.

[52] G. A. Olah, "After oil and gas: methanol economy," *Catal. Lett*, vol. 93, no. 1/2, pp. 1–2, Mar. 2004, doi: 10.1023/B:CATL.0000017043.93210.9c.

[53] C. Yang, Z. Ma, N. Zhao, W. Wei, T. Hu, and Y. Sun, "Methanol synthesis from CO2-rich syngas over a ZrO2 doped CuZnO catalyst," *Catal. Today*, vol. 115, no. 1–4, pp. 222–227, Jun. 2006, doi: 10.1016/j.cattod.2006.02.077.

[54] J. Ma *et al.*, "A short review of catalysis for CO2 conversion," *Catal. Today*, vol. 148, no. 3–4, pp. 221–231, Nov. 2009, doi: 10.1016/j.cattod.2009.08.015.

[55] K. Fujimoto and Y. Yu, "Spillover effect on the stabilization of Cu-Zn catalyst for CO2 hydrogenation to methanol," in *New Aspects of Spillover Effect in Catalysis - For Development of Highly Active Catalysts, Proceedings of the Third International Conference on Spillover*, vol. 77, Elsevier, 1993, pp. 393–396.

[56] T. Inui and T. Takeguchi, "Effective conversion of carbon dioxide and hydrogen to hydrocarbons," *Catal. Today*, vol. 10, no. 1, pp. 95–106, Aug. 1991, doi: 10.1016/0920-5861(91)80077-M.

[57] B. J. Liaw and Y. Z. Chen, "Liquid-phase synthesis of methanol from CO2/H2 over ultrafine CuB catalysts," *Applied Catalysis A: General*, vol. 206, no. 2, pp. 245–256, Jan. 2001, doi: 10.1016/S0926-860X(00)00601-3.

[58] X.-L. Liang, X. Dong, G.-D. Lin, and H.-B. Zhang, "Carbon nanotube-supported Pd–ZnO catalyst for hydrogenation of CO2 to methanol," *Appl. Catal. B*, vol. 88, no. 3–4, pp. 315–322, May 2009, doi: 10.1016/j.apcatb.2008.11.018.

[59] S. T. Oyama, "Preparation and catalytic properties of transition metal carbides and nitrides," *Catal. Today*, vol. 15, no. 2, pp. 179–200, Jun. 1992, doi: 10.1016/0920-5861(92)80175-M.

[60] S. Xie, W. Zhang, X. Lan, and H. Lin, "CO2 reduction to methanol in the liquid phase: A review.," *ChemSusChem*, vol. 13, no. 23, pp. 6141–6159, Dec. 2020, doi: 10.1002/cssc.202002087.

[61] H. Nieminen, G. Givirovskiy, A. Laari, and T. Koiranen, "Alcohol promoted methanol synthesis enhanced by adsorption of water and dual catalysts," *Journal of CO2 Utilization*, vol. 24, pp. 180–189, Mar. 2018, doi: 10.1016/j.jcou.2018.01.002.

[62] S. Xie *et al.*, "Eliminating carbon dioxide emissions at the source by the integration of carbon dioxide capture and utilization over noble metals in the liquid phase," *J. Catal.*, vol. 389, pp. 247–258, Sep. 2020, doi: 10.1016/j.jcat.2020.06.001.

[63] R. A. Köppel, C. Stöcker, and A. Baiker, "Copper- and Silver–Zirconia Aerogels: Preparation, Structural Properties and Catalytic Behavior in Methanol Synthesis from Carbon Dioxide," *J. Catal.*, vol. 179, no. 2, pp. 515–527, Oct. 1998, doi: 10.1006/jcat.1998.2252.

[64] T. Wang, J. Wang, and Y. Jin, "Slurry Reactors for Gas-to-Liquid Processes: A Review," *Ind. Eng. Chem. Res.*, vol. 46, no. 18, pp. 5824–5847, Aug. 2007, doi: 10.1021/ie070330t.

[65] A. T. Aguayo, J. Ereña, D. Mier, J. M. Arandes, M. Olazar, and J. Bilbao, "Kinetic Modeling of Dimethyl Ether Synthesis in a Single Step on a CuO−ZnO−Al_2O_3 /γ-Al_2O_3

Catalyst," *Ind. Eng. Chem. Res.*, vol. 46, no. 17, pp. 5522–5530, Aug. 2007, doi: 10.1021/ie070269s.

[66] M. Nilsson, L. J. Pettersson, and B. Lindström, "Hydrogen Generation from Dimethyl Ether for Fuel Cell Auxiliary Power Units," *Energy Fuels*, vol. 20, no. 5, pp. 2164–2169, Sep. 2006, doi: 10.1021/ef050419g.

[67] T. A. Semelsberger, K. C. Ott, R. L. Borup, and H. L. Greene, "Generating hydrogen-rich fuel-cell feeds from dimethyl ether (DME) using Cu/Zn supported on various solid-acid substrates," *Applied Catalysis A: General*, vol. 309, no. 2, pp. 210–223, Aug. 2006, doi: 10.1016/j.apcata.2006.05.009.

[68] F. Yaripour, F. Baghaei, I. Schmidt, and J. Perregaard, "Synthesis of dimethyl ether from methanol over aluminium phosphate and silica–titania catalysts," *Catal. Commun.*, vol. 6, no. 8, pp. 542–549, Aug. 2005, doi: 10.1016/j.catcom.2005.05.003.

[69] Q. Zhang, Y.-Z. Zuo, M.-H. Han, J.-F. Wang, Y. Jin, and F. Wei, "Long carbon nanotubes intercrossed Cu/Zn/Al/Zr catalyst for CO/CO2 hydrogenation to methanol/dimethyl ether," *Catal. Today*, vol. 150, no. 1–2, pp. 55–60, Feb. 2010, doi: 10.1016/j.cattod.2009.05.018.

[70] T. Takeguchi, K. Yanagisawa, T. Inui, and M. Inoue, "Effect of the property of solid acid upon syngas-to-dimethyl ether conversion on the hybrid catalysts composed of Cu–Zn–Ga and solid acids," *Applied Catalysis A: General*, vol. 192, no. 2, pp. 201–209, Feb. 2000, doi: 10.1016/S0926-860X(99)00343-9.

[71] X. An, Y.-Z. Zuo, Q. Zhang, D. Wang, and J.-F. Wang, "Dimethyl Ether Synthesis from CO_2 Hydrogenation on a CuO−ZnO−Al_2O_3 −ZrO_2 /HZSM-5 Bifunctional Catalyst," *Ind. Eng. Chem. Res.*, vol. 47, no. 17, pp. 6547–6554, Sep. 2008, doi: 10.1021/ie800777t.

[72] S. Wang, D. Mao, X. Guo, G. Wu, and G. Lu, "Dimethyl ether synthesis via CO2 hydrogenation over CuO–TiO2–ZrO2/HZSM-5 bifunctional catalysts," *Catal. Commun.*, vol. 10, no. 10, pp. 1367–1370, May 2009, doi: 10.1016/j.catcom.2009.02.001.

[73] J.-L. Tao, K.-W. Jun, and K.-W. Lee, "Co-production of dimethyl ether and methanol from CO2 hydrogenation: development of a stable hybrid catalyst," *Appl. Organomet. Chem.*, vol. 15, no. 2, pp. 105–108, Feb. 2001, doi: 10.1002/1099-0739(200102)15:2<105::AID-AOC100>3.0.CO;2-B.

[74] A. T. Aguayo, J. Ereña, I. Sierra, M. Olazar, and J. Bilbao, "Deactivation and regeneration of hybrid catalysts in the single-step synthesis of dimethyl ether from syngas and CO2," *Catal. Today*, vol. 106, no. 1–4, pp. 265–270, Oct. 2005, doi: 10.1016/j.cattod.2005.07.144.

[75] "The CO_{2} Hydrogenation toward the Mixture of Methanol and Dimethyl Ether: Investigation of Hybrid Catalysts -Bulletin of the Korean Chemical Society | Korea Science." https://doi.org/10.5012/BKCS.1998.19.4.466 (accessed Feb. 03, 2025).

[76] K. Sun, W. Lu, M. Wang, and X. Xu, "Low-temperature synthesis of DME from CO2/H2 over Pd-modified CuO–ZnO–Al2O3–ZrO2/HZSM-5 catalysts," *Catal. Commun.*, vol. 5, no. 7, pp. 367–370, Jul. 2004, doi: 10.1016/j.catcom.2004.03.012.

[77] H. Zhong, H. Yao, J. Duo, G. Yao, and F. Jin, "Pd/C-catalyzed reduction of NaHCO3 into CH3COOH with water as a hydrogen source," *Catal. Today*, vol. 274, pp. 28–34, Oct. 2016, doi: 10.1016/j.cattod.2016.05.010.

[78] J. Hietala, A. Vuori, P. Johnsson, I. Pollari, W. Reutemann, and H. Kieczka, "Formic Acid," in *Ullmann's encyclopedia of industrial chemistry*, Wiley-VCH Verlag GmbH & Co. KGaA, Ed. Weinheim, Germany: Wiley-VCH Verlag GmbH & Co. KGaA, 2000, pp. 1–22.

[79] "Potassium formate market value globally 2027 | Statista." https://www.statista.com/statistics/1079898/global-potassium-formate-market-size/#:~:text=Global%20market%20value%20of%20potassium%20formate%202018%2D2027&text=The%20global%20market%20of%20potassium,potassium%20salt%20of%20formic%20acid (accessed Nov. 25, 2024).

[80] A. Álvarez *et al.*, "Challenges in the greener production of formates/formic acid, methanol, and DME by heterogeneously catalyzed CO2 hydrogenation processes.," *Chem. Rev.*, vol. 117, no. 14, pp. 9804–9838, Jul. 2017, doi: 10.1021/acs.chemrev.6b00816.

[81] Z. Zhang, S. Hu, J. Song, W. Li, G. Yang, and B. Han, "Hydrogenation of CO2 to formic acid promoted by a diamine-functionalized ionic liquid.," *ChemSusChem*, vol. 2, no. 3, pp. 234–238, 2009, doi: 10.1002/cssc.200800252.

[82] Y. Gao, J. K. Kuncheria, H. A. Jenkins, R. J. Puddephatt, and G. P. A. Yap, "The interconversion of formic acid and hydrogen/carbon dioxide using a binuclear ruthenium complex catalyst," *J. Chem. Soc., Dalton Trans.*, no. 18, pp. 3212–3217, 2000, doi: 10.1039/b004234j.

[83] Y. Wu *et al.*, "*110th Anniversary:* Ionic Liquid Promoted CO_2 Hydrogenation to Free Formic Acid over Pd/C," *Ind. Eng. Chem. Res.*, vol. 58, no. 16, pp. 6333–6339, Apr. 2019, doi: 10.1021/acs.iecr.9b00654.

[84] G. A. Filonenko, W. L. Vrijburg, E. J. M. Hensen, and E. A. Pidko, "On the activity of supported Au catalysts in the liquid phase hydrogenation of CO2 to formates," *J. Catal.*, vol. 343, pp. 97–105, Nov. 2016, doi: 10.1016/j.jcat.2015.10.002.

[85] M. Asif, W. Yoon, J. Lee, and J. Kim, "Hydrogen production, storage, and decarbonization via heterogenous catalytic CO2 hydrogenation," *Korean J. Chem. Eng.*, vol. 42, no. 8, pp. 1561–1586, Jul. 2025, doi: 10.1007/s11814-025-00454-9.

[86] "Challenges and Opportunities in the Catalytic Conversion of CO_2 to Value-Added Chemicals – STM Journals."

https://journals.stmjournals.com/jocc/article=2024/view=174632/ (accessed Dec. 18, 2025).

[87] J. Słoczyński *et al.*, "Catalytic activity of the M/(3ZnO·ZrO2) system (M=Cu, Ag, Au) in the hydrogenation of CO2 to methanol," *Applied Catalysis A: General*, vol. 278, no. 1, pp. 11–23, Dec. 2004, doi: 10.1016/j.apcata.2004.09.014.

[88] J. Toyir, P. R. de la Piscina, J. Llorca, J.-L. G. Fierro, and N. Homs, "Methanol synthesis from CO2 and H2 over gallium promoted copper-based supported catalysts. Effect of hydrocarbon impurities in the CO2/H2 source," *Phys. Chem. Chem. Phys.*, vol. 3, no. 21, pp. 4837–4842, Oct. 2001, doi: 10.1039/b105235g.

[89] M. Agnelli, M. Kolb, and C. Mirodatos, "Co hydrogenation on a nickel catalyst .," *J. Catal.*, vol. 148, no. 1, pp. 9–21, Jul. 1994, doi: 10.1006/jcat.1994.1180.

[90] U. Y. Qazi, "Future of Hydrogen as an Alternative Fuel for Next-Generation Industrial Applications; Challenges and Expected Opportunities," *Energies*, vol. 15, no. 13, p. 4741, Jun. 2022, doi: 10.3390/en15134741.

[91] J. M. M. Arcos and D. M. F. Santos, "The Hydrogen Color Spectrum: Techno-Economic Analysis of the Available Technologies for Hydrogen Production," *Gases*, vol. 3, no. 1, pp. 25–46, Feb. 2023, doi: 10.3390/gases3010002.

[92] H. M. U. Ayub, S. Y. Alnouri, M. Stijepovic, V. Stijepovic, and I. A. Hussein, "A cost comparison study for hydrogen production between conventional and renewable methods," *Process Safety and Environmental Protection*, vol. 186, pp. 921–932, Jun. 2024, doi: 10.1016/j.psep.2024.04.080.

[93] M. M. Hossain Bhuiyan and Z. Siddique, "Hydrogen as an alternative fuel: A comprehensive review of challenges and opportunities in production, storage, and transportation," *Int. J. Hydrogen Energy*, vol. 102, pp. 1026–1044, Feb. 2025, doi: 10.1016/j.ijhydene.2025.01.033.

[94] B. Wu, Y. Gao, F. Jin, J. Cao, Y. Du, and Y. Zhang, "Catalytic conversion of NaHCO3 into formic acid in mild hydrothermal conditions for CO2 utilization," *Catal. Today*, vol. 148, no. 3–4, pp. 405–410, Nov. 2009, doi: 10.1016/j.cattod.2009.08.012.

[95] C. He, G. Tian, Z. Liu, and S. Feng, "A mild hydrothermal route to fix carbon dioxide to simple carboxylic acids.," *Org. Lett.*, vol. 12, no. 4, pp. 649–651, Feb. 2010, doi: 10.1021/ol9025414.

[96] J. Duo *et al.*, "NaHCO3-enhanced hydrogen production from water with Fe and in situ highly efficient and autocatalytic NaHCO3 reduction into formic acid.," *Chem. Commun.*, vol. 52, no. 16, pp. 3316–3319, Feb. 2016, doi: 10.1039/c5cc09611a.

[97] B. Jin, L. Luo, and L. Xie, "Pathways and Kinetics for Autocatalytic Reduction of CO2 into Formic Acid with Fe under Hydrothermal Conditions.," *ACS Omega*, vol. 6, no. 17, pp. 11280–11285, May 2021, doi: 10.1021/acsomega.1c00119.

[98] K. Michiels, B. Peeraer, W. Van Dun, J. Spooren, and V. Meynen, "Hydrothermal conversion of carbon dioxide into formate with the aid of zerovalent iron: the potential of a two-step approach.," *Faraday Discuss.*, vol. 183, pp. 177–195, Sep. 2015, doi: 10.1039/c5fd00104h.

[99] H. Zhong *et al.*, "Highly efficient water splitting and carbon dioxide reduction into formic acid with iron and copper powder," *Chemical Engineering Journal*, vol. 280, pp. 215–221, Nov. 2015, doi: 10.1016/j.cej.2015.05.098.

[100] Y. Le, H. Zhong, Y. Yang, R. He, G. Yao, and F. Jin, "Mechanism study of reduction of CO 2 into formic acid by in-situ hydrogen produced from water splitting with Zn: Zn/ZnO interface autocatalytic role," *Journal of Energy Chemistry*, Mar. 2017, doi: 10.1016/j.jechem.2017.03.013.

[101] H. Zhong, L. Wang, Y. Yang, R. He, Z. Jing, and F. Jin, "Ni and Zn/ZnO Synergistically Catalyzed Reduction of Bicarbonate into Formate with Water Splitting.," *ACS Appl. Mater. Interfaces*, vol. 11, no. 45, pp. 42149–42155, Nov. 2019, doi: 10.1021/acsami.9b14039.

[102] G. Yao, X. Zeng, Y. Jin, H. Zhong, J. Duo, and F. Jin, "Hydrogen production by water splitting with Al and in-situ reduction of CO 2 into formic acid," *Int. J. Hydrogen Energy*, vol. 40, no. 41, pp. 14284–14289, Nov. 2015, doi: 10.1016/j.ijhydene.2015.04.073.

[103] J. I. del Río, E. Pérez, D. León, Á. Martín, and M. D. Bermejo, "Catalytic hydrothermal conversion of CO2 captured by ammonia into formate using aluminum-sourced hydrogen at mild reaction conditions," *Journal of Industrial and Engineering Chemistry*, vol. 97, pp. 539–548, May 2021, doi: 10.1016/j.jiec.2021.03.015.

[104] L. Lyu, X. Zeng, J. Yun, F. Wei, and F. Jin, "No catalyst addition and highly efficient dissociation of H2O for the reduction of CO2 to formic acid with Mn.," *Environ. Sci. Technol.*, vol. 48, no. 10, pp. 6003–6009, May 2014, doi: 10.1021/es405210d.

[105] Y. Chen, Z. Jing, J. Miao, Y. Zhang, and J. Fan, "Reduction of CO2 with water splitting hydrogen under subcritical and supercritical hydrothermal conditions," *Int. J. Hydrogen Energy*, vol. 41, no. 21, pp. 9123–9127, Jun. 2016, doi: 10.1016/j.ijhydene.2015.11.157.

[106] "Standard Reduction Potentials Table." https://www.chm.uri.edu/weuler/chm112/refmater/redpottable.html (accessed Nov. 29, 2024).

[107] L. Lyu, F. Jin, H. Zhong, H. Chen, and G. Yao, "A novel approach to reduction of CO_2 into methanol by water splitting with aluminum over a copper catalyst," *RSC Adv.*, vol. 5, no. 40, pp. 31450–31453, 2015, doi: 10.1039/C5RA02872H.

[108] A. Behr, J. Eilting, K. Irawadi, J. Leschinski, and F. Lindner, "Improved utilisation of renewable resources: New important derivatives of glycerol," *Green Chem.*, vol. 10, no. 1, pp. 13–30, 2008, doi: 10.1039/B710561D.

[109] Z. Shen, Y. Zhang, and F. Jin, "From NaHCO3 into formate and from isopropanol into acetone: Hydrogen-transfer reduction of NaHCO3 with isopropanol in high-temperature water," *Green Chem.*, vol. 13, no. 4, p. 820, 2011, doi: 10.1039/c0gc00627k.

[110] D. Esposito and M. Antonietti, "Chemical conversion of sugars to lactic acid by alkaline hydrothermal processes.," *ChemSusChem*, vol. 6, no. 6, pp. 989–992, Jun. 2013, doi: 10.1002/cssc.201300092.

[111] M. I. Chinchilla, F. A. Mato, Á. Martín, and M. D. Bermejo, "Hydrothermal CO2 reduction by glucose as reducing agent and metals and metal oxides as catalysts.," *Molecules*, vol. 27, no. 5, Mar. 2022, doi: 10.3390/molecules27051652.

[112] Y. Zhu, Y. Yang, X. Wang, H. Zhong, and F. Jin, "Pd/C-catalyzed reduction of $NaHCO_3$ into formate with 2-pyrrolidone under hydrothermal conditions," *Energy Sci. Eng.*, vol. 7, no. 3, pp. 881–889, Jun. 2019, doi: 10.1002/ese3.317.

[113] Z. Shen, Y. Zhang, and F. Jin, "The alcohol-mediated reduction of CO_2 and $NaHCO_3$ into formate: a hydrogen transfer reduction of $NaHCO_3$ with glycerine under alkaline hydrothermal conditions," *RSC Adv.*, vol. 2, no. 3, pp. 797–801, 2012, doi: 10.1039/C1RA00886B.

[114] X. Wang, Y. Yang, H. Zhong, T. Wang, J. Cheng, and F. Jin, "Molecular H_2 O promoted catalytic bicarbonate reduction with methanol into formate over $Pd_{0.5}$ $Cu_{0.5}$ /C under mild hydrothermal conditions," *Green Chem.*, vol. 23, no. 1, pp. 430–439, 2021, doi: 10.1039/D0GC02785E.

[115] M. Konstantinova, "Biomass-assistedcatalytic reduction of carbon dioxide to value-added products underhydrothermal conditions," Doctoral dissertation, University of Sheffield, 2022.

[116] B. M. Kabyemela, T. Adschiri, R. M. Malaluan, and K. Arai, "Kinetics of glucose epimerization and decomposition in subcritical and supercritical water," *Ind. Eng. Chem. Res.*, vol. 36, no. 5, pp. 1552–1558, May 1997, doi: 10.1021/ie960250h.

[117] B. M. Kabyemela, T. Adschiri, R. M. Malaluan, and K. Arai, "Glucose and fructose decomposition in subcritical and supercritical water: detailed reaction pathway, mechanisms, and kinetics," *Ind. Eng. Chem. Res.*, vol. 38, no. 8, pp. 2888–2895, Aug. 1999, doi: 10.1021/ie9806390.

[118] D. A. Cantero, A. Álvarez, M. D. Bermejo, and M. J. Cocero, "Transformation of glucose into added value compounds in a hydrothermal reaction media," *J. Supercrit. Fluids*, vol. 98, pp. 204–210, Mar. 2015, doi: 10.1016/j.supflu.2014.12.015.

[119] H. R. Holgate, "Oxidation chemistry and kinetics in supercritical water : hydrogen, carbon monoxide, and glucose," Doctoral dissertation, Massachusetts Institute of Technology, Dept. of Chemical Engineering, 1993.

[120] F. Jin *et al.*, "High-yield reduction of carbon dioxide into formic acid by zero-valent metal/metal oxide redox cycles," *Energy Environ. Sci.*, vol. 4, no. 3, p. 881, 2011, doi: 10.1039/c0ee00661k.

[121] X. Liu, H. Zhong, C. Wang, D. He, and F. Jin, "CO_2 reduction into formic acid under hydrothermal conditions: A mini review," *Energy Sci. Eng.*, vol. 10, no. 5, pp. 1601–1613, May 2022, doi: 10.1002/ese3.1064.

[122] H. Zhong, K. Fujii, Y. Nakano, and F. Jin, "Effect of CO_2 Bubbling into Aqueous Solutions Used for Electrochemical Reduction of CO_2 for Energy Conversion and Storage," *J. Phys. Chem. C*, vol. 119, no. 1, pp. 55–61, Jan. 2015, doi: 10.1021/jp509043h.

[123] M. Andérez-Fernández *et al.*, "Formic acid production by simultaneous hydrothermal CO2 reduction and conversion of glucose and its derivatives," *Journal of the Taiwan Institute of Chemical Engineers*, vol. 139, p. 104504, Oct. 2022, doi: 10.1016/j.jtice.2022.104504.

[124] M. Locatelli, D. Melucci, G. Carlucci, and C. Locatelli, "Recent hplc strategies to improve sensitivity and selectivity for the analysis of complex matrices," *Instrum. Sci. Technol.*, vol. 40, no. 2–3, pp. 112–137, Mar. 2012, doi: 10.1080/10739149.2011.651668.

[125] S. E. Hunter and P. E. Savage, "Quantifying rate enhancements for acid catalysis in CO_2 -enriched high-temperature water," *AIChE J.*, vol. 54, no. 2, pp. 516–528, Feb. 2008, doi: 10.1002/aic.11392.

[126] M. Sasaki, K. Goto, K. Tajima, T. Adschiri, and K. Arai, "Rapid and selective retro-aldol condensation of glucose to glycolaldehyde in supercritical water," *Green Chem.*, vol. 4, no. 3, pp. 285–287, Jun. 2002, doi: 10.1039/b203968k.

[127] P. Gao *et al.*, "Preparation of lactic acid, formic acid and acetic acid from cotton cellulose by the alkaline pre-treatment and hydrothermal degradation," *Industrial Crops and Products*, vol. 48, pp. 61–67, Jul. 2013, doi: 10.1016/j.indcrop.2013.04.002.

[128] F. Jin, Z. Zhou, H. Enomoto, T. Moriya, and H. Higashijima, "Conversion mechanism of cellulosic biomass to lactic acid in subcritical water and acid–base catalytic effect of subcritical water," *Chem. Lett.*, vol. 33, no. 2, pp. 126–127, Feb. 2004, doi: 10.1246/cl.2004.126.

[129] R. I. Mainil, N. Paksung, and Y. Matsumura, "Determination of retro-aldol reaction type for glyceraldehyde under hydrothermal conditions," *J. Supercrit. Fluids*, vol. 143, pp. 370–377, Jan. 2019, doi: 10.1016/j.supflu.2018.09.013.

[130] C. A. Ramírez-López, J. R. Ochoa-Gómez, S. Gil-Río, O. Gómez-Jiménez-Aberasturi, and J. Torrecilla-Soria, "Chemicals from biomass: synthesis of lactic acid by alkaline hydrothermal conversion of sorbitol," *J. Chem. Technol. Biotechnol.*, vol. 86, no. 6, pp. 867–874, Jun. 2011, doi: 10.1002/jctb.2602.

[131] M. Trincado, H. Grützmacher, and M. H. G. Prechtl, "CO2-based hydrogen storage – Hydrogen generation from formaldehyde/water," *Physical Sciences Reviews*, vol. 3, no. 5, May 2018, doi: 10.1515/psr-2017-0013.

[132] H. Kishida, F. Jin, Z. Zhou, T. Moriya, and H. Enomoto, "Conversion of Glycerin into Lactic Acid by Alkaline Hydrothermal Reaction," *Chem. Lett.*, vol. 34, no. 11, pp. 1560–1561, Nov. 2005, doi: 10.1246/cl.2005.1560.

[133] G. Wang, Y. Meng, J. Zhou, and L. Zhang, "Selective hydrothermal degradation of cellulose to formic acid in alkaline solutions," *Cellulose*, vol. 25, no. 10, pp. 5659–5668, Oct. 2018, doi: 10.1007/s10570-018-1979-9.

[134] C. A. Ramírez-López, J. R. Ochoa-Gómez, M. Fernández-Santos, O. Gómez-Jiménez-Aberasturi, A. Alonso-Vicario, and J. Torrecilla-Soria, "Synthesis of lactic acid by alkaline hydrothermal conversion of glycerol at high glycerol concentration," *Ind. Eng. Chem. Res.*, vol. 49, no. 14, pp. 6270–6278, Jul. 2010, doi: 10.1021/ie1001586.

[135] "Agilent MetaCarb 87H Organic Acids Column H+ Form ," 2013, Accessed: Nov. 26, 2024. [Online]. Available: chrome-extension://efaidnbmnnnibpcajpcglclefindmkaj/https://www.agilent.com/cs/library/usermanuals/public/Agilent%20MetaCarb%2087H%20A5214%20300x6.5mm.pdf.

[136] "Phenols, Alcohols and Carboxylic Acids - pKa Values." https://www.engineeringtoolbox.com/paraffinic-benzoic-hydroxy-dioic-acids-structure-pka-carboxylic-dissociation-constant-alcohol-phenol-d_1948.html (accessed Nov. 26, 2024).

[137] M. J. Kamlett, *Organic Electronic Spectral Data*. New York ; London: Interscience, 1960, 1960.

[138] J. P. Phillips, and F and C. Nachod, *Organic Electronic Spectral Data*, vol. 4. New York: Interscience, 1963.

[139] O. H. Wheeler, and Lloyd and A. Kaplan, *Organic Electronic Spectral Data*, vol. 3. New York: Interscience, 1966.

[140] J. P. Phillips, Robert, and Paul E. Lyle, and Raymond Jones, " ," in *Organic Electronic Spectral Data*, vol. 5, New York: Interscience, 1969.

[141] J. P. Phillips, Leon, and J D. Freedman, and Cymerman Craig, *Organic Electronic Spectral Data*, vol. 6. New York: Wiley-Interscience, 1970.

[142] J. P. Phillips, Joseph, and Rip C. Dacons, and G. Rice, *Organic Electronic Spectral Data*, vol. 7. New York: Wiley- : Interscience, 1972.

[143] Z. Shen *et al.*, "The mechanism for production of abiogenic formate from CO2 and lactate from glycerine: uncatalyzed transfer hydrogenation of CO2 with glycerine under alkaline hydrothermal conditions," *RSC Adv.*, vol. 4, pp. 15256–15263, 2014.

[144] "CN102911035A - Method for preparing propionic acid from ethyl acetate through carbonylation - Google Patents." https://patents.google.com/patent/CN102911035A/en (accessed May 17, 2025).

[145] S. Letichevsky *et al.*, "The role of m-ZrO2 in the selective oxidation of ethanol to acetic acid employing PdO/m-ZrO2," *J. Mol. Catal. A: Chem*, vol. 410, pp. 177–183, Dec. 2015, doi: 10.1016/j.molcata.2015.09.012.

[146] V. V. Brei, M. E. Sharanda, S. V. Prudius, and E. A. Bondarenko, "Synthesis of acetic acid from ethanol–water mixture over Cu/ZnO–ZrO2–Al2O3 catalyst," *Applied Catalysis A: General*, vol. 458, pp. 196–200, May 2013, doi: 10.1016/j.apcata.2013.03.038.

[147] B. Voss, N. C. Schjødt, J.-D. Grunwaldt, S. I. Andersen, and J. M. Woodley, "Kinetics of acetic acid synthesis from ethanol over a Cu/SiO2 catalyst," *Applied Catalysis A: General*, vol. 402, no. 1–2, pp. 69–79, Jul. 2011, doi: 10.1016/j.apcata.2011.05.030.

[148] C. P. Rodrigues, P. C. Zonetti, C. G. Silva, A. B. Gaspar, and L. G. Appel, "Chemicals from ethanol—The acetone one-pot synthesis," *Applied Catalysis A: General*, vol. 458, pp. 111–118, May 2013, doi: 10.1016/j.apcata.2013.03.028.

[149] Y. Hu, J. Pan, M. A. Nawaz, X. Li, and D. Liu, "Kinetic study on the carbonylation of ethanol to propionic acid using homogeneous Rh complex catalyst at low water content," *Reac. Kinet. Mech. Cat.*, vol. 129, no. 1, pp. 235–251, Feb. 2020, doi: 10.1007/s11144-019-01692-9.

[150] H. Li *et al.*, "Thermodynamics Foundation and Separation Process Design for Production of Propionic Acid from Ethanol Carbonylation Catalyzed by Iodide," *Ind. Eng. Chem. Res.*, vol. 59, no. 13, pp. 6090–6101, Apr. 2020, doi: 10.1021/acs.iecr.9b06505.

[151] L. Xu, Y. Hu, M. A. Nawaz, X. Li, and D. Liu, "Kinetic study of carbonylation of ethanol to propionic acid using homogeneous rhodium complex catalyst in the presence of diphosphine ligand," *Fuel Processing Technology*, vol. 213, p. 106716, Mar. 2021, doi: 10.1016/j.fuproc.2020.106716.

[152] S. Yacob, S. Park, B. A. Kilos, D. G. Barton, and J. M. Notestein, "Vapor-phase ethanol carbonylation with heteropolyacid-supported Rh," *J. Catal.*, vol. 325, pp. 1–8, May 2015, doi: 10.1016/j.jcat.2015.02.004.

[153] S. Yacob, B. A. Kilos, D. G. Barton, and J. M. Notestein, "Vapor phase ethanol carbonylation over Rh supported on zeolite 13X," *Applied Catalysis A: General*, vol. 520, pp. 122–131, Jun. 2016, doi: 10.1016/j.apcata.2016.04.006.

[154] S. Sabater *et al.*, "Mechanistic Investigation of the Nickel-Catalyzed Carbonylation of Alcohols," *Organometallics*, vol. 39, no. 6, pp. 870–880, Mar. 2020, doi: 10.1021/acs.organomet.0c00082.

[155] G. Peng, S. J. Sibener, G. C. Schatz, S. T. Ceyer, and M. Mavrikakis, "Co_2 hydrogenation to formic acid on ni(111)," *J. Phys. Chem. C*, vol. 116, no. 4, pp. 3001–3006, Feb. 2012, doi: 10.1021/jp210408x.

[156] C.-L. Chiang, K.-S. Lin, and H.-W. Chuang, "Direct synthesis of formic acid via CO 2 hydrogenation over Cu/ZnO/Al 2 O 3 catalyst," *J. Clean. Prod.*, vol. 172, pp. 1957–1977, Jan. 2018, doi: 10.1016/j.jclepro.2017.11.229.

[157] D. Bröll *et al.*, "Chemistry in supercritical water.," *Angew. Chem. Int. Ed*, vol. 38, no. 20, pp. 2998–3014, Oct. 1999, doi: 10.1002/(SICI)1521-3773(19991018)38:20<2998::AID-ANIE2998>3.0.CO;2-L.

[158] F. Jin and H. Enomoto, "Rapid and highly selective conversion of biomass into value-added products in hydrothermal conditions: chemistry of acid/base-catalysed and oxidation reactions," *Energy Environ. Sci.*, vol. 4, no. 2, pp. 382–397, 2011, doi: 10.1039/C004268D.

[159] M. Watanabe *et al.*, "Glucose reactions with acid and base catalysts in hot compressed water at 473 K.," *Carbohydr. Res.*, vol. 340, no. 12, pp. 1925–1930, Sep. 2005, doi: 10.1016/j.carres.2005.06.017.

[160] Y. Yang *et al.*, "Synergetic conversion of microalgae and CO_2 into value-added chemicals under hydrothermal conditions," *Green Chem.*, vol. 21, no. 6, pp. 1247–1252, 2019, doi: 10.1039/C8GC03645D.

[161] M. Elsner, L. Zwank, D. Hunkeler, and R. P. Schwarzenbach, "A new concept linking observable stable isotope fractionation to transformation pathways of organic pollutants.," *Environ. Sci. Technol.*, vol. 39, no. 18, pp. 6896–6916, Sep. 2005, doi: 10.1021/es0504587.

[162] D. A. Singleton, S. R. Merrigan, J. Liu, and K. N. Houk, "Experimental geometry of the epoxidation transition state," *J. Am. Chem. Soc.*, vol. 119, no. 14, pp. 3385–3386, Apr. 1997, doi: 10.1021/ja963656u.

[163] S. R. Merrigan, V. N. Le Gloahec, J. A. Smith, D. H. R. Barton, and D. A. Singleton, "Separation of the primary and secondary kinetic isotope effects at a reactive center using starting material reactivities. Application to the FeCl3-Catalyzed oxidation of C□H bonds with tert-butyl hydroperoxide," *Tetrahedron Lett.*, vol. 40, no. 20, pp. 3847–3850, May 1999, doi: 10.1016/S0040-4039(99)00637-1.

[164] G. Wen, Y. Xu, Z. Xu, and Z. Tian, "Characterization and Catalytic Properties of the Ni/Al2O3 Catalysts for Aqueous-phase Reforming of Glucose," *Catal. Lett*, vol. 129, no. 1–2, pp. 250–257, Apr. 2009, doi: 10.1007/s10562-008-9810-0.

[165] R. D. Cortright, R. R. Davda, and J. A. Dumesic, "Hydrogen from catalytic reforming of biomass-derived hydrocarbons in liquid water.," *Nature*, vol. 418, no. 6901, pp. 964–967, Aug. 2002, doi: 10.1038/nature01009.

[166] I. Coronado, M. Stekrova, M. Reinikainen, P. Simell, L. Lefferts, and J. Lehtonen, "A review of catalytic aqueous-phase reforming of oxygenated hydrocarbons derived from biorefinery water fractions," *Int. J. Hydrogen Energy*, vol. 41, no. 26, pp. 11003–11032, Jul. 2016, doi: 10.1016/j.ijhydene.2016.05.032.

[167] Y. Xu, Z. Tian, G. Wen, Z. Xu, W. Qu, and L. Lin, "Production of CO *x* -free Hydrogen by Alkali Enhanced Hydrothermal Catalytic Reforming of Biomass-derived Alcohols," *Chem. Lett.*, vol. 35, no. 2, pp. 216–217, Feb. 2006, doi: 10.1246/cl.2006.216.

[168] K. Michiels, J. Spooren, and V. Meynen, "Production of hydrogen gas from water by the oxidation of metallic iron under mild hydrothermal conditions, assisted by in situ formed carbonate ions," *Fuel*, vol. 160, pp. 205–216, Nov. 2015, doi: 10.1016/j.fuel.2015.07.061.

[169] E. Ghali, *Corrosion resistance of aluminum and magnesium alloys: understanding, performance, and testing*. Wiley, 2010.

[170] C. Vargel, "The corrosion of aluminium," in *Corrosion of Aluminium*, Elsevier, 2020, pp. 41–61.

[171] L. Calabrese, L. Bonaccorsi, D. D. Pietro, and E. Proverbio, "Effect of process parameters on behaviour of zeolite coatings obtained by hydrothermal direct synthesis on aluminium support," *Ceramics International*, vol. 40, no. 8, pp. 12837–12845, Sep. 2014, doi: 10.1016/j.ceramint.2014.04.138.

[172] M. Nordio, M. Eguaras Barain, L. Raymakers, M. Van Sint Annaland, M. Mulder, and F. Gallucci, "Effect of CO2 on the performance of an electrochemical hydrogen compressor," *Chemical Engineering Journal*, vol. 392, p. 123647, Jul. 2020, doi: 10.1016/j.cej.2019.123647.

[173] X. Zeng, G. Yao, and J. Zhao, "Study on the Highly Efficient Reduction of CO_2 to Formate Using Zinc under Mild Hydrothermal Conditions," *J. Phys.: Conf. Ser.*, vol. 2168, no. 1, p. 012024, Jan. 2022, doi: 10.1088/1742-6596/2168/1/012024. Sciwheel inserting bibliography...